Fondo Sociale Europeo

Ministero dell'Istruzione dell'Università e della Ricerca

Università degli studi di Catania

Ministero dell'Istruzione dell'Università e della Ricerca

Università degli studi di Catania

Tesi di Dottorato in Ingegneria Geotecnica

XXIII Ciclo

Massimo Nicolosi

Seismic analysis of inclined shallow granular deposits

Coordinatore

Prof. Ing. Michele Maugeri

Tutor

Prof. Ing. Michele Maugeri

Co - Tutor

Prof. Ing. Claudio di Prisco

(Politecnico di Milano)

Catania, Dicembre 2011

to Vanessa

NTRODUCTION

In the last decades many attempts for understanding the cyclic and dynamic behaviour of soils have been done by the scientific community.

The importance of this emerging topic has been highlighted by the empirical evidence that seismic hazard is strongly affected by the soil behaviour and consequently a better understanding of the dynamic soil behaviour could lead to a reduction in human casualties and a decreased loss of money due to earthquakes events.

From a modelling point of view, because of the intrinsic challenging characteristics of the problem under examination, the approaches adopted can be essentially subdivided between empirical and theoretical.

The first has showed their capabilities of modelling the full complexity of the dynamic soil behaviour, even if their main drawback lies essentially on the very limited possibility of being generalized if the model is not accurately calibrated for soils taken from the site under analysis. Furthermore many peculiar effects could not be observed or physically understood.

The latter approach is aimed at concerning a quite general constitutive relationship capable of highlighting the soil dynamic response by modifying mechanical models taken from literature, already calibrated on the static mechanical response.

The aim of this thesis consists to investigate the mechanical response of two granular materials (Hostun and Toyoura sand) under cyclic/dynamic conditions.

In many cases in literature, the displacements based approach appears to provide a compromise between the more simple pseudo-static approach, by a single or partial factors of safety, which works only on the safety side, and the more comprehensive finite element method of analysis, producing detailed performance data but whose implementation requires a high level of sophistication in selection of material properties, constitutive laws, and mesh discretization. From a practical point of view, the displacement-based approach offers the advantage of giving a rapid and yet quantitative assessment of the movement of earth structures under seismic loading.

In this thesis such a hypothesis is numerically discussed.

In the last years the research of prof. R. Nova and of prof. C. di Prisco of Politecnico of Milan has been devoted to lab experiments and to formulate a constitutive model for the

behaviour of granular soils. For this reason part of the thesis has been performed at the Politecnico of Milan.

Starting from the recent works of Imposimato (1998), Zambelli (2002) and Pisanò (2007), the code VIBRAZIONE, implementing an elastoviscoplastic model, has been improved and tested, studying the dynamic instability of an infinitely long slope under real Italian earthquakes (Database SISMA) and comparing the results with those obtained by means of the displacement method, that is widespread employed among engineers.

Recently many authors have established empirical relationships between the expected permanent displacement, the soil dynamic characteristics, and the earthquake engineering parameters. The critical acceleration ratio, which is defined as the ratio of the critical acceleration (k_c) of the sliding block to the peak acceleration (a_{max}) of the earthquake, has been shown to be a parameter that has an important influence on the magnitude of the permanent displacement.

Thus, in the literature, the seismic displacement of a potential sliding soil mass computed using Newmark's theory has been traditionally expressed as a function of the critical acceleration ratio (k_c/a_{max}).

In this paper some relationships between permanent displacement, evaluated by means of the code VIBRAZIONE and the Newmark method, and earthquake parameters, such as critical acceleration ratio, Arias Intensity and Destructive Potential, have been finally investigated.

CHAPTER 1 GENERAL REVIEW

General

The analysis and the understanding of the mechanical behaviour and stability conditions of either cyclically or dynamically loaded soils is one of the most stimulating subjects of soil mechanics, especially by the light of deaths, injuries and damages, which the seismic hazards cause each year around the world.

In the last decades these aspects have been subject of increasing attention, both for the development of knowledge on the complex cyclic behaviour of soils, and because the consequences of many seismic events have shown that a substantial part of the damage caused to the affected area is related to instability of natural slopes and earth structures for which an event may be the cause. In many cases, in fact, extensive damages to structures and infrastructures as well as the loss of human lives can not occur as a result of the direct effects of the earthquake, but because of instability affecting the structures and infrastructures that are based on the slope or which can be interested by any instability phenomenon induced by seismic event. In high-intensity Japan earthquakes from 1964 to 1980, for example, more than half of the victims is due to instability generated by seismic events (Kobayashi, 1981). More than half of the damage caused by the earthquake in Alaska in 1964, instead, were caused by the many landslides caused by the seismic event (Youd, 1978; Wilson and Keefer, 1985).

The conditions of seismic stability of slope or structure on earth are affected by many factors and a reliable stability analysis should consider the influence of each of them.

Particularly important are the morphologic characteristics and hydraulic conditions of slope or soil structure considered, the nature of soils and characteristics of the seismic event. Because of this multiplicity of factors the modelling of seismic response is remarkably complex.

Since the first studies performed great importance was attributed to the influence that the seismic phenomena characterizing the complex cyclic behaviour of soils can exercise on seismic stability conditions.

Numerous other experiences have shown that analyses of seismic stability conditions that do not take into account the effects of the cyclic behaviour of soils can lead to unreliable assessments and, above all, not much precautionary. Table 1.1, for example, shows some widely documented cases in the literature of natural slopes, earth dams and embankments where disastrous effects have occurred in consequence of several earthquakes. For many of the cases described in Table 1.1, some stability analyses

conducted without taking into account the effects of the reduction in shear strength of the soil have led to estimate adequate margins of safety of the structures to collapse. For most of the cases shown in Table 1.1 the studies carried out have shown that the effects of the cyclic behaviour of soils are, in some cases, the only explanation key of the instability phenomena occurred; in other cases the instability phenomena was influenced as by the decay of the soil shear strength as the destabilizing effect caused by the seismic motion.

The above considerations emphasize the importance of phenomena related to the cyclic behaviour of soils on the seismic stability conditions of a natural slope or soil structure.

In the present paper will therefore examine the seismic instability on slopes, in particular in terms of displacements.

SEISMIC INSTABILITY PHENOMENA

Classification

Depending on the nature of the causes of a phenomenon of instability during a seismic event, the more general distinction (Kramer, 1996) includes two categories: the instability phenomena of inertial nature, indicated in the international literature as *"inertial instability"*, and instability phenomena caused by a marked reductions in shear strength of soil, usually indicated as *"weakening instability"*.

At the first type of phenomena (inertial instability) we refers when the cyclic behaviour of the soil, due to the cyclic load history imposed by the seismic event, is such that not to cause any reduction in shear strength; the phenomenon of deformation produced by the seismic event is, therefore, only due to the destabilizing effect related to the inertial actions induced by the ground motion. At the second type of phenomena (weakening instability) we refers, however, when the behaviour of soil subjected to cyclic loading imposed by the seismic event is such to manifest a substantial reduction in shear strength. In this case it is the decrease in resistance to produce the phenomenon of instability and to govern its evolution.

A so clear division of phenomena is, in fact, unlikely. The cyclic behaviour of soil is, indeed, always characterized by changes in shear strength even if in very small quantities. Moreover, also in the case of significant reduction in resistance, inertial actions always provide a certain contribution to the deformation induced. Therefore, conditions of seismic stability of a slope and the possible phenomenon of induced stability are always influenced by the inertial effect and by the effects of the cyclic behaviour of soils; this consideration is also supported by the fact that these phenomena, as well as concomitant, are closely linked. It is well known that the mechanical behaviour experienced by a soil under conditions of cyclic loading deeply depends on its stress and strain state.

With regard to the effects produced by an earthquake on a slope, it is also worth nothing that the manner in which a possible phenomenon of instability manifests is, however, related to the stability conditions of the slope in the phase before the event. In general, a seismic phenomenon of instability occurs when the seismic resistance of the soil mass potentially unstable is exceeded by the destabilizing actions acting as a result of the earthquake and the stress-strain state pre-existing the event. The seismic behaviour of a slope is, therefore, always influenced by its conditions of static stability.

Based on these considerations it is considered appropriate to use the term *"inertial instability"* or phenomenon of instability of inertial nature to describe those phenomena in which the reduction in shear strength is so small that it can be neglected for all practical purpose; any deformative phenomenon induced by the seismic event can, therefore, be regarded as being predominantly inertial.

If, however, the reduction in shear strength of soil is high enough to minimize the influence of the destabilizing action of inertial nature it is reasonable to assume that the possible deformative phenomenon is mainly caused by the effects of the cyclic behaviour of soils, at these phenomena we can report with the term *"weakening instability"* or instability phenomena caused by the reduction in shear strength of soil.

Finally, when both aspects are important for the response of the slope, the deformative phenomenon is of dual nature and its analysis can not ignore any of the two cases. In this case we will refer in the following to these phenomena with the term *"inertial-weakening instability"* or instability phenomena produced by inertial effects and by reduction in the shear strength of soil.

In this regard it should be noted that the possibility of occurrence of a phenomenon governed only by the reduction in shear strength of the soil or the possibility that the phenomenon is of double nature must be checked in relation to the initial conditions of stability of the slope. Once again, therefore, it is clear that the analysis of the condition of seismic stability of a slope can not, in any way, regardless of knowledge of the conditions of static stability.

The experience gained in the last decades has shown that to instability phenomena of different nature correspond, in general, permanent deformation of different entities and, therefore, damage to the affected area of different entity.

METHODS FOR THE ANALYSIS OF STABILITY

General

The issues related to the analysis of the seismic stability conditions of structures on earth and slopes are discussed for over sixty years (Terzaghi, 1950). Since at the same times the knowledge on the subject and the solving techniques of related problems have evolved, in literature there are many approaches of different nature to the problem.

In general, the approaches traditionally followed for seismic stability analyses can be divided into three categories:

- methods of dynamic analysis of the seismic response;
- methods of analysis based on the principle of limit equilibrium or limit analysis;
- empirical methods and solutions.

The methods of dynamic analysis of the seismic response of soil structure have found various applications in the study of seismic instability of the slopes whether with regard to the phenomena of inertial nature or with regard to phenomena in which the variation in shear strength of soli is a concomitant cause or even trigger.

The methods of analysis that make use of the principle of limit equilibrium analysis are certainly among the best known and most popular in geotechnical engineering and have had numerous applications also in relation to the evaluation of seismic stability conditions of slopes. The best-known approaches that use these types of analysis are the so-called pseudo-static method and the displacement method traditionally attributed to the study of Newmark (1965).

The empirical methods and solutions are born mainly by post observation and the subsequent analysis of many phenomena of instability caused by earthquakes occurred in different parts of the world.

In the following we will briefly recall the main features of the most common used methods, in order to highlight the applicability to the instability phenomena in this study, for solving problems of seismic stability of slopes and structures on earth. In particular, we will examine the characteristics of the pseudo-static approach, the method of displacements and the dynamic analysis of seismic response.

The pseudo-static approach

Pseudo-static methods are probably the most common approach for the seismic design of soil structures. The basic premise in pseudo-static methods is that the soil structure behaves as a rigid plastic material and it is at a state of limit equlibrium under the action of acceleration-induced inertia forces superimposed on static forces. The implementation of

a pseudo-static analysis requires input of the peak design acceleration, geometry of the considered soil structure and Mohr-Coulomb soil strength parameters (c and ϕ). The stability of the soil structure under the peak inertia force is determined by the calculation of the dynamic safety factor which is the ratio of the total resisting force to the total destabilizing force. Once dynamic safety factor is below the unit, an instant, but non-quantified, failure is assumed to occur.

An analysis of this type greatly simplifies the problem, although, for different reasons, does not allow a proper analysis. The application of the pseudo-static method through the method of the global limit equilibrium is more widespread than that through the limit analysis. The first application in this sense goes back to a study by Terzaghi (1950) and consisted of an extension to the case of the slopes of the theory developed by Okabe (1926) and Mononobe (1929) for the calculation of the increasing of the thrust of the soils on the rigid framework because of the earthquake. To both applications that refer to the method of the limit equilibrium and limit analysis a limited validity is recognized, as at the basis of the pseudo-static approach there are some assumptions that, from a theoretical point of view, are not correct and, therefore, can lead to unreliable estimations on the stability. In fact, with this approach at least in its initial formulation, any aspect of the cyclic behaviour of soils and the dynamic response of any structure on earth are not taken in any way in consideration. Nevertheless, for a long time, this methodology has been applied both to the lack of an alternative of practical use and because the assumption at the basis of the pseudo-static approach, which is to schematize the seismic action with inertial forces statically applied, allows to consider the problem in a manner substantially similar to the static case and, therefore, to refer to the extensive treatment on the topic provided in the scientific literature.

Traditionally, the method is applied to analyse in plane strain condition and, for a given collapse mechanism, provides the search of the area, defined critical, to which is due to the minimum value of the safety factor. In analogy to the static case, except for particular patterns, the analysis conditions of equilibrium limit can be made only in terms of overall equilibrium for particular schemes for which the problem results statically determined. In the other cases the problem is solved with the known method of the strips, making that some assumptions about the state of stress within the soil mass, makes the problem statically determined and solvable by means of the only equilibrium equations of the statics and the failure criteria.

The result of an analysis conducted according to the pseudo-static approach is highly dependent on the choices made about the seismic acceleration value and the shear strength parameters of soil.

The hypothesis to assume that the potential landslide mass behaves as a rigid body would impose a maximum value of the inertial actions proportional to the maximum value of seismic acceleration at the ground. The actual deformation of the soil and the

consideration that the maximum value of acceleration acts on a reduced period of time have made that the acceleration value selected for analysis is usually considerably lower than the maximum value. Both in the literature (Hynes-Griffin and Franklin, 1984) and in the standards of different countries there are many indications in this regard. In most cases, however, the experience and wisdom (engineering judgment) play a fundamental role in the choice of an appropriate value of the seismic acceleration the stability verify.

With regard to the choice of the parameters of shear strength of soil it is necessary to consider the possible effects on seismic stability conditions that some of the features of the complex cyclic behaviour of soils can have. In particular, the aspects related to the reduction in shear strength that can characterize the dynamic response of many soils must be taken into account.

In this case the approach traditionally followed is to take values of the shear strength parameters appropriately reduced or to make an assessment of the possible variation of pore pressure that can occur in the soil following the history of cyclic loading at which the earthquake is submitted.

This approach to the problem remains, however, of limited validity so that, in presence of soils that can shown significant changes in strength and deformability, some standards, including the Eurocode 8 (2002), prescribe not to carry out stability analyses through pseudo-static approach. These considerations, together with an awareness that the actual stability conditions of a slope or structure on earth are governed by the extent of deformations related to the seismic response, make that the pseudo-static method can not be considered a reliable analysis tool.

The displacement-based method

The displacement method has been originated by a work proposed by Newmark in 1965, to estimate the permanent displacements of slopes on earth dams or embankments induced by earthquakes. The method, often referred to as the Newmark method is, probably, one of the most popular analytical tools used in seismic geotechnical engineering. Because of its generality, in fact, the method is provided in many different applications for seismic stability analyses of slopes and structure on earth; moreover, the approach is so general that it became widely used in other fields of seismic geotechnical engineering.

Displacement-based methods require a certain functional relationship between the expected permanent displacement of the sliding soil mass, the critical acceleration and representative characteristic parameters of the earthquake record. The amount of movement of the soil structure can be estimated from the given relationship once the peak ground acceleration exceeds the critical acceleration of the soil structure. The critical acceleration is defined here as the minimum horizontal ground acceleration required to overcome frictional resistance along the sliding boundary of the soil mass and bring the

dynamic safety factor to one. Thus, the implementation of a displacement-based analysis requires, first, an iterative pseudo-static procedure to determine the critical acceleration of the considered soil structure, and then an evaluation of the required characteristic parameters of the input earthquake.

The use of a methodology of analysis based on the evaluation of the permanent displacements is justified by the fact that the stability seismic conditions and the post-seismic functionality of a slope or structure on earth are closely related to the magnitude of permanent deformations that an earthquake can cause. To the magnitude of the induced deformation is, in fact, related to the damage that any deformative phenomenon, established by the event, can have on structures or infrastructure that are located on a slope or on those invested by the mass of soil became unstable. It should be noted that the configuration of collapse, that the pseudo-static method predicts for values of the safety factor less than unit, is not, in practice, in any way defined. Indeed, the consideration that during an earthquake the safety factor of the slope takes, for a few seconds, values lower than unit does not necessarily mean the achieving of a state of collapse.

In some cases (Wilson and Keefer, 1984), for example, was found that, despite the pseudo-static method foresaw a situation of collapse, the extent of permanent deformations produced by the earthquake was so small not to affect, in any way, the conditions of stability and functionality of the slope.

When, as a result of the destabilizing seismic actions, the safety coefficient of the slope falls below the unit value, the potentially unstable soil mass is no longer in equilibrium and it is subjected to displacements due to the accelerations to which it is subjected, as a result of forces no longer balanced.

The soil mass is assumed to be a rigid block that fails in a rigid-plastic manner when the ground acceleration exceeds the critical acceleration of the slope. The critical acceleration is the seismic acceleration value at which the stress state acting in all along the potential sliding surface is such that to establish a condition of limit equilibrium for the slope. This definition requires, therefore, that the critical acceleration of a slope depends on the shear strength available under seismic conditions along the analyzed surface of potential sliding.

Once sliding commences, it is assumed to continue at a constant acceleration equal to the critical acceleration until the relative velocity between the sliding mass and the base became zero. A graphical interpretation of Newmark's sliding block theory is illustred in Fig.1.1, where:

g is the gravitational constant, $a(t)$ is the horizontal ground acceleration function with time t, $k_m g$ is the peak value of $a(t)$ and $k_c g$ is the critical acceleration of the sliding block.

Reached the limit conditions, the equilibrium of the slope is no longer guaranteed, and it will begin to store up permanent displacements until the seismic acceleration, reversing the sign, will cancel the relative velocity of the landslide mass. From that moment the

slope will not manifest displacements until the critical value of acceleration will be exceeded. In this case the permanent displacements will accumulate in the same manner described again above.

The displacement method is traditionally applied using acceleration time histories obtained from dynamic analyses of the seismic response or, more simply, the accelerograms recorded on the ground.

For a fixed history of seismic accelerations, the evaluation of permanent displacements, totally cumulate from the slope, requires the determination of the differential equation of the relative motion and its integration in all moments of time in which the relative velocity of landslide mass is non-zero.

The equation of motion to take into consideration is different depending on the examined collapse mechanism. Although, in fact, the analogy to the base of the method proposed by Newmark (1965) is related to a sliding on a plane surface, the generality of the method has allowed its extension to failure mechanisms of different types and patterns of slope of any geometry.

The typical result of a permanent displacement analysis made with the method proposed by Newmark (1965) is shown in Figure 1.2.

The use of this approach allows to overcome many of the limitations imposed by the pseudo-static analysis. In this case, it is taken into account the entire history of seismic loading, to which the slope is subject, overcoming the problem, typical of a pseudo-static approach, of choosing a suitable value of the acceleration for the analyses.

Furthermore, as will be shown later, the generality which characterizes the displacement method allows appropriate changes oriented to examine the effects that the local seismic amplification phenomena can have on the seismic response and the effects of the cyclic behavior of soils.

Hypotheses of the method

The approach proposed by Newmark (1965) for the evaluation of permanent displacements presents a number of hypotheses that characterize the traditional application and that, therefore, must be analyzed in detail; the main hypotheses can be summarized as follows:

- the use of acceleration time histories evaluated by dynamic analyses of the seismic response, made without considering the effects of flows associated with the onset of permanent displacements, implies that the response of the considered structure and the onset of permanent displacements are two processes independent or uncoupled;
- the evaluation of permanent displacements, made by assuming that the critical acceleration of the slope has a constant value over time, implies not to consider

the phenomena of variation of the shear strength of soils that typically can characterized their response to cyclic stresses;

- the evaluation of displacements is usually carried out assuming that these can be accumulated only in the downhill direction of motion.

The hypothesis that the potential unstable soil mass behaves as a rigid body involves two remarkable simplifications of the problem. In a rigid body all points move the same way and the body motion can be described by referring to the center of the masses. The hypothesis that the body is rigid also allows to assume that the inertial action, which the body is subjected, is directly proportional to the seismic acceleration imposed on the ground. This allows to execute the analyses of displacements by directly using the time histories of accelerations from accelerometer recordings, rather than stories of accelerations measured by dynamic analysis of the seismic response of the structure under consideration. In fact, the accelerations, which a slope is subjected during an earthquake, vary from area to area of the slope in relation to the manner in which the seismic response of the structure occurs. Therefore, the motion to which different areas of the slope are subjected depends on geometry and stiffness characteristics of the structure, but also by the amplitude and frequency content of the imposed seismic motion. In general, in a structure on earth consisting of very rigid soils or subject to seismic forcing characterized by low values of fundamental frequencies, the displacements of different parts of the structure are in phase with each other. Conversely, in structures consisting of very deformable soil or subjected to seismic forcing characterized by higher fundamental frequencies, the motion of different parts of the structure may not be in phase. The assumption of rigid body totally neglects these aspects.

Simplified methodologies for assessing the effects of amplification of the seismic responses on the extent of permanent displacements, without the need of dynamic analyses of the response and maintaining the assumption of rigid body, have been proposed by Crespellani et al. (1994), with reference to the limit equilibrium analysis, and by Chen and Liu (1990), using the limit analysis.

The displacement analysis is often performed by using stories of seismic accelerations obtained from analyses of seismic response carried out by assuming that, in the structure examined, does not happen any sliding associated with the onset of permanent displacements. This process, usually indicated as an uncoupled analysis, implicitly assumes that the response of the slope or structure and the permanent deformations that it can be subjected to are two different processes and do not interact with each other. Several authors have examined this extremely tricky aspect of the displacement method.

Lin & Whitman (1983), using a model with more degrees of freedom consisting of a set of concentrated masses connected by elastic springs and viscous dampers, have studied the seismic response of earth dams. The model predicts the possible presence of an element that allows the horizontal sliding to simulate the presence of a sliding surface in

the soil mass. The position of this element in the proposed model allows to schematize shallow, intermediate or deep phenomena of sliding. The possible absence of the element can, however, analyze the uncoupled response of the structure. Using both harmonic forcing and artificial accelerograms and performing displacement analyses, using the histories of accelerations obtained from both types of analyses, the authors observe that the approach that uses the results of the uncoupled analyses provides, in general, conservative results. The displacements, in this case, are always longer than those obtained by coupled analysis and the difference is maximum for seismic forcing with a predominant period close to the fundamental period of the structure on earth. The difference between the results of these two types of analyses depends on the type of sliding considered in the model and in particular for surface sliding is negligible, is approximately 20% for sliding of intermediate depth and it is finally equal to 100% for deep sliding.

Gazetas & Uddin (1994) have studied the problem using a two-dimensional dynamic analysis, performed with the finite element method, taking into consideration the presence of elements that allow the plastic flow of the soil. Even in this case the presence or not of such elements allows to evaluate the response coupled or uncoupled of the structure. The displacement method is applied using the histories of the accelerations obtained from both types of analyses. The authors observe that the assumption of uncoupled analysis does not significantly affect the amount of permanent displacements in the case of forcing with predominant frequencies far from the values of the fundamental frequencies of the structure. Only in the case of seismic forcing with a predominant period close to the fundamental period of the structure, uncoupled analysis provides values of the displacement more conservative of approximately 100%.

Kramer & Smith (1997), finally, have developed an approach involving the use of a model with two or more degrees of freedom that takes into account the deformability of the system and the potential sliding that may occur along a surface. Again, the slope is modeled as a set of masses connected by elastic springs and viscous dampers. The results of the study show that, for instability that involve shallow or very rigid sliding surfaces, the effect of soil deformation is practically negligible and evaluations of permanent displacements, made using the results of uncoupled analysis of the seismic response, are generally precautionary. For instability involving very deformable soil or very deep sliding surfaces, neglecting the effect of the real deformation of the soil is, however, precautionary; the permanent displacements, in this case, are overstimated of approximately 100%. The results of a response analysis of the uncoupled type may, however, not be on the safe side for structures made of very deformable materials such as municipal solid waste landfills. In this case, the permanent displacements may be underestimated by a factor of about 1.5. With regard to the influence of the frequency content of seismic forcing the conclusions of Kramer & Smith (1997) are similar to those of Gazetas and Uddin (1994) and Lin and Whitman (1983).

These indications, together with other reported in literature (Chopra and Zhang, 1991; Rathje and Bray, 1998), allow to assert that, overall, the use of an uncoupled approach leads to results anyway precautionary because it concerns the evaluation of induced permanent displacements.

The definition provided by Newmark (1965) implies that the critical acceleration value is strictly dependent on the shear strength of the available soil, under seismic conditions, along the potential sliding surface examined. Because the soils subjected to cyclic loading histories may experience changes in shear strength, quite generally, it is not permissible to assume that the critical acceleration of the slope will remain constant over the time and the displacement analyses should be made taking into consideration this change. Although this aspect has been neglected for a long time and although the assumption of a critical value of the acceleration is traditionally associated with the Newmark method (1965), it should be noted that the same author underlines the importance of a careful analysis of the possible dynamic behavior of the soil in assessing the critical acceleration of the slope:

"In the determination of the value of sliding resistance the dynamic properties of the material must be considered. This involves the dynamic effects on the pore-water pressure, and the effect of the motion or shearing strain itself on the volume change and the pore pressure change. "

If the cyclic behavior of the soil is such as to cause a reduction in shear strength, the critical acceleration of the slope is reduced consequently; a displacement analysis that does not take into account this aspect can provide unreliable and, above all, not precautionary assessments of the seismic stability conditions and of the post-seismic functionality of the structure. Newmark (1965) has clearly demonstrated the need to take into account the effects that, on the seismic response of a slope, can have the cyclic behavior of soils, highlighting the possibility of phenomena of collapse that would not have occurred in the absence of changes in shear strength of soil:

"However, at some localities, natural soil strata are encountered which can lose part or almost all their shearing resistance under shock conditions, either because of increased hydrostatic pressing or owing to loss in shearing strength from even slight remoulding. Under such conditions, major failures can occur, and have occurred in embankments or under the foundations of dams which otherwise would not have suffered difficulties ".

In some studies, in literature, the permanent displacement analysis is performed taking into account some of the aspects that may characterize the cyclic behavior of soils.

The approach traditionally followed (Sarma, 1975; Hadj-Hamou and Kavazanjian 1985; Crespellani et al., 1990; Dobry & Baziar, 1991, 1992; Dobry et al., 1992), rather than carry out displacement analyses assuming a critical value of acceleration variable over time, examines a constant value over time but determined taking into account the effects of the

reduction in shear strength of soil. In case of phenomena considering a reduction in shear strength, displacement analyses of this kind are certainly cautionary.

In relation, however, at the way in which there is a variation in time of the critical acceleration and in relation at the way in which there is a reduction in shear strength of the soil, this approach may be too precautionary. This is shown by studies in which the permanent displacement analysis is performed considering a change in critical acceleration over time that reflect the ways in which the reduction in shear strength of the soil occurs (Williams and Dent, 1986; Lemos and Coelho, 1991; Crespellani et al., 1992, 1996; Tika-Vassilikos et al., 1993; Lemos et al., 1994; Cascone et al., 1998). Therefore, a more reliable prediction of permanent displacements can be done by examining the ways in which the reduction of shear strength of soil occurs and evaluating, as a consequence, the ways in which there is a variation in the time of the critical acceleration of slope.

The hypothesis that the displacements of slope accumulate only in the downhill direction is made in view of the fact that the critical acceleration value relative to the upward motion is so large that it can be hardly exceeded during a seismic event. This consideration may be valid, in general, with reference to soils that, under conditions of cyclic loading, do not show an appreciable reduction in shear strength. Otherwise, this hypothesis, still precautionary, can not be verified. In this case, the displacement analysis should be made without excluding a priori the possibility of an accumulation of displacements even in the uphill direction of motion. Analysis of this type have been proposed by Matasovic et al. (1998) for the evaluation of the stability conditions of the covers made in municipal solid waste landfills.

Validation of the method

The reliability of the results provided by the displacement method is related to different factors and has often been analyzed in the literature.

In general, the prediction of the displacement that this approach provides is, obviously, related to the accuracy with which the history of seismic accelerations used has been chosen and the manner in which the possible effects of the cyclic behavior of soils has been schematized. The studies in this regard (Ambraseys and Sarma, 1967; Ambraseys, 1972; Sarma, 1974, 1979, 1981; Franklin & Chang, 1977; Gazetas et al., 1981; Wilson and Keefer, 1984; Ambraseys & Menu, 1988) generally agree that the forecasts provided by the displacement method can be considered reliable if the destabilizing actions, induced by the earthquake on the potential unstable mass, and the shear strength actually available, under seismic conditions, along the potential sliding surface were properly evaluated.

In literature a number of studies that have validated the use of the displacement method in forecasting through experimental analyses on scale models (Goodman and Seed, 1966; Weekes and Wang, 2001) are also present. Other authors (Tanaka, 1982; Wilson and

Keefer, 1983; Jibson and Keefer, 1993; Rathje and Bray, 1998), however, have verified the reliability of the forecasts provided by the displacement method using back-analysis and in situ observations of instability occurred during recent earthquakes. For these reasons the displacement method is now considered an effective alternative to complex dynamic analyses. Eurocode 8 (2002) and CR4 (CR4 ISSMGE, 1999), for example, involve the use of this method to perform the seismic stability analyses of slopes.

Critical value of displacement

With regard to slopes consisting in soils potentially subject to variations of the shear strength, the displacement method was used for a long time without considering any form of critical acceleration reduction for the slope.

In this case, the forecasts provided by the method are unreliable because the analysis is performed by considering only the inertial effect and neglecting the effect of the reduction of shear strength of soil that can contribute, also in a significant way, to the induced deformation. The uncertainty on the evaluation of permanent displacements is, however, linked to the entity of the resistance reduction shown by the soil during the cyclic loading history. A priori we can not, therefore, know the extent of the error that was made analyzing, with a traditional approach, a deformation phenomenon that, at least potentially, can be caused by the only effect of reducing the shear strength (inertial instability) or may, in case, be of dual nature (inertial-weackening instability).

With regard to this problem some authors have shown that the application of the displacement method, made without examining any form of reduction in shear strength of the soil, may be considered significant only if the values of the evaluated permanent displacements are lower than a threshold value defined critical displacement. This parameter has found different definitions in literature; in general, we refer to it as a threshold value of the permanent displacement above which it is reasonable to assume that in the masses of soil affected by the instability phenomenon wake up deformations of entity such that to configure a significant reduction in shear strength.

In these conditions can manifest phenomena of complete collapse of the slopes that are not predictable with an approach that does not take into account the effects of reduction in shear strength of soil. In this respect a critical value of the displacement can, therefore, to establish the validity range of a traditional approach or of a displacement analysis performed neglecting the effects of the reduction of soil shear strength.

If the value of the permanent displacement, evaluated with a traditional approach, exceed the critical threshold, some authors (Jibson, 1993; Jibson and Keefer, 1993; Romeo, 2000) suggest to perform an analysis of static stability of the slope related to post-earthquake conditions using values of the parameters of the shear strength appropriately reduced or valued with reference to the residual conditions which the soil may reach in presence of large deformations.

The evaluation of a critical value of the displacement, for the meaning given to this parameter, it is very complex. In general (Jibson, 1993; Romeo, 2000), very deformable soils can experience very large deformations without necessarily reaching a state of collapse; soils with a softening behaviour can support lower displacements and cause, therefore, sudden and rapid phenomena of collapse of slopes. The choice of a critical threshold of displacement also requires the knowledge of the cyclic behavior of materials, forming the potentially unstable soil mass, and the assessment of the deformation levels, beyond which is acceptable to assume that the shear strength of the soil has been subjected to decreasing no more negligible.

The indications given in literature are very limited, confirming the complexity of this evaluation. Wieczorek et al. (1985), for example, with reference to the phenomena of collapse of slopes occurred during the earthquake in San Mateo County (California), have defined a critical value of the displacement of 5 cm. Keefer and Wilson (1989) have instead used a value of 10 cm as a critical threshold of displacement relative to the phenomena of collapse that occurred in California and classified by the same authors as sliding and slip without weathering of the landslide mass (coherent slides) occurred in slopes very or moderately acclive and characterized by rapid and deep movements. Jibson and Keefer (1993), finally, have used the range 5-10 cm as the critical threshold for permanent displacement caused by some instability phenomena occurring in the Mississippi Valley.

Admissible value of the displacement

Using the displacement method, an assessment of the effects that an earthquake can cause on a slope or on a structure on earth can be expressed by comparing the displacement value calculated and a value considered to be admissible. This type of analysis can be arranged, then, as part of a geotechnical design at the limit states.

In this regard, the Eurocode 8 (2002) defines a limit state for a natural slope or a structure on earth as the state to whom is owing permanent displacements of the mass of soil that are unacceptable in a depth of significant interest for the structures on the slope or for those located in the vicinity:

"A verification of ground stability shall be carried out for structures to be erected on or near natural or artificial slopes, in order to ensure that the safety and / or serviceability of the structures is preserved under the design earthquake. Under earthquake loading conditions, the limit state for slopes is defined as that associated with unacceptable large permanent displacement of the soil mass within a depth which is significant both for the structural and functional effects on the structures."

The definition of an admissible value of the displacement must therefore be made taking into account the characteristics of the slope or structure on earth examined and the extent of the damage potentially caused in relation to the features and functionality of structures

that are located in the slope or structures that may be potentially affected by the instability phenomenon.

For the definition of an admissible threshold of displacement must be, therefore, analyzed the effects that the permanent displacement may have on the possible loss of functionality, on the possible loss of human lives, on cost and time to restart the operativeness of the structure and the importance that the condition of temporary non-exercise of the structure has on the economic and social life of the region in which it is located. The complexity of the problem means that, even at the international level, the normative indications to that effect are extremely lacking; in most cases, therefore, the opinion on the admissibility or not of a displacement value is left to the experience. In this regard may, however, be useful the few evidences found in the scientific literature.

Hynes-Griffin and Franklin (1984), recommend a maximum value of 100 cm as the value of the displacement can be tolerated by a dam on earth without that his integrity has been completely compromised, but for which the dam results significantly damaged. Cascone and Rampello (2002), with reference to the dam Marana Capaciotti (Foggia), establish a permissible value of the displacement of 50 cm equal to approximately one-fifth of the franco of the dam. Wilson and Keefer (1985) have carried out a microzonation of some sites in California assuming that for the building structures present in this area the functionality was not compromised for values of maximum induced displacement approximately of 2 cm for slopes composed of coherent soils with a translational failure mechanism and equal to about 10 cm for rocky slopes with complex structure. Legg et al. (1982),on the base of observation of the functionality of structures located on slopes that have experienced different displacements after some earthquakes, have suggested the correlation between values of the induced displacement and produced damage as given in Table 1.6. Idriss (1985), finally, shows the values of the admissible displacement fixed by the Alaska Geotechnical Evaluation Criteria Committee (Table 1.2).

Dynamic analysis

The dynamic analysis of the seismic response is probably one of the most complete and comprehensive approach to carry out a through analysis of the performance of soil structure subjected to seismic loading.

It allows to analyze the behaviour of a structure on earth or a natural slope minimizing the approximations which, however, characterize other methods of analysis. The dynamic analysis, in fact, using constitutive models more or less complex and of more or less immediate practical application and examining the problem without resorting to the artificial separation of stress aspects from those deformative, allows to evaluate the response in time of a structure to a given seismic input. In practical applications the dynamic analysis is performed by means of codes that solve the problem by different numerical approaches, the most common of which are the method of finite differences and finite element method. The typical result of an analysis conducted with these methods is the distribution, in time and space, of the stress and deformation state induced by the seismic event in the structure considered. In the context of dynamic analysis methods can be distinguish different approaches that take into account, more or less reliable, the complex cyclic behaviour of soils, the dynamic interaction between the fluid phase and solid phase and how perform the analysis of seismic response in one-dimensional, two-dimensional or three-dimensional field. The reliability of the result of a dynamic analysis is, in general, highly dependent on the degree of knowledge of the nature and dynamic behaviour of the soils and the reliability with which you have checked the history of seismic accelerations used for the analyses.

Complex and accurate modelling of the problem is possible by means of codes appropriately developed; often, however, the constitutive models implemented in these codes make use of parameters of difficult experimentally evaluation or, even, empty of physical meaning.

The displacements-based approach appears to provide a compromise between the simplistic pseudo-static approach, which produces a single factor of safety as the only safety factor, and the more comprehensive finite element method of analysis, which produces detailed performance data but whose implementation requires a high level of sophistication in selection of material properties, constitutive laws, and mesh discretization. From a practical point of view, the displacement-based approach offers the advantage of giving a rapid and yet quantitative assessment of the movement of earth structures under seismic loading. The practical value of a displacement-based analysis is that if predicted deformations are significant, a more refined method is warranted to further analyze the performance of the considered soil structure.

In this paper will be used a finite differences code, called VIBRAZIONE. The results are then compared with those obtained using the Newmark method.

Solutions and procedures for the instability analyses

For the evaluation of seismic stability conditions and post-seismic functionality of structures on earth and slopes, in literature there are many solutions and calculation procedures, some of which allow to take into account the effects that the cyclic behaviour of soils may have on the seismic response.

Deformation phenomena of inertial nature

The stability analyses related to mainly inertial phenomena that are traditionally dealt using all three approaches described in Section 1.3.

The pseudo-static analysis has been, and still is, widely used mainly for practical purposes. About the reliability of the results provided by this approach to the problem has been discussed previously by highlighting how, in general, the use of this method is acceptable only in cases in which the seismic response of the structure under consideration is not significantly influenced by the cyclic behaviour of constitutive soils.

Dynamic analyses has been carried out since the 70s using finite element codes developed primarily by the school of Berkeley, in particular, the traditional approaches followed for the dynamic analyses are the equivalent linear method and the effective dynamic analysis in the time domain.

With regard to analysis by displacement method, in literature there are many applications made using the traditional approach proposed by Newmark (1965). Revisions and modifications to the original approach have been proposed by several authors to make it applicable to different patterns of slope and to perform the analysis both in terms of effective stress and of total stress.

In literature, moreover, numerous empirical solutions have been proposed based on the use of statistical relationships and / or abaci obtained by regression analysis of permanent displacement measured by applying the method to a more or less extensive series of histories of seismic accelerations and referring to different patterns of slope (Newmark, 1965; Ambraseys, 1972; Sarma, 1975; Franklin and Chang, 1977; Makdisi and Seed, 1978; Sarma, 1979, 1981; Lin and Whitman, 1986; Ambraseys and Menu, 1988; Yegian et al., 1991; Jibson, 1993; Srbulov and Ambraseys, 1994; Simonelli and Viggiani, 1995; Cai and Bathurst, 1996; Count and Rizzo, 1996; Madiais and Vannucchi, 1997; Crespellani et al., 1998; Jibson et al., 1998; Romeo, 1998; Pergalani and Luzi, 2000; Romeo, 2000).

Deformation phenomena caused by increases in interstitial pressure

The stability analyses related to the phenomena induced by the reduction of soil shear strength (deformation failure) are aimed at assessing the entity of the potential permanent displacement induced by the seismic event. In literature are available different solutions in part empirical and in part referable to the displacement method.

The empirical solutions have been developed in an attempt to correlate some parameters, that describe the characteristics of the slope and those of the seismic motion, to permanent displacement values measured in situ as a result of damage caused by seismic activity (Hamada et al., 1986; Youd and Perkins, 1987; Bartlett and Youd, 1992, 1995; Rauch, 1997) or measured in lab during test on scale models (Towata et al., 1992), the approaches used to develop predictive models are usually of statistical nature.

Solutions related to the displacement method, however, was obtained in part through energetic approaches (Byrne, 1991) and in part in the attempt to modify the original model proposed by Newmark (1965) in order to take into account the effects of reduction in shear strength of the slope on the response in terms of cumulative displacements.

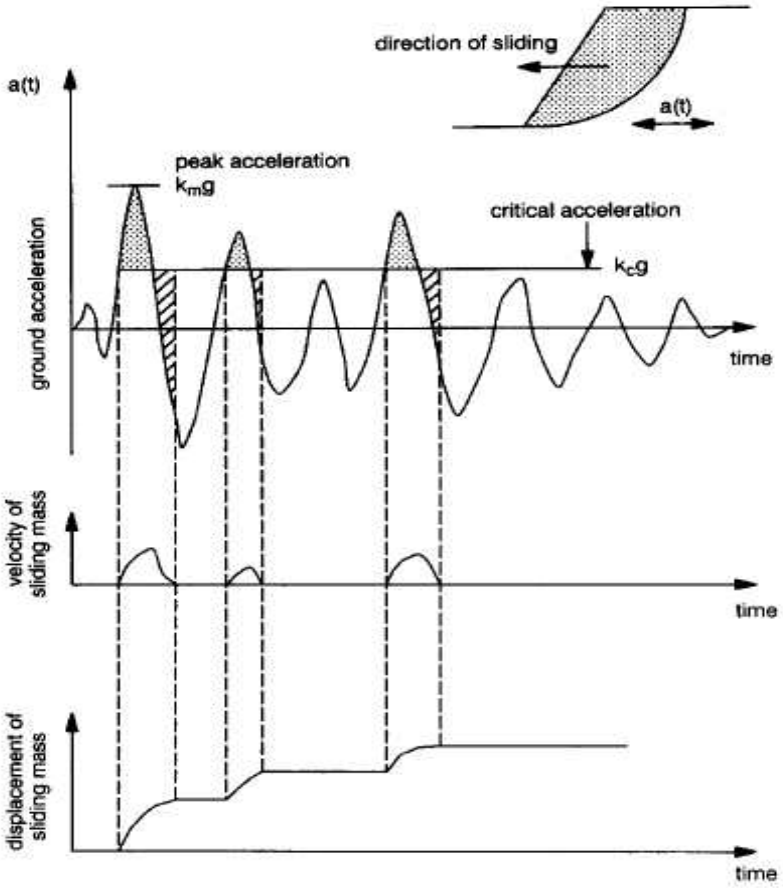

Fig. 1. Illustration of Newmark's sliding block method to calculate permanent displacement of earth structures (unsymmetrical displacement).

Figure 1.1: Illustration of Newmark's sliding block method to calculate permanent displacement of earth structures (unsymmetrical displacement). (Cay and Bathurst, 1996).

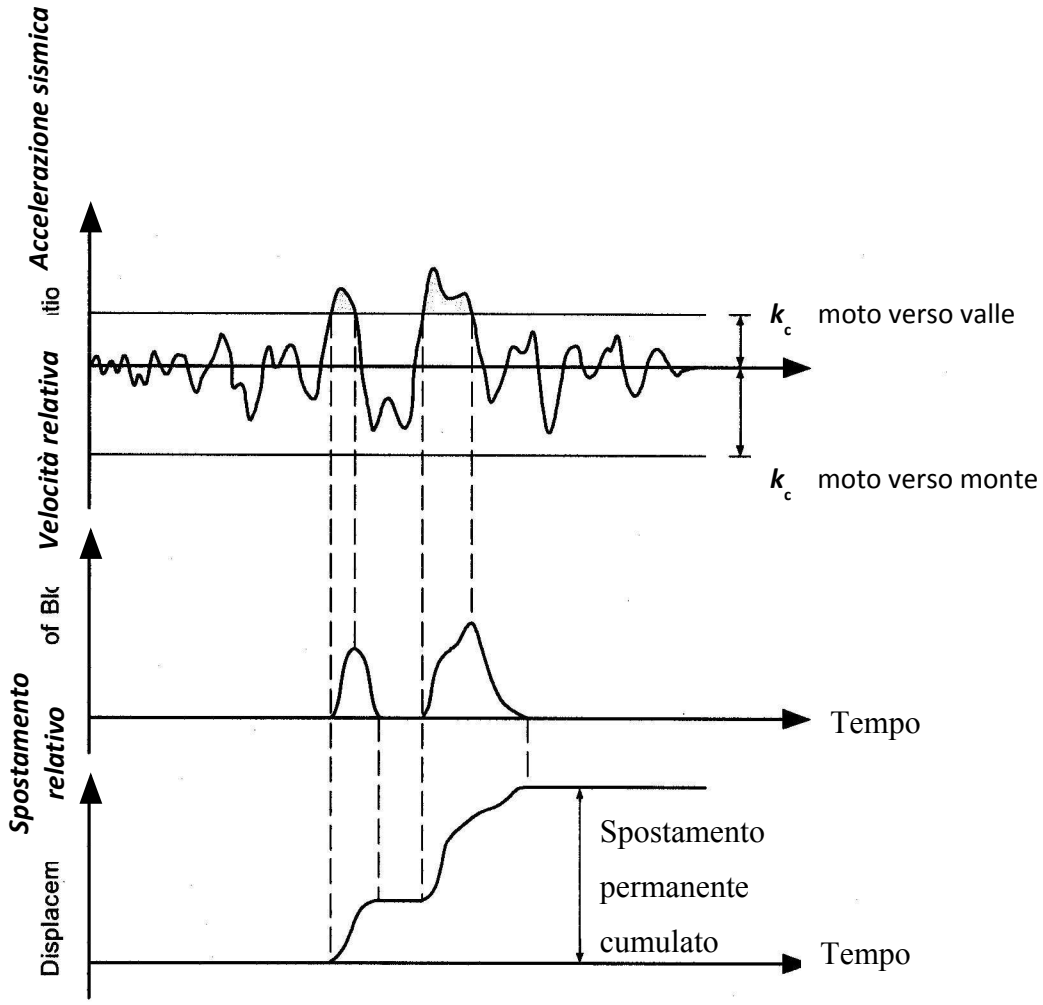

Fig. 1.2: Tipico risultato di una analisi degli spostamenti permanenti effettuata con il metodo proposto da Newmark (1965) (adattata da Wilson & Keefer, 1985).

Table 1.1: Casi documentati di crolli di pendii e strutture in terra.

Earthquake	Struttura e caratteristiche			Effetto	Fonte
Santa Barbara (1925) M=6.3	Sheffield dam	k_H=0.10	F_d=1.2	Collasso per liquefazione	Seed (1979 b)
San Fernando (1971) M_w=6.6	San Fernando dam (Lower)	k_H=0.15	F_d=1.3	Collasso per liquefazione	Seed (1979 b)
San Fernando (1971) M_w=6.6	San Fernando dam (Upper)	k_H=0.15	F_d=2÷2.5	Collasso per liquefazione d≈180cm	Seed (1979 b)
-	Tailing Dam (Japan)	k_H=0.20	F_d≈1.3	Collasso per riduzione di resistenza al taglio	Seed (1979 b)
Kozani-Grevena (1995) M_s=6	Embankment of Rimino bridge	k_c°=0.325		Collasso per effetto inerziale e per riduzione di resistenza al taglio d_H=0.8-2m	Tika & Pitilakis (1999)
Hokkaido-Nansei-Ohi (1994)	Embankment	"*sufficient resistance against seismic inertia forces*"		Collasso per riduzione di resistenza al taglio e per effetto inerziale	Towhata & Mizutani (1999)
Kushiro-Oki (1993) M_{JMA}=7.8	Argine sinistro del fiume Kushiro	H = 6.5m ,	β_{av}=17°	Collasso per liquefazione c≈ 2-3m	Finn (1999)
Kushiro-Oki (1993) M_{JMA}=7.8 k_{max}=0.5	Rilevato in prossimità dell'aeroporto di Kushiro	H = 65m Δu^*_{max} =0.2	β_{av} =22°	Spostamenti al piede per riduzione di resistenza al taglio e per effetto inerziale d_V=2÷4 cm d_H =10 cm	Iai *et al.* (1999)
Aegion (1995) M_S=6.2 k_{max}≥0.29	Linea di costa di Eratini (Golfo di Corinto)	β_{av}=9.6° k_c°=0.38	F_s=3.3	Collasso per effetto inerziale	Bouckovalas *et al.* (1998)
Aegion (1995) M_S=6.2 k_{max}≥0.29	Linea di costa di Eratini (Golfo di Corinto)	β_{av}=6.8° k_c°=0.11	F_s =2.0	Collasso per effetto inerziale e per riduzione di resistenza al taglio	Bouckovalas *et al.* (1998)
Aegion (1995) M_S=6.2 k_{max}≥0.29	Linea di costa di Eratini (Golfo di Corinto)	β_{av}=6.8° k_c°=0.17	F_s =2.5	Collasso per effetto inerziale e per riduzione di resistenza al taglio	Bouckovalas *et al.* (1998)
Aegion (1995) M_S=6.2 k_{max}≥0.29	Linea di costa di Eratini (Golfo di Corinto)	β_{av}=10.2° k_c°=0.09	F_s =1.5	Collasso per effetto inerziale e per riduzione di resistenza al taglio	Bouckovalas *et al.* (1998)

Legenda:

F_d:	Fattore di sicurezza valutato con il metodo pseudo-statico in corrispondenza di un valore k_H·g dell'accelerazione sismica
k_{max}:	Valore massimo dell'accelerazione sismica imposta espresso come frazione dell'accelerazione di gravità
k_c°:	Valore dell'accelerazione critica determinato senza tenere conto della riduzione di resistenza al taglio del terreno
d, d_H, d_V:	Valori dello spostamento (d) e delle sue due componenti (d_H, d_V) indotto dall'evento sismico
H , β_{av}:	Valori medi dell'altezza e della pendenza dei pendii o delle strutture esaminate
F_S:	Fattore di sicurezza statico
Δu^*_{max}:	Valore dell'incremento di pressione interstiziale indotto normalizzato rispetto alla tensione verticale efficace

Table 1.2: Admissible displacement values by *Alaska Geotechnical Evaluation Criteria Committee* (Idriss, 1985).

Classe	Damage	Displacement (cm)
I	modesto	<3
II	medium	15
III	high	30
IV	very high	90
V	Catastrofico	300

CHAPTER 2: CONSTITUTIVE MODELLING OF SAND

State of the art

In the last years much of the Geotechnical research, developed at the Structural Engineering Department of Politecnico of Milan on soil mechanics, has been devoted to laboratory experiments and modelling of the mechanical behaviour of sands, with the aim of reproducing the observed mechanical behaviour along very different loading paths by means of a unique constitutive model. This is very complex since it depends on numerous factors such as:

- both previous loading history and the initial stress state;
- presence of interstitial liquid phase;
- type of applied load paths (monotonic, cyclic, etc.).
- load application rate.

The combination of all these aspects determines the enormous variability that can be found on site and that only by means of laboratory tests can be carefully studied: the strong nonlinearity of the mechanical behaviour, the irreversibilities, the deviatoric-volumetric interaction typical of granular soils, the hysteresis under loading cycles, possible instability (liquefaction) in presence of water, viscosity, etc.. All these phenomena are strongly dependent on the stress state and relative density, whereby traditionally it is possible to distinguish between loose sand (low D_R), and dense sand (high D_R), passing through out intermediate states (medium dense sand). Sands belonging to these two different categories are quite different, especially in terms of volumetric behaviour, also responsible of the manner of collapse.

However, the granular nature of the material considered suggests to be unsuitable a rigid classification of the two categories: depending upon the imposed stress paths, for example, a dense sand may present dilatancy such that to make it more like a loose sand, at the end of the process, for the next loading paths, and vice versa for a loose sand that compacts. The possibility for the same material to change mechanical properties has important implications, especially in cyclic dynamics where the seismic stresses applied locally determine a continuous alternation of contractive and dilatant phases.

Several years needed to arrive at constitutive formulations able to reproduce such a variety of phenomenological aspects, though still the research on this topic cannot be considered to be completed.

The ambition to describe so many phenomena by means of a single formulation leads necessarily to a complex and onerous (to be calibrated) models; add to this the inherent difficulty in obtaining in-situ, with simple techniques, undisturbed sand samples for

laboratory tests. The commitment required by the theoretical understanding and parametric identification of these constitutive models still makes their use very difficult in routine professional applications, also because they are not currently used by even the most common commercial codes.

Nearly all constitutive models used until recently in seismology for predicting ground motion induced by earthquakes have been based on the assumption of linear viscoelastic behaviour for the soil.

Only few authors, in recent times, have shown the capabilities of taking into account nonlinear soil behaviour in parallel finite element codes for large-scale applications (Xu et al., 2003).

As was emphasized by Xu et al. (2003), this lack of numerical tools capable of solving solid dynamic problems in nonlinear field is basically due to three main factors:

1) for years nonlinear soil amplification has been routinely taken into account in geotechnical engineering practice by employing nonlinear elasticity (Seed et al., 1969);

2) the lack of satisfying constitutive models capable of capturing time rate dependence in the nonlinear field;

3) the scarce evidence of nonlinear effects in the observed motion, other than liquefaction.

However in the last decades, the viscoplastic constitutive approach has grown significantly in importance among the solid dynamic scientific community, thanks to the effort devoted by many authors. This approach seems to be very promising in order to study accurately nonlinear propagation phenomena with numerical schemes based on explicit time advancing discretization. Concerning the third issue, a large number of accelerograms has been recorded during strong earthquakes that have made possible to infer nonlinear response of soli, like reduction in shear wave velocity and change in soil damping with increasing loads (Hardin et al., 1972).

It is worth noting that the non-local viscoplastic constitutive model is conceived to take into account both the characteristic time and the spatial characteristic length of the granular assembly, since, according to the authors, the superimposition of the two effects is misleading.

The model implemented in the code, employed for the numerical analyses in this paper, is based on the elastoplastic at anisotropic strain hardening developed by di Prisco (1993), that was born as a development and generalization of the simpler “Sinfonietta Classica” by Nova (1998).

In the following a more detailed description of this constitutive rule is reported.

Elastic behaviour

Experimental results indicate that the elastic properties are function of the soil element, i.e. they may expressed in terms of the soil density (or void ratio) and the stress acting on the soil. For a given void ratio, the elastic properties have been shown to vary with the mean normal stress as well as the deviatoric stress.

Soils behaviour in unloading-reloading is by no means perfectly elastic: hysteresis and ratcheting, observed in cyclic tests, are evident signs of the occurrence of irrecoverable strains even in this region.

Therefore it is necessary the use of a non-linear elastic law, and neglecting cyclic loads in small strains, the hypothesis of the elastic domain conservation may be accepted and a hyperelastic potential may be assumed.

For characterizing a non-linear hyperelastic rule, a different function *W*, elastic potential, defined in the stress hyperspace, must be introduced:

$$W = W(\sigma_{ij}) \tag{2.1}$$

from which:

$$\varepsilon_{ij}^{e} = \partial W / \partial \sigma_{ij} \tag{2.2}$$

and

$$\dot{\varepsilon}_{ij}^{e} = \partial W^{2} / \partial \sigma_{ij} \partial \sigma_{hk} \dot{\sigma}_{hk} \tag{2.3}$$

The elastic potential is defined in suitable way introducing some simple hypotheses, as the assumption that the elastic behaviour is isotropic and the ratio R'=G/K is constant (where K indicates the bulk modulus, while G the shear modulus). The same hypotheses have been assumed in the recently hyperelastic models of Lade and Nelson (1987).

All details concerning the model implemented are reported in Lade-Nelson (1998).

The plastic potential is so defined:

$$W = X^{1-\lambda} / (18 B_0 (1-\lambda)) \tag{2.4}$$

where B_0 and λ are two constants characteristic of the material, while X is obtained by:

$$X = I_1^2 + R^* (\sqrt{J_2^{'}})^2 \tag{2.5}$$

So the constitutive elastic parameters are three: B_0, R^*, λ.

$\dot{\varepsilon}_{ij}^{el}$ is defined by starting from the definition of an elastic potential (Lade and Nelson, 1987) from which the elastic incremental compliance matrix C_{ijhk}^{el} can be derived.

Such law can capture the intrinsic non linearity of the behaviour in unloading - reloading, but its major disadvantage is in considering isotropic the behaviour of the material.

The hypothesis violates the experimental evidence, since the acquired anisotropic structure plays a role even within the elastic domain.

The compliance matrix is defined as:

$$C_{ijhk}^{el} = \frac{\partial^2 W}{\partial \sigma_{ij} \partial \sigma_{hk}} = \frac{\left(\frac{1}{3} - R_F\right)\frac{\delta_{ij}\delta_{hk}}{3} + \frac{R_F}{2}\left(\delta_{ih}\delta_{jk} + \delta_{ik}\delta_{jh}\right)}{B_R} - 2B_1 \frac{\left(\frac{p'}{3}\delta_{ij} + R_F s_{ij}\right)\left(\frac{p'}{3}\delta_{hk} + R_F s_{hk}\right)}{B^2} \tag{2.6}$$

where:

δ_{ij} is the Kronecker's delta;

p' is the effective mean pressure;

s_{ij} is the deviatoric tensor of stress;

$B = B_R (p'^2 + R_F J_2)^{\lambda}$ with J_2 second invariant of s_{ij};

$B_1 = B_R (p'^2 + R_F J_2)^{\lambda - 1}$;

with B_R, R_F and λ elastic constitutive parameters.

The non linearity of the law is determined by the second term of eq. 2.6 in which, by means of the parameter λ, it is possible to govern the dependence of compliances by the stress state.

The Lade and Nelson's model can be reduced to Hooke's law with appropriate choice of parameters, thus reducing to the case of linear elasticity. It is enough to inhibit the non-linearity imposing $\lambda = 0$ and then to determine by comparison the law between the B_R and R_F parameters and the usual engineering constants, obtaining:

$$\begin{cases} B_R = \dfrac{E}{3(1-2\nu)} = K \\ R_F = \dfrac{K}{2G} = \dfrac{1+\nu}{3(1-2\nu)} \end{cases} \tag{2.7}$$

Viscoplastic mechanism

The constitutive model implemented is characterized by constitutive parameters depending on the current relative density that has been chosen by the authors.

The viscoplastic mechanism is characterised by a single plastic potential, by a non-associated constitutive relationship, by an anisotropic strain hardening and by a viscoplastic Perzyna's type flow rule.

The model is conceived in small strains; the strain rate tensor $\dot{\varepsilon}_{ij}$ can be defined by the superimposition of an instantaneous elastic strain rate tensor $\dot{\varepsilon}_{ij}^{el}$ and a delayed plastic strain rate tensor $\dot{\varepsilon}_{ij}^{vp}$:

$$\dot{\varepsilon}_{ij} = \dot{\varepsilon}_{ij}^{el} + \dot{\varepsilon}_{ij}^{vp} \tag{2.8}$$

On the contrary, the viscoplastic strain rate tensor depends on the assumptions concerning the flow rule, the constitutive factors, the hidden variables and their hardening rules that will be briefly outlined here in the following.

The flow rule

According to Perzyna (Perzyna P., 1963; Perzyna P., 1966), the viscoplastic strain increment tensor is defined as follows:

$$\dot{\varepsilon}_{ij}^{vp} = \phi(f)\frac{\partial g}{\partial \sigma_{ij}^{'}} \tag{2.9}$$

where *f* is the yield function, *g* the plastic potential, $\phi(f)$ is the viscous nucleus which is generally defined as a function of *f* and $\sigma_{ij}^{'}$ the effective stress rate tensor. The chosen flow rule (Equation 2.9) allows us to introduce the time dependency of the material mechanical response and to avoid the consistency rule.

The yield function *f* may be positive or negative, without any constraint, i.e. the stress state may be external or internal to the yield locus. The plastic potential defines the direction of the viscoplastic strain rate tensor, while the yield function influences its modulus by means of the viscous nucleus ϕ.

The choice of this flow rule (Equation 2.9) derives from the aim of achieving four distinct goals:

- the simulation of the time dependent stable and unstable mechanical behaviour of granular materials during drained and undrained creep tests (Lindenberg and Koning, 1981; di Prisco and Imposimato, 1996);
- to reproduce the dependency on the time factor of the mechanical behaviour of sands when these latter are subject to dynamic actions of large intensity;
- to describe the dependency of the mechanical behaviour on the current relative density. In fact, when the consistency rule is avoided, the updating of constitutive parameters on the relative density becomes very simple (di Prisco et al., 2002);
- to introduce the viscosity for treating the localization problems. Even in this case the definition of the viscous nucleus becomes crucial.

The viscous nucleus definition is crucial in the description of the mechanical response of the material both during creep tests and impulsive and dynamic tests. The numerical analyses described in following have been performed by implementing a particular

nonlinear expression for ϕ, characterized by two different branches that is capable of capturing the time dependency of the mechanical response of the material when the strain rate is small (creep tests) as well as when this latter is very large (fast loading tests):

$$\phi_1 = \bar{\gamma} p^i \exp(\alpha f) \qquad \text{if } f \le f_0 \tag{2.10}$$

$$\phi_2 = \beta p^i \sqrt{\log(\zeta f)} \qquad \text{if } f > f_0$$

in which p' is the effective pressure, $\bar{\gamma}$, α, β, ζ and f_0 are positive constitutive parameters. As is evident from Figure 2.1, the viscous nucleus shape is mainly governed by the dimensionless parameter f_0, by increasing whom the mechanical response of the material, when fast loading are imposed, becomes more rapid and instantaneous, whereas β and ζ are calculated by imposing the continuity of ϕ and of its first derivate term when $f = f_0$. As a consequence they are not independent and do not have to be calibrated. Equation (2.10) implies that even when the effective state of stress is within the yield locus (i.e. when f <0) irreversible strains may take place.

During creep tests, if the imposed load increment sizes are small, the strain rate tensor value are also very small and this implies that, during the evolution of time, the f values are either positive but very small or negative. For this reason, thanks to creep tests (di Prisco et al., 1996) $\bar{\gamma}$ and α can be calibrated. In Figure 2.2 a calibration example in a semi-logarithmic plane is represented: $\bar{\gamma}$ [s^{-1}] is linked to the material characteristic time describing the evolution rate of the material micro-structure, whereas α is a dimensionless parameter influencing the shape of the creep curve.

Only in the last decade, some authors have experimentally considered the dependency of the mechanical behaviour on the loading frequency and showed that the shear modulus depends linearly and not dramatically on loading frequency, while the damping ratio dependency is severe and highly nonlinear. According to di Prisco et al. (2007), the nonlinearity is due to two antagonistic factors: the time dependency of the material mechanical behaviour (dominant at low frequencies) and the dynamic effects associated with high frequencies.

To summarize the cited experimental results in Figure 2.3, the trend of the damping ratio *D* versus the loading frequency is schematically illustrated (together with the theoretical responses that can be obtained by means of viscoplastic, viscoelastic and elasto-hysteretic constitutive models, respectively.

The yield function and the plastic potential

For defining eq. 2.9, the yield locus *f* and the plastic potential *g* must be introduced.

As is described in di Prisco (1993), *f* and *g* depend on the effective state of stress, on a set of hidden variables and on a dimensionless constitutive parameter γ:

$$f = f(\sigma'_{ij}, \chi_{ij}, r_c, \beta_f) \tag{2.11}$$

$$g = g(\sigma'_{ij}, \chi_{ij}) \tag{2.12}$$

χ_{ij} is a state variable tensor which takes in account of the anisotropy induced by the straining process, r_c defines the size of the yield function *f* and is equivalent to the isotropic preconsolidation pressure for an isotropic material, finally β_f controls the yield locus shape. This implies that *f* is not fixed but widens, rotates and changes shape with viscoplastic straining; on the contrary the plastic potential may only rotate.

Figure 2.4 shows as the yield function *f* is centred on the axis directed as χ_{ij} , which is rotated with respect to δ_{ij} .

The stress tensor can be written as

$$\sigma'_{hk} = s^*_{hk} + r\chi_{hk} \tag{2.13}$$

where

$$r = \sigma'_{hk}\chi_{hk} \tag{2.14}$$

As shown in Figure 2.5, in geometric terms, *r* gives the component of the stress vector σ'_{ij} along the axis χ_{ij} in the six-dimensional stress space, while s^*_{hk} gives the orthogonal component of σ'_{ij} ($s^*_{hk}\chi_{hk} = 0$). It is also convenient to define a tensor η^*_{hk} such that:

$$\eta^*_{hk} = \sqrt{3}s^*_{hk} / r \tag{2.15}$$

For an isotropic material, no preferential orientation exists and $\chi_{ij} = \delta_{ij}/\sqrt{3}$ so that $r = p'\sqrt{3}$ where p' is the mean pressure, s^*_{hk} coincides with the classical deviatoric part of σ'_{ij} and $\eta^*_{hk} = s_{hk}/p' = \eta_{hk}$ where η_{hk} is a stress variable. When $\chi_{ij} = \delta_{ij}/\sqrt{3}$ the standard definition used by many authors (Nova et al., 1980; Adachi et al., 1982) for isotropic constitutive models is obtained.

The analytic definition of the yield function *f* (Figure 2.4) is the following:

$$f = 3\beta_f(\gamma - 3)Ln(r/r_c) - \gamma J_{3\eta^*} + 9/4(\gamma - 1)J_{2\eta^*} = 0 \tag{2.16}$$

where γ is the dimensionless constitutive parameter previously cited, while $J_{2\eta^*}$ and $J_{3\eta^*}$ are the second and third invariants of η^*_{hk}:

$$J_{2\eta^*} = \eta^*_{ij}\eta^*_{ji} \tag{2.17}$$

$$J_{3\eta^*} = \eta^*_{ij}\eta^*_{jk}\eta^*_{ki} \tag{2.18}$$

The plastic potential *g* is assumed to be given by an expression similar to that of yield surface:

$$g = 3\beta_g(\gamma - 3)Ln(r/r_c) - \gamma J_{3\eta^*} + 9/4(\gamma - 1)J_{2\eta^*} = 0 \tag{2.19}$$

with the only difference of the parameter β_g. Plastic potential and yield function coincides when $\beta_g = \beta_f$. In general, until now, the parameter β_g has been assumed equal to 3, while β_f is lower than β_g and is a function of the plastic strains, so that the flow rule results to be non-associated.

For each hidden variable an appropriate evolution rule complete of constitutive parameters is introduced. r_c depends on both volumetric and deviatoric plastic strains via three parameters: the volumetric plastic compliance B_p, ξ_c and ξ_e, which are linked to the dilatancy at failure in compression and in extension. r_c is limited from below by r_{c0} which gives the size of an initial nucleus within which the deformations are considered to be elastic. β_f varies between two limits β_{f0} and $\hat{\beta}_f$; t_p rules the rate of its variation. χ_{ij} can vary only within a limit cone, fully characterized by two angles $\hat{\theta}_c$ and $\hat{\theta}_e$ linked in a complex but unique way to the friction angle in compression and in extension. Its rate evolution is governed by parameter c_p.

It is important to underline that in the case of granular materials, as many experimental results show (Oda, 1972; Oda et al., 1978; Cambou and Lanier, 1988), when failure is approached and large irreversible strains take place, internal fabric – i.e. directional microstructure characteristics – does not change any more. This is equivalent to assume that the tensor χ_{ij} reaches asymptotically a limit tensor $\hat{\chi}_{ij}$, which is a function only of the stress state at failure and not of the straining process. As a consequence, the locus of the $\hat{\chi}_{ij}$ may be assumed to be isotropic. In order to identify the limit micro-structure of the material (i.e. to identify the current $\hat{\chi}_{ij}$) towards which the system is evolving, an

incrementally linear mapping rule is conceived. $\hat{\chi}_{ij}$ depends on the current state of stress and on the current anisotropic tensor χ_{ij} .

The constitutive parameters

The elasto-viscoplastic mechanism so far presented is characterised by sixteen parameters: two elastic (E, ν), eleven plastic (γ, r_{c0}, $\hat{\theta}_c$, $\hat{\theta}_e$, ξ_c , ξ_e , t_p , c_p , B_p , β_{f0} , $\hat{\beta}_f$) and three viscous (α, $\bar{\gamma}$ and f_0). The plastic constitutive parameters are calibrated on the basis of the results obtained in one isotropic loading-unloading test, two drained triaxial compression/extension tests and two undrained triaxial compression/extension tests all performed in strain-controlled conditions (Figure 2.6).

In particular, the parameters γ, $\hat{\theta}_c$, $\hat{\theta}_e$, ξ_c , ξ_e are linked to the failure behaviour and are calibrated on the drained triaxial compression and extension tests. B_p , which is the plastic logarithmic volumetric compliance, can be directly established from a loading-unloading isotropic test, while $\hat{\beta}_f$, linked to the yield function shape, can be determined loading the specimen up to failure in triaxial compression and then unloading it. Finally parameters c_p and t_p control the rate of evolution of the yield locus and therefore the stiffness of the material.

The two viscous constitutive parameters α and $\bar{\gamma}$, which describe the system evolution rate, are calibrated on the basis of creep test experimental data (Figure 2.2), while f_0 is imposed equal to 0.2 (Pisanò, 2007).

All the eleven plastic constitutive parameters are assumed to depend on the current relative density D_r (di Prisco et al., 2002). This dependency can be easily introduced when the consistency rule is avoided and it is necessary for capturing the softening regime of dense sands.

Implementation of the constitutive model

The use of the described model enables to establish laws of variation of the constitutive parameters to take into account how the mechanical properties of the same material depends upon the density. For the implementation of the law within the code has therefore proceeded as follows (di Prisco and Imposimato, 1996):

1) was initially carried out laboratory tests on samples of loose (D_R = 20%) and dense (D_R = 90%) sand; 20% and 90% are considered the real physical extremes of the range of variability of the relative density, although its formal definition allows excursions from 0 to 100%. On the base of experimental data obtained, the elastoplastic model is calibrated for the material in the two limit conditions of compaction;

2) the integration procedure step by step of the nonlinear law consider D_R function of the void index and therefore of the volume, like an internal variable. Its value, therefore, is updated after each load step, assuming, for hypothesis that only the irreversible part of the volumetric strain is employed to change it;

3) Identified an evolutive law for D_R and having the two sets of parameters, it must to be choose how to extrapolate to different values of density. The choice carried out was as simple as possible and is the linear interpolation: called x any constitutive parameter and x_S and x_D its values for loose and dense sand, respectively, will in general:

$$x = x_S + \frac{x_D - x_S}{90 - 20}(D_R - 20) \tag{2.20}$$

Thus the numerical analysis always need of an initial value of relative density, from which to get through (2.20) the initial constitutive parameters. This operation is repeated with each update of the relative density.

With regard to a drained compression test on loose sand, it is possible to note how to take account of the evolution of D_R and parameters gives, for high deformations, a change in the volumetric behaviour, consistent with the fact that a loose sand compressed gradually decreases its volume (see Figure 2.7).

With regard to dense sands, however, this effect manifests, on the contrary, with a decrease in dilation as the sample dilates. According to the calculation scheme described, the dilation implies a deterioration of mechanical properties and so the possibility of simulating a softening response (such as the elastoplastic model was not able to do, see Fig. 2.8).

Focusing on what happens under cyclic loading conditions, the simulation of cyclic drained triaxial tests (and asymmetric) of loose sand through the viscous model is shown in Figure 2.9.

Thanks to the established definition of the viscous nucleus, viscoplastic strains can develop also for negative values of *f*, so that the loading-unloading cycles are not perfectly reversible and a slight accumulation of strains (deviatoric and volumetric) is made possible. During undrained cyclic tests this implies a progressive increase in pore pressure and a decrease in the average effective pressure p' (see Figure 2.10).

The model just discussed allows a substantial progress compared with the original at instantaneous plasticity. However, it is not yet fully satisfactory in the description of the cyclic behaviour, fundamental for seismic dynamic applications.

The numerical method

To obtain the solution of the formulated problem a Finite Difference Method has been chosen enchouraged by the availability of a code designed to solve problems of the type under consideration. This program was developed by S. Imposimato in the PhD thesis (1998) and also tested by Pisanò (2007): it was considered advantageous to make use of an existing instrument, at the same time helping to improve it.

The method of finite differences

The finite difference method belongs to the so-called grid-point methods, in which the space-time domain is discretized by means of a grid (regular in the simplest version) and every function is represented through its assessments to the nodes of the grid itself.

The key feature of the method consists of a rewrite of the resolving differential equations, in which the derivatives are replaced and approximated by incremental ratios on finite intervals. The Finite Difference Method is quite simple, versatile and relatively easy to implement, so it is still of widespread use for dynamic problems, in particular for 1D geometries as in the considered case.

To the different algorithms, and in general to any numerical approximation methods, are required the following properties of:

- Consistency, for which the difference between the original differential equation and its approximation to the finite difference must become negligible when the steps of spatial and temporal discretization tend to zero. This property is not inherent to the solution of the problem, but concerns only the quality of the discrete representation of the solving system (and hence the truncation error);
- Stability, defined as the ability to produce a limited numerical solution when the real solution of the problem is limited;

- Convergence, which is satisfied if the numerical solution approximates at best the real solution when the spacing of the grid in time and space tend to zero.

The analytical study of such conditions is usually only achievable for problems of linear elasticity, while we are considering a totally non-linear material: this necessarily requires to proceed with caution in defining the characteristics of the numerical model, in order to avoid that the solution is affected by rough errors and / or excessive approximations.

The calculation program

The calculation code, which often will be referred to as VIBRAZIONE, used for the numerical analyses in this paper makes use at its inside of an explicit solution scheme: the unknown factors in the various nodes of the grid are calculated at a given instant of time, individually and sequentially; an implicit scheme, however, would require a simultaneous resolution by inversion of a matrix at the level of entire grid.

The discretization shown in Figure 2.11 has been used. The crosses represent the places along the coordinate where the velocities in the directions *z* and *x* have been calculated, while the circles represent the points along which the viscoplastic strains, the stresses and the elastic compliance matrix have been evaluated.

This is a staggered formulation in which the velocity components, on the one hand, and stresses, strains and compliances, on the other, have their own dedicated location on the grid.

As for the reformulation at the finite difference of the equations, the approximation rule of the *centred difference* has been used, both in space and time.

After these premises the running of the program can be summarized in the following operation, it:

1) reads the constitutive parameters of the material;

2) opens and associates the names of files that will contain the results;

3) reads the relative initial state for each point;

4) uses, for each point, the associated constitutive law for a path at zero increments of $d\sigma_z$, $d\tau_{zx}$ and deformations with the remaining components of the stress tensor, generating initial velocity and acceleration throughout the layer;

5) for each point and each time instant:

- imposes the velocity vector at the base of the layer;

- calculates the components of the elastic matrix and the viscoplastic variables of the solving system;

- prints the results relative to a chosen time instant;

- solves the finite difference system and determines the velocity vector in the internal points of the slope;

- prints the results related to a certain point;

- obtains from the velocity vector the axial and shear strain increment $d\varepsilon_z$ and $d\gamma_{zx}$, then proceeding, through the constitutive law, to the calculation of the other stress-strain magnitudes and updating the internal variables;

- imposes the condition of free surface;

- updates the velocity and displacement vectors.

The initial state

As is mentioned above, the simulation can not start without the acquisition of the initial state of the system. This necessity occurs whenever step by step non-linear analyses is performed, being essential the information about the history of the system. With reference to geotechnical problems, it is usually necessary to simulate the deposition process: to

conduct in a realistic way this operation, detailed informations about the geological history of the deposit would be necessary.

In the present work that the sand layer is assumed to be deposited, in time, on the substrate: it is as if successive strips, from the bottom, of soil, consisting of identical volume elements, had overlapped in time according to the following stress paths:

$$\dot{\sigma}_z = \gamma \cos\alpha dz, \quad \dot{\tau}_{xz} = \gamma sen\alpha dz, \quad \dot{\varepsilon}_x = \dot{\varepsilon}_y = \dot{\gamma}_{zy} = \dot{\gamma}_{xy} = 0 . \tag{2.21}$$

The two components of stress σ_z and τ_{zx} are isostatic, as a result of the simplification of indefinitely equilibrium due to the symmetries of the problem. In case of horizontal layer (α = 0) this stress path leads to a deposition under edometric conditions.

So the code VIBRAZIONE requires an auxiliary routine (just available) that can provide the initial state of the system. This routine has been realized starting from the basic procedure used to simulate a load path at the level of volume element: the deposition, in fact, has been simulated numerically from top to the bottom, the imposing path (2.21) on a fictitious material point, which return the status whenever tensions σ_z and τ_{zx} correspond to the discretization heights of the deposit.

To simulate the deposition was used the elastoplastic model, assuming that this process has been completed as a long ago to be considered completed the transient describable with the viscoelasticity.

The dampers

In its initial conception the considered problem involves the generation of an input signal at the interface between soil and bedrock, which behaves, when input is completed, like a stiff boundary, in any case ensuring the continuity of the velocity vector in that point. This has the important consequence that the wave is forced throughout the duration inside the layer; indeed during the reflection considering stiff interface there is conservation of energy between incident wave and reflected wave: if it were propagating in perfectly elastic medium (non-dissipative) then you would have an infinite duration of the motion within the system.

In nature, instead a possible bedrock is not normally so much stiffer than the ground above to be modelled as perfectly rigid. Therefore, once the generated input has been reflected on the surface and come back to the starting point, what really happens is that a portion of the energy is transmitted into the rock (refracted wave), while the remaining portion is reflected back into the layer: in this way it is possible to understand how, also with elastic material, the seismic motion is destined to weaken in time.

To simulate this aspect the numerical model should provide a discretization of the entire domain studied (in this case unlimited).

It is used, instead, a particular numerical “trick”, designed by Zienkiewicz et al. (1999), which is summarized below.

The basic principle is, for this one-dimensional case, the introduction of an artificial boundary on which to impose a condition of transparency, capable of allowing to a portion of the kinetic energy to radiate in the half-space rock. This can be done introducing at the interface the viscous dampers characterized by the usual rheological law $\sigma = \eta \dot{u}$: the parameter η should be calibrated by that condition of transparency, i.e. by imposing the continuity of strains between soil and bedrock.

In Figure 2.12 it is shown how dampers work along both directions of the plane, z and x, are required: in fact, despite being generated seismic input of pure shear, the volumetric-shear coupling introduced by the viscoplasticity will spontaneously generate, in any case, a pressure wave, for which will be valid the same observations about reflection in contact with the rock.

The calibration of the parameter μ (actually two, one for each direction) is obtained by requiring that in the viscous dashpot will be produced the same state of stress of the rock really present. For this scope it is necessary an explicit analytical link between stress and velocity. Such a link exists in simple form only for the case of linear elasticity, to which we

lead for the sake of simplicity. It can be shown that, in the 1D geometric conditions considered, the following relations are valid in general, related to increases in stress due to the passage of the wave:

$$\begin{cases} \tau_{zx} = \rho V_S \dfrac{\partial u_x}{\partial t} \\ \sigma_z = \rho V_P \dfrac{\partial u_z}{\partial t} \end{cases} \qquad 2.22$$

Where p is the density, while V_S and V_P are the velocities of elastic propagation of the the shear and pressure waves:

$$\begin{cases} V_S = \sqrt{\dfrac{G}{\rho}} \\ V_P = \sqrt{\dfrac{E_{ed}}{\rho}} = \sqrt{\dfrac{E(1-\nu)}{(1+\nu)(1-2\nu)}} \end{cases} \qquad 2.23$$

with E, G and ν usual elastic constants and E_{ed} edometric modulus. With these relations it is possible to derive the analytical expression of the coefficient η, simply by imposing:

$$\begin{cases} \tau_{zx} = \eta_x \dot{u}_x = \rho V_S \dot{u}_x \\ \sigma_z = \eta_z \dot{u}_z = \rho V_P \dot{u}_z \end{cases} \Rightarrow \begin{cases} \eta_x = \rho V_S \\ \eta_z = \rho V_P \end{cases} \qquad 2.24$$

The calibration of the dampers, therefore, requires knowledge of the mechanical properties of the rock, here assumed linear-elastic. If the layer of soil is discretized into N sub-layers, in the calculation code the integral motion of soil and rock is imposed exactly at the interface (z=N*Δz), while the behaviour of the rock is expressed at an additional dummy substrate (z=(N+1)*Δz). Therefore, if $\bar{t}$ is the seismic input duration and Δz is the spatial discretization gap, we have:

$$\begin{cases} v_z(z=(N+1)\Delta z,t) = v_z(z=(N+1)\Delta z,t) = 0 & \forall t \le \bar{t} \\ v_z(z=(N+1)\Delta z,t) = \dfrac{\sigma_z\big|_{z=N\Delta z} - \gamma H \cos\alpha}{\eta_z} \wedge v_x(z=(N+1)\Delta z,t) = \dfrac{\tau_{zx}\big|_{z=N\Delta z} - \gamma H \sin\alpha}{\eta_x} & \forall t > \bar{t} \end{cases} \qquad 2.25$$

The second of equation 2.25 implicitly involve that at the base the stress-velocity linear relationship is valid also for the soil, restoring, using the definition of η_x and η_z, the continuity of stress at the interface.

It was realized over time (Pisanò, 2007) that the inclusion in the calculation of the definition at times of the boundary condition (2.25) introduces in the solution a discontinuity in the velocity field, which obviously takes in time in the drift of the displacements. This fact is remedied by extending to all the time instants the second of (2.25), i.e. activating the dampers from the beginning of the analysis: this will introduce a slight attenuation of the input signal, which has verified to be negligible compared to the dissipations immediately due to the viscoplastic link.

For the numerical analyses described in this work, it was decided not to activate the dampers, as long as the evaluation of the seismic response of the slope was performed in a time equal to the duration of the seismic input, not considering the instants after.

Indeed, the use of the code VIBRAZIONE is very expensive in terms of duration of the processing (even several hours) and the evaluation of permanent displacements of the considered slope slightly depends on the instants after the seismic input.

By choosing not to activate the dampers, however, results cautionary.

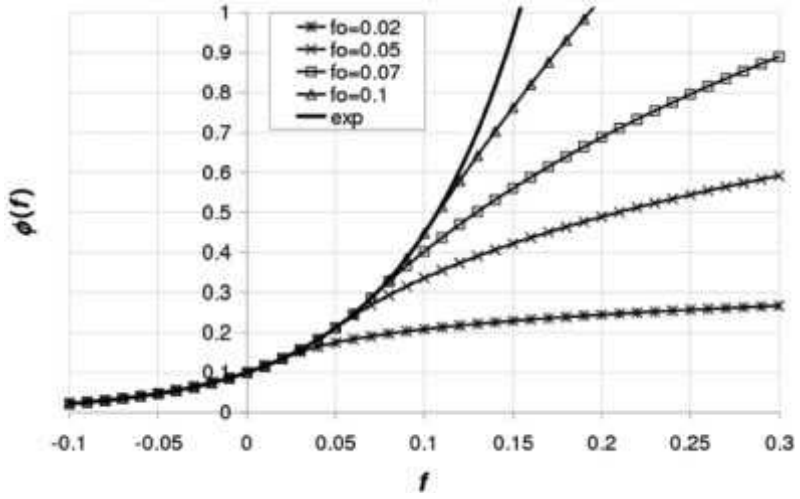

Figure 2.1 Viscous nucleus definition for different values of f_0 (di Prisco et al., 2007).

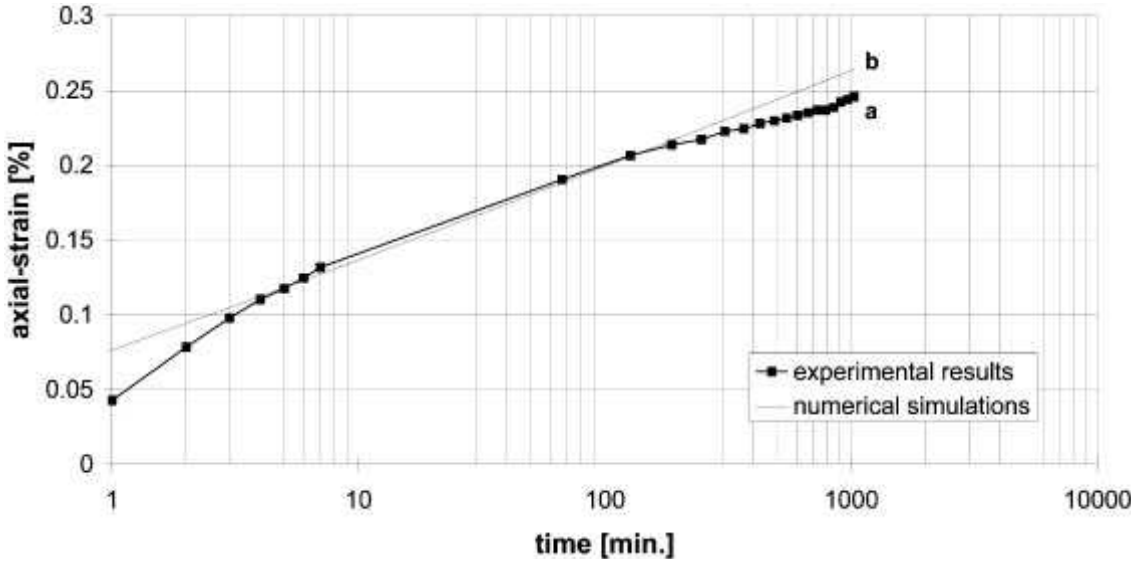

Figure 2.2. Creep test experimental data (a) and numerical simulations (b) obtained by means of the viscoplastic model corresponding to an instantaneous axial load increment of 5 kPa (cell pressure of 100 kPa, mobilized friction angle of 16°) (di Prisco and Imposimato, 1996).

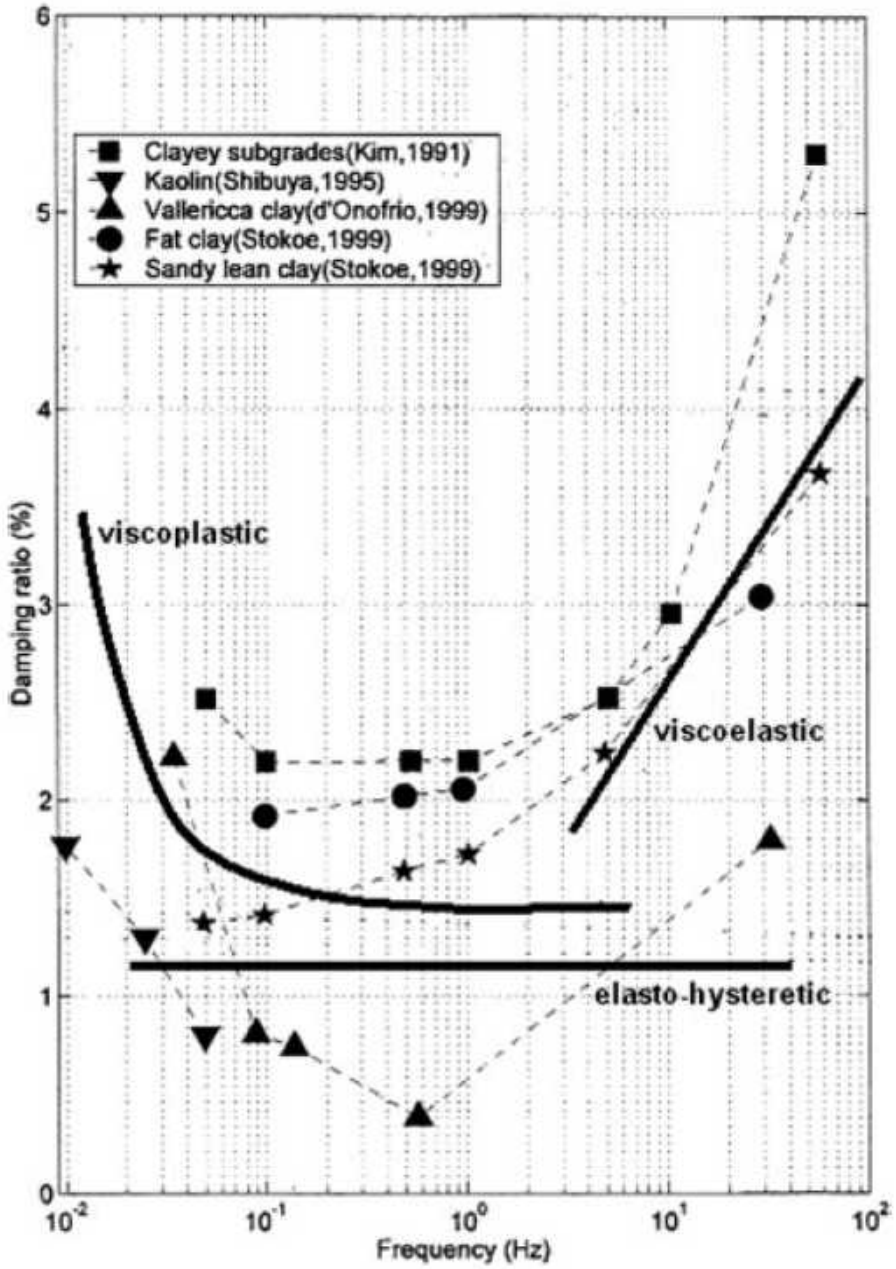

Figure 2.3. Experimental trends of damping ratio with the frequency and theoretical responses of viscoplastic, viscoelastic and elasto-hysteretic models (di Prisco et al., 2006).

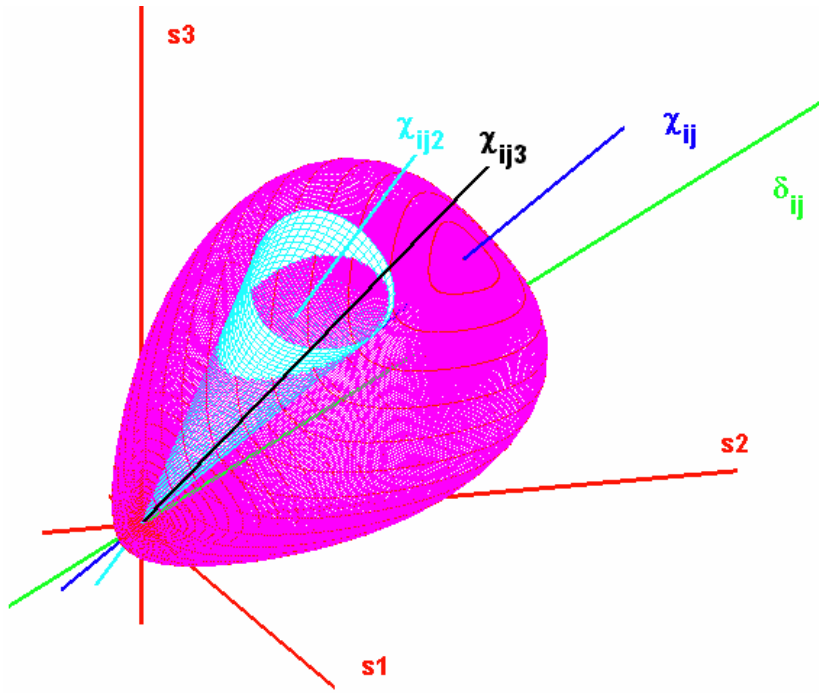

Figure 2.4 The two yield surfaces in principal stress space (Zambelli, 2006).

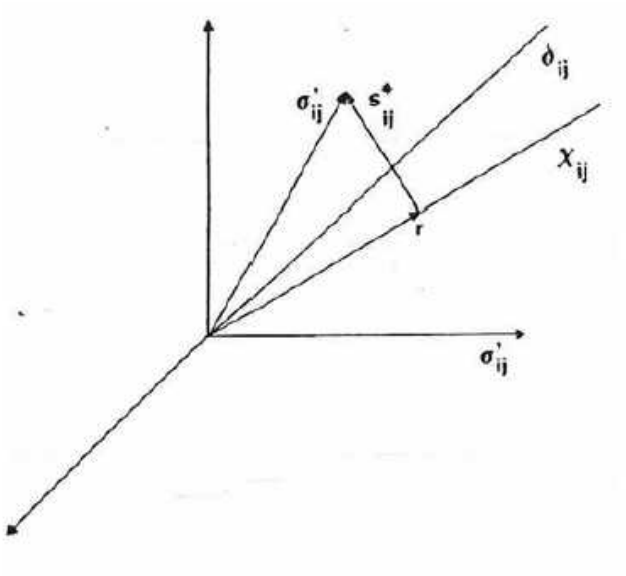

Figure 2.5 Stess space – definition of stress variables (di Prisco, 1993).

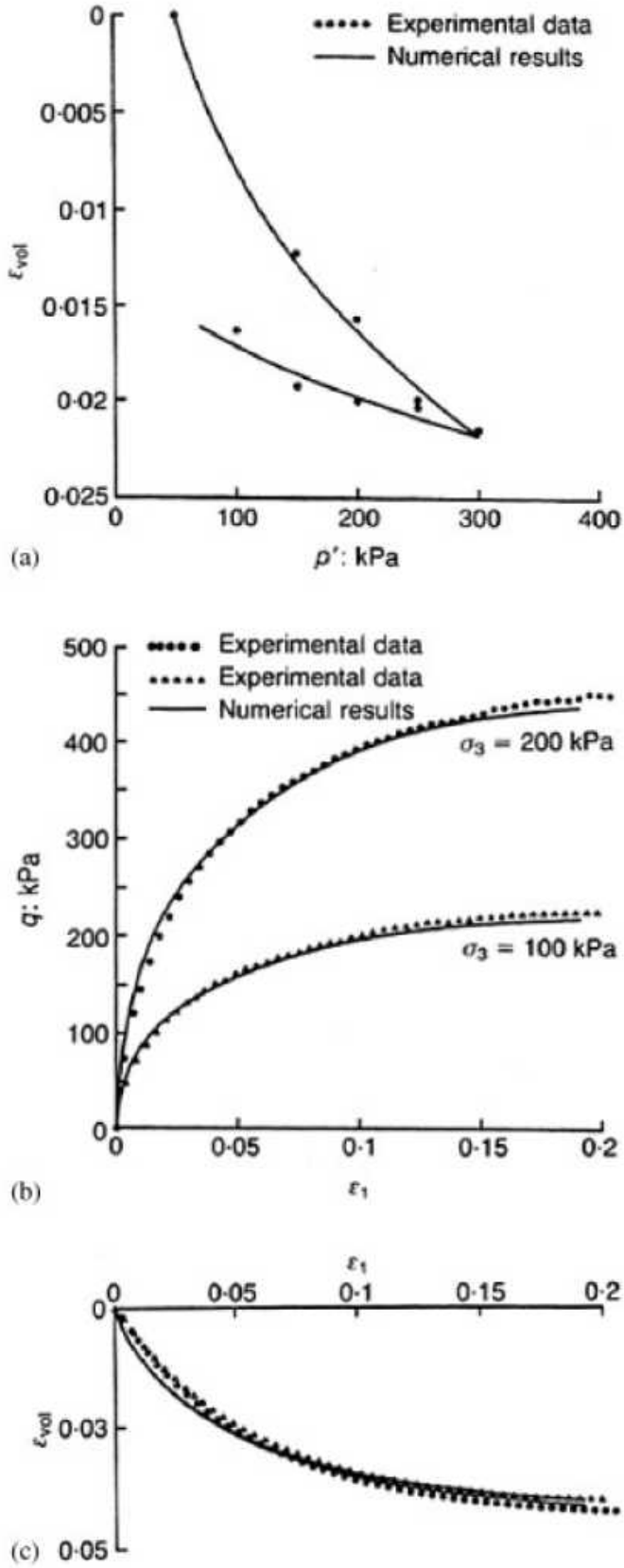

Figure 2.6. Comparison of experimental and numerical results: (a) isotropic loading-unloading standard drained triaxial compressions; (b) deviatoric stress-strain behaviour and (c) volumetric response (di Prisco et al., 1995).

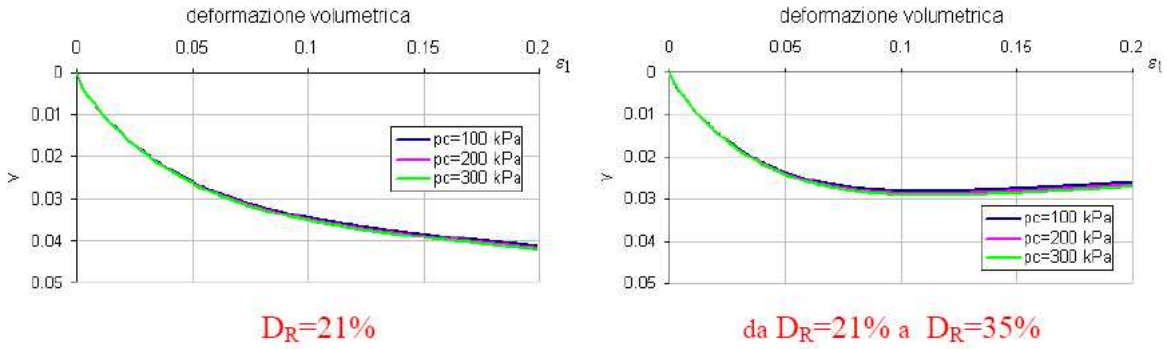

Figure 2.7 Simulation of the volumetric behaviour of loose sand in drained triaxial compression tests: elastoplastic model (on the left) and elastoviscoplastic (on the right). (Zambelli, 2002).

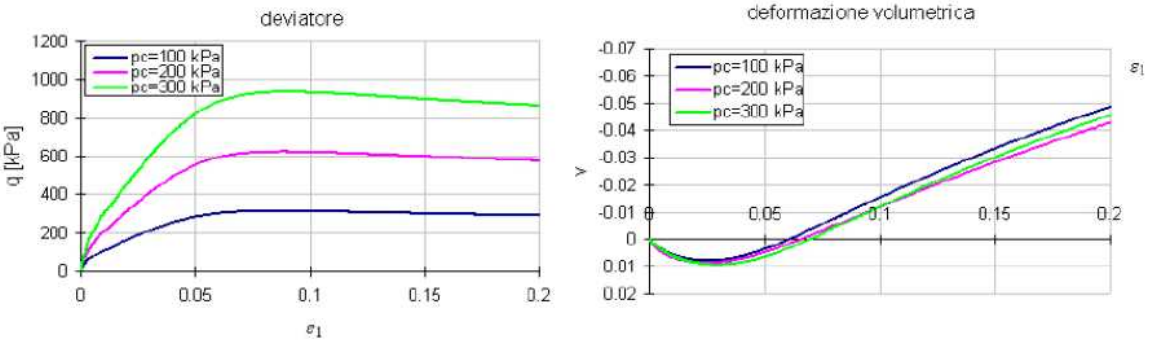

Figure 2.8 Drained compression tests on dense sand by elastoviscoplastic model (Zambelli, 2002).

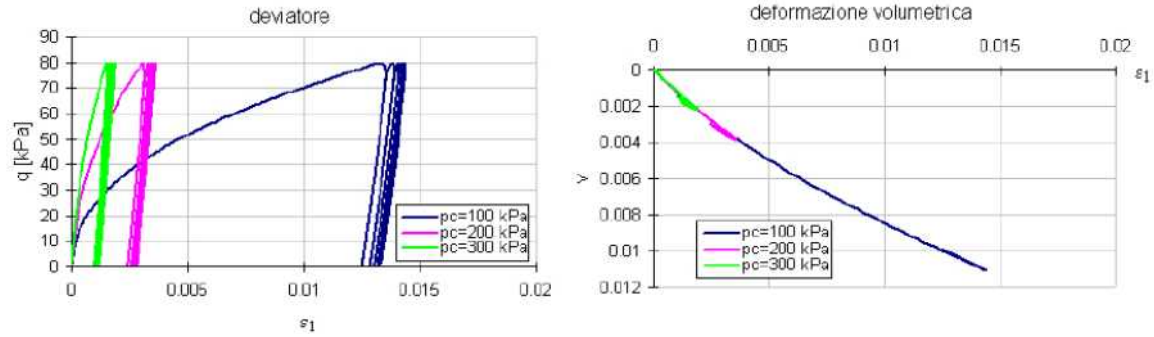

Figure 2.9 Drained cyclic tests on loose sand by the elastoviscoplastic model (Zambelli, 2002).

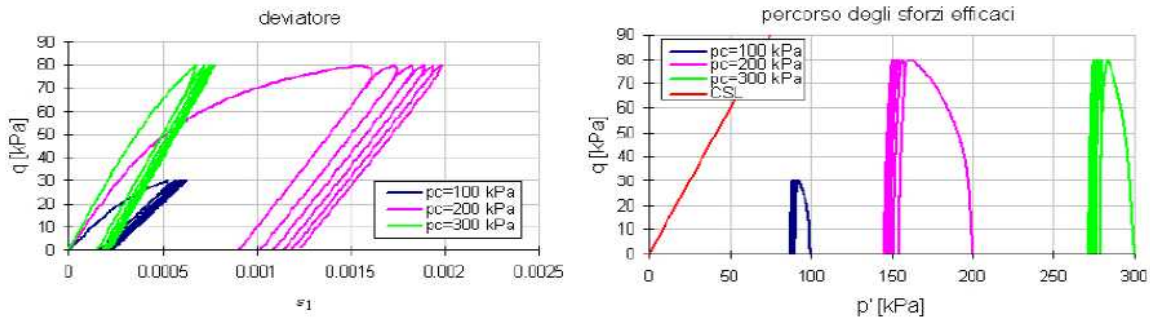

Figure 2.10 Cyclic undrained tests on loose sand through elastoviscoplastic model (Zambelli, 2002).

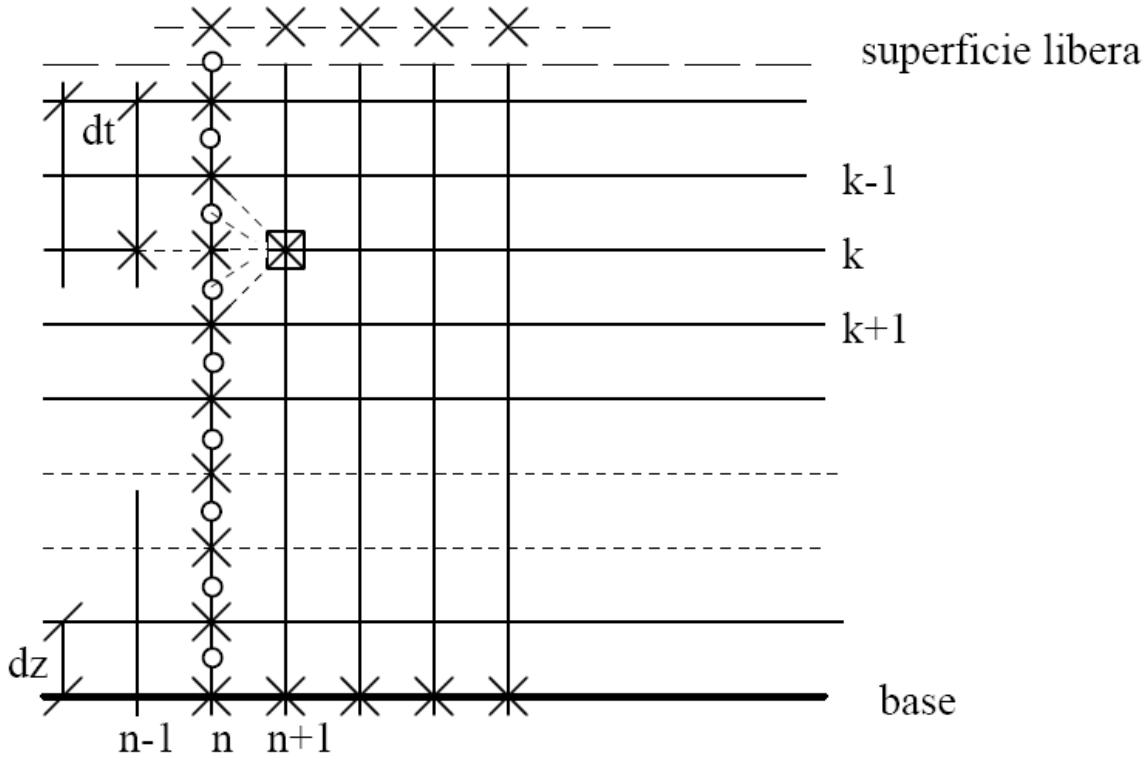

Figure 2.11 Discretization used to solve the finite difference system (Imposimato, 1998).

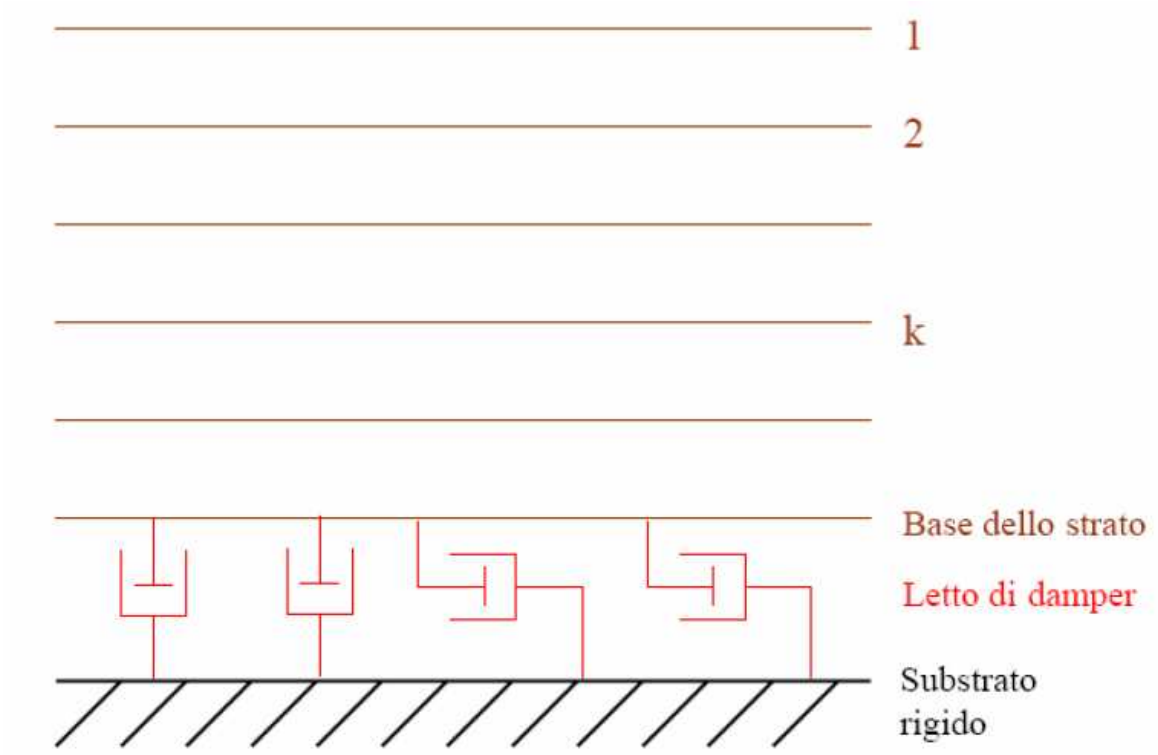

Figure 2.12. Scheme of the placement of the dampers at the interface between layer and bedrock.

CHAPTER 3: THE SEISMIC INPUT

3.1. *Accelerograms database*

In many applications of seismic engineering, particularly if linear dynamic analyses (both of civil and geotechnical structures) are required, may be used real accelerograms, which have characteristics as far as possible close to those of the earthquake that mainly affects the seismic hazard of the site in terms of peak values, magnitude and distance, but also fault mechanism. For this purpose in recent years several accelerograms databases, available on internet, have been organized. Among them we recall only a few of particular interest:

- European Strong Motion Database: collects more than 3000 accelerometric records from Europe and neighboring regions;
- PEER Strong Motion Database: collects accelerometric data from major earthquakes in the world, with particular reference to those Californians;
- SISMA (Site of Italian Strong-Motion Accelerograms): is an archive of strong motion accelerograms recorded in Italy during the period 1972-2002. It includes 247 three-components uniformly processed recording related to 89 earthquakes and 101 recording stations. The web-site allows to search data through three selection criteria (i.e. “Search Eqk”, “Search Station” and “Search Recording”). Selected Strong-Motion accelerograms and associated earthquake, station and ground motion parameters can be displayed and downloaded. The Database is the result of a joint project between the Sapienza Università di Roma and University of California, Los Angeles (UCLA).

The seismic input, employed for the numerical analyses performed for this research, are the five strong motion accelerograms, from the database SISMA, with higher PGA for each site classification A, B and C, according to EC8; in some cases the accelerograms has been conveniently amplified to reach the critical acceleration value (Kc) for the analyses performed by means of Newmark method (Figure 3.1 a, b and c; Figure 3.2 a and b; Figure 3.3 a, b and c; Figure 3.4 a, b and c).

Under seismic actions of considerable duration the soil deposit can enter in the phase of *forced movement*, this phase is dominated by the characteristics of the stress. So, if it is established a steady response under the prolonged action of the different harmonic components of the signal, in dynamics the understanding of the change becomes crucial (filtering), that those components suffer through the layer depending on its mechanical properties and boundary conditions.

The proper functioning of VIBRAZIONE in case of analysis of real earthquakes has been tested (Pisanò, 2007) comparing the results with the experimental data obtained on shaking table by Fukuy et al. (2007a, b).

3.2. *Parameters of severity of the seismic motion*

It is well known that damages depend both on the nature of earthquake and the structure characteristics.

The severity of an accelerogram in terms of effects on soils or structures depends on many parameters associated with it. In this section are described some of the parameters most used in engineering.

1) Maximum Ground Acceleration or Peak Ground Acceleration of earthquake signal: PGA. The Peak Ground Acceleration is currently used because it is directly related to the inertial forces of rigid structures.

2) The Arias intensity was initially defined (Arias, 1970) as:

$$\vartheta_I = \frac{\pi}{2g}\int_0^{t_0} a^2(t)dt \tag{3.1}$$

and was called scalar intensity. Dimensionally the Arias intensity is a velocity. It is directly quantifiable through the acceleration record *a(t)*, integrating it over the total duration of the earthquake. By definition, it is the trace of a second-order tensor. This is the reason why it is an invariant; therefore it is not dependent on the accelerograph axis orientation.

Unlike PGA, it considers the full range of frequencies recorded and included in the accelerogram and the duration of the ground motion. The Arias intensity is claimed to be a measure of the total seismic energy absorbed by the ground. Therefore, Arias intensity is better than PGA for responding the geohazard induced by earthquakes (Jibson, 1993).

Arias (1970) also defined the scalar intensity on the horizontal plane as:

$$I_h = \frac{\pi}{2g}\int_0^{t_0} a_h^2(t)dt \tag{3.2}$$

He pointed out the importance of this variable, because, among other reasons, man-made structures are more sensitive to horizontal ground motion than that vertical.

3) The Destructive Potential (Saragoni, 1981) is defined as:

$$P_d = \frac{I_A}{f_d^c} \tag{3.3}$$

where I_A is Arias Intensity, f_d is signal central frequency and c is a parameter determined from a statistical analysis on acceleration hazard processes equals 2.

4) The Fourier Spectra is a parameter on the frequency content.

5) Tm is the mean period of the accelerogram, as defined by Rathje et al. (1998):

$$T_m = \frac{\sum C_i^2 \left(\frac{1}{f_i}\right)}{\sum C_i^2} \tag{3.4}$$

with C_i and f_i being the Fourier amplitudes and the corresponding frequencies.

6) The predominant period is the period corresponding to the maximum amplitude of the Fourier spectrum.

7) Duration of seismic motion: for the purposes of the resistance of older buildings to seismic actions, as well as the stability of soil under dynamic conditions, the duration of motion, in terms of number of cycles of significant amplitude, is a critical parameter, indeed it could start up fatigue phenomena at a low number of cycles and, in soils, an accumulation of interstitial pressure. The devastating effects of some recent large earthquakes in subduction zone on both buildings and soils (i.e.: Mexico, 1985, the Philippines, 1990; Turkey, 1999), suggest that the problem of duration should be faced more explicitly. Eurocode 8, Part 1, establishes that, for the generation of artificial accelerograms for dynamic analysis of structures in seismic areas, the duration must be compatible with the magnitude and other characteristics of the seismic event that most influence the seismic hazard of the site.

Then remains the problem of the quantitative definition of the duration or to determine which is the time interval in which the seismic motion is significant from an engineering point of view.

For this purpose are often used two definitions:

- duration based on the overcoming of a threshold value (*bracketed duration*): is defined a threshold, usually 0.05 g, above which it is deemed that the motion has engineering relevance, the duration is equal to the time interval between the first and the last overcoming of such value;

- duration based on the intensity of motion: the Arias intensity function is calculated and it is normalized to the maximum value, the duration is equal to the time interval $t_2 - t_1$, where $I_A(t_1) = 0.05$ and $I_A(t_2) = 0.95$.

The calculation of the duration of an accelerogram, according to one of the two definitions above, in some cases shows the variability in the quantification of this parameter; in fact, for example, in case of prolonged but modest oscillations in the final part of the signal, the *bracketed duration* may be twice that one based on the intensity of motion (Faccioli and Paolucci, 2005).

In general, $D_{5\text{-}95}$ (Trifunac and Brady, 1975) is the time interval between the points where the 5% and 95% of the total energy has been registered.

3.3. *The frequency domain*

In addition to the time domain, it is important to evaluate the results of the numerical analyses, shown in the following chapters, even in the frequency domain. The purpose of this approach is to understand the filtering action of the analyzed system in relation to the stress imposed: thus it is possible to understand what is the soil action on each frequency component of the signal, allowing to predict the hazard of the earthquake from the knowledge of its frequency band, as well as the mechanical and geometrical properties of the system.

In Figure 3.5 it is shown a uniform layer of soil of height *H*, based on a perfectly rigid half-space rock, infinitely extended in the *x* and *y* direction; at the base of the layer, considered linear elastic with density ρ and velocity of S wave *Vs*, is imposed a harmonic tangential stress $e^{i\omega t}$ of unitary amplitude.

The motion of the layer is determined by the superposition of an incident wave (upward) and a reflected one (downwards), of amplitude A and B respectively and pulsation ω. The motion is not dissipated by any transfer in the rocky half-space, as it, being rigid, forces the entire energy to stay within the layer.

The horizontal displacement field is:

$$s_x = Ae^{i\omega(t+z/V_S)} + Be^{i\omega(t-z/V_S)} \tag{3.5}$$

The amplitudes A and B are determined by imposing the condition of free surface and continuity of the displacement at the interface with bedrock, namely:

$$\begin{cases} \tau_{xz}(z=0,t) = \rho V_S \dfrac{ds_x(z=0,t)}{dt} = 0 \\ s_x(z=H,t) = e^{i\omega t} \end{cases} \tag{3.6}$$

After simple analytical developments, the expression of the displacement field is:

$$s_x(z,t) = \frac{\cos\left(\dfrac{\omega z}{V_S}\right)}{\cos\left(\dfrac{\omega H}{V_S}\right)} e^{i\omega t} \tag{3.7}$$

It is useful now obtain the relationship between surface displacement and input at the base:

$$\frac{s_x(z=0,t)}{s_x(z=H,t)} = \frac{1}{\cos\left(\dfrac{\omega H}{V_S}\right)} = \frac{1}{\cos\left(\dfrac{2\pi f H}{V_S}\right)} = H(f) \tag{3.8}$$

H(f) is the so-called *transfer function*: regardless of the time, it quantifies the amplitude transformation of a generic harmonic from the base to the surface.

It may be demonstrated that *H(f)* has the vertical asymptotes (Figure 3.6) at all odd multiples of $V_S/4H$: next to these values could occur the so-called phenomenon of resonance, ie a high dynamic amplification of certain frequencies of the signal.

In a real case, the identification of the resonant frequencies is fundamental to determine the danger of an earthquake for a site.

The Fourier Spectra, for the considered accelerograms for only site classification A, are obtained by means of the code SeismoSignal (Figure 3.7 a and b).

SeismoSignal constitutes an easy and efficient way to process strong-motion data, featuring a user-friendly visual interface and being capable of deriving a number of strong-motion parameters often required by engineer seismologists and earthquake engineers.

SeismoSignal calculates:

- elastic and constant-ductility inelastic response spectra;
- Fourier and Power spectra;
- Arias (I_a) intensity;
- Cumulative Absolute Velocity (CAV) and Specific Energy Density (SED);
- Root-mean-square (RMS) of acceleration, velocity and displacement;
- Sustained maximum acceleration (SMA) and velocity (SMV);
- Effective design acceleration (EDA) Acceleration (ASI) and velocity (VSI) spectrum intensity;
- predominant (T_p) and mean (T_m) periods;
- Bracketed, uniform, significant and effective durations.

The program is able to read accelerograms defined in both single and multiple values per line formats (the two most popular formats used by strong-motion database), and can apply baseline correction and filtering prior to time integration of the signal (to obtain velocity and displacement time-histories).

In the present work two types of sand are considered: Hostun and Toyoura. For the first one, imposing V_S = 120 m/s, the resonant frequencies of the system are included in the range between 1.5 Hz (for a height H of the slope equal to 20 m) and 6 Hz (H = 5m). In this range are included many of the peak frequencies of the earthquakes considered, except for the Campobello di Mazara and Umbria-Marche 1st earthquakes.

Considering Toyoura sand and imposing V_S = 229 m/s, the resonance frequencies are included in the range between 2.85 Hz and 11.5 Hz. In this range, on the contrary, are mainly included Campobello di Mazara and Umbria-Marche 1st earthquakes.

More detailed considerations about the analysis in the frequency domain are given in the following chapters.

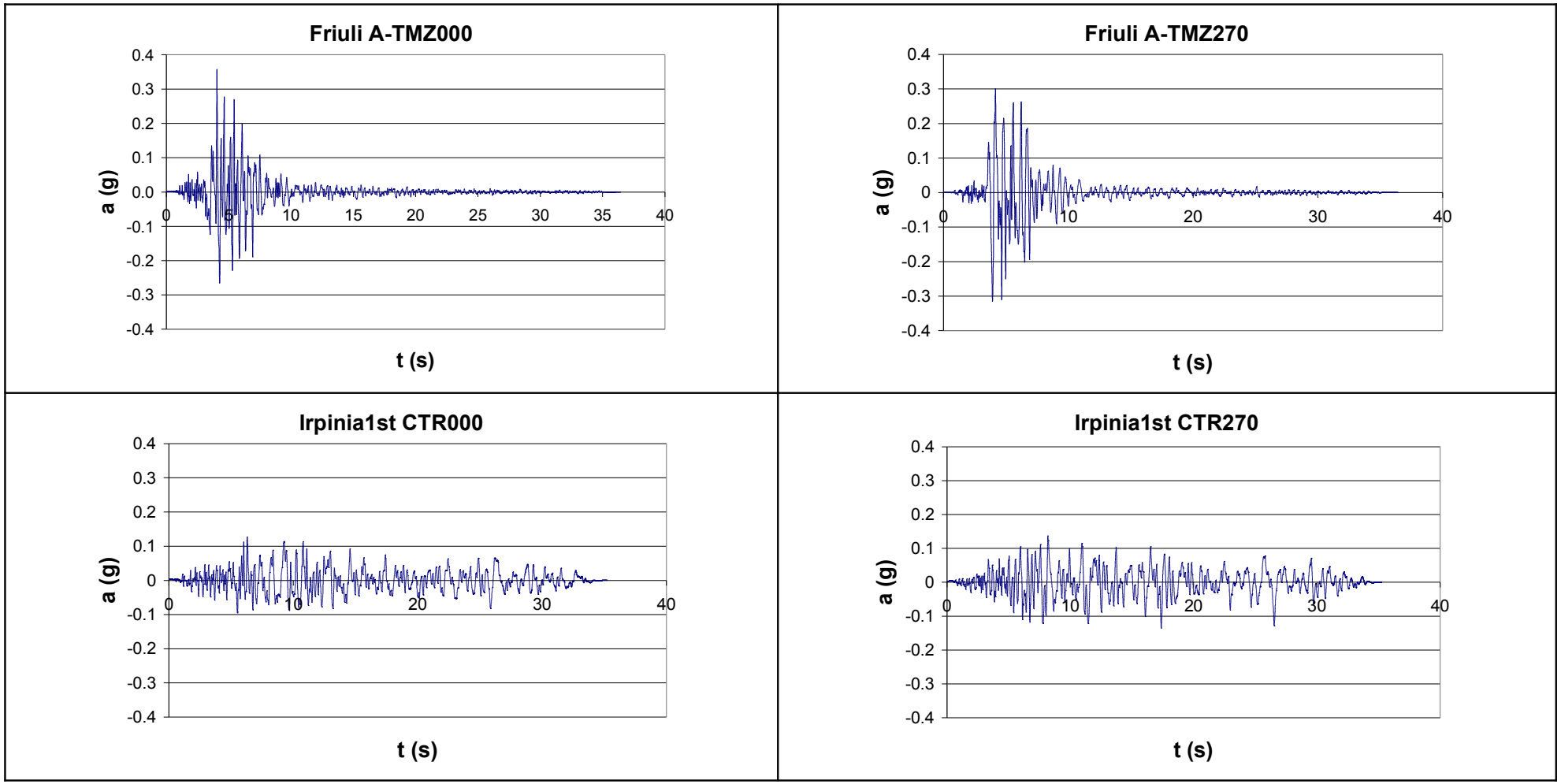

Figure 3.1 a. Strong motion accelerograms, site classification A: Friuli earthquake, Tolmezzo – Diga Ambiesta station (NS-WE); Irpinia 1st earthquake, Calitri station (NS-WE).

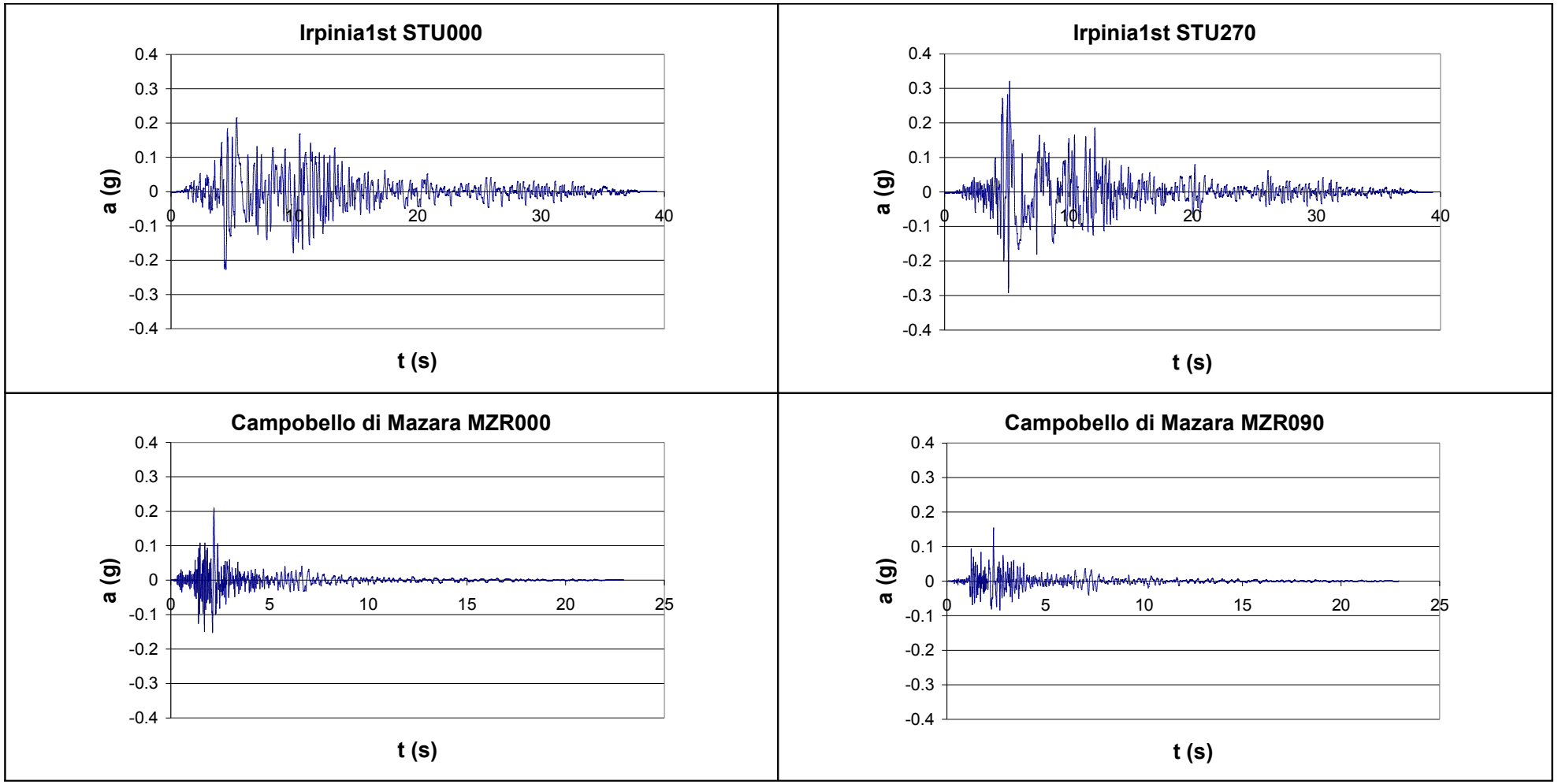

Figure 3.1 b. Strong motion accelerograms, site classification A: Irpinia 1st earthquake, Sturno station (NS-WE); Campobello di Mazara earthquake, Mazara del Vallo station (NS-WE).

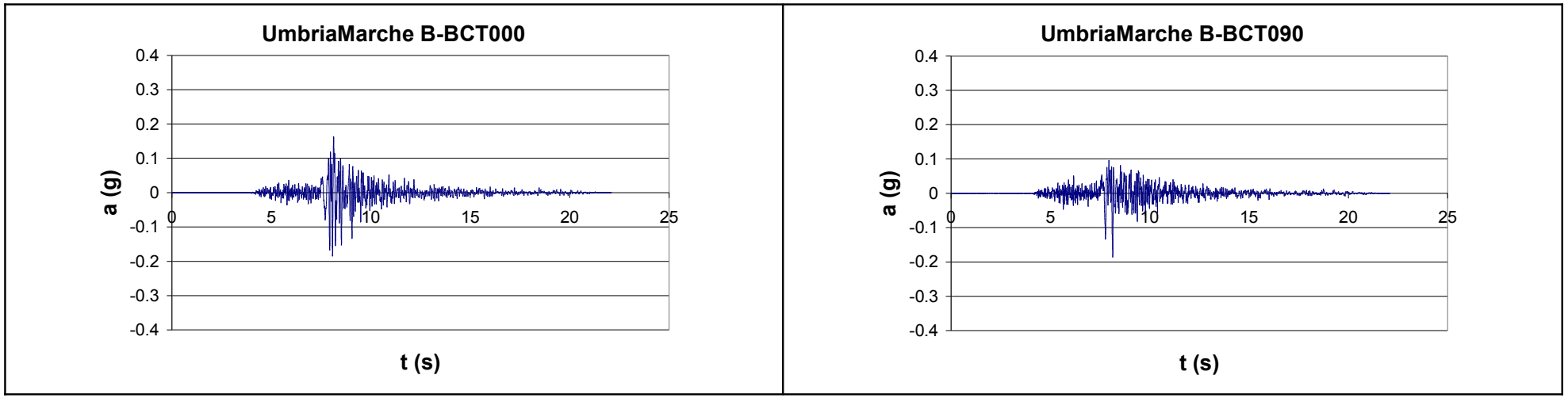

Figure 3.1 c. Strong motion accelerograms, site classification A: Umbria Marche 1st earthquake, Borgo-Cerreto Torre station (NS-WE).

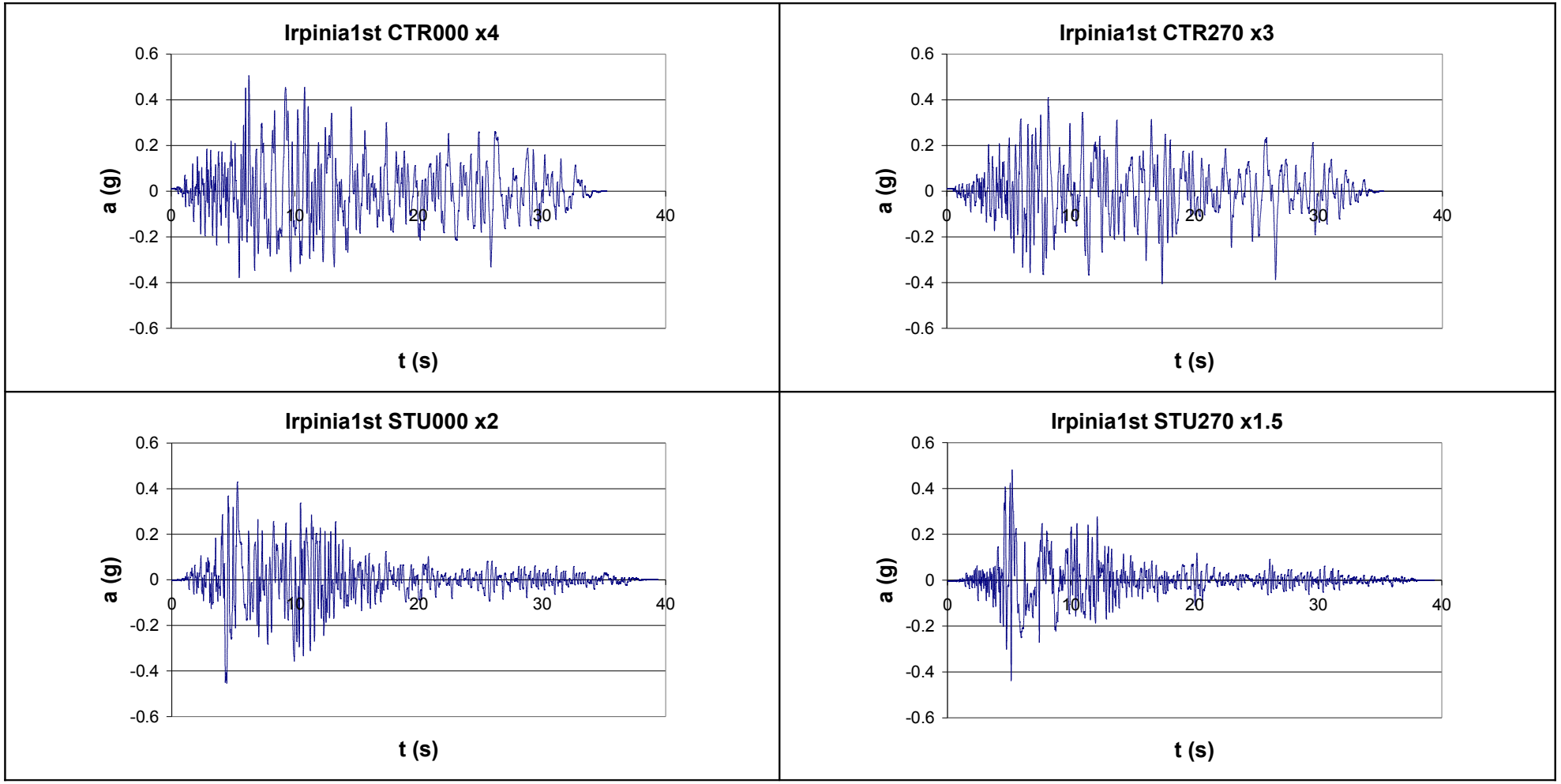

Figure 3.2 a. Strong motion amplified accelerograms, site classification A: Irpinia 1st earthquake, Calitri and Sturno station (NS-WE).

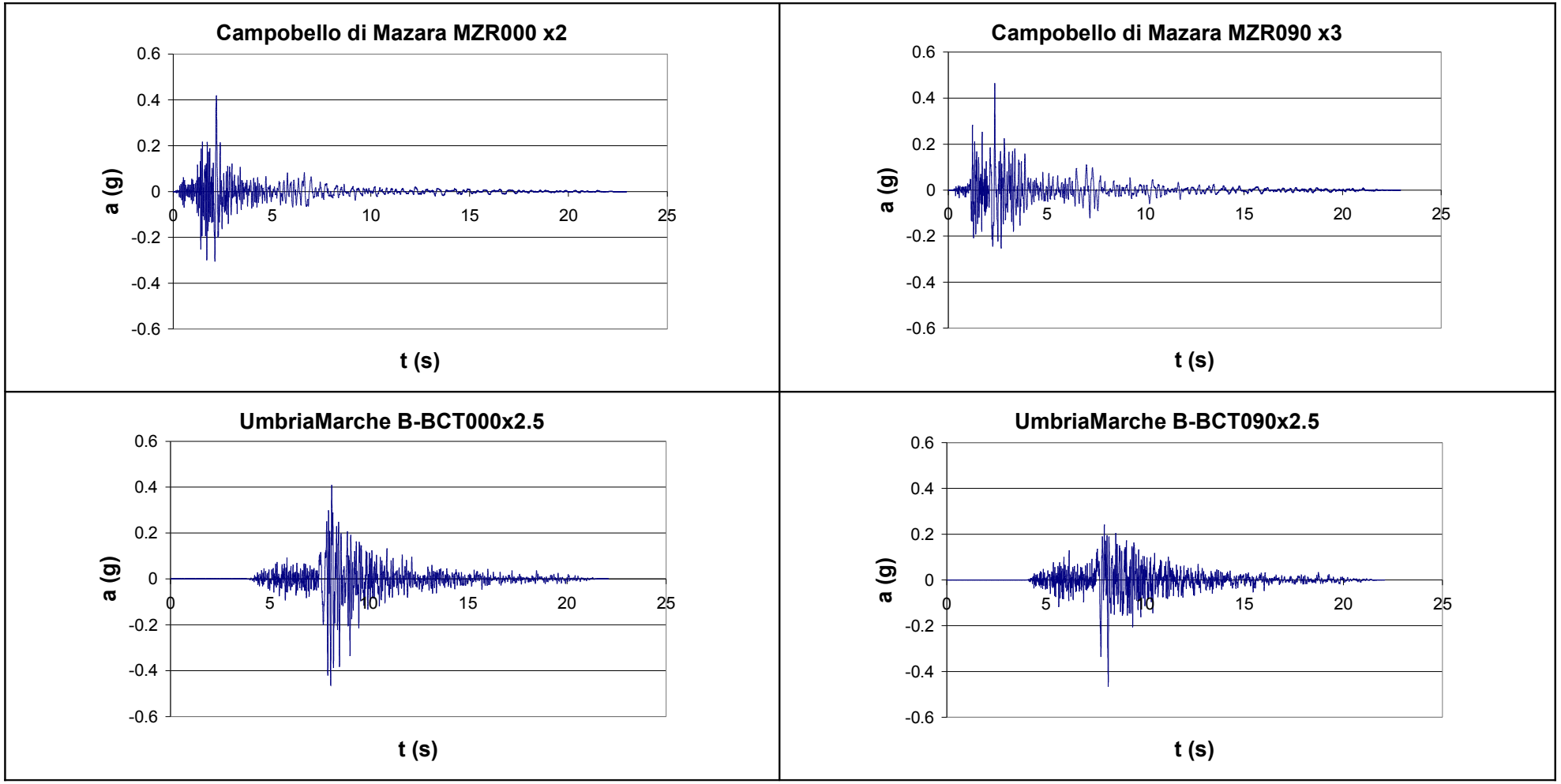

Figure 3.2 b. Strong motion amplified accelerograms, site classification A: Campobello di Mazara earthquake, Mazara del Vallo station (NS-WE), Umbria Marche 1st earthquake, Borgo-Cerreto Torre station.

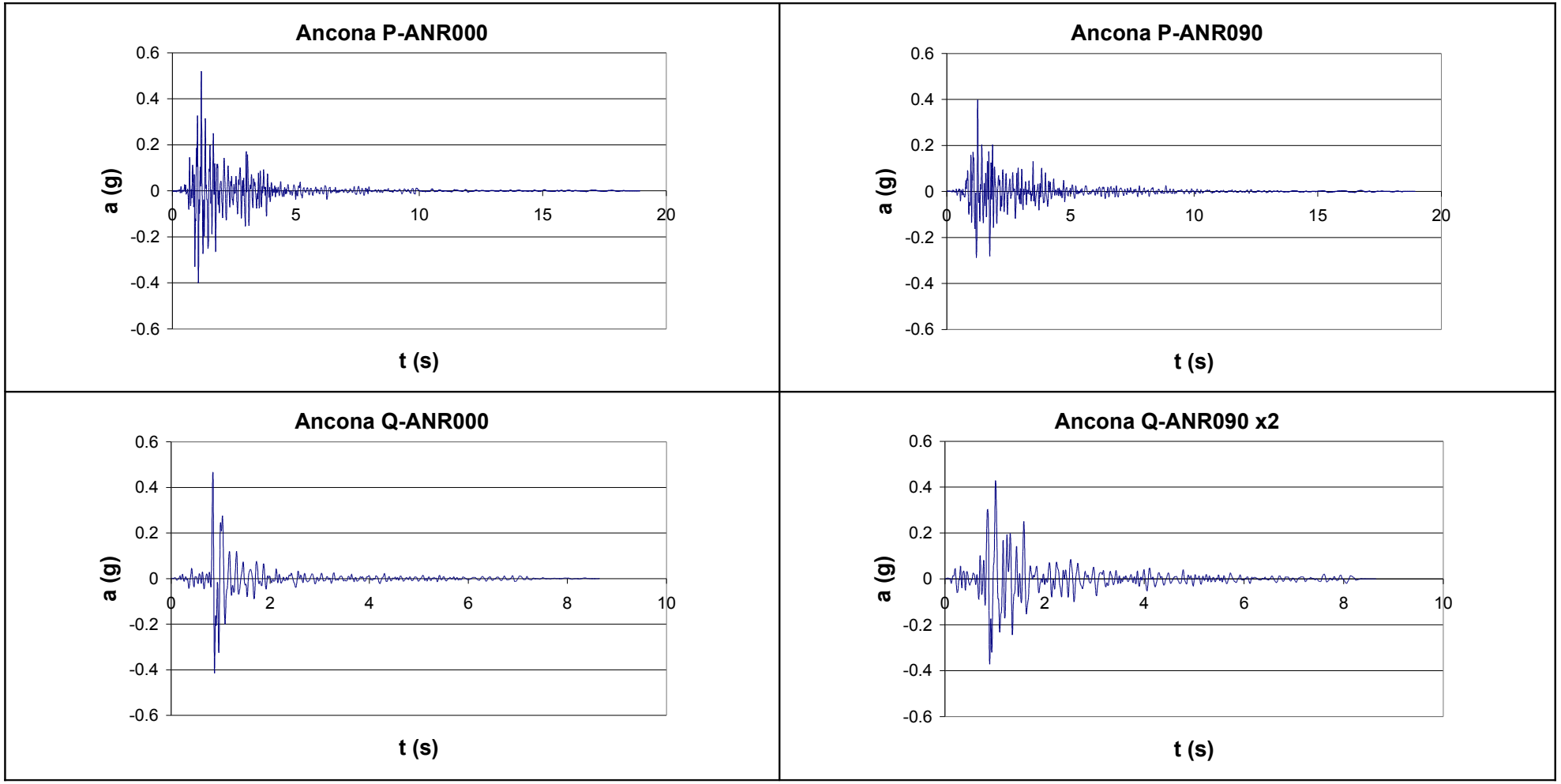

Figure 3.3 a. Strong motion accelerograms (amplified or not), site classification B: Ancona earthquake, Ancona Rocca station (NS-WE).

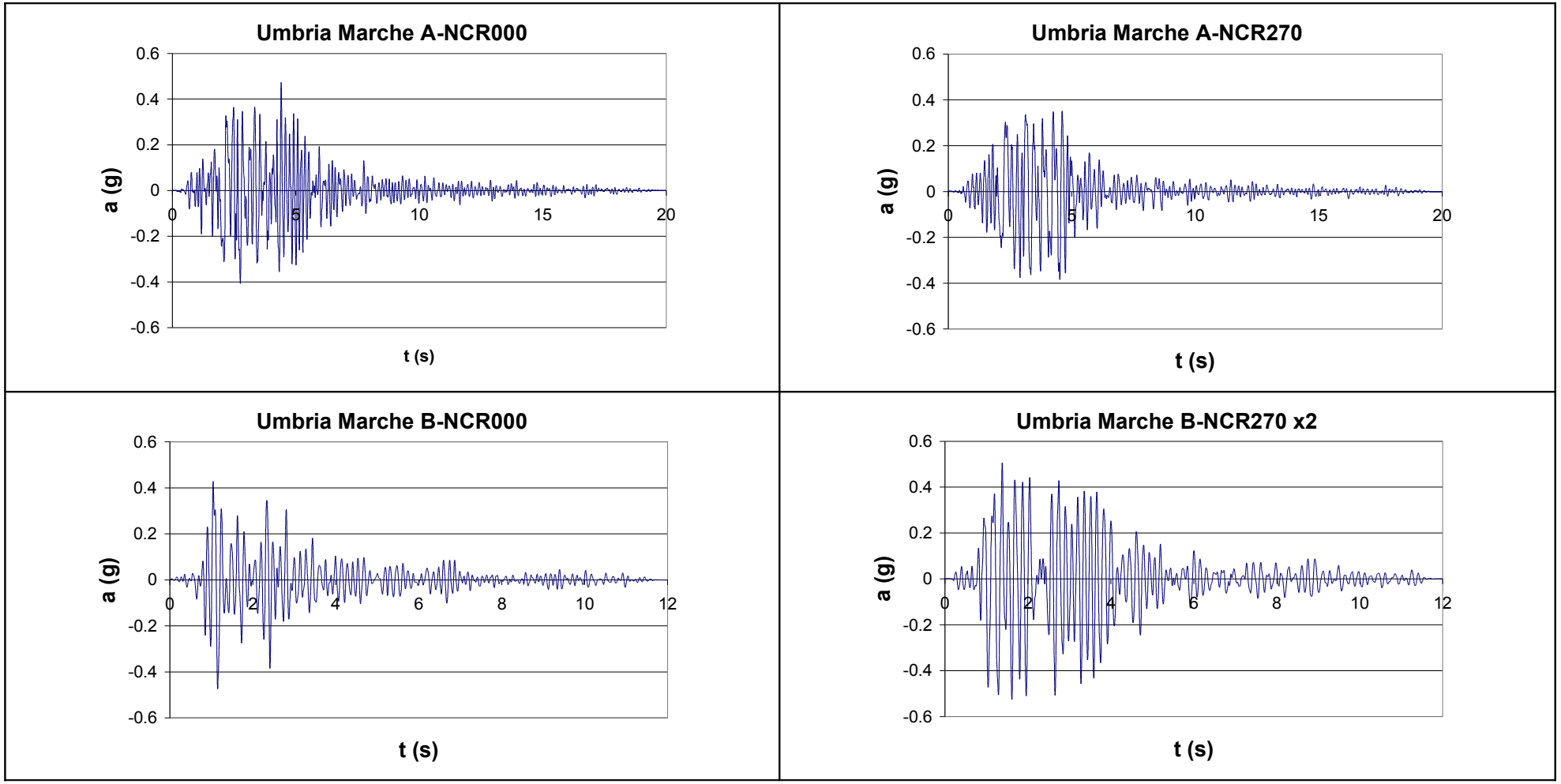

Figure 3.3 b. Strong motion accelerograms (amplified or not), site classification B: Umbria Marche 2nd and 1st earthquake, Nocera Umbra station (NS-WE).

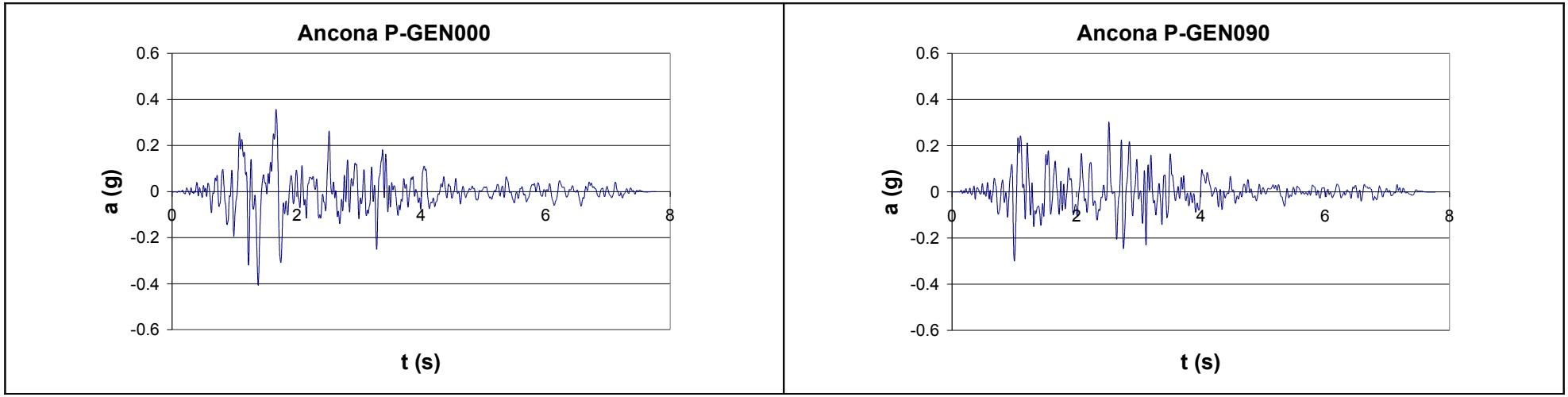

Figure 3.3 c. Strong motion accelerograms, site classification B: Ancona earthquake, Genio-Civile station (NS-WE).

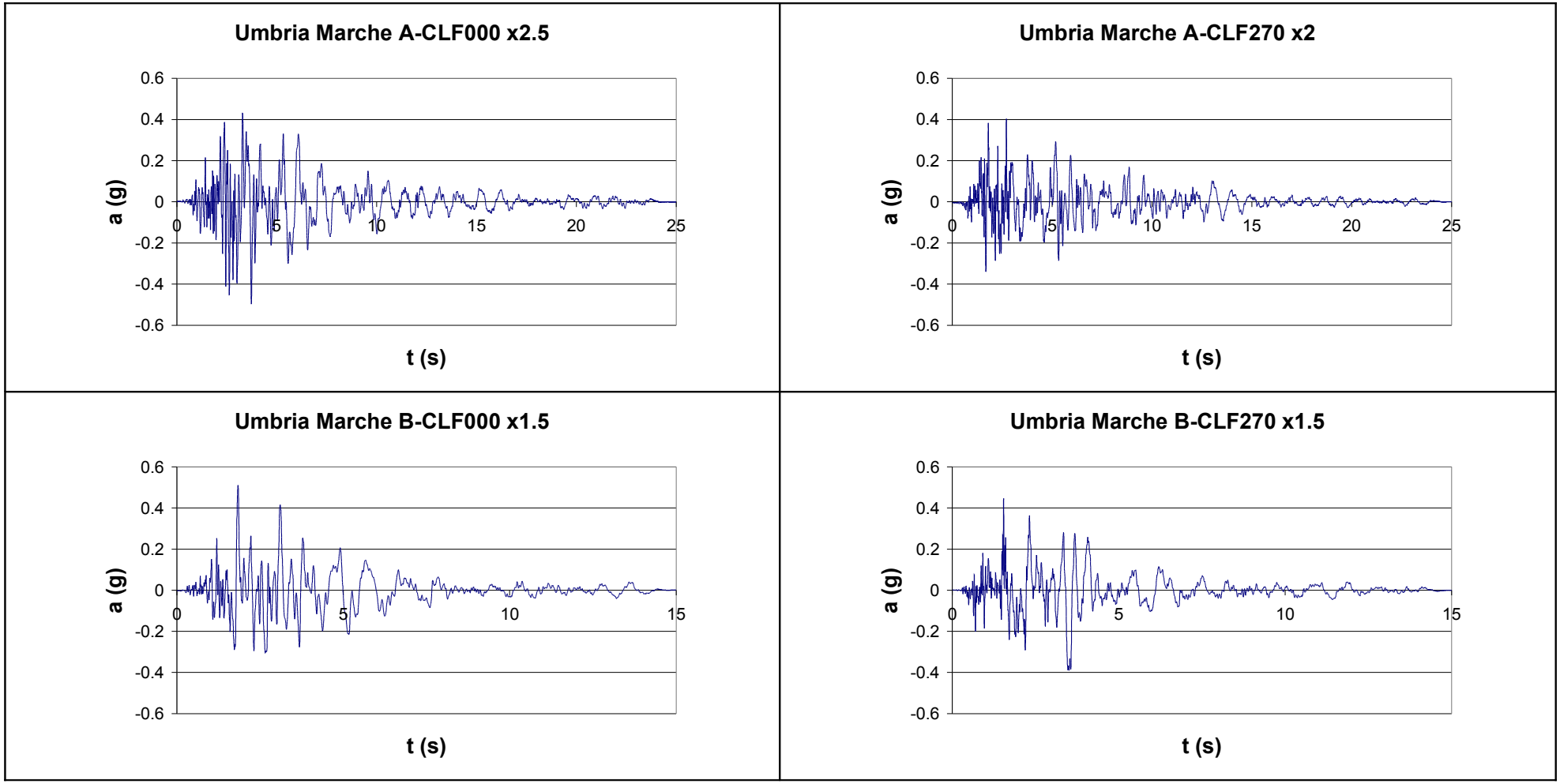

Figure 3.4 a. Strong motion amplified accelerograms, site classification C: Umbria Marche 2nd and 1st earthquake, Colfiorito station (NS-WE).

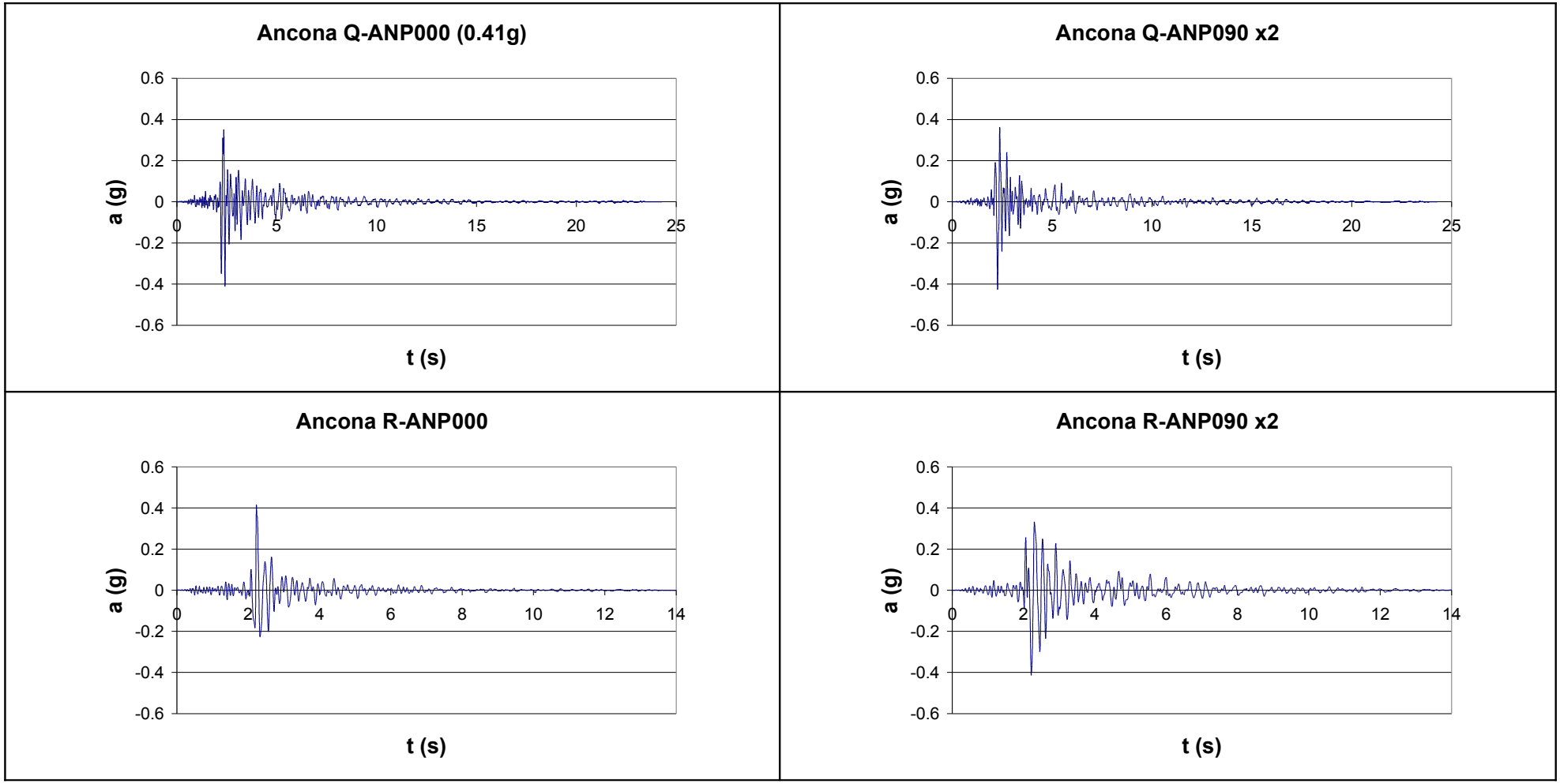

Figure 3.4 b. Strong motion accelerograms (amplified or not), site classification C: Ancona earthquake, Ancona Palombina station (NS-WE).

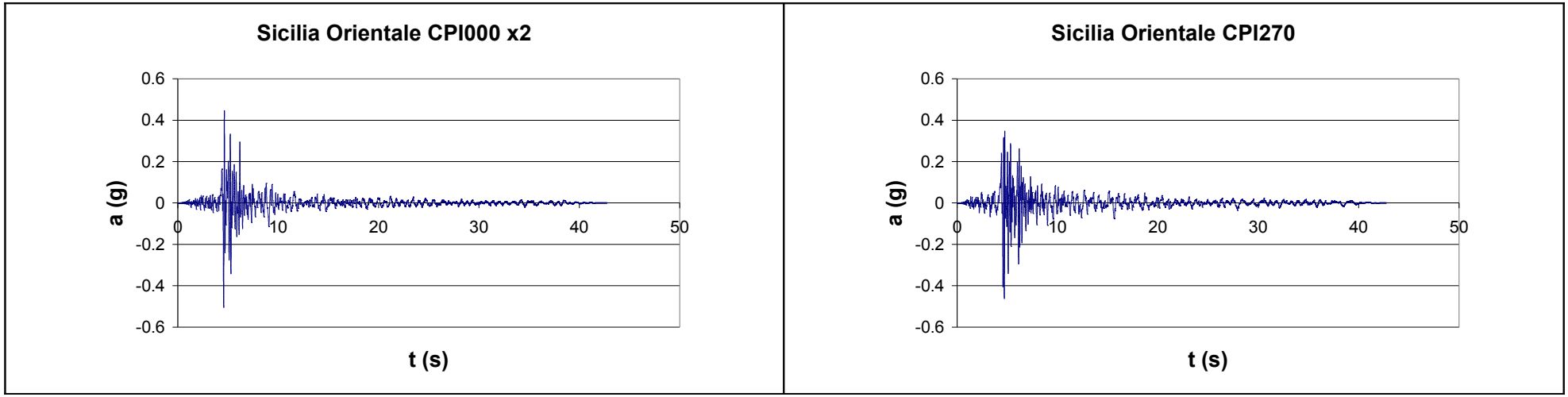

Figure 3.4 c. Strong motion accelerograms (amplified or not), site classification C: Sicilia Orientale earthquake, Catania - Piana station (NS-WE).

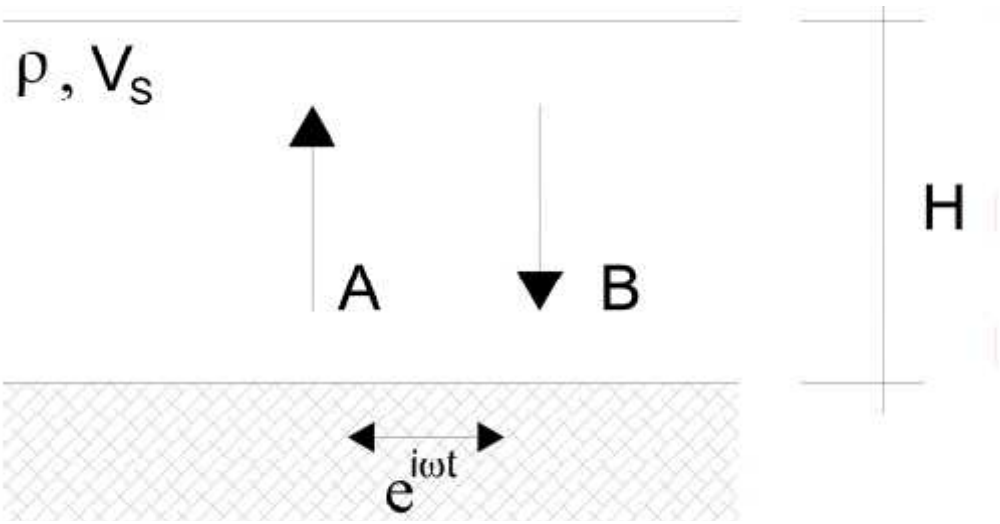

Figure 3.5: Layer on rigid half-space subjected to harmonic stress (Pisanò, 2007).

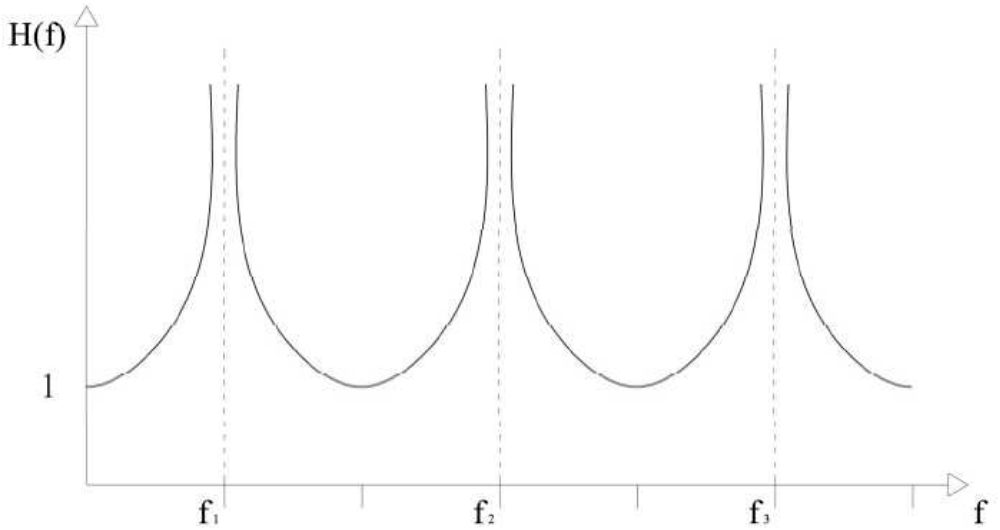

Figure 3.6: Transfer function of the elastic layer on rigid half-space (Pisanò, 2007).

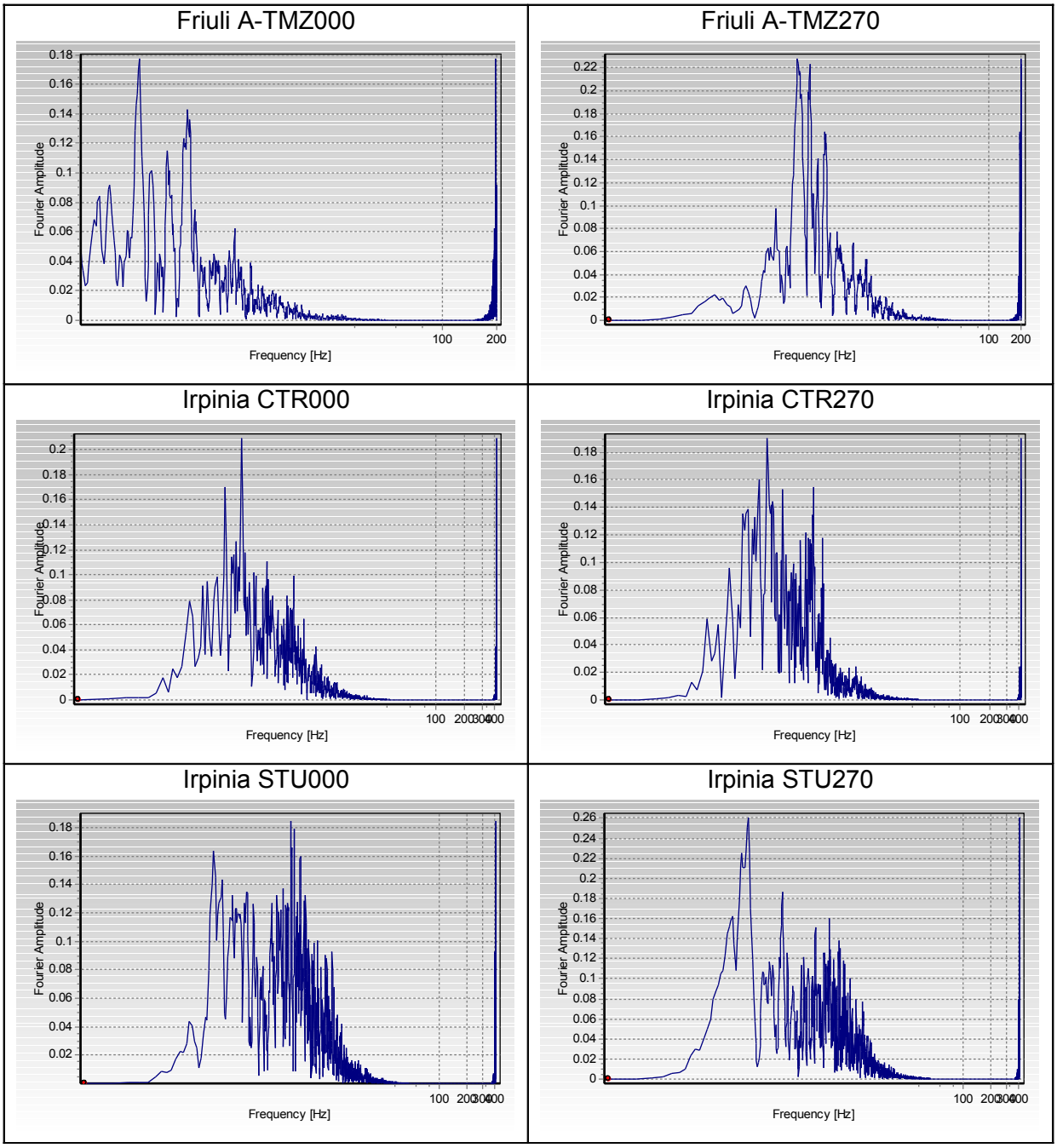

Figure 3.7 a. Fourier Spectra: Friuli earthquake, Tolmezzo – Diga Ambiesta station; Irpinia 1st earthquake, Calitri and Sturno stations.

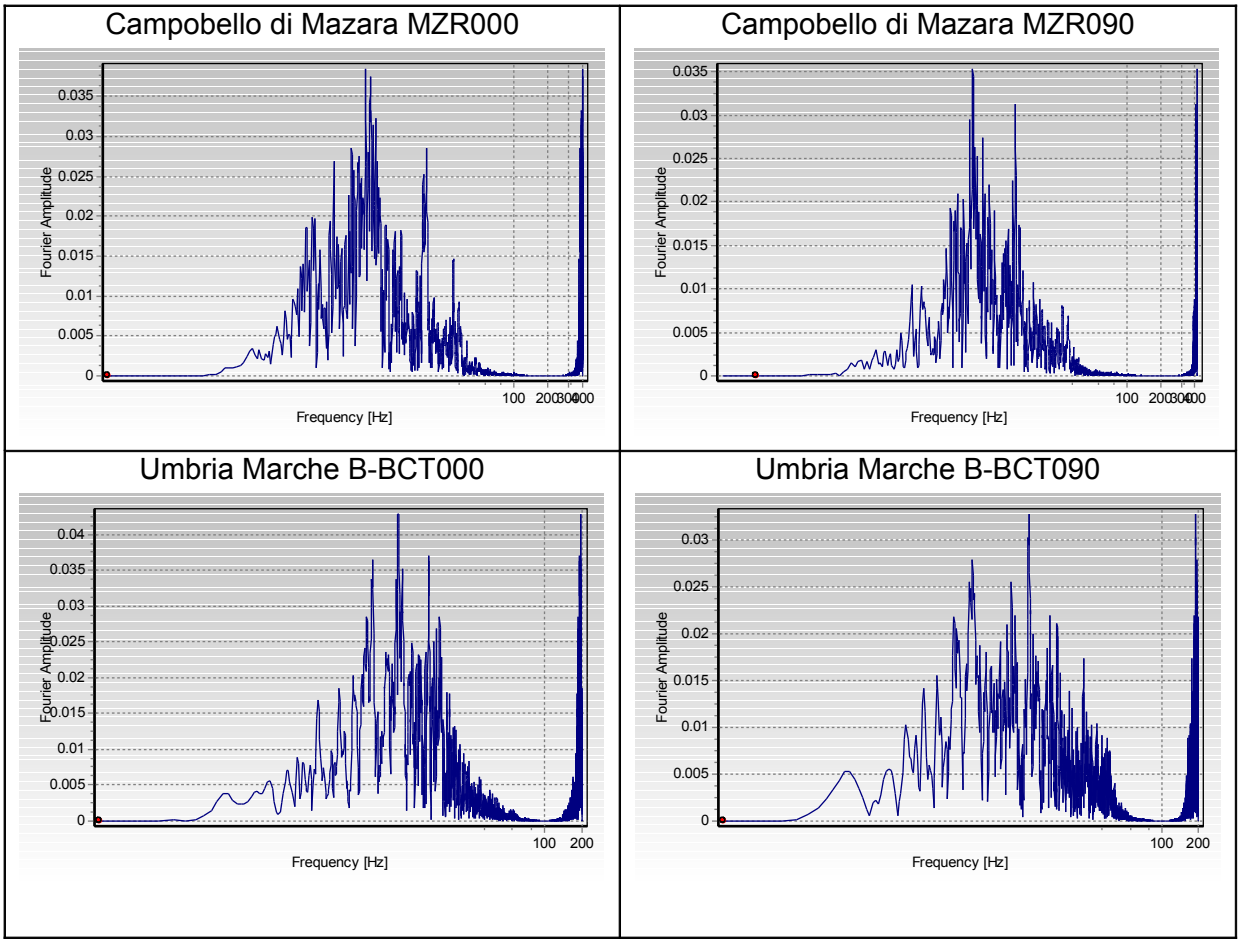

Figure 3.7 b. Fourier Spectra: Campobello di Mazara earthquake, Mazara del Vallo station; Umbria Marche 1st earthquake, Borgo - Cerreto Torre station.

CHAPTER 4: ELASTOVISCOPLASTIC NUMERICAL ANALYSES OF INCLINED SHALLOW SLOPES OF HOSTUN SAND UNDER SEISMIC ACTION

3.4. *Introduction*

In this chapter the first results, obtained using the code VIBRAZIONE, are illustrated; in particular the author focuses on the mechanical response of Hostun RF sand.

An inclined shallow infinitely long slope was considered four different angles of inclination (15°, 20°, 25° and 30°) are accounted for; the heights H considered for the slope are 5, 10, 15 and 20m.

The spatial discretization Δz was set equal to 0.2m; more details about this choice are presented in Appendix A.

The characteristics of the seismic input considered have already been illustrated in the previous chapter.

As was already explained in the previous chapters, before proceeding with the dynamic analyses is necessary to simulate the deposition process, to obtain the initial state of stress and initial internal variables. This operation was conducted as previously described, by adopting a purely elastoplastic model and by imposing for Hostun sand γ = 17 kN/m^3.

3.5. *Mechanical characterization of Hostun sand*

In this section the parameters used for the constitutive model are detailed. These have been obtained by simulating the experimental results of laboratory tests on Hostun sand.

The elastoviscoplastic model requires two sets of parameters (Table 4.1), representative of loose (D_R = 20%) and dense sands (D_R = 90%), in whose range the characteristics for layers of intermediate relative density are included.

In Figure 4.1 the results of standard drained compression tests simulated, for three different values of cell pressure are provided, these refer to sand specimens with initial density of 20% and another of 90%, respectively.

Looking at the results, by varying the parameters given by the viscoplasticity, the loose sand shows beyond a certain level of deviatoric strain its tendency to compact, while dense sand shows dilatancy and softening. The routine used to simulate the behaviour of the volume provides at each step the value of D_R. The final value are reported in Table

4.2. It is possible to recognize the influence of cell pressure even on the final value of the relative density: if the confining pressure p_c increases than the tendency to compact for loose sand grow up, while the tendency to dilate for dense sand decreases.

The analyses performed refer to dense Hostun sand.

Finally, through the load paths in the p'-q plane is possible a "Mohr-Coulomb" interpretation of the shear strength characteristics of the material. Evaluating the maximum loading ratio M, obtained in the test, can be deduced (less than tenths of a degree) a friction angle of 32° for loose sand and 38° (angle of peak) for the dense. Of course, this is a forced interpretation of a complex constitutive model using a simplified scheme: clearly the results of this operation may vary, for the same material, depending on the type of simulating test. In the following analyses, as explained in more details in the next paragraphs, a friction angle of 37.1° for dense Hostun sand was considered (Pisanò, 2007).

3.6. *Analysis of the dynamic response under amplified real accelerograms*

In this paragraph the author has taken, as seismic input, the amplified accelerograms for the soil types A, B and C. The ground motion parameter values for these accelerograms are reported in Table 4.3.

In Figure 4.2 (a, b, c, d, e and f) the time histories of the main variables of the system monitored at the base, middle and surface of the slope, are illustrated which are:

a) tangential stress and strain; displacement, velocity and acceleration in *x* direction;

b) normal stress and strain; displacement, velocity and acceleration in *z* direction;

c) relative density;

d) loading cycles in $\gamma_{xz} - \tau_{xz}$ plane;

e) friction angle along a horizontal plane, defined as the angle whose tangent is equal to the ratio between τ_{xz} and σ_z.

All these variables have been considered for the Friuli earthquake, Tolmezzo - Diga Ambiesta station (TMZ000), and geometry α = 15° and H = 5 m, while in the following only the most interesting variables will be analyzed.

In Figure 4.3 the isochrones, or the spatial profile given for 4 different time instants (variable depending on the accelerograms considered) are shown for TMZ000 (α = 15° and H = 5 m). In this paragraph the author will neglect the Friuli earthquake, which will be considered in the following with the other not amplified accelerograms for soil type A.

Analyzing the results obtained by the code VIBRAZIONE, for the Irpinia earthquake the permanent parallel (to the plane of the slope) displacements are of several meters, especially for an inclination angle of the slope α = 30° (Figures 4.4, 4.5, 4.6 and 4.7).

The higher displacement is equal to 17 m, for the registration CTR000, amplified by a factor of 4, and for the geometry α = 30° and height H = 20 m.

Using as seismic input the records of Campobello di Mazara and Borgo - Cerreto Torre permanent horizontal displacement are much smaller, resulting less than 50 cm (Figures 4.8, 4.9, 4.10 and 4.11).

Such extreme values are real singularity, hence the use of the term "localization", for the distributions of the system variables, which are regular in the remaining areas of the domain.

The instability condition of the system manifests, therefore, considering a slope of very dense material, through the formation of a plane of weakness (shear band), characterized by a decreased relative density, because of dilatancy, and thus a degradation of initial mechanical properties. After the formation of this plane is acceptable to assume that the sliding of the top part of the domain on the lower takes place along it, if rigid. To confirm this, it is enough to examine the displacement profiles in the x direction, where the isochrones show visibly the singularity discussed above (Figure 4.12), with a reduction of relative density of the ground, decreasing from 90% to about 26%.

Thus the rigid body scheme often used in practice seems not be suitable: it can possibly be effective for studying the dynamics of rock masses, in which the planes of discontinuity, usually present, constitute preferential pathways for sliding of some blocks on the masses below.

In the present case the soil-rock interface could be a plane of weakness, except to note that the localizations do not always occur at the maximum depth, remaining on the contrary rather superficial. For this reason in earth slopes will occur the first phase of the wave propagation in deformable soil and then could establish a sliding mechanism with good approximation rigid, of course this second stage will occur only if the initial stress-strain state and the magnitude of the stress are such as to trigger localization.

Therefore, it is necessary to define strategies for the identification of possible planes of weakness due to instability caused by previous earthqauke.

In general, imposing an angle of inclination of the slope, the displacements are growing with increasing of the slope height.

Exceptions are cases STU000x2, with α = 30°, B-BCT000x2.5 and B-BCT090x2.5, with α = 25°, for which the higher displacements occur at the lower height H = 5 m of the slope.

The higher surface settlements take place, instead, for accelerograms CTR000x4, for the condition α = 25° and H = 15m, and STU000x2, for the condition α = 30° and H = 5m, and they are approximately equal to 0.5 m; in both cases there are localization phenomena with a reduction in relative density below 30% (see Figure 4.13).

In addition to the failures several cases of heave of the ground level have also occurred, the highest value equal to 0.14 m has been for the accelerograms CTR000x4 and CTR270x3, in both cases for the geometry α = 20° and H = 20m (see Figure 4.14).

With regard to the horizontal acceleration there is a large damping of the negative acceleration values for a slope inclination of 30° and, in particular, for height H = 20 m; some examples are reported in Figures 4.13 and 4.14.

Concerning the friction angle mobilized in many cases the limit breaking value of material, equal to 37.1°, is exceeded; for the considered accelerograms of Irpinia earthquake it happens in the 30% of cases, while for the registration Campobello di Mazara and Borgo-Cerreto Torre in at least the 20% of cases. In Figure 4.15 are reported three examples of exceeding the limit value, in particular, the last case shows how the geometry α = 25° and H = 5m is the most disadvantageous.

As was mentioned, the output of VIBRAZIONE provides the values of the variables calculated in the middle and at the surface of the slope, in particular, for the mobilized friction angle can be said that the highest values are usually recorded in the middle of the layer, where is also higher the frequency of exceeding the limit value.

Finally looking at the load cycles (at the middle of the layer) can be seen that there are many yielding. Considering the Irpinia earthquake and the accelerograms CTR000x4 (α=25°, H=15m) and STU000x2 (α=30° and H=5m) the deformations are equal to 45% and 90% respectively, while for the other accelerograms they remain under 0.5% (Figure 4.15).

For the considered earthquake for soil type B and C, only the horizontal displacement are discussed (Figures 4.16 to 4.35), being useful in the next paragraph for the comparison with those obtained using the displacement method.

The higher values are obtained for the Umbria Marche earthquake, geometry α = 30° and H = 30m, registration A-NCR000 (soil type B) and A-CLF000 (soil type C), amplified by a factor 2, equal to 5.85 m and 17.3 m, respectively.

Also in these cases such high displacements are due to localization, in the upper part of the slope, with a reduction of relative density from 90% to less than 30%.

64.. *Comparison with Newmark method (amplified accelerograms).*

In this section the results already obtained by code VIBRAZIONE, in terms of displacement, are compared with those obtained employing the Newmark method.

This is useful to assess if and how the model in question is able to overcome the limits of old design procedures as Newmark method, that in any case provides approximate results but still very useful for evaluating the reliability of analysis more complex, resulting for this, as well as for its simplicity, very popular among engineers.

The Newmark method assumes that the entire slope can be designed as a single block, of longitudinal extent irrelevant but rigid, being this the most important simplification made by the method. The rigid block is supposed to overcome a rocky substrate, to which it is linked by means of an interface to pure friction (non-cohesive) and flat (no dilation). If a

seismic input of pure shear comes close to this interface and triggers the motion of the system, the block can:

1) jointly move to the bedrock, as long as the resistance offered by the interface, assumed at Mohr-Coulomb, is able to balance the various static or inertial actions applied;

2) accelerating under the maximum force transmitted from the sliding plane, in case such resistance is not sufficient. Only in this case relative sliding between bedrock and overlying block will occur, which then stop when the values of base acceleration are such that the interface resistance was not overcome. (See Figure 4.36)

The dynamic of the slope so described is reduced to the motion of a rigid body along a rough surface, whose constitutive law is rigid-plastic. The friction between the block and the substrate tends to dissipate the relative motion, when present, reducing the force of inertia acting on the first, thus the response of the system will be stable in all cases (relative displacement of the system always limited), due to the dissipation and the indeformability of the contact below the breaking point, hence the impossibility to observe resonance phenomena.

Furthermore, this contact is perfectly flat so an input of pure shear can never create motion components in the normal direction, possibility allowed only in presence of dilatancy.

In displacement methods derived from the rigid block Newmark model (1965), the seismic action is defined by a time function, eg. an accelerogram, and the response of slope to the seismic action is evaluated in terms of cumulated displacements, being the integration in the time of the equation of relative motion between the potentially unstable mass and bedrock.

The potential landslide body, subject to the weight force and the seismic action, moves along the sliding surface whenever the acceleration at the base, a(t), exceeds a threshold value, called critical acceleration K_c, characteristic of the incipient collapse conditions; the displacement vanishes when the acceleration, changing of sign, is such as to cancel the relative velocity between the landslide body and the stable ground.

In case of dry slope:

$$K_c = \frac{\cos\alpha * tg\varphi' - \sin\alpha}{\sin\alpha * tg\varphi' + \cos\alpha}$$

where φ' is the friction angle and α the inclination angle of the slope. The values of K_c for different inclinations are shown in Table 4.4.

Therefore, the final displacement will be greater the greater is the number of times the acceleration, caused by the earthquake, exceeds the critical acceleration and especially the greater the time interval in which this situation occurs. This means that the displacement strongly depends on the frequency content of the seismic action, further than its size, and on geometric and geotechnical characteristics of the slope, of which also the critical acceleration is function.

To perform the analysis using the Newmark method was necessary to calibrate the model in order to compare the results with those already available from VIBRAZIONE.

Having already defined height and inclination of the slope, as well as the specific weight of the soil, the only uncertainty concerns the value of the friction angle for two reasons:

1) Newmark method refers to the roughness of the rock-soil interface, which in finite difference model does not really exist;

2) even if it is assumed as interface friction angle that of the above ground, it must be remembered that among the parameters of the elastoviscoplastic model the friction angle does not explicitly appear.

So the equivalent friction angle should be identified by simulating the nonlinear relationship of laboratory tests; in particular a sample consolidated under a effective isotropic pressure of 100 kPa was considered and submitted to a simple shear test, tying the displacement in direction 2 and 3 and keeping constant the value of σ_1, applying at the boundary a shear stress σ_{13} and inducing an angular distortion in the sample γ_{13}.

It is worth noting that this test is precisely the same kinematic constraint conditions to which all points of the undefined slope are subjected. In this case the determination of the friction angle is immediate because $\varphi' = \arctan(t/\sigma_1)$ (Figure 4.37).

The angle friction is therefore equal to 37.1, more details are given in Pisanò (2007).

For the calculation of displacements with Newmark method, in this paper was used a simple code, implemented using Matlab software.

To compare the displacements obtained with VIBRAZIONE (d_{vibr}) and those obtained with the Newmark method, it is used the ratio Δ/d_{vibr}, where Δ is the difference of the displacements calculated with the two methods ($d_{vibr} - d_{newark}$). This ratio is reported in Figure 4.38 in function of the ratio K_c/a_{max}, the Arias Intensity 5-95% and the Destructive Power 5-95% respectively.

It is worth noting that in the 95% of the results, the values of the displacement calculated with the Newmark method are lower than the 20% of those obtained by means of VIBRAZIONE.

5.4. ***Analysis of the dynamic response under real accelerograms***

In this paragraph the author has taken, as seismic input, the accelerograms for the soil types A (Database SISMA). The ground motion parameter values for these accelerograms are reported in Table 4.3.

Analyzing the results obtained by the code VIBRAZIONE, the higher permanent parallel (to the plane of the slope) displacements have been occurred for the Irpinia earthquake, Sturno station: in particular for STU000 accelerograms and the geometry α=30, H =15 and 20 m, the displacements are equal to 16 m and 6.7 m, respectively; while for STU270 accelerograms and the geometry α=30, H =10 and 20 m, the displacements are equal to

5.3 m and 5.6 m, respectively. (Figures 4.39, 4.40, 4.41, 4.42, 4.43 and 4.44). In all these cases, such high values are due to localization and an amplification of the accelerograms on surface; examining the displacement profiles in the x direction, the isochrones visibly show these singularities, with a reduction of the relative density of the ground, decreasing from 90% to less than 30%. (Figure 4.49).

Using as seismic input the records of Campobello di Mazara and Borgo - Cerreto Torre permanent horizontal displacement are much smaller, resulting less than 5 cm (Figures 4.45, 4.46, 4.47 and 4.48).

In general, imposing an angle of inclination of the slope, the displacements are growing with increasing of the slope height, also if for TMZ station higher displacements occur for H=15 m and not for H=20 m.

The higher surface settlement takes place, instead, for accelerogram TMZ270, for the condition α = 15° and H = 20m, and it is approximately equal to 0.04 m (Figure 4.50); for this geometry the higher vertical displacements are recorded. The case STU000, geometry α = 30° and H = 15m, represent an exception with a vertical displacement equal to 1m.

In addition to the failures several cases of heave of the ground level have also occurred, the highest value equal to 0.05 m has been recorded for the accelerogram TMZ000, geometry α = 30° and H = 10m (see Figure 4.51).

Considering Mazara and Umbria Marche earthquakes, the vertical displacements are lower than 1 cm.

With regard to the horizontal acceleration there is the well known damping of the negative acceleration values for a slope inclination of 30° as it can be seen from Figure 4.51.

Concerning the friction angle mobilized in many cases the limit breaking value of material, equal to 37.1°, is exceeded; for the considered accelerograms of Irpinia and Friuli earthquakes it happens in the 20-30% of cases, while for the registration Campobello di Mazara and Borgo- Cerreto Torre in happens only for the geometry α = 25° and H = 5m; this geometry is characterized by high values of φ' (Figure 4.52).

As the previous case, the highest values of the mobilized friction angle are usually recorded in the middle of the layer, where is also higher the frequency of exceeding the limit value.

Finally looking at the load cycles (at the middle of the layer), considering Irpinia earthquake, the deformations vary from 20% to 80%, while for Friuli earthquake are lower than 5%.

64.. ***Comparison with Newmark method (real accelerograms).***

In this section the results already obtained by code VIBRAZIONE, in terms of displacement, are compared with those obtained employing the Newmark method.

The code used shows how the seismic input is amplified as it goes through the layer and as the relative density can greatly decrease, aspects not taken into account by the Newmark method.

For this reason, the accelerogram obtained by VIBRAZIONE in the middle and at the surface of the slope (for any geometry), in addition to the those considered for soil type A, are used as seismic input, imposing the friction angle corresponding to the real relative density: such values are obtained by interpolation of limit values $\varphi' = 32°$($D_R = 20\%$) and $\varphi' = 37.1°$($D_R = 90\%$).

Also in this case, the ratio Δ/d_{vibr} is reported in Figure 4.53 in function of the ratio K_c/a_{max}, the Arias Intensity 5-95% and the Destructive Power 5-95% respectively.

By the comparison of results, in terms of displacements, obtained with the two methods appears that:

- using as seismic input the accelerogram at the base, in 98% of the cases the displacement evaluated with Newmark method are the 20% of those calculated using VIBRAZIONE;
- using as seismic input the accelerogram in the middle of the layer, this percentage drops to 92% and in 2% of cases Δ results negative;
- using that one on the surface, only in the 20% of the cases the displacements calculated with Newmark method are less than 20% of those calculated with VIBRAZIONE and in 13% of cases Δ results negative.

This shows how the two methods are closer when it is taken into account the amplification of the accelerogram in the soil and the decreasing of relative density.

The negative values of Δ are due to the dynamic amplification of seismic input, in particular for the geometry $\alpha = 25°$ and H = 5m.

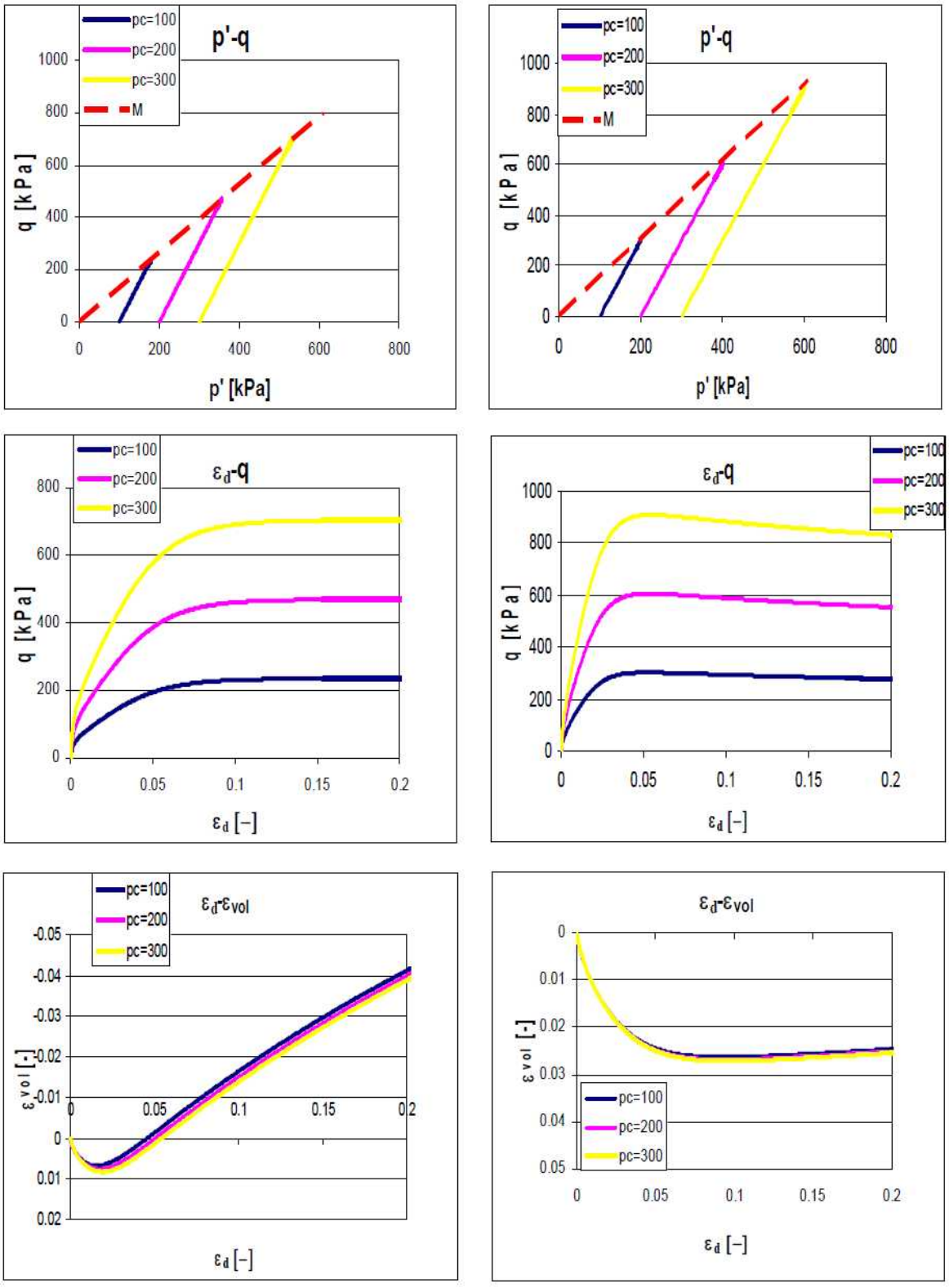

Figure 4.1. Standard drained compression tests on loose and dense Hostun sand simulated by elastoviscoplastic model.

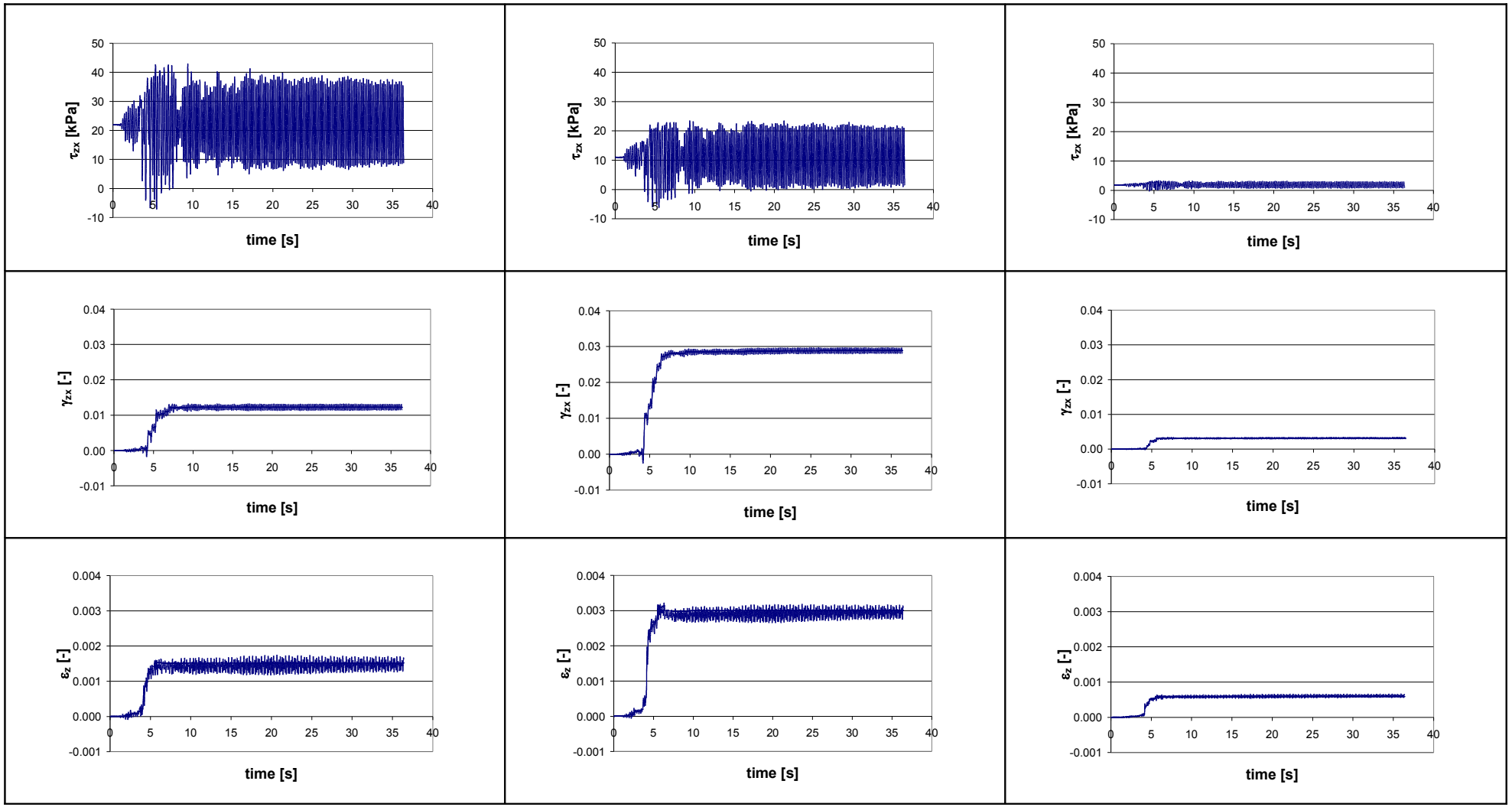

Figure 4.2 (a). Tangential stress and strain, vertical strain (base, middle and top of the layer), Hostun sand.

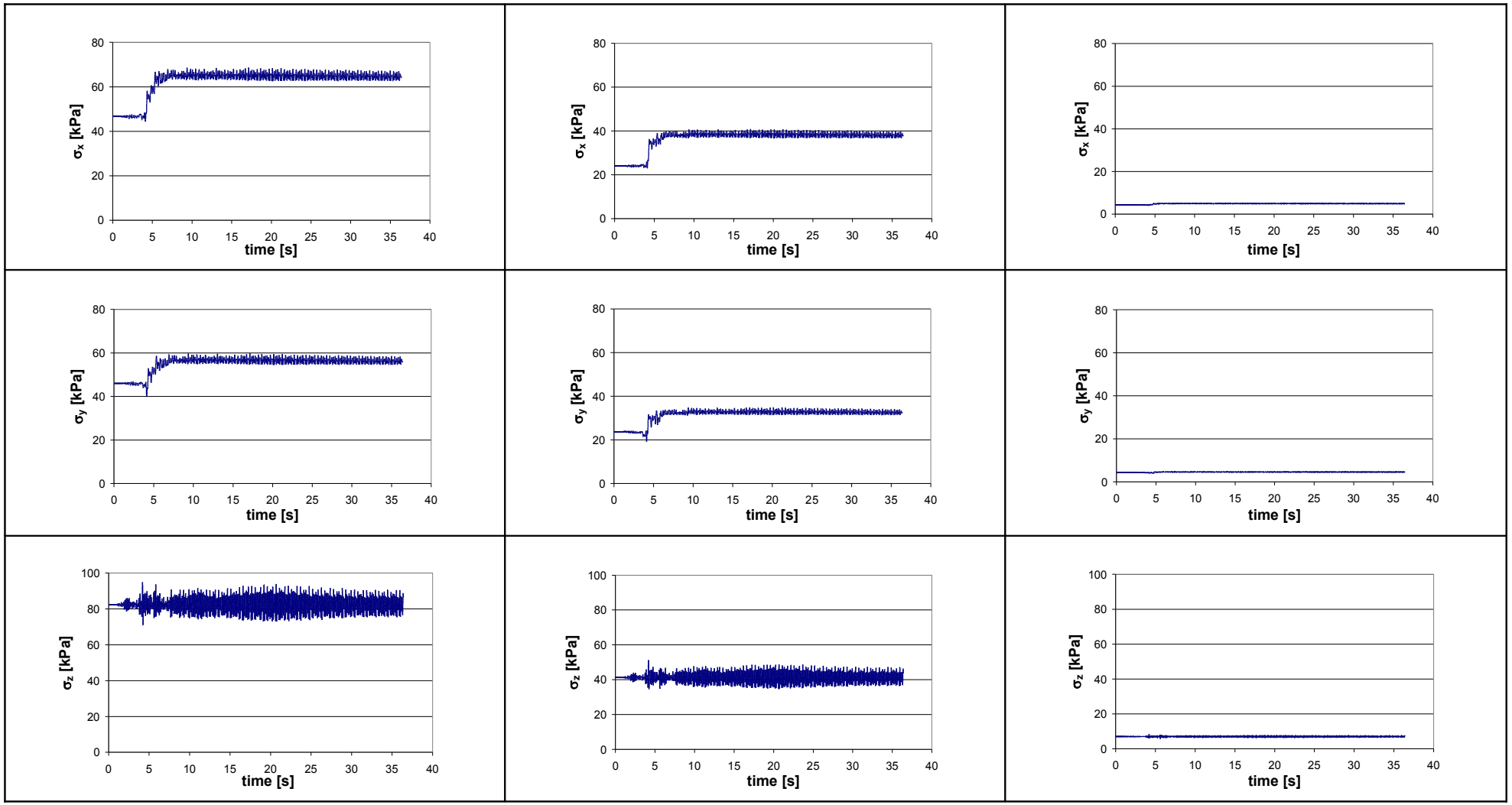

Figure 4.2 (b). Stress in x, y and z direction (base, middle and top of the layer), Hostun sand.

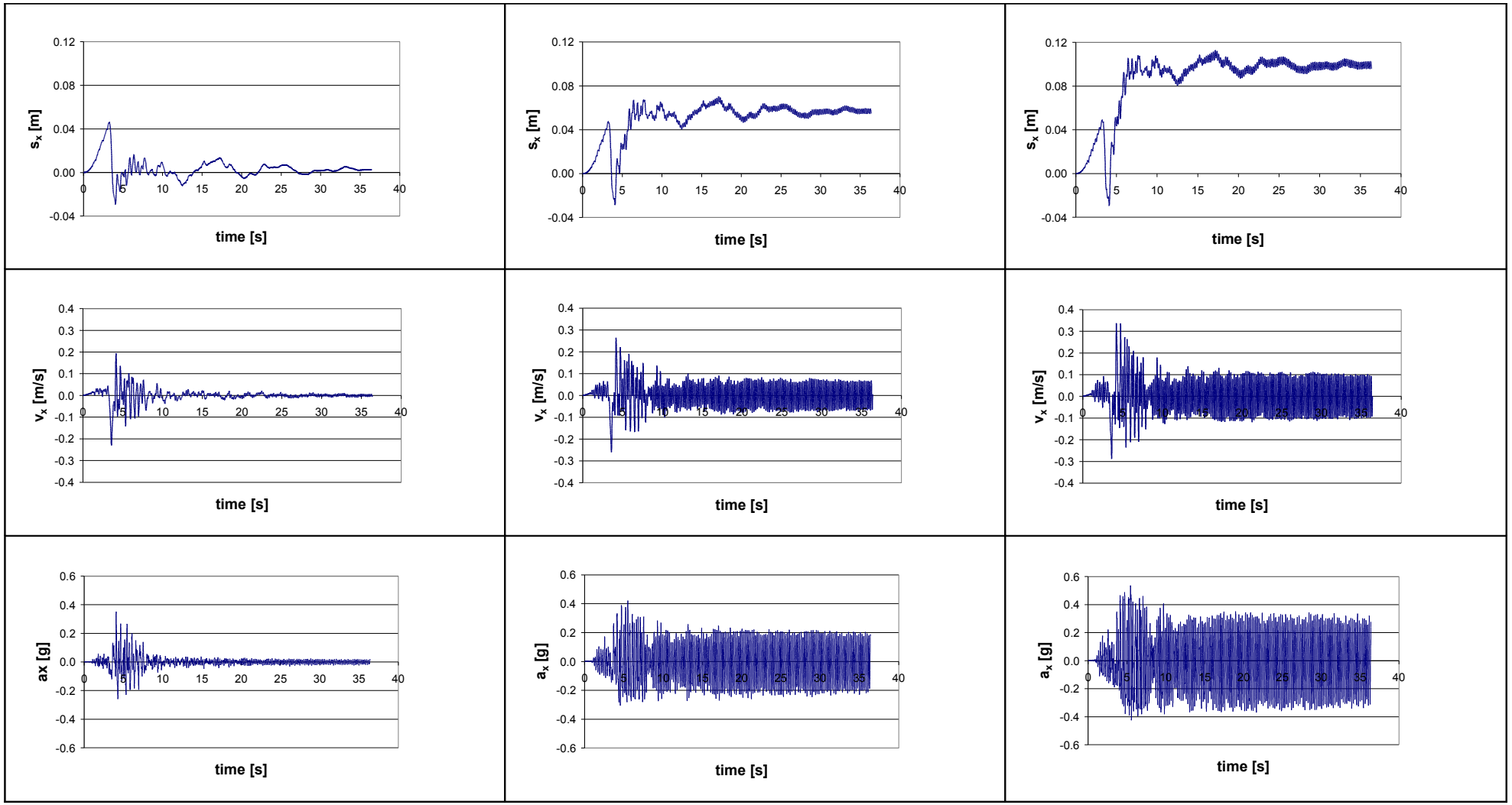

Figure 4.2 (c). Displacement, velocity and acceleration in x direction (base, middle and top of the layer), Hostun sand.

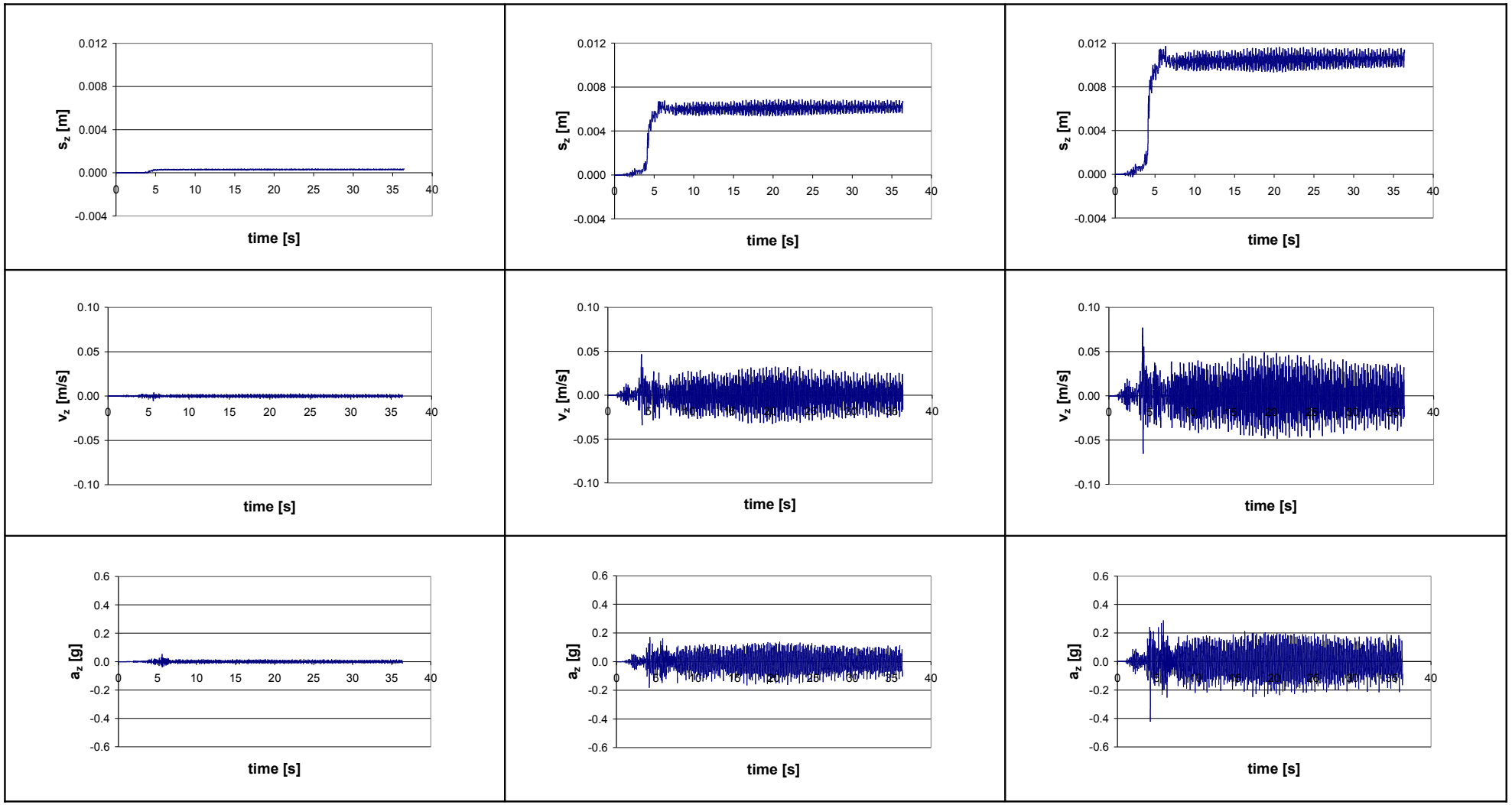

Figure 4.2 (d). Displacement, velocity and acceleration in z direction (base, middle and top of the layer), Hostun sand.

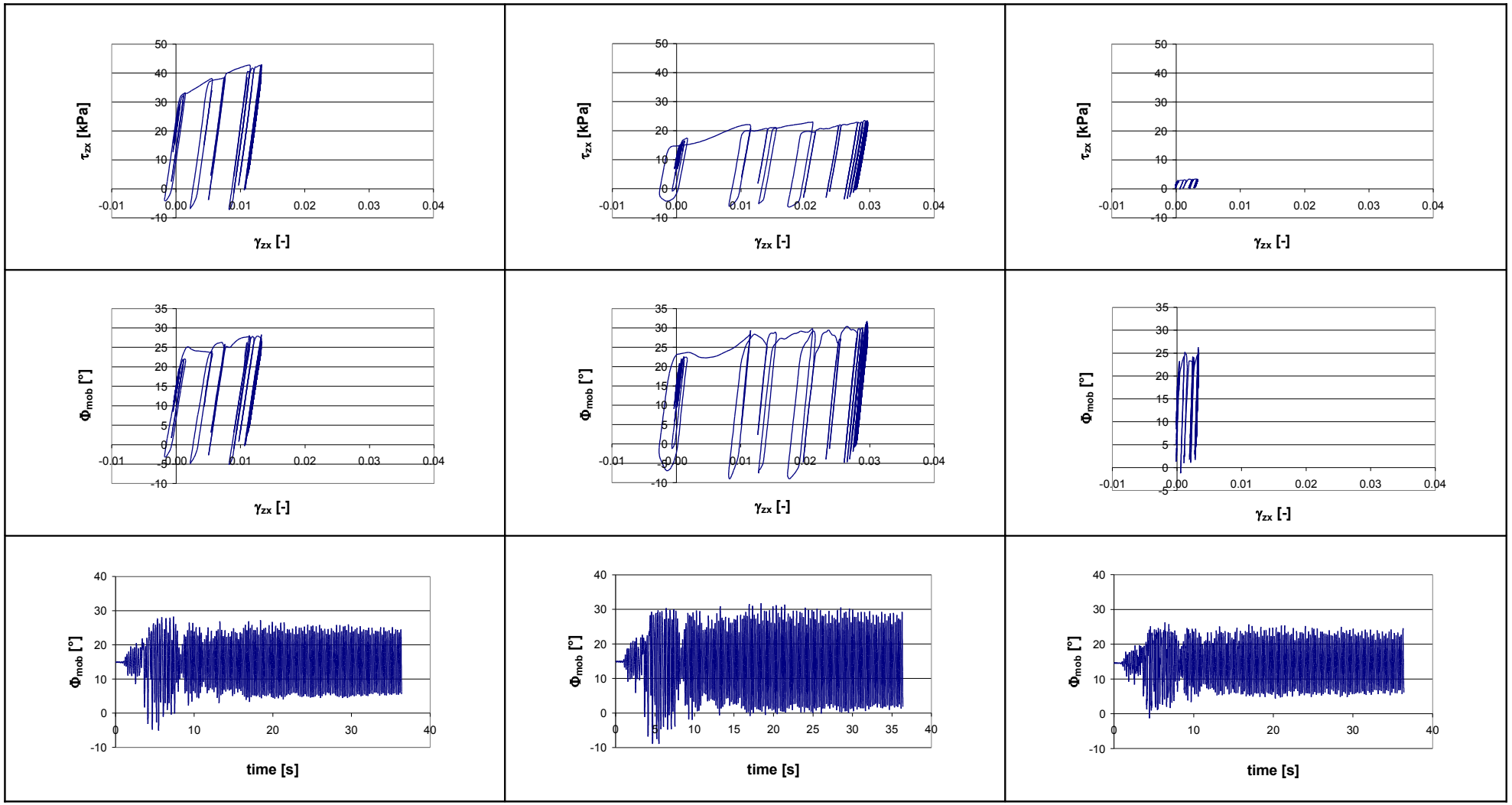

Figure 4.2 (e). Loading cycles and friction angle (base, middle and top of the layer), Hostun sand.

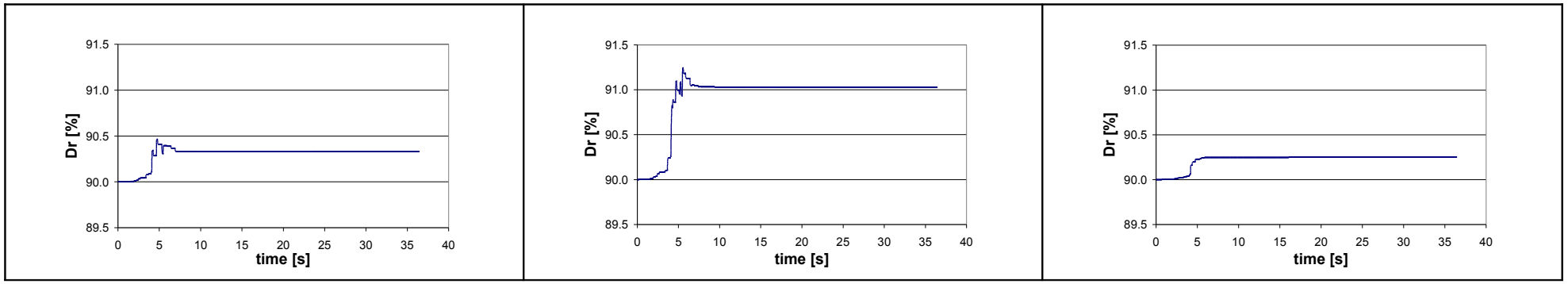

Figure 4.2 (f). Relative density (base, middle and top of the layer), Hostun sand.

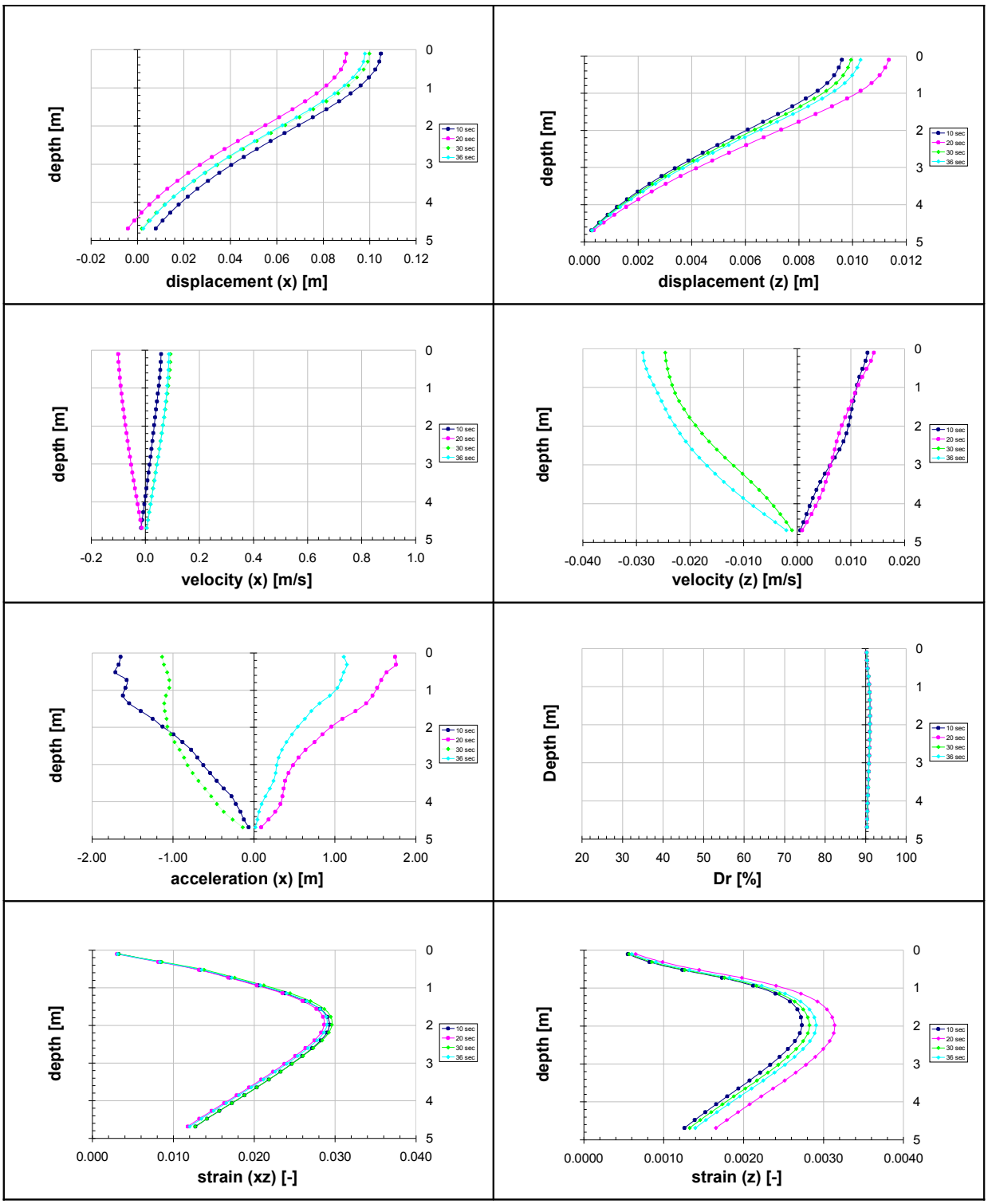

Figure 4.3. Isochrones of displacement and velocity (x and z), acceleration (x), relative density and strain, Hostun sand.

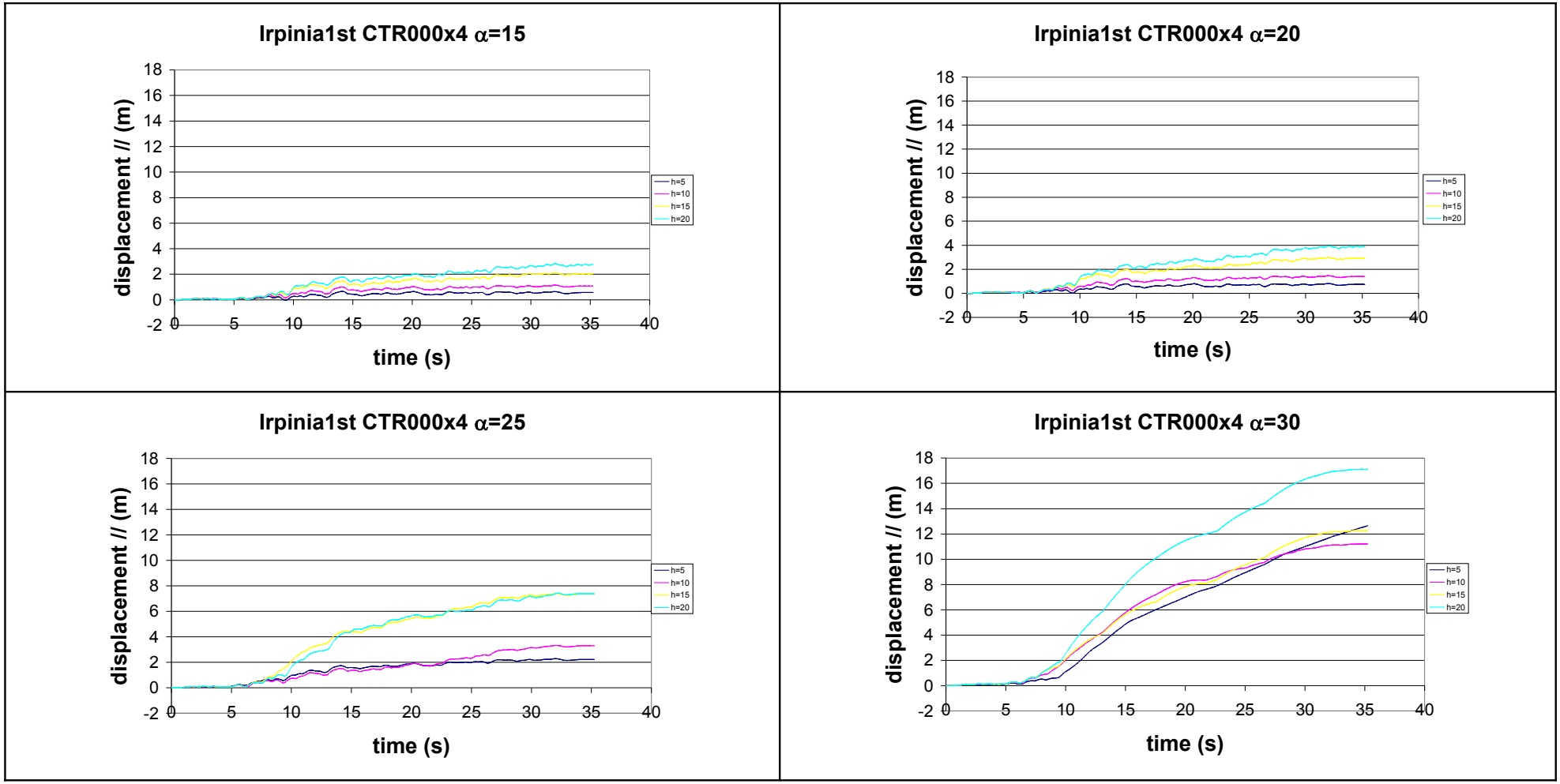

Figure 4.4. Permanent horizontal displacements, accelerogram CTR000, amplification factor 4, soil type A.

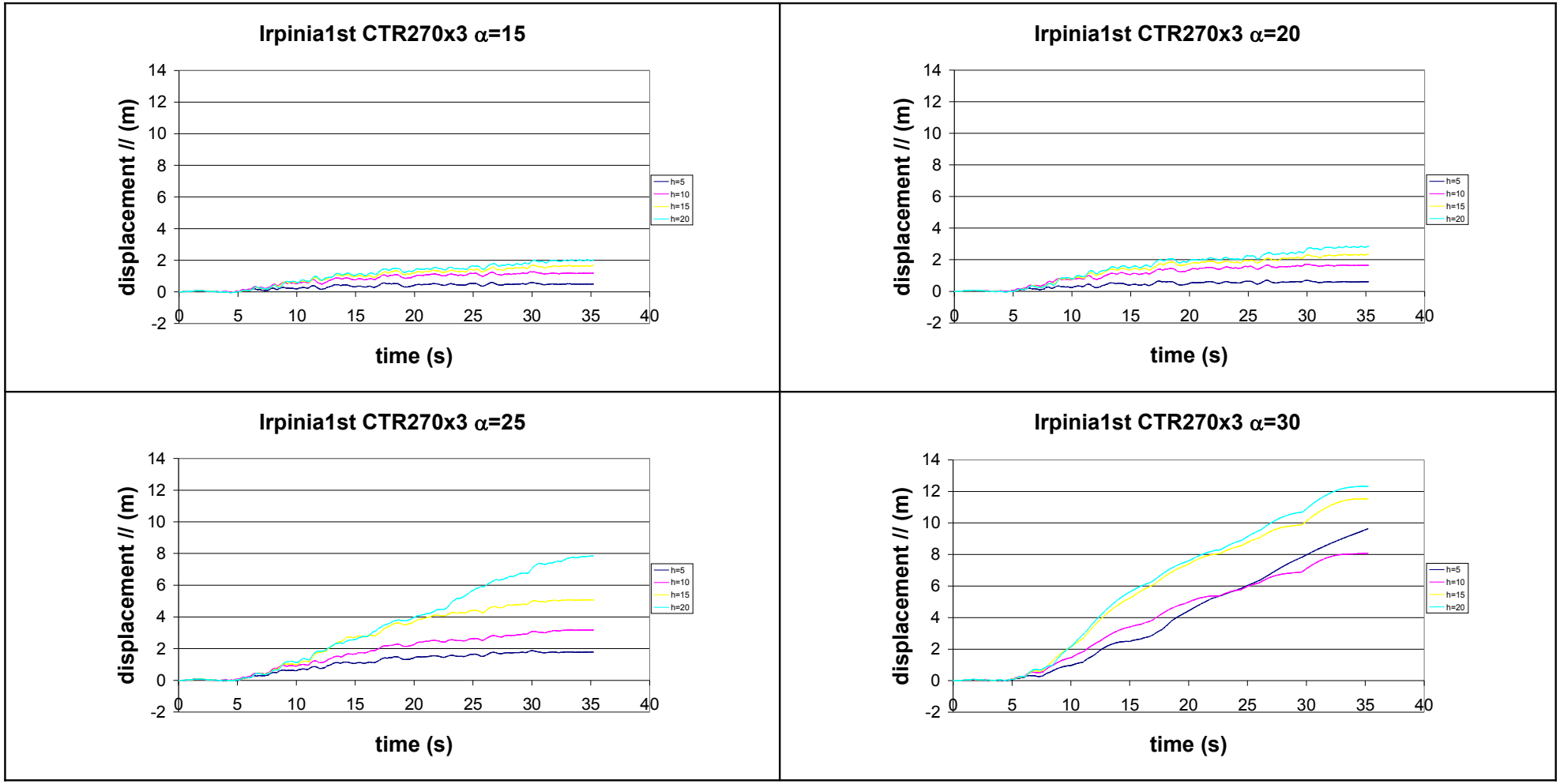

Figure 4.5. Permanent horizontal displacements, accelerogram CTR270, amplification factor 3, soil type A.

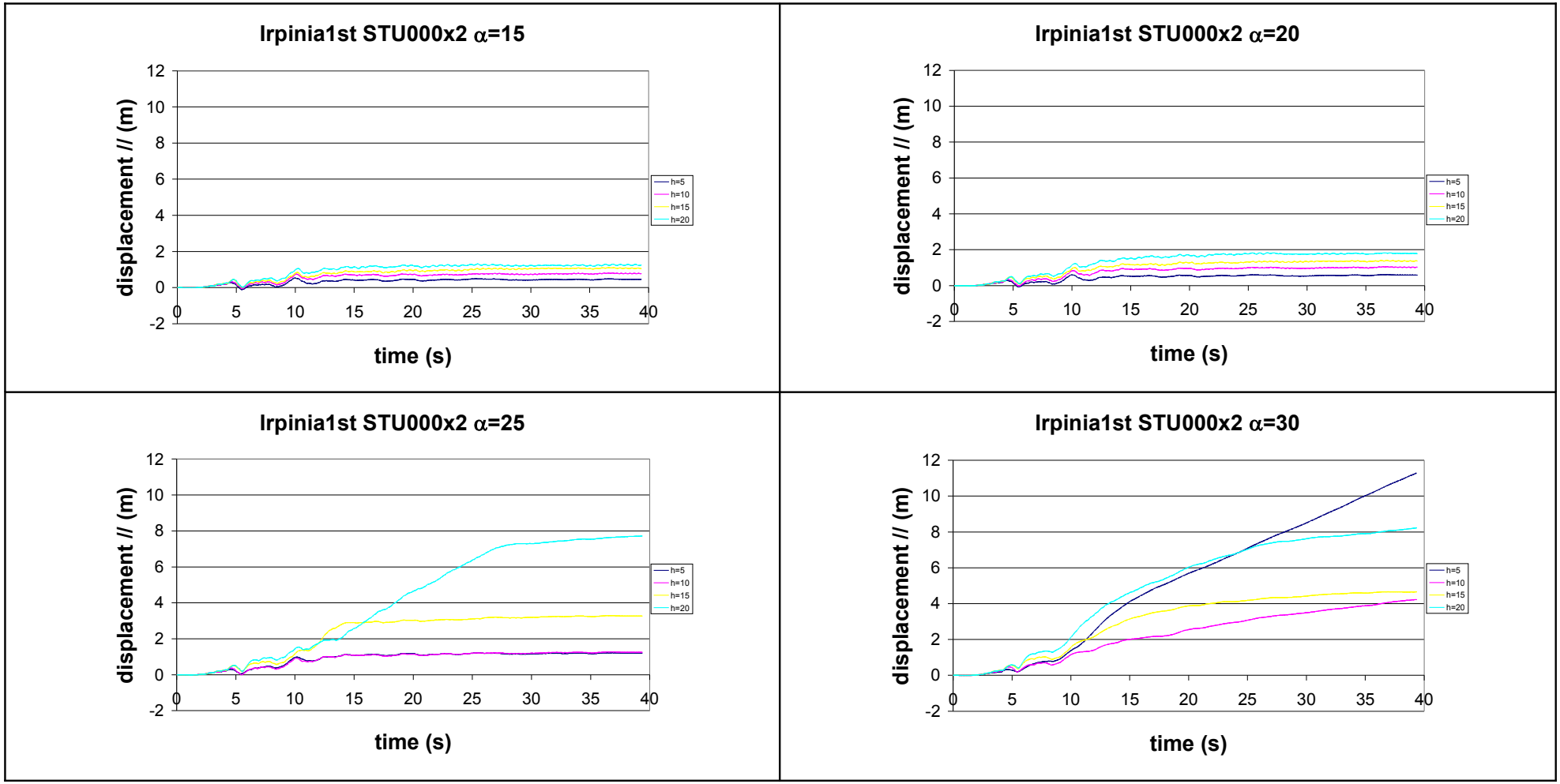

Figure 4.6. Permanent horizontal displacements, accelerogram STU000, amplification factor 2, soil type A.

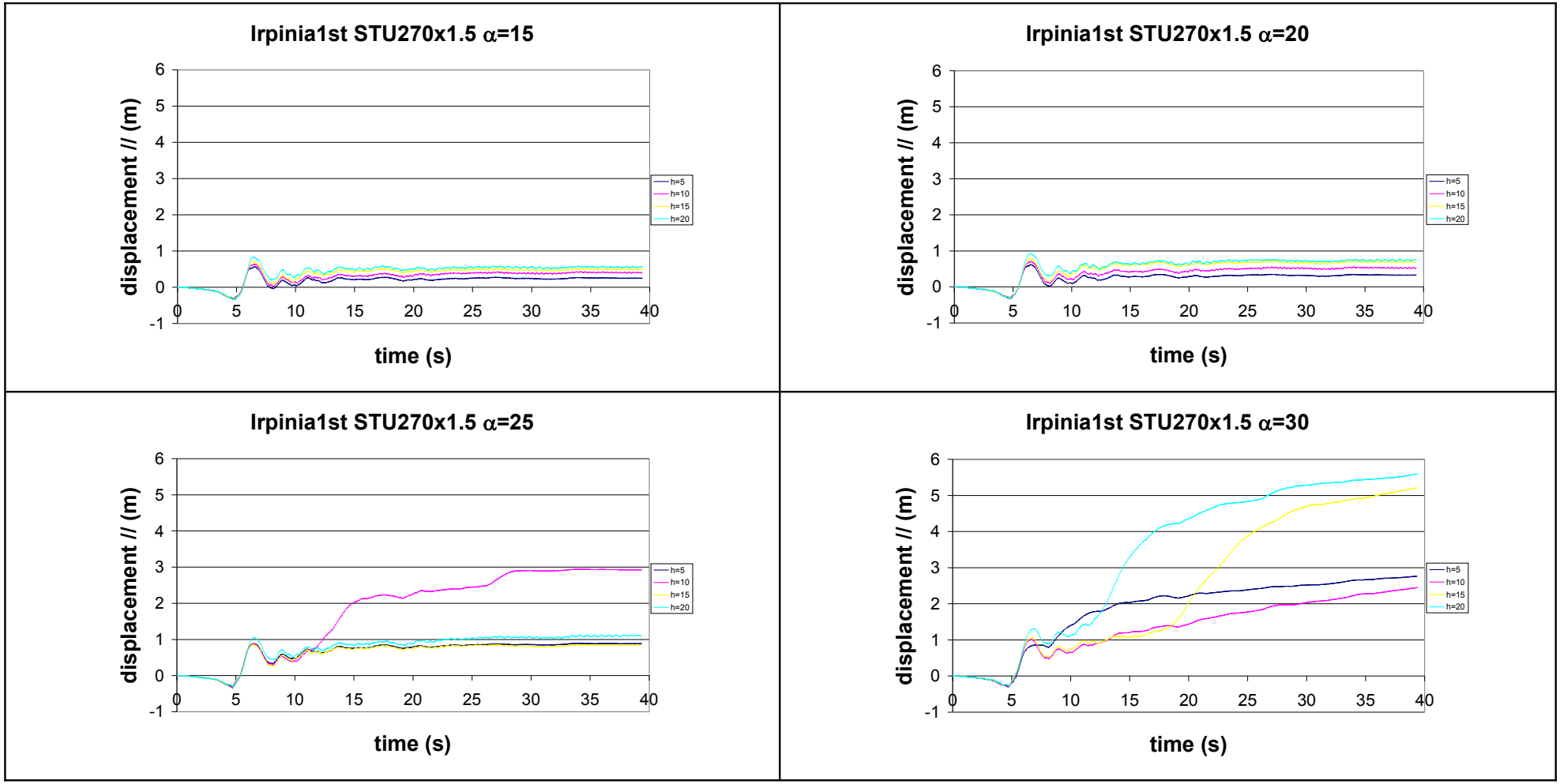

Figure 4.7. Permanent horizontal displacements, accelerogram STU270, amplification factor 1.5, soil type A.

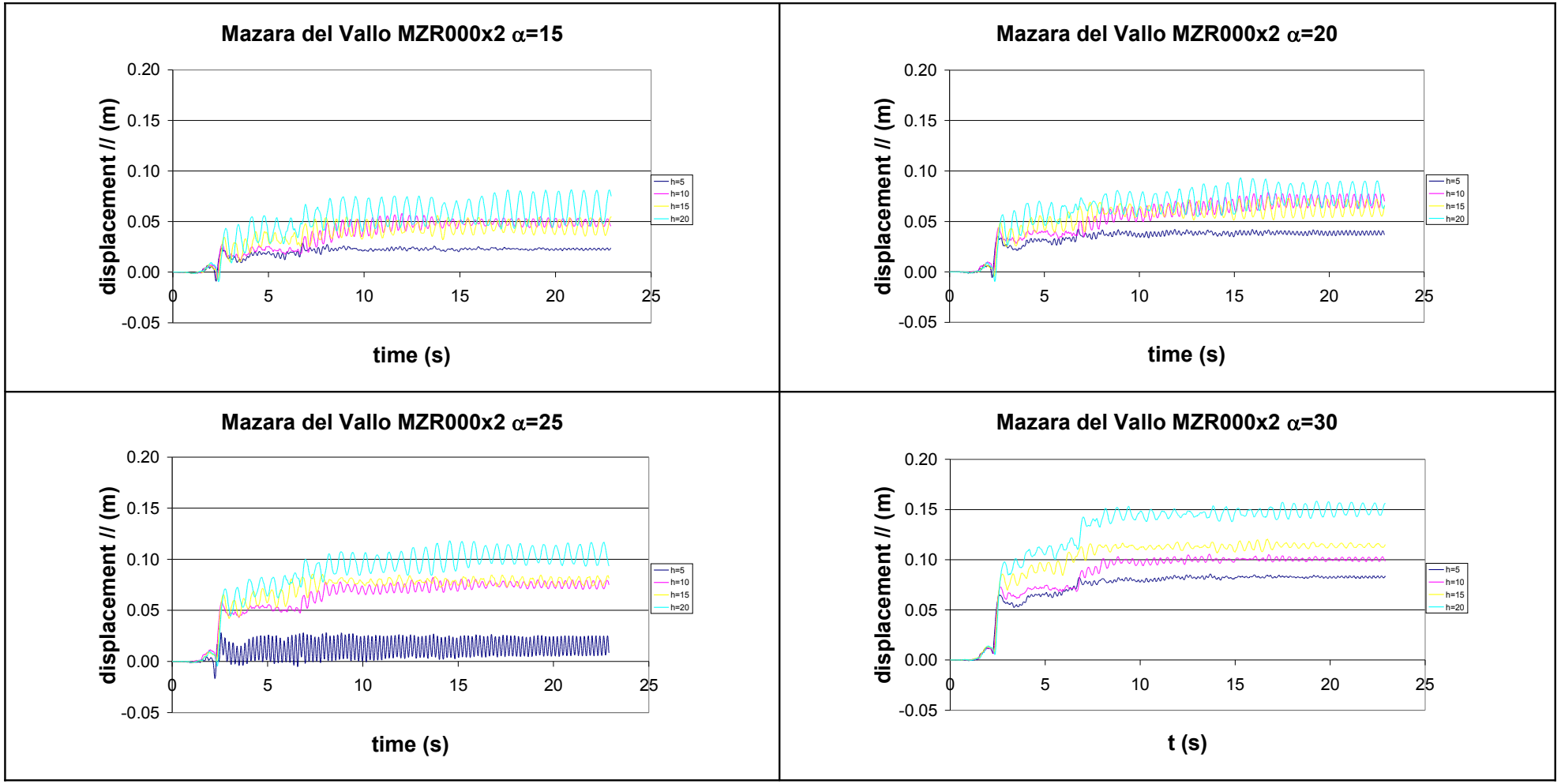

Figure 4.8. Permanent horizontal displacements, accelerogram MZR000, amplification factor 2, soil type A.

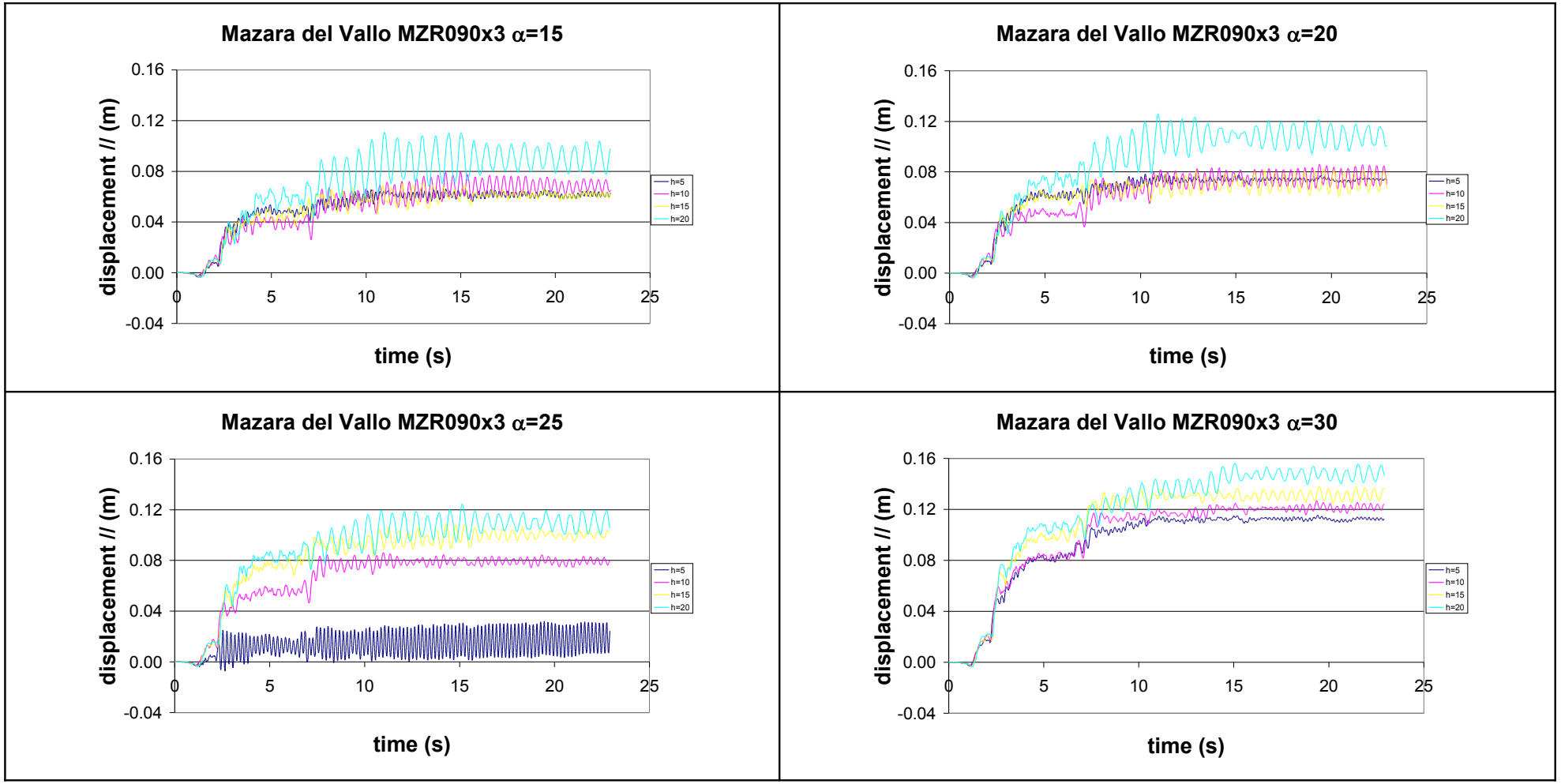

Figure 4.9. Permanent horizontal displacements, accelerogram MZR090, amplification factor 3, soil type A.

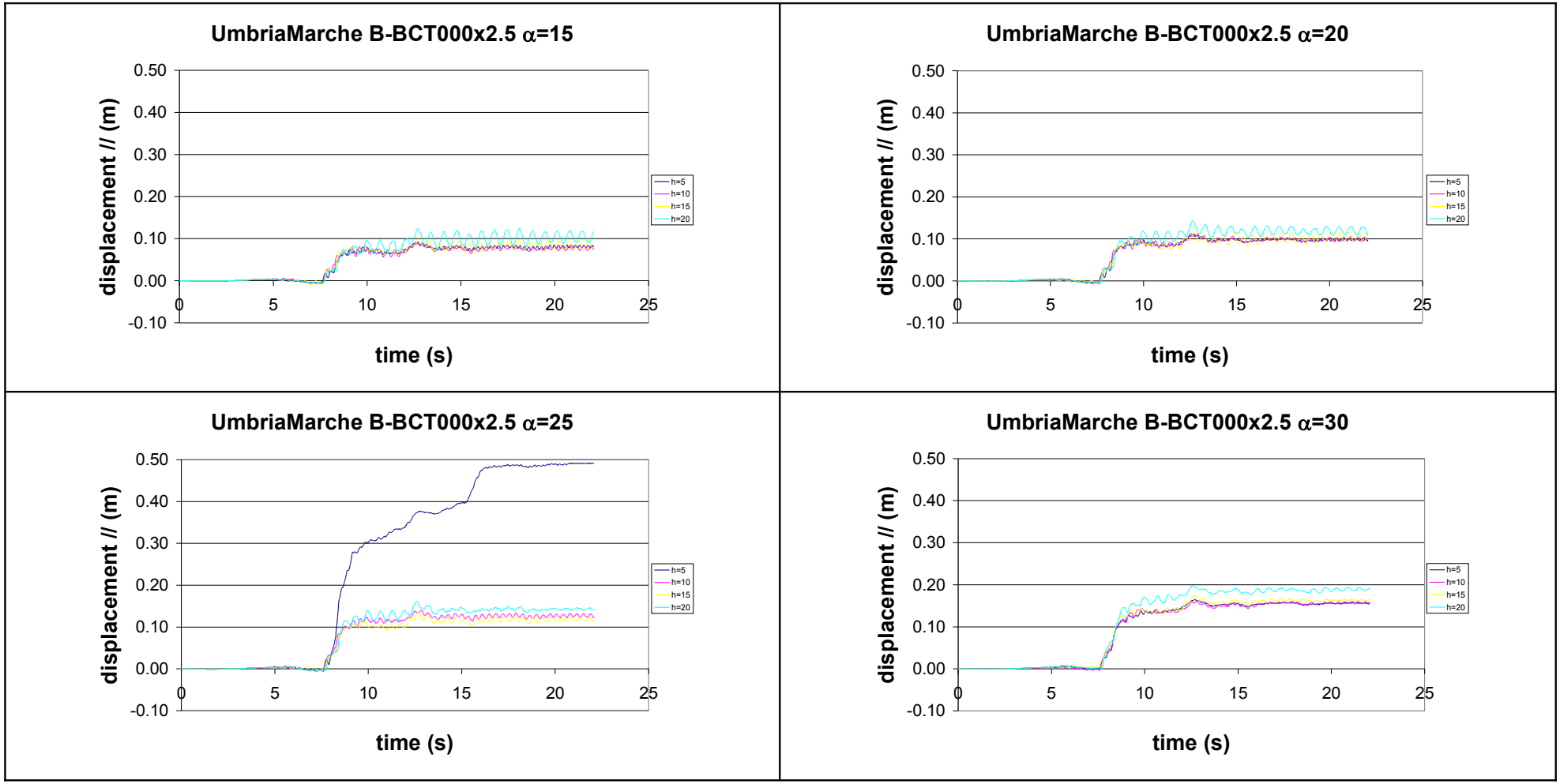

Figure 4.10. Permanent horizontal displacements, accelerogram B-BCT000, amplification factor 2.5, soil type A.

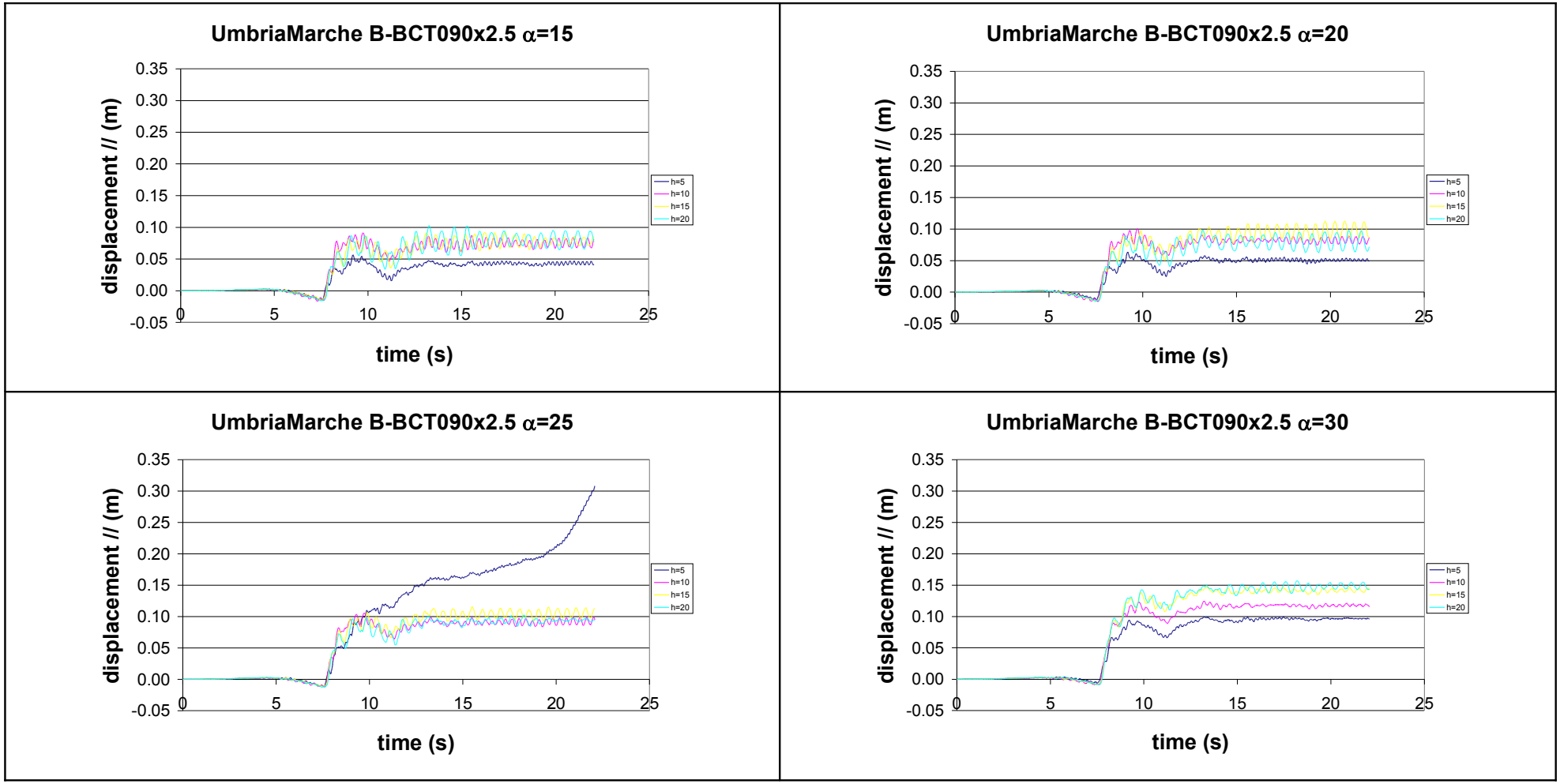

Figure 4.11. Permanent horizontal displacements, accelerogram B-BCT090, amplification factor 2.5, soil type A.

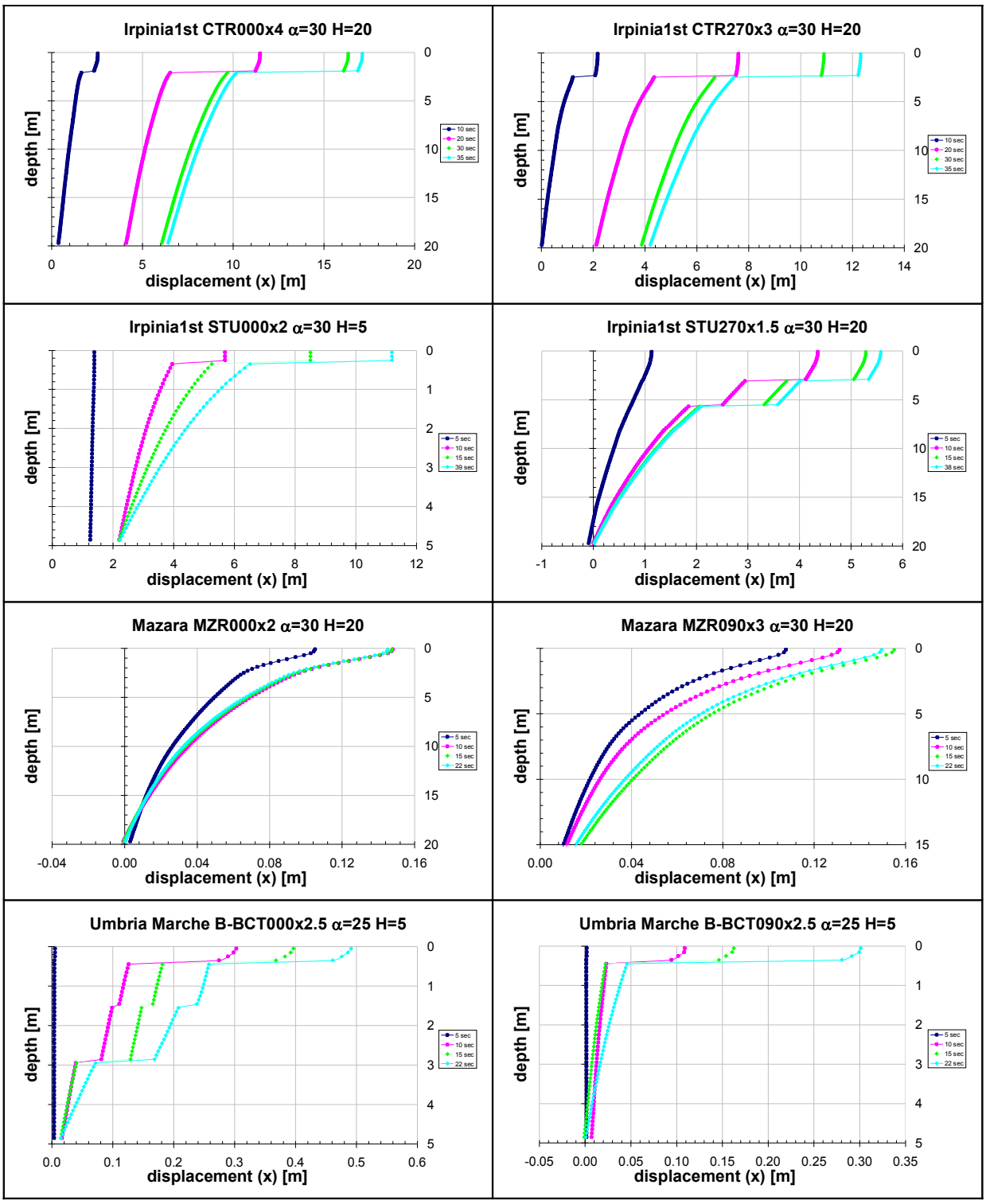

Figure 4.12. Isochrones for maximum horizontal displacements.

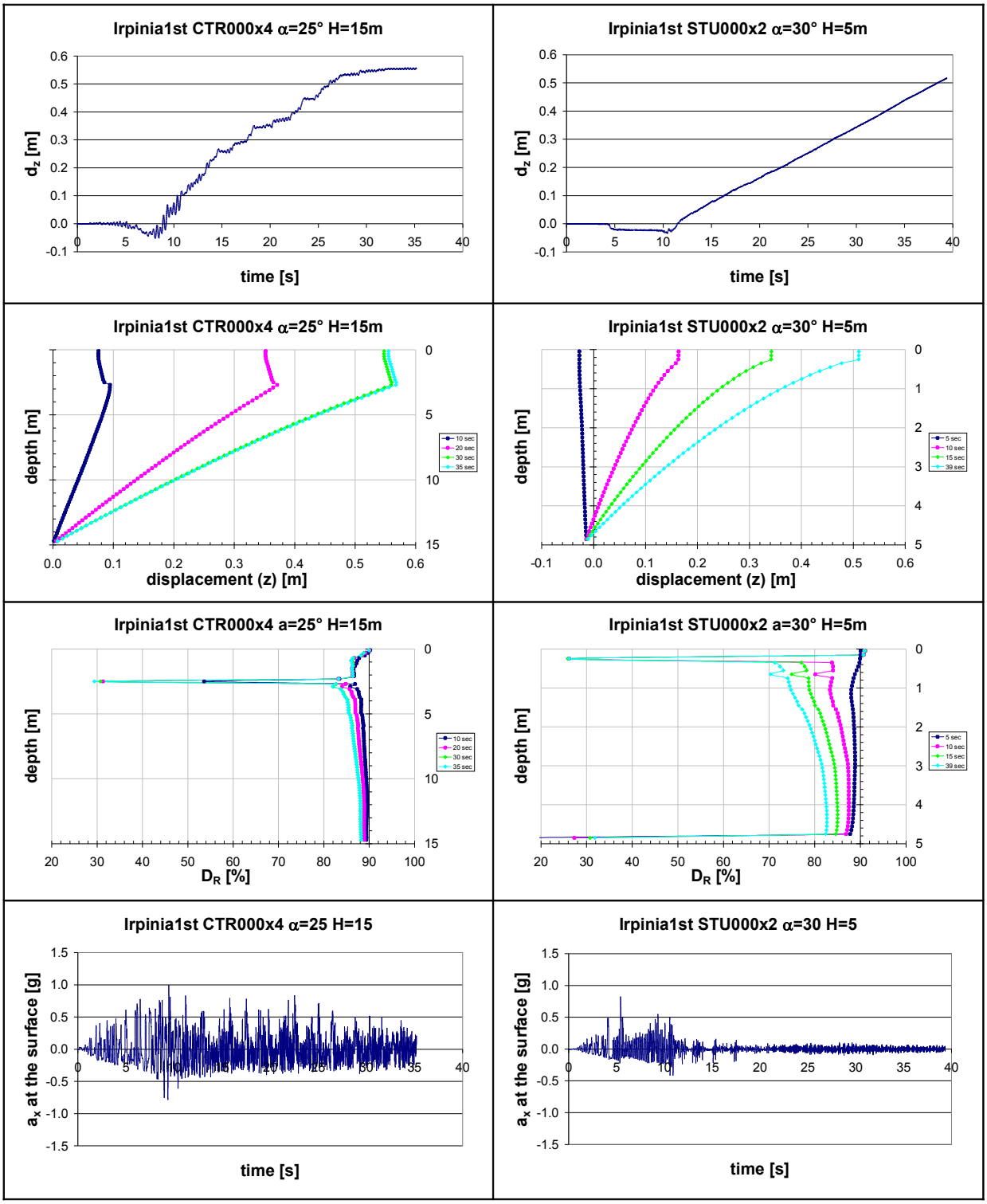

Figure 4.13. Vertical displacements and relative isochrones; horizontal acceleration.

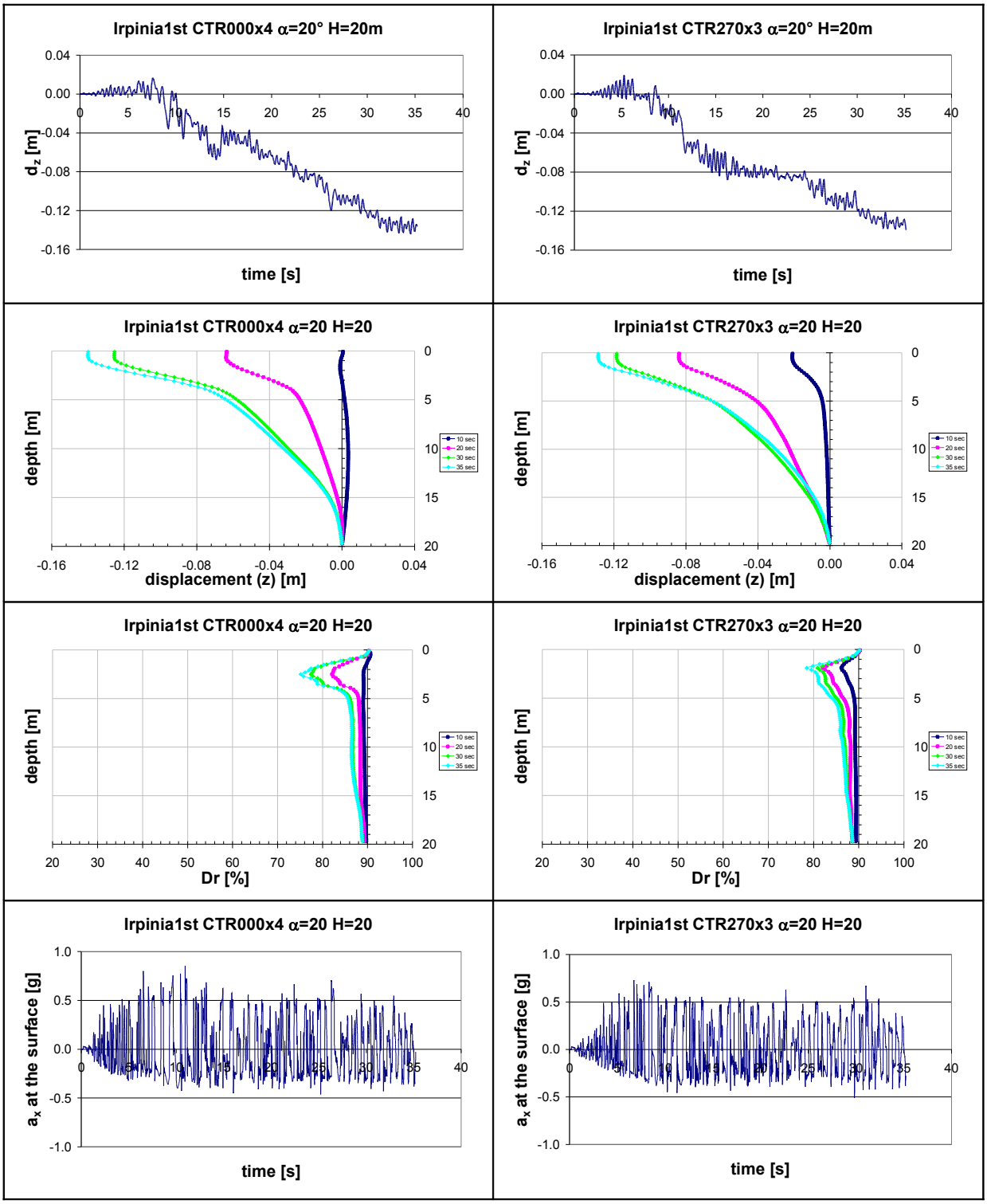

Figure 4.14. Vertical displacements and relative isochrones; horizontal acceleration.

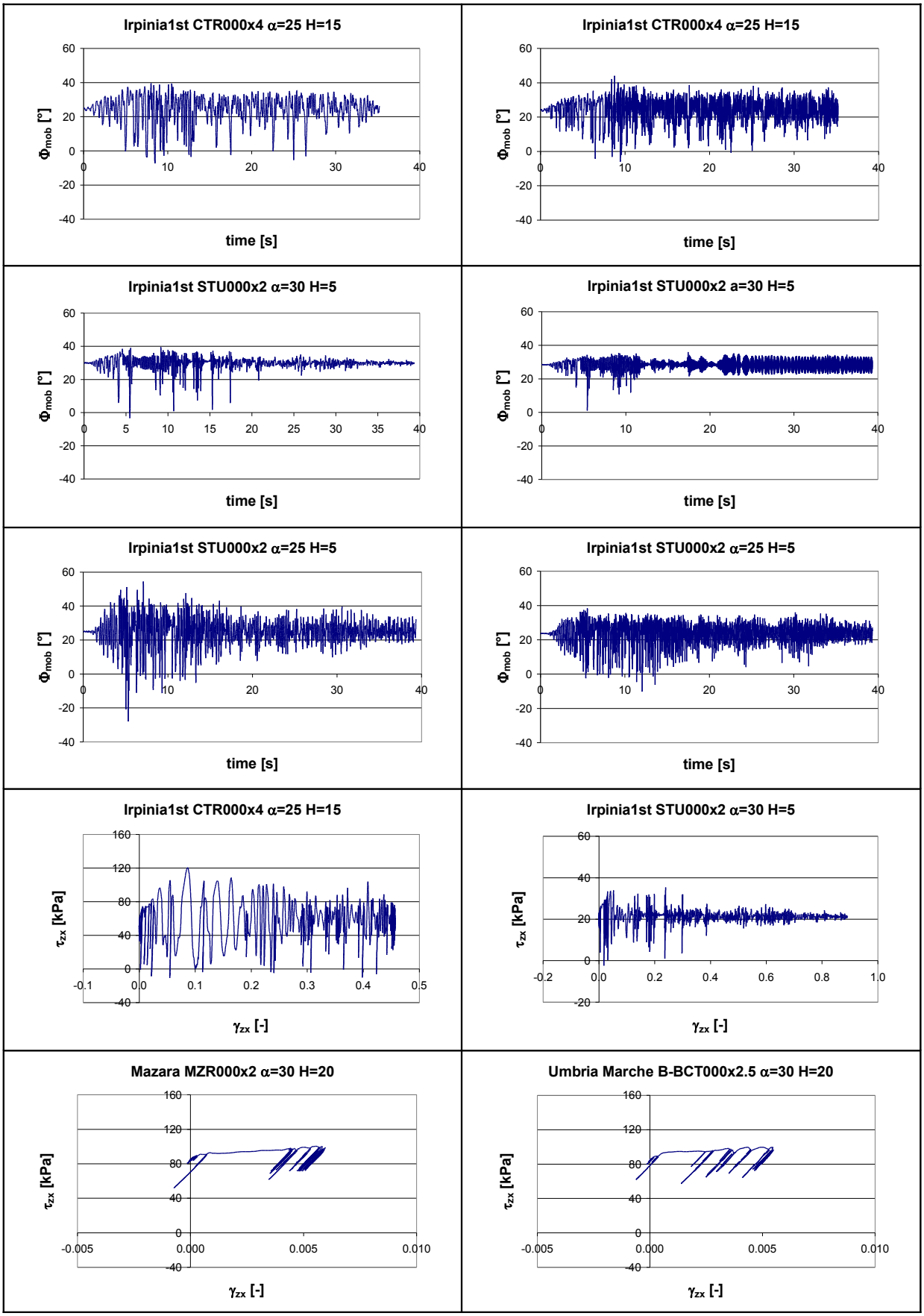

Figure 4.15. Friction angle mobilized (at the middle and on the surface of the slope) and load cycles (at the middle).

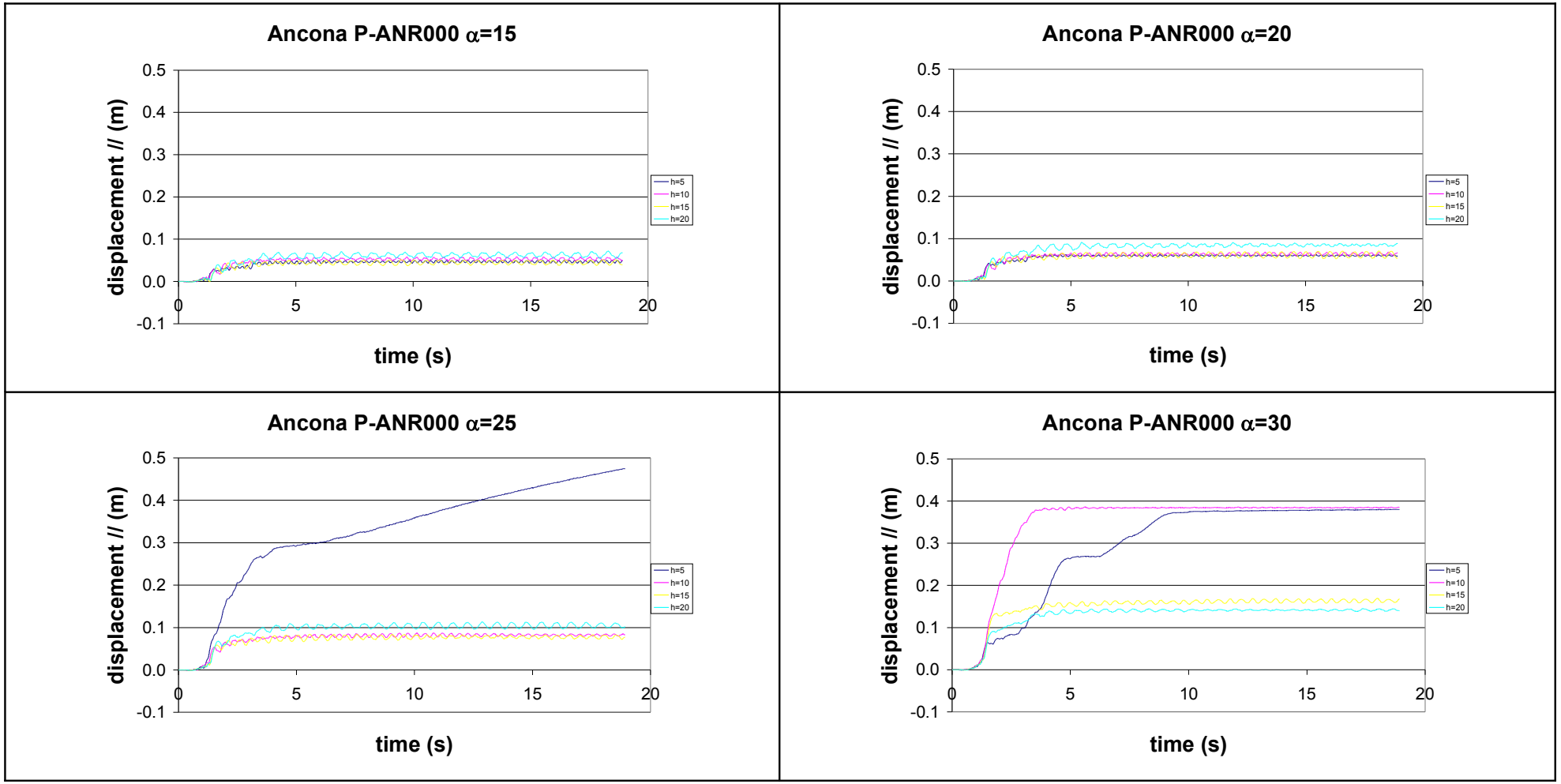

Figure 4.16. Permanent horizontal displacement, accelerogram P-ANR000, soil type B.

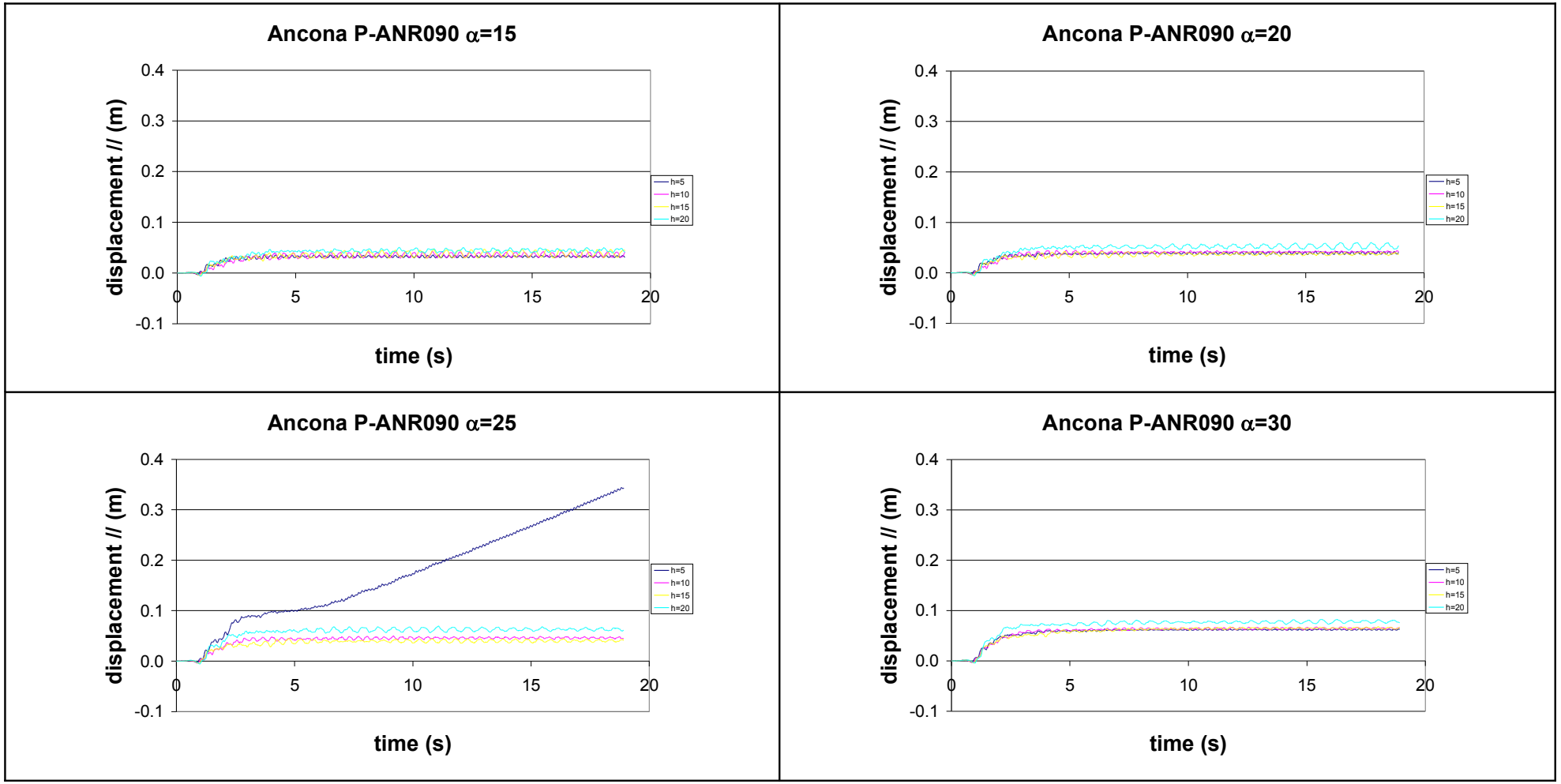

Figure 4.17. Permanent horizontal displacement, accelerogram P-ANR090, soil type B.

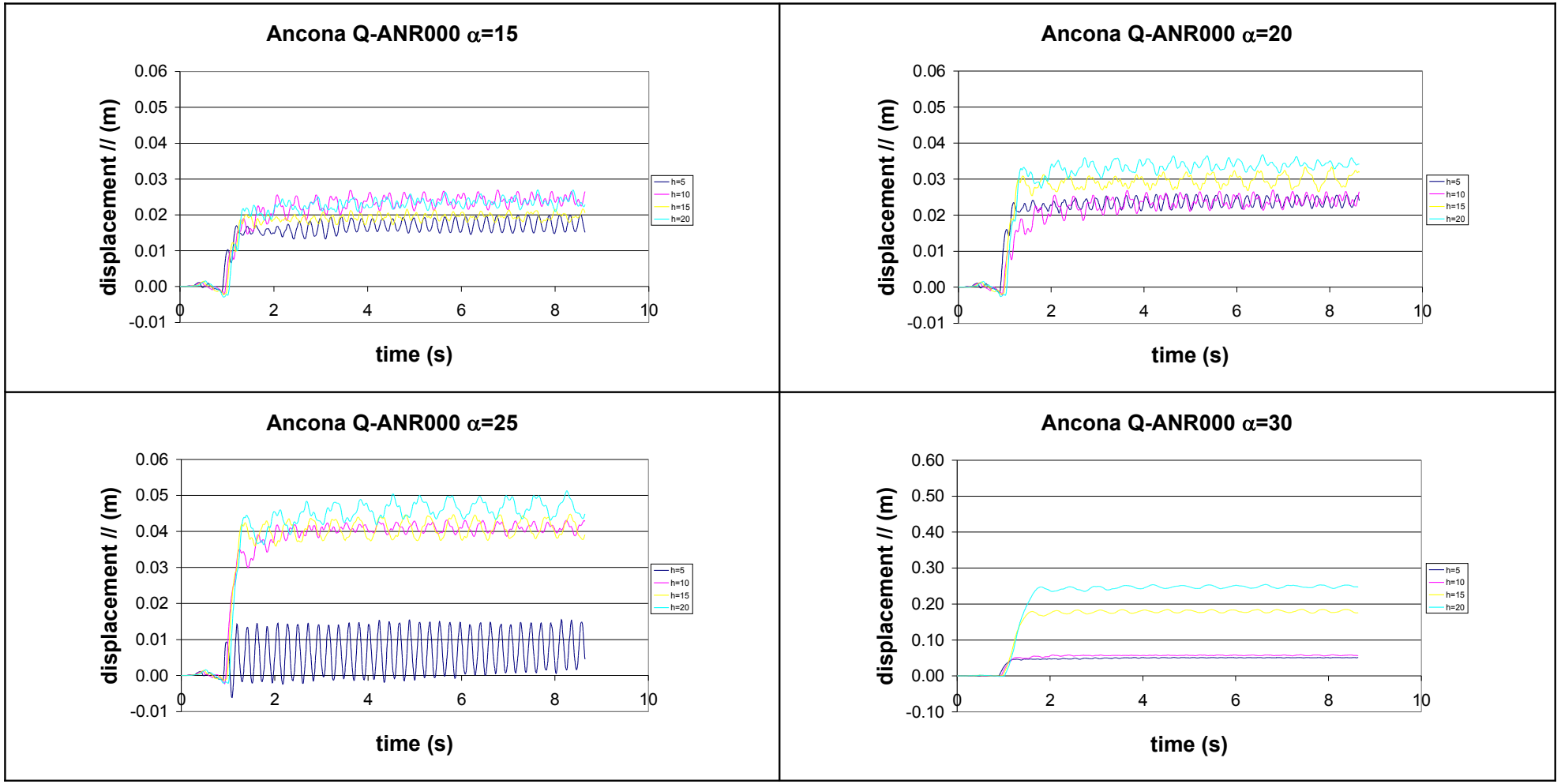

Figure 4.18. Permanent horizontal displacement, accelerogram Q-ANR000, soil type B.

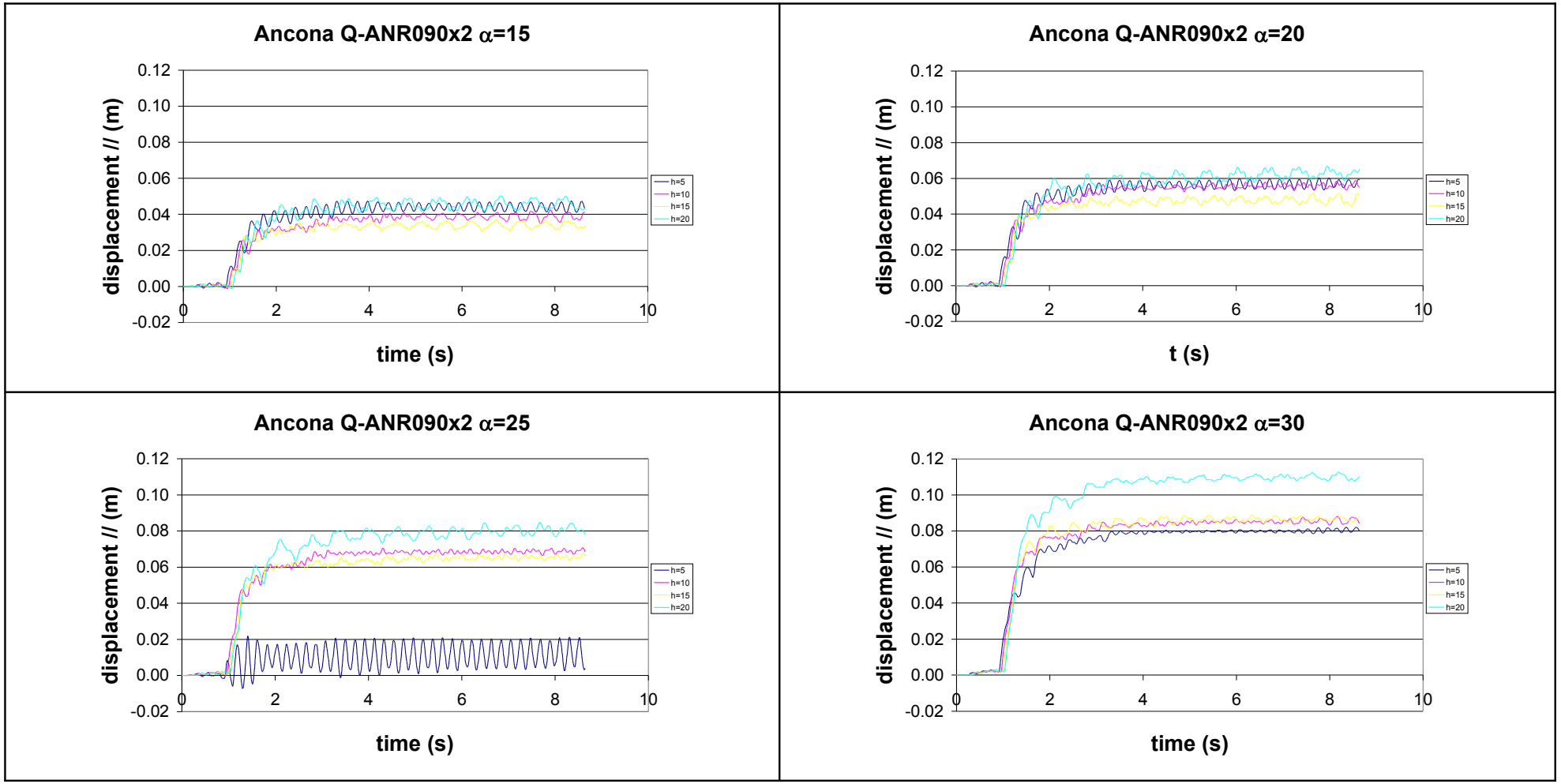

Figure 4.19. Permanent horizontal displacement, accelerogram Q-ANR090, amplification factor 2, soil type B.

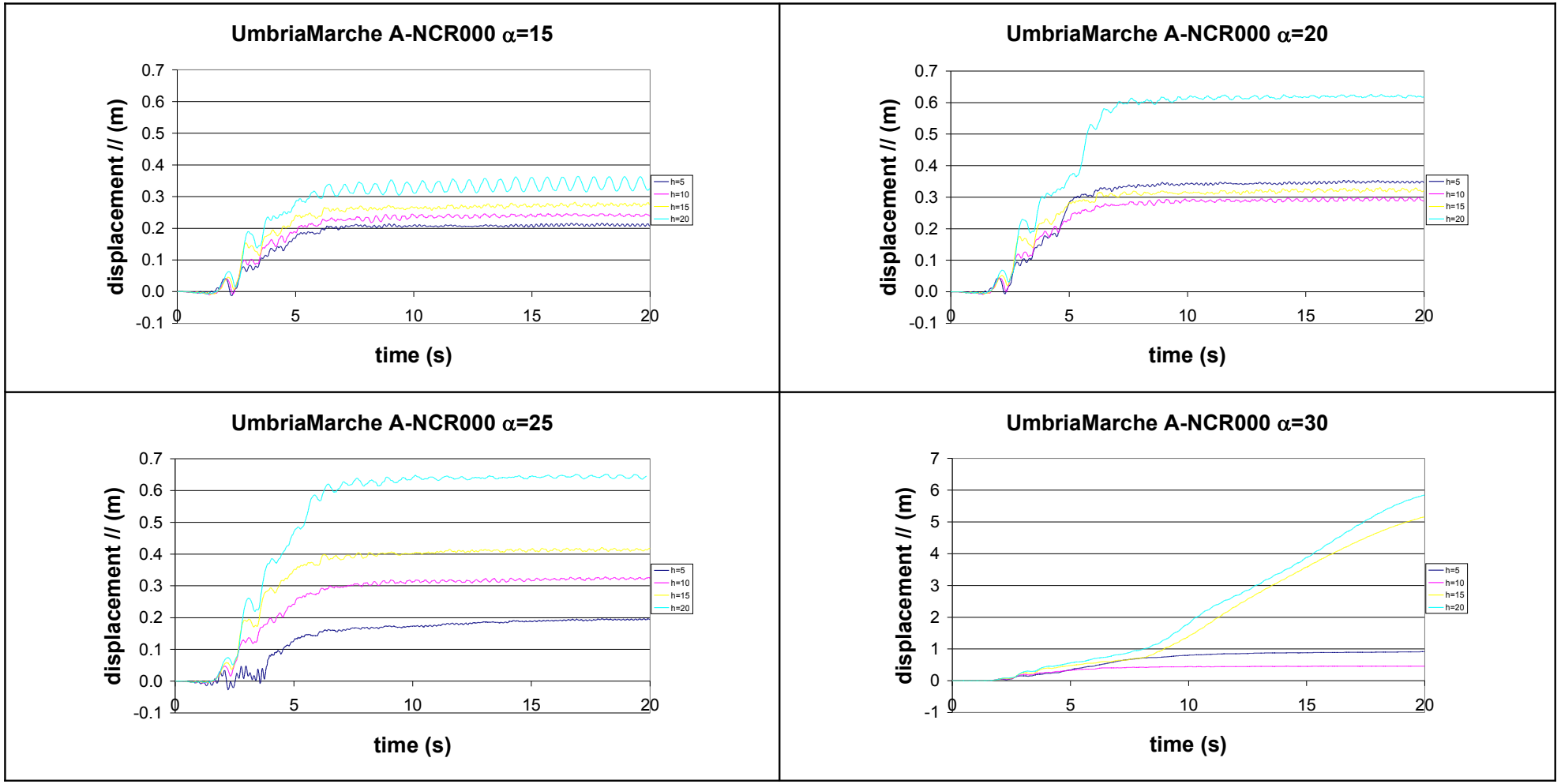

Figure 4.20. Permanent horizontal displacement, accelerogram A-NCR000, soil type B.

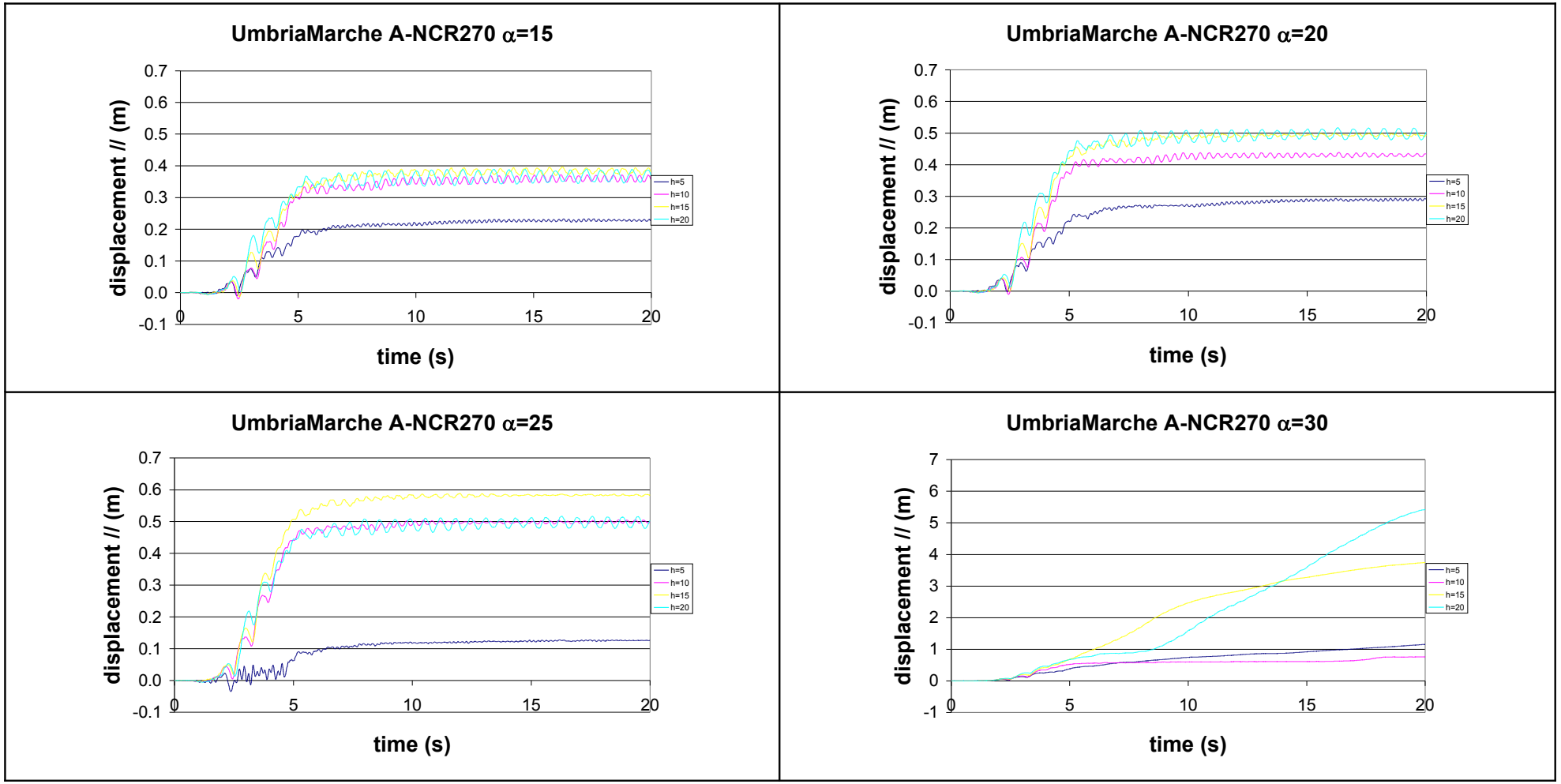

Figure 4.21. Permanent horizontal displacement, accelerogram A-NCR270, soil type B.

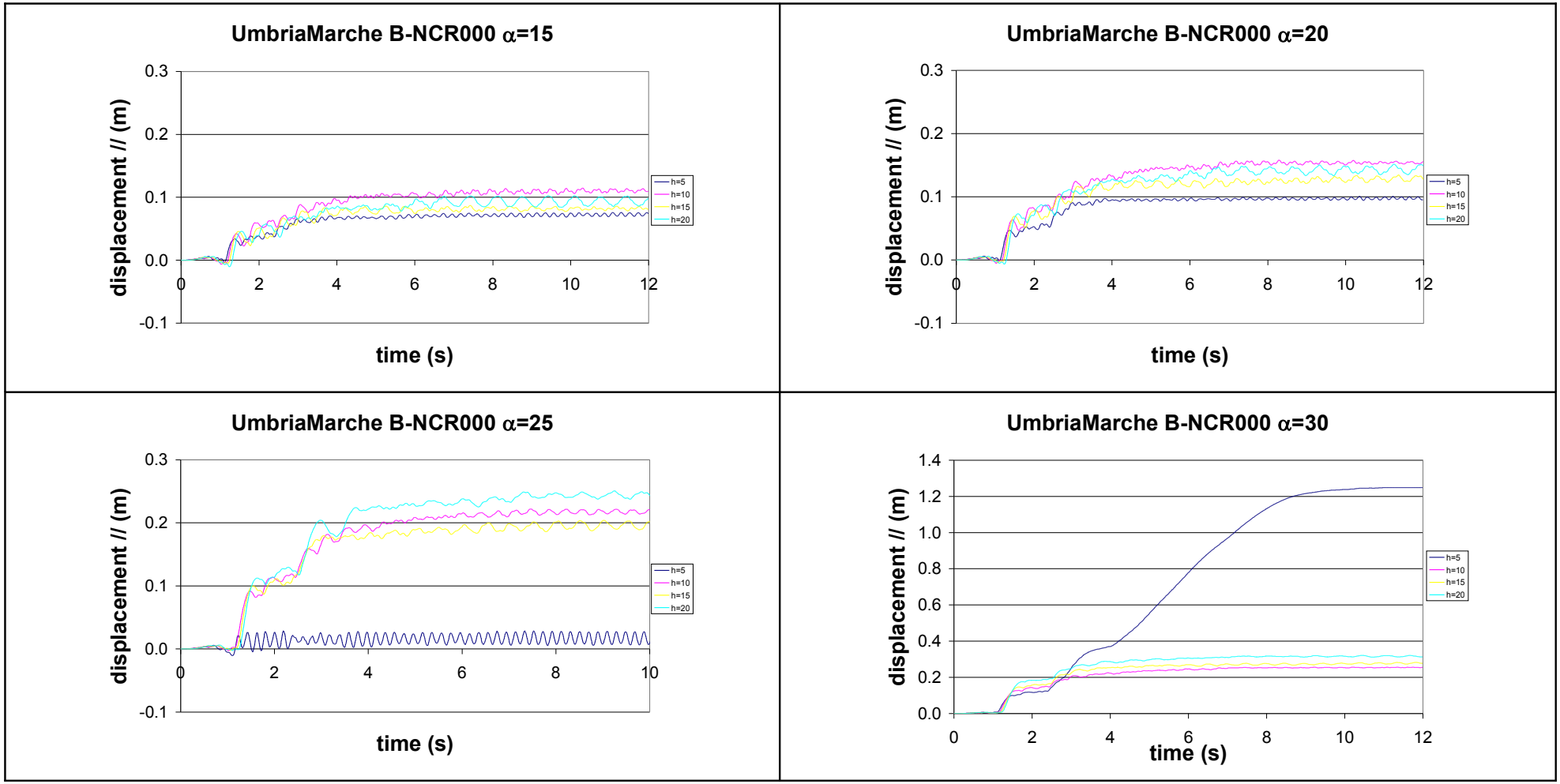

Figure 4.22. Permanent horizontal displacement, accelerogram B-NCR000, soil type B.

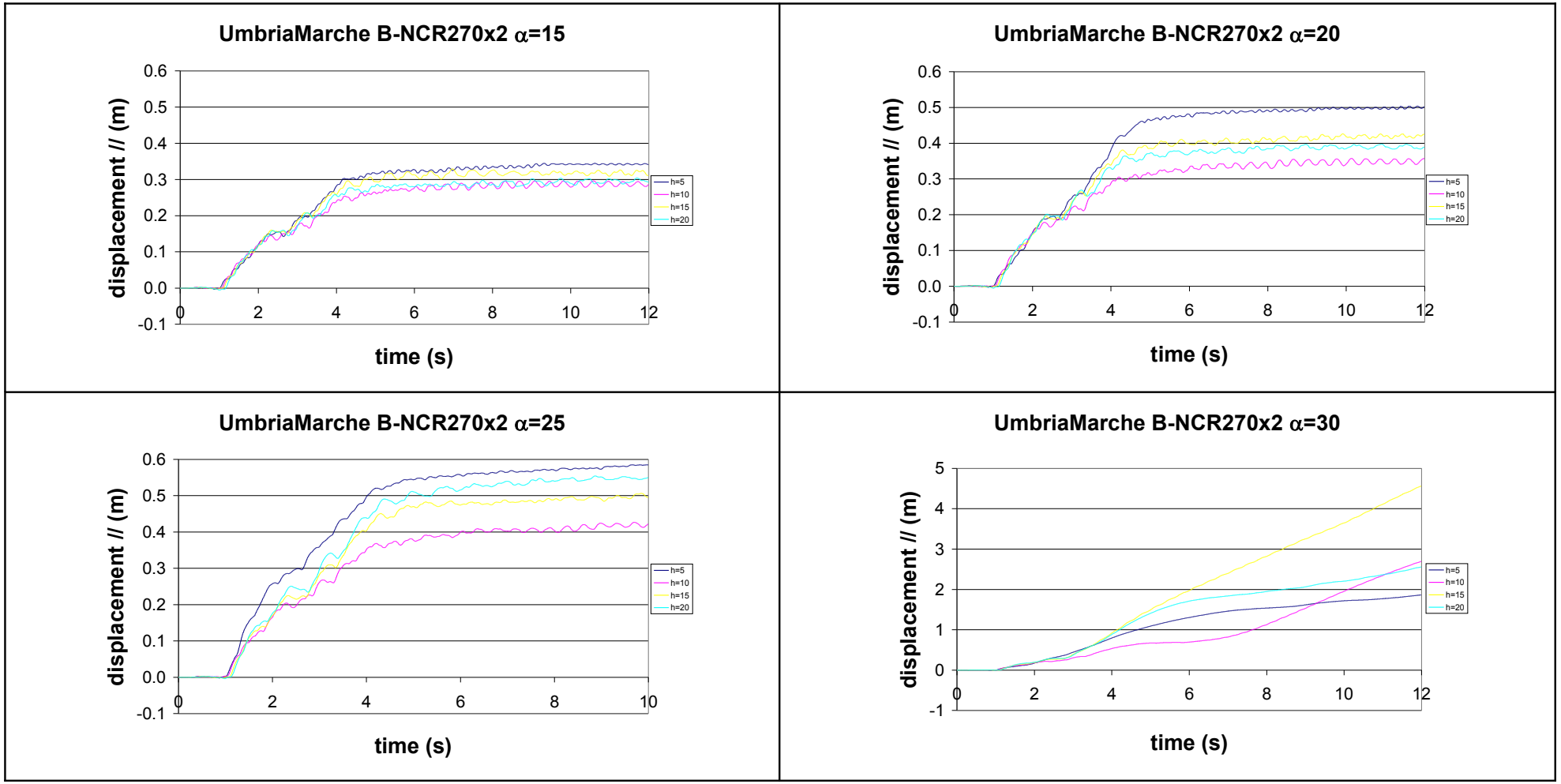

Figure 4.23. Permanent horizontal displacement, accelerogram B-NCR270, amplification factor 2, soil type B.

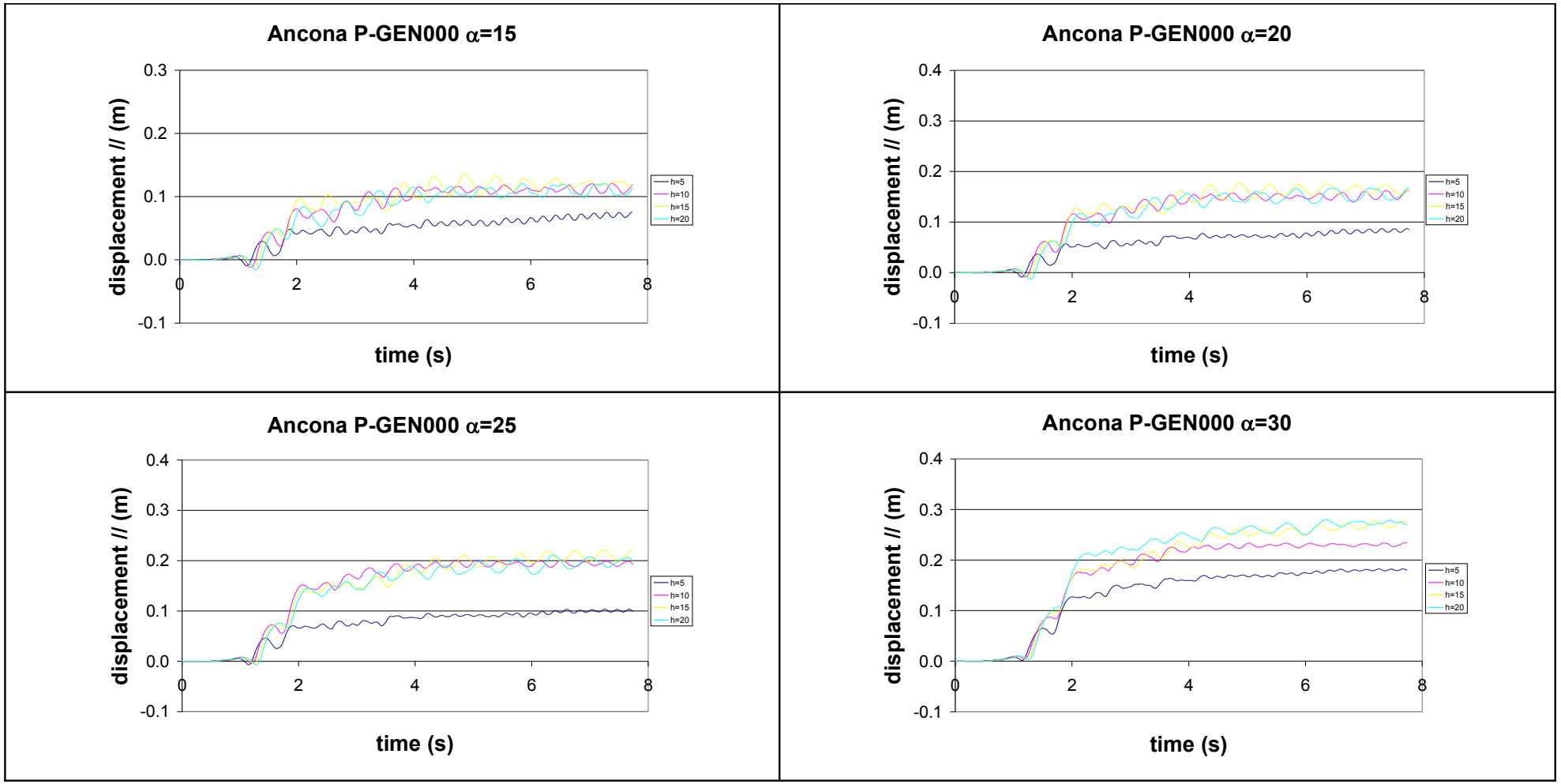

Figure 4.24. Permanent horizontal displacement, accelerogram P-GEN000, soil type B.

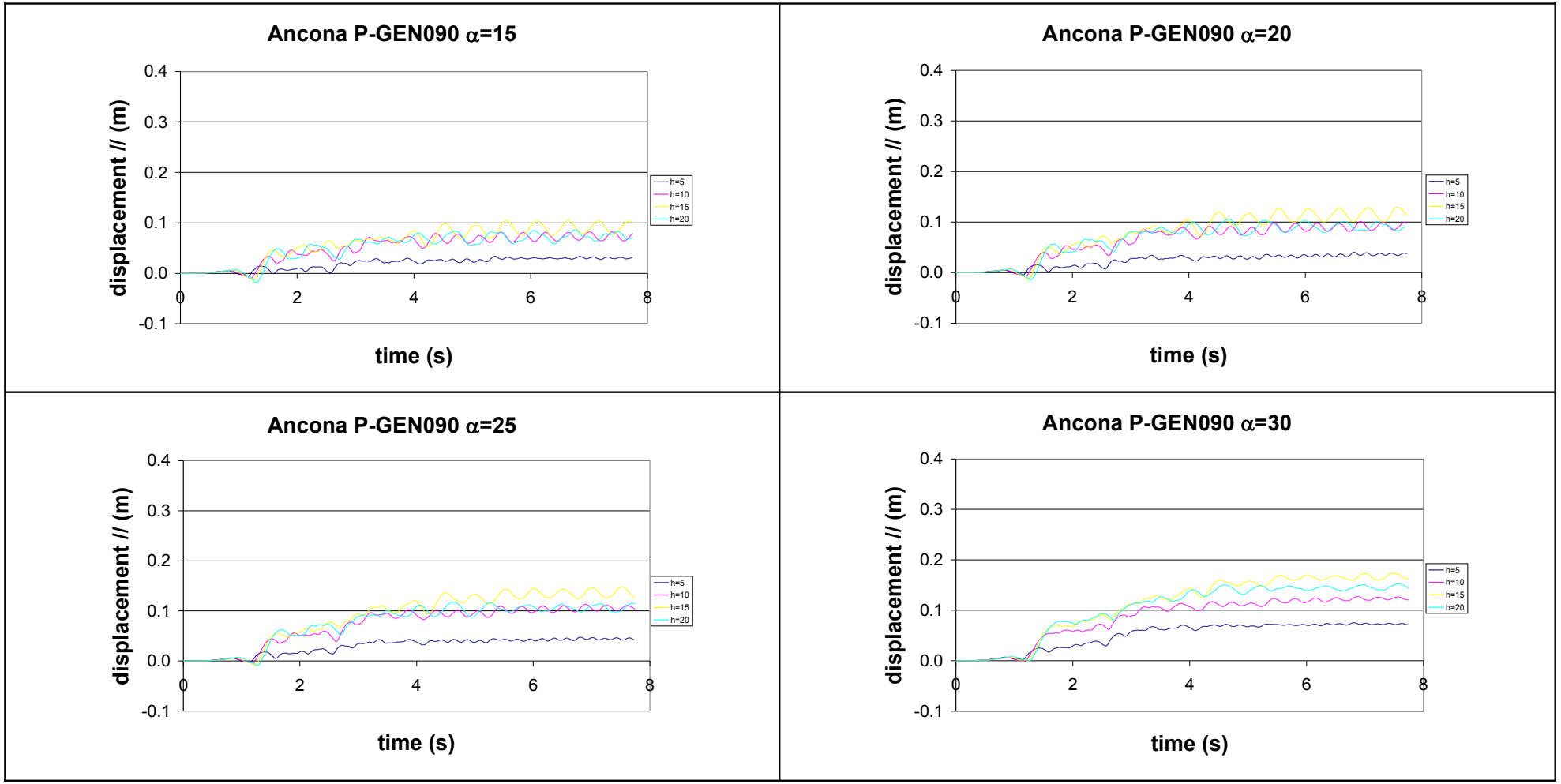

Figure 4.25. Permanent horizontal displacement, accelerogram P-GEN090, soil type B.

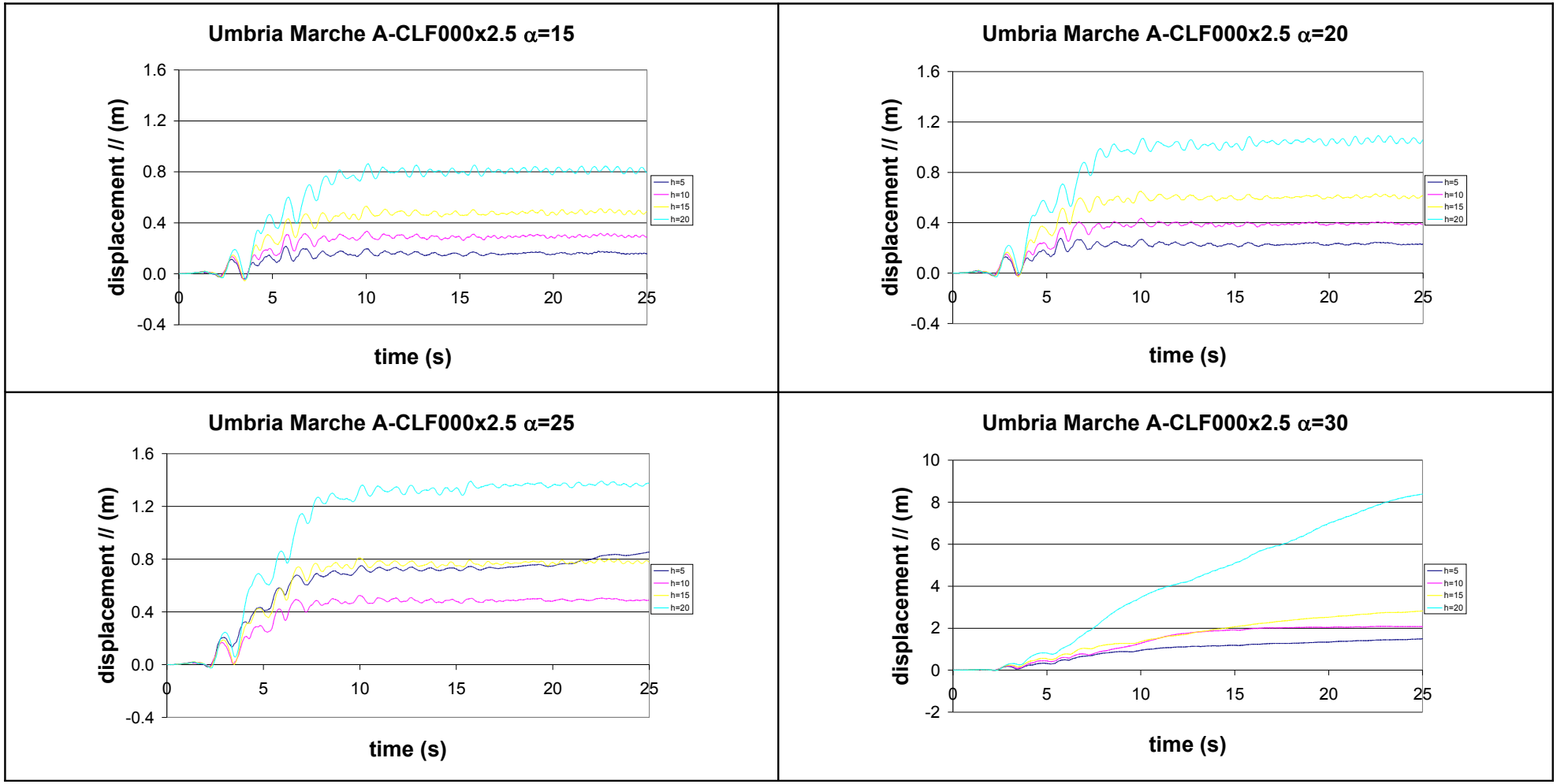

Figure 4.26. Permanent horizontal displacement, accelerogram A-CLF000, amplification factor 2.5, soil type C.

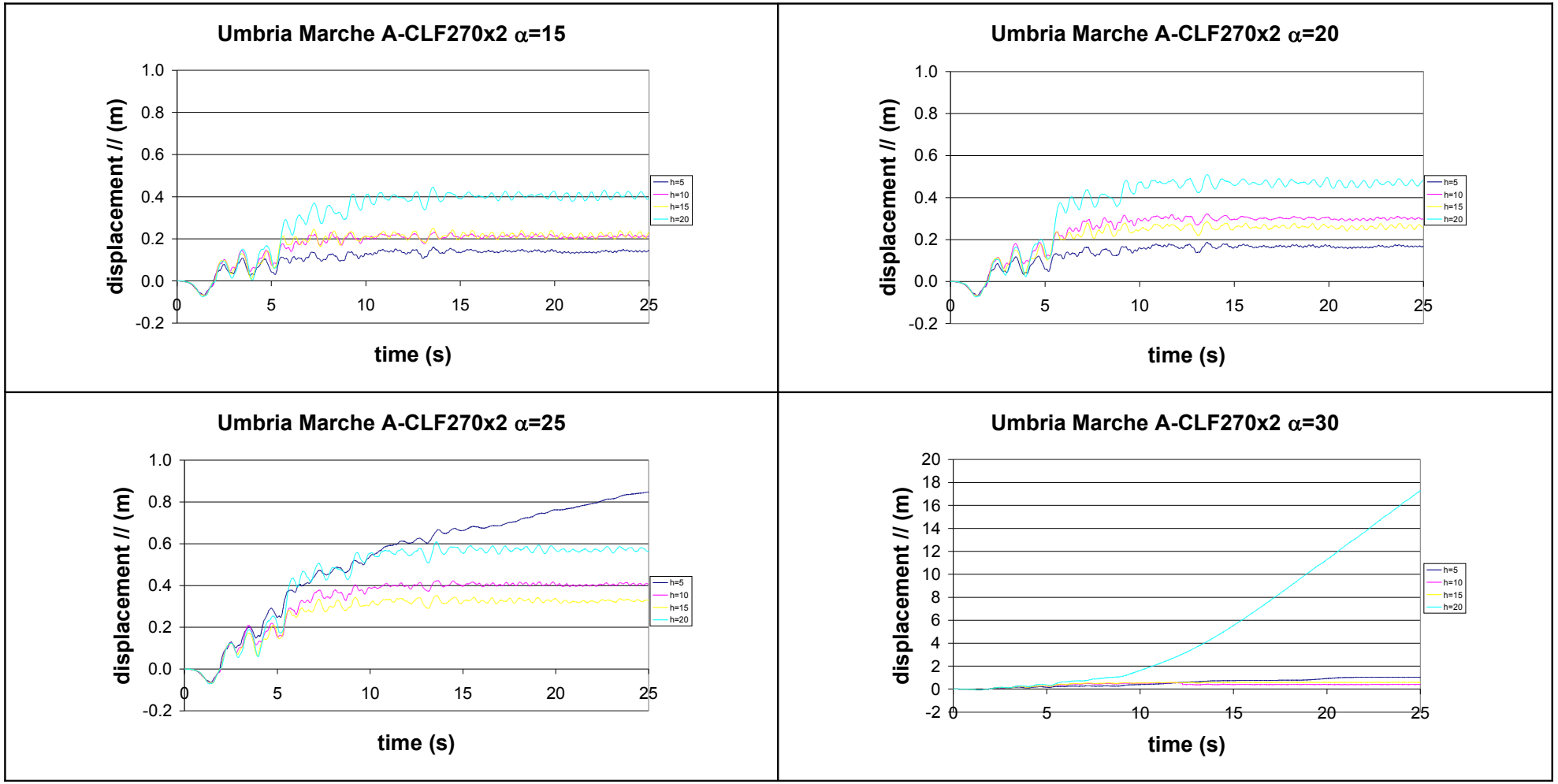

Figure 4.27. Permanent horizontal displacement, accelerogram A-CLF270, amplification factor 2, soil type C.

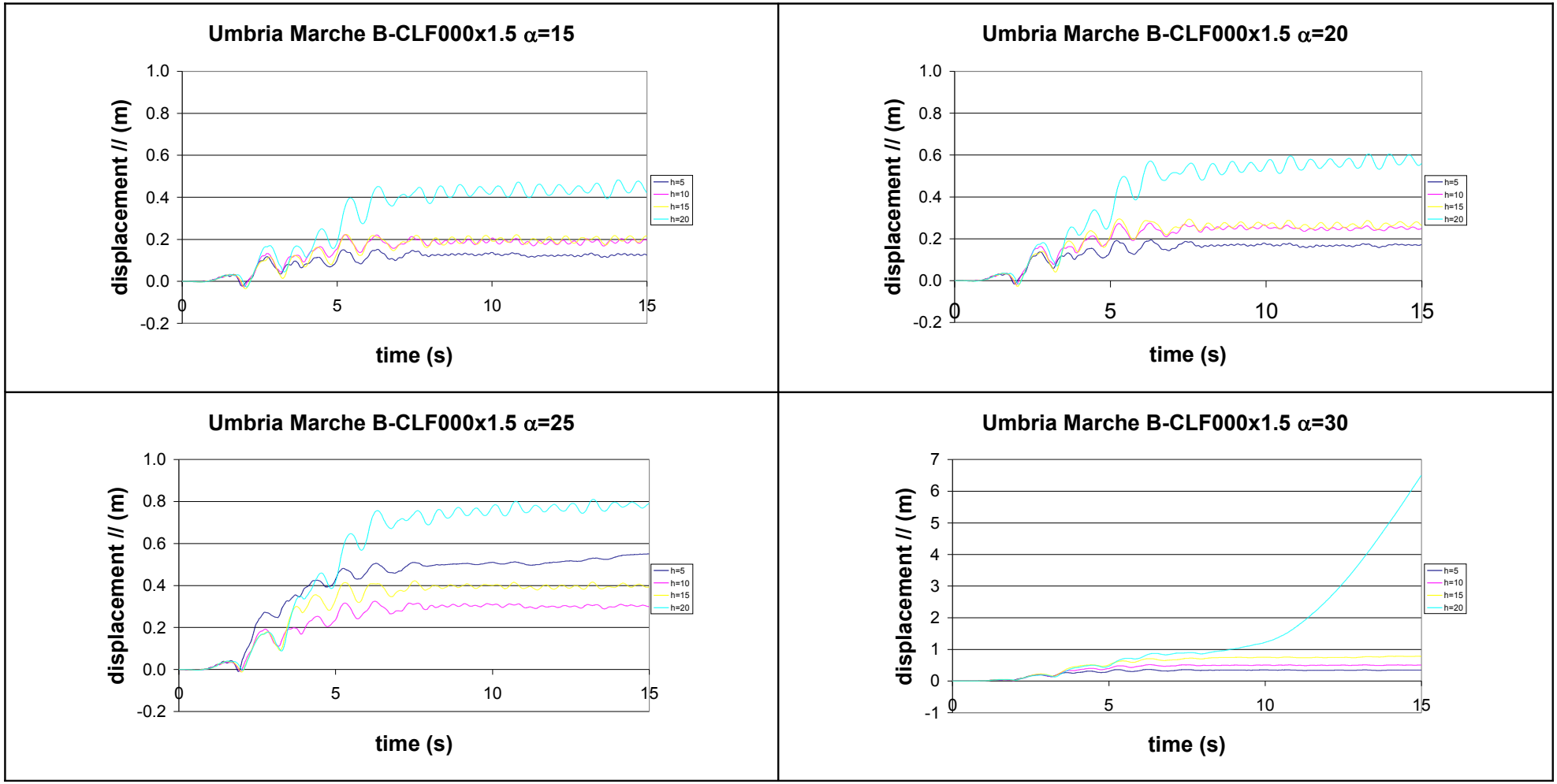

Figure 4.28. Permanent horizontal displacement, accelerogram B-CLF000, amplification factor 1.5, soil type C.

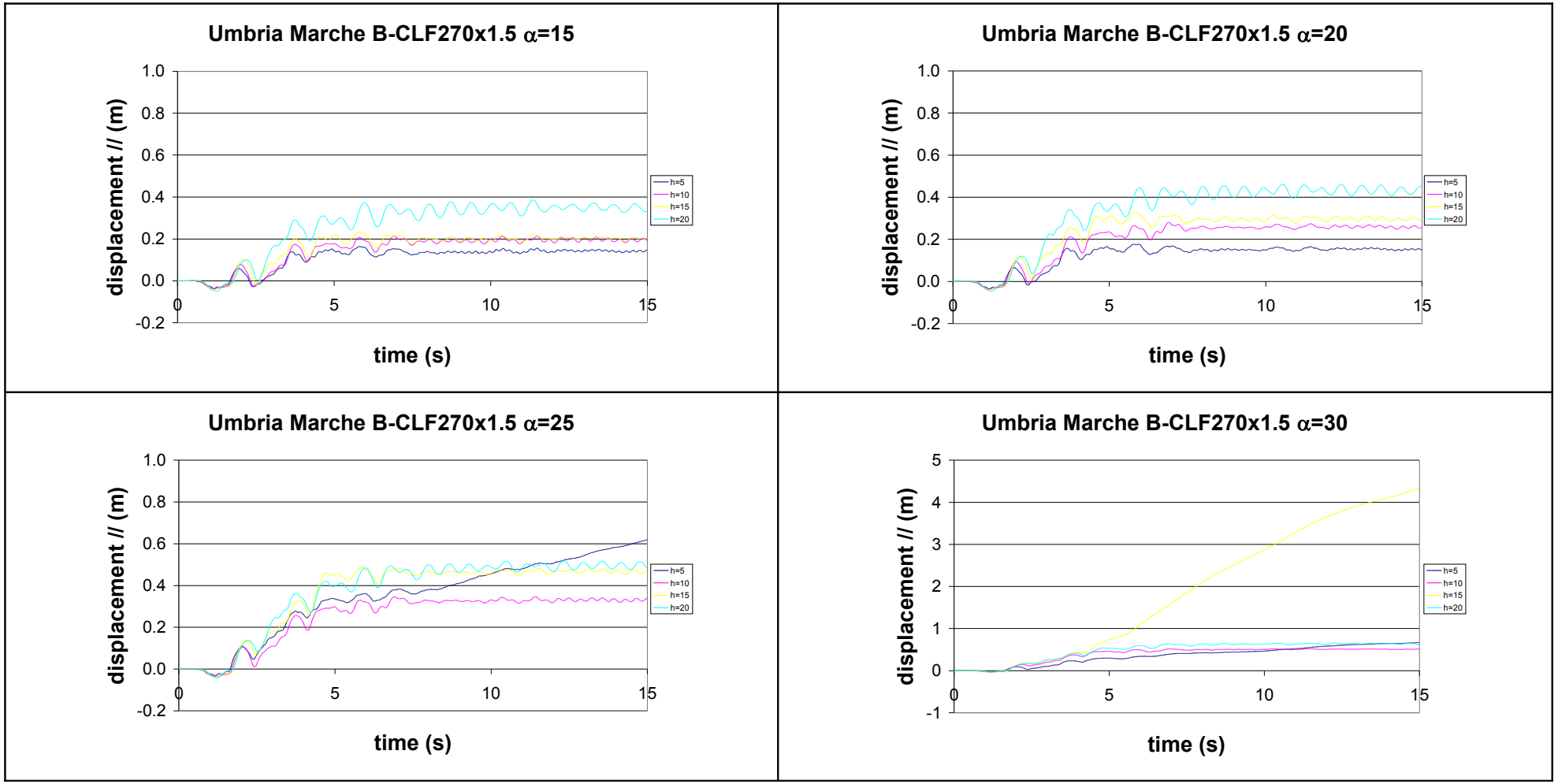

Figure 4.29. Permanent horizontal displacement, accelerogram B-CLF270, amplification factor 1.5, soil type C.

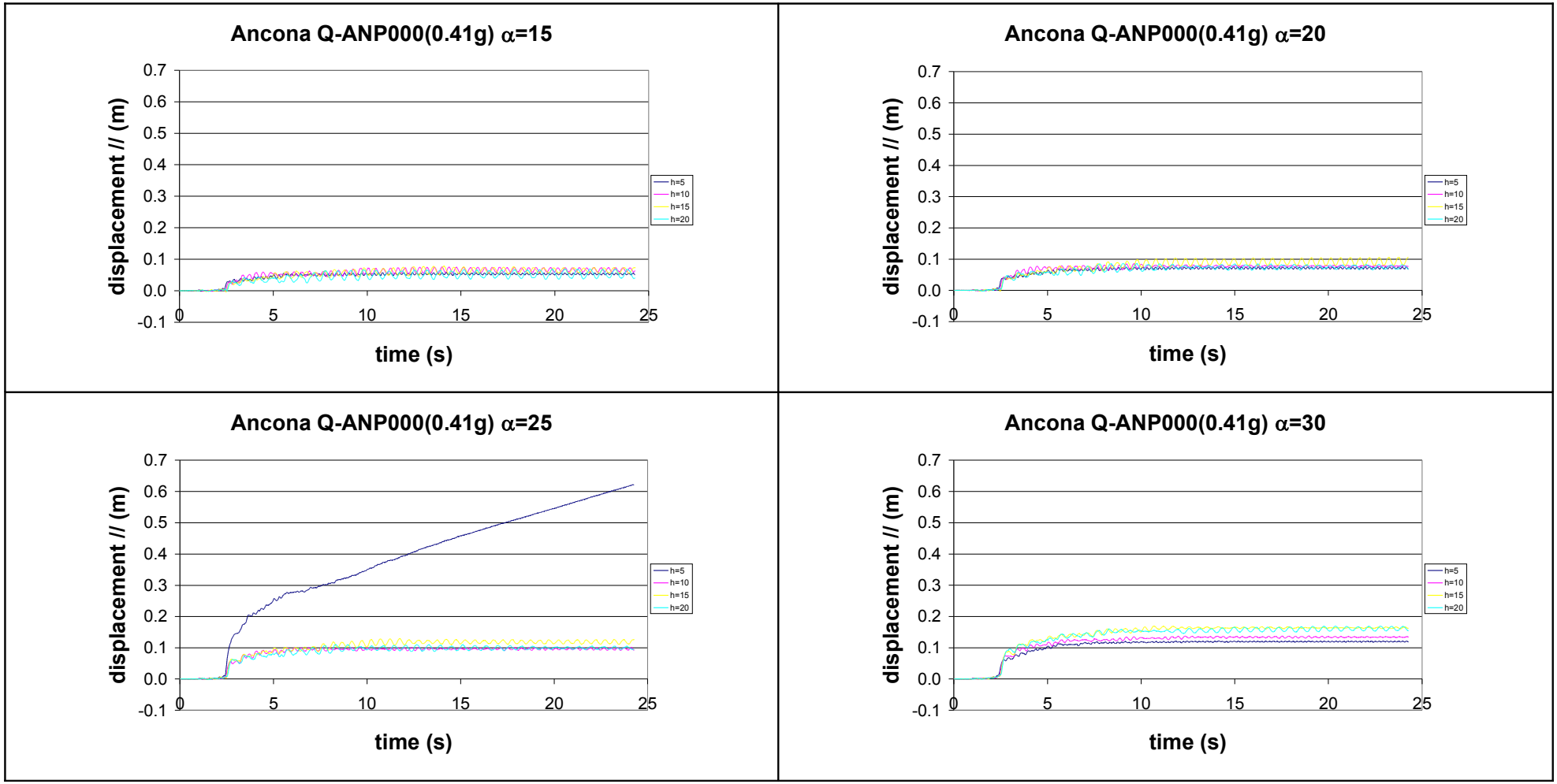

Figure 4.30. Permanent horizontal displacement, accelerogram Q-ANP000, amplified to 0.41g, soil type C.

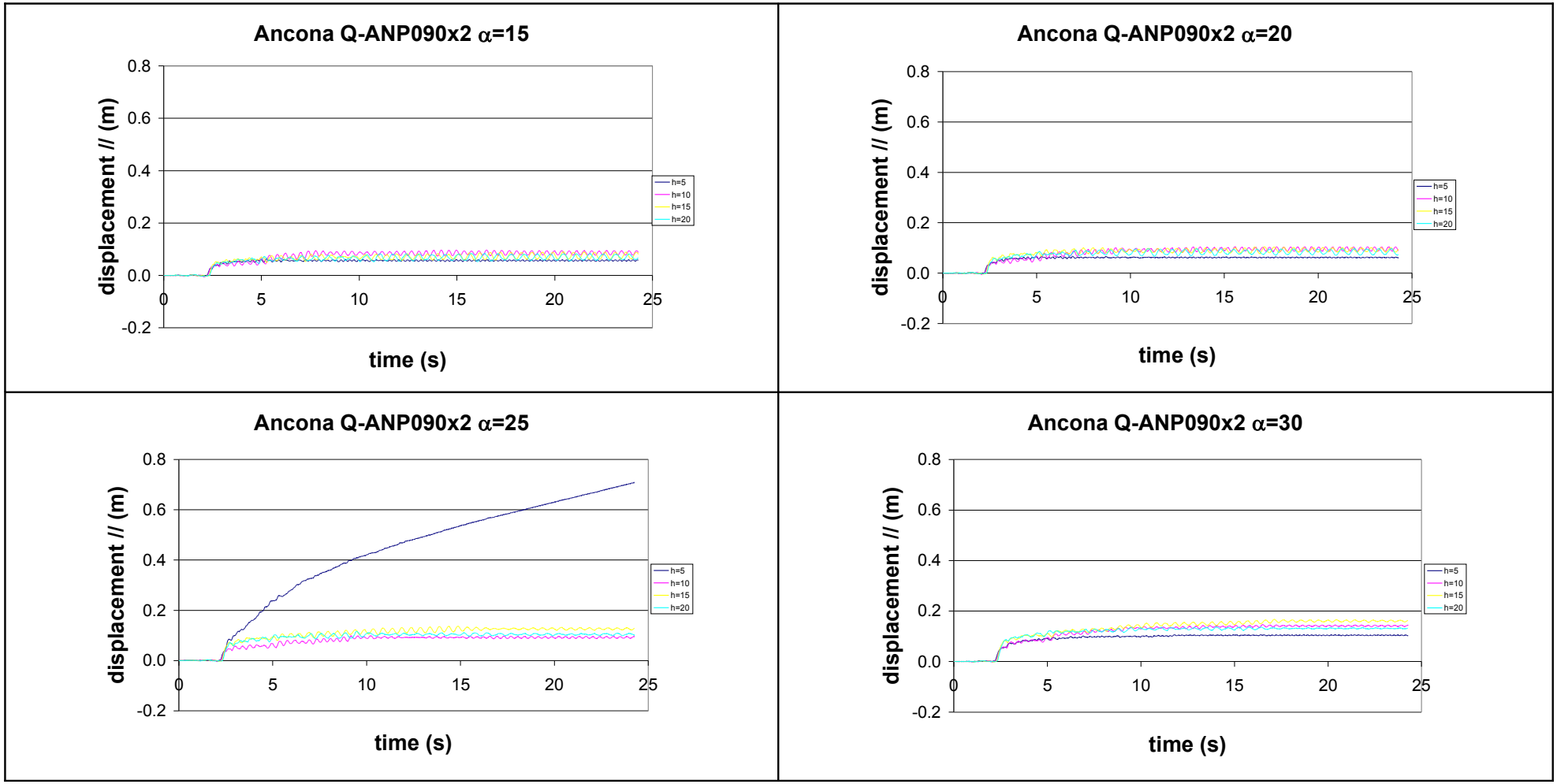

Figure 4.31. Permanent horizontal displacement, accelerogram Q-ANP090, amplification factor 2, soil type C.

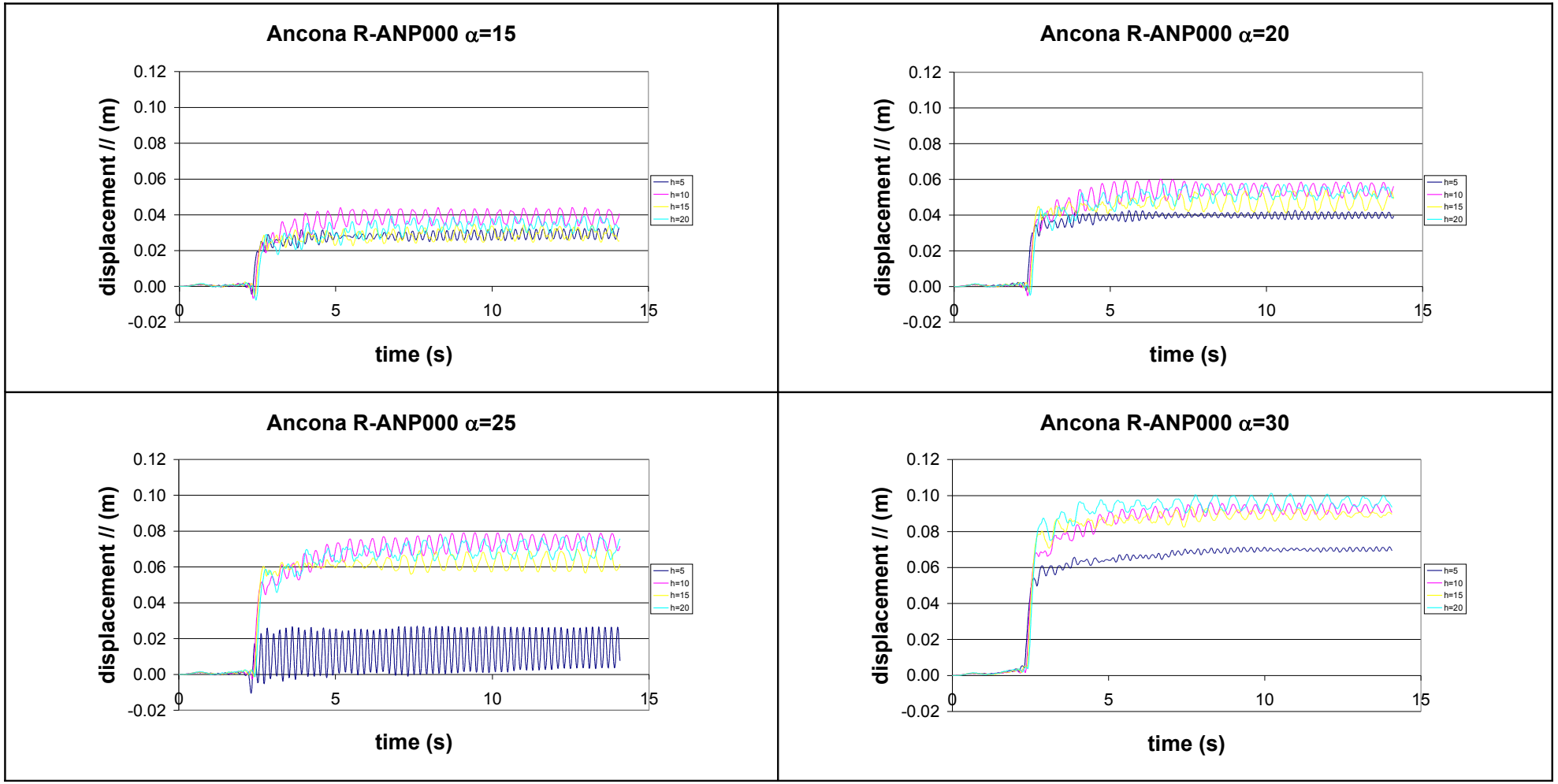

Figure 4.32. Permanent horizontal displacement, accelerogram R-ANP000, soil type C.

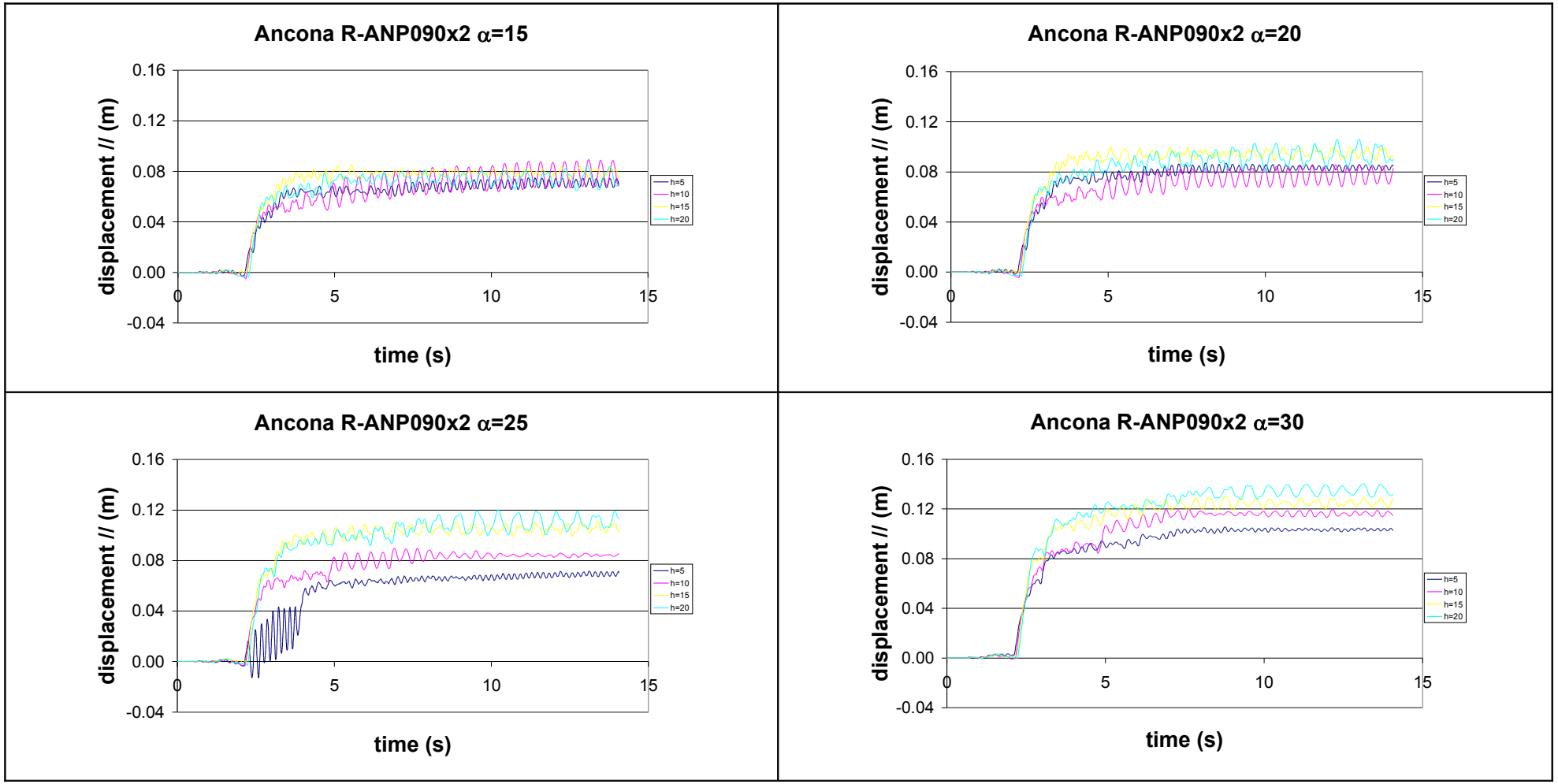

Figure 4.33. Permanent horizontal displacement, accelerogram R-ANP090, amplification factor 2, soil type C.

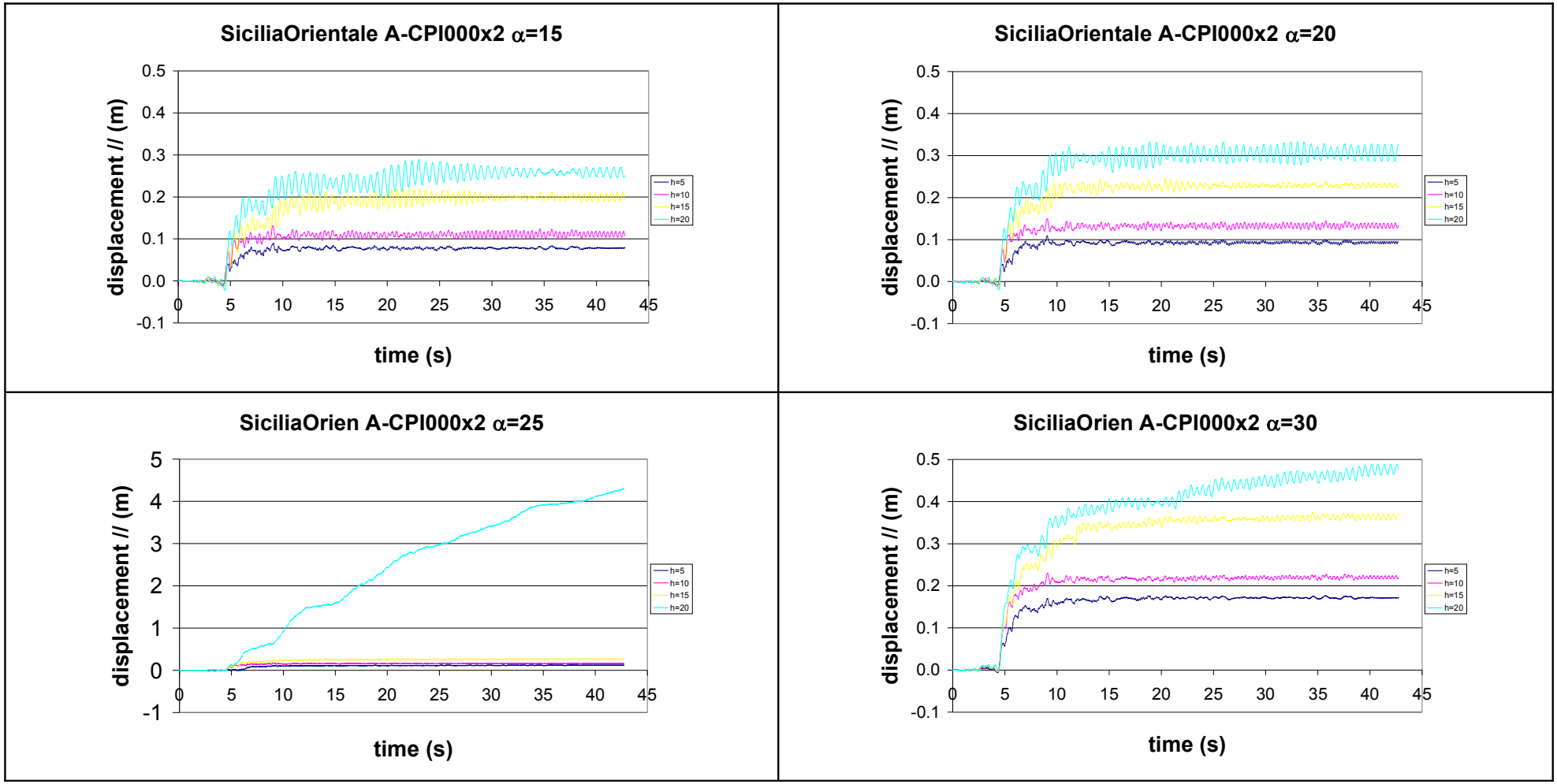

Figure 4.34. Permanent horizontal displacement, accelerogram A-CPI000, amplification factor 2, soil type C.

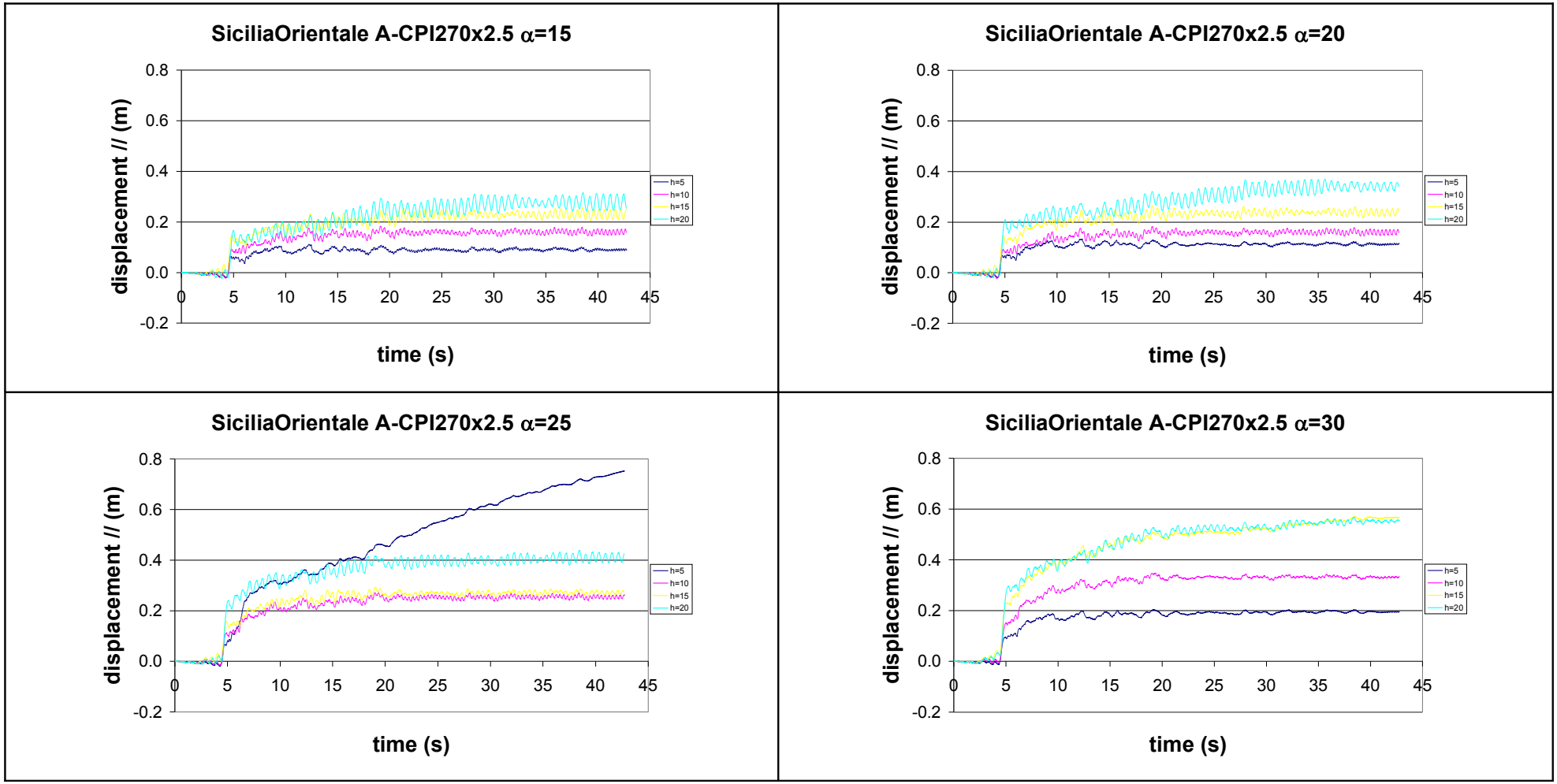

Figure 4.35. Permanent horizontal displacement, accelerogram A-CPI270, amplification factor 2.5, soil type C.

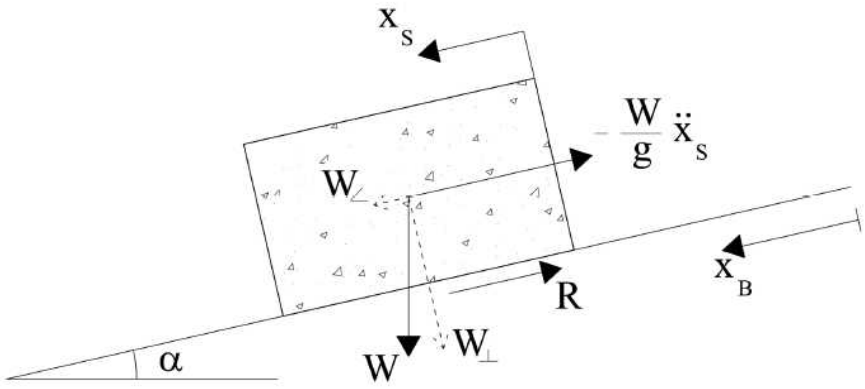

Figure 4.36. Equilibrium of rigid block on Newmark method.

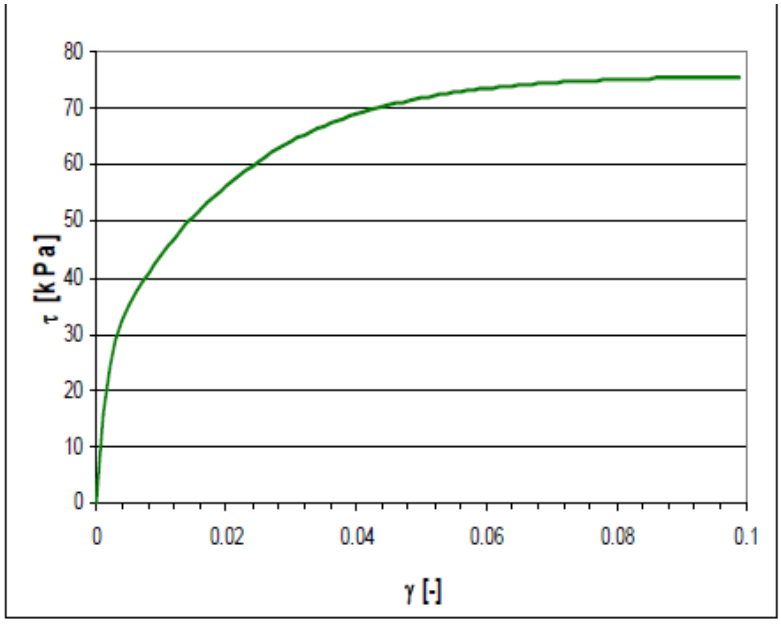

Figure 4.37. Simulation of simple shear test.

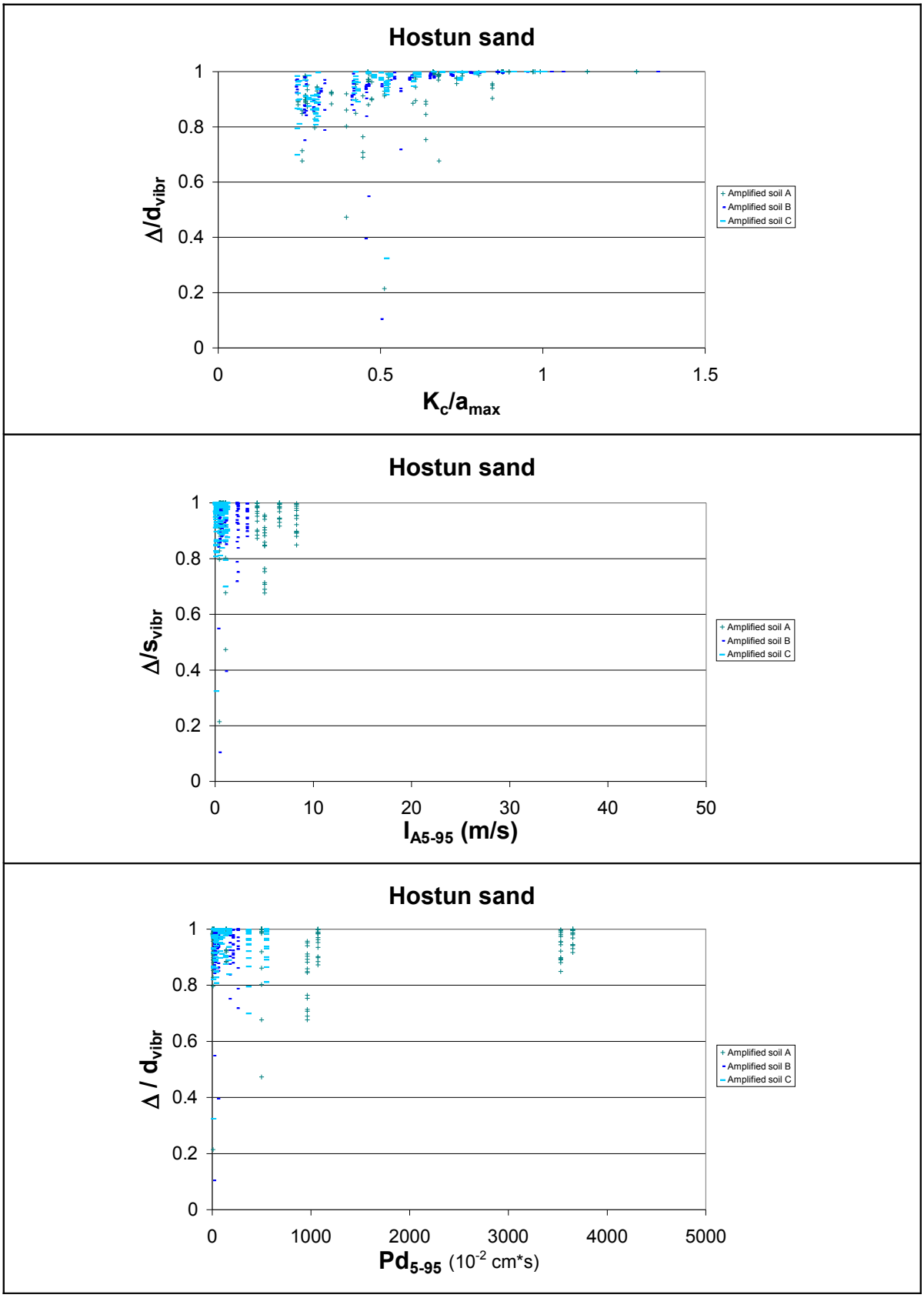

Figure 4.38. Ratio Δ/d_{vibr} in function of K_c/a_{max}, I_{A5-95} and P_{D5-95} respectively.

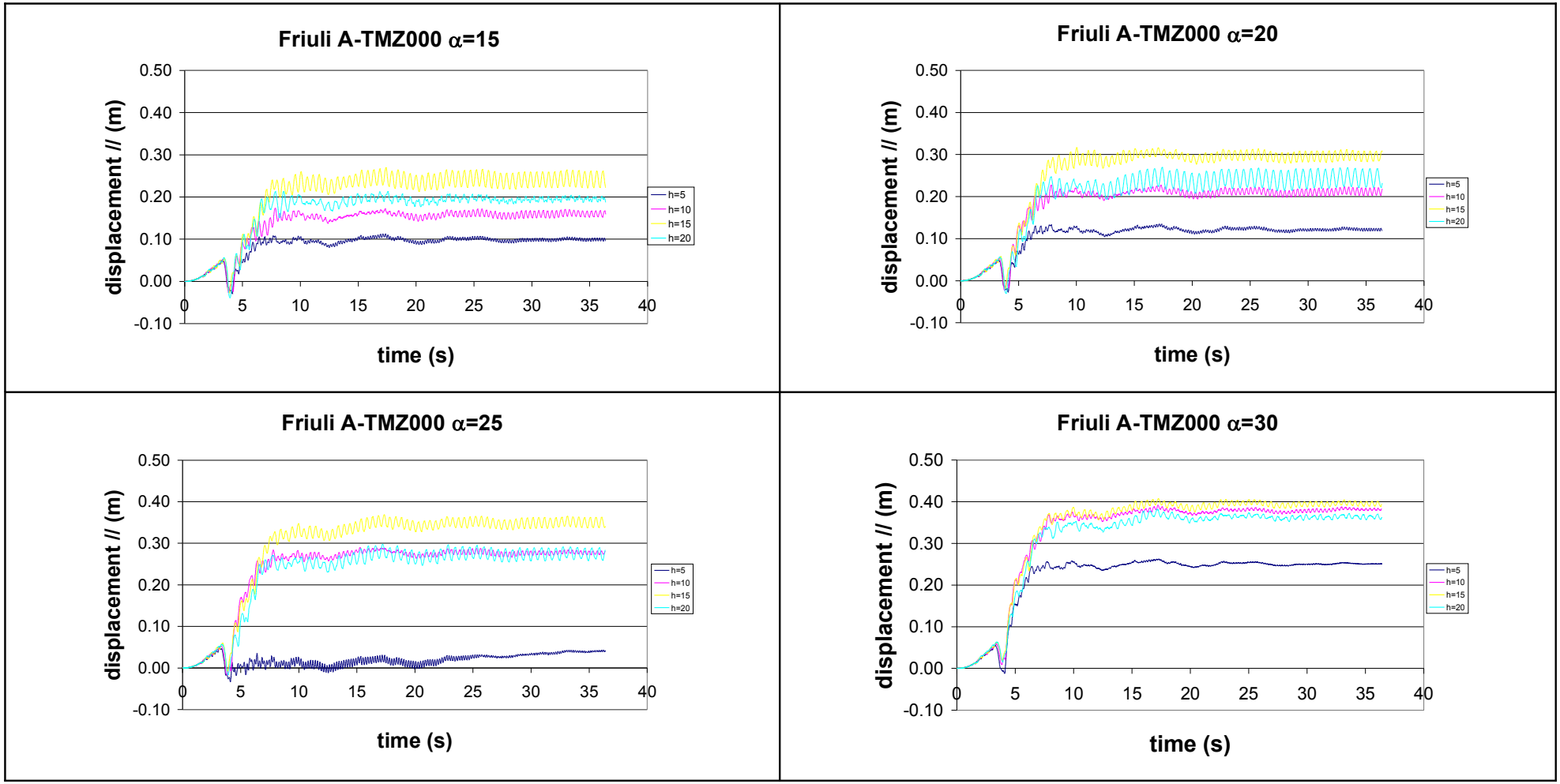

Figure 4.39. Permanent horizontal displacement, accelerogram A-TMZ000, soil type A.

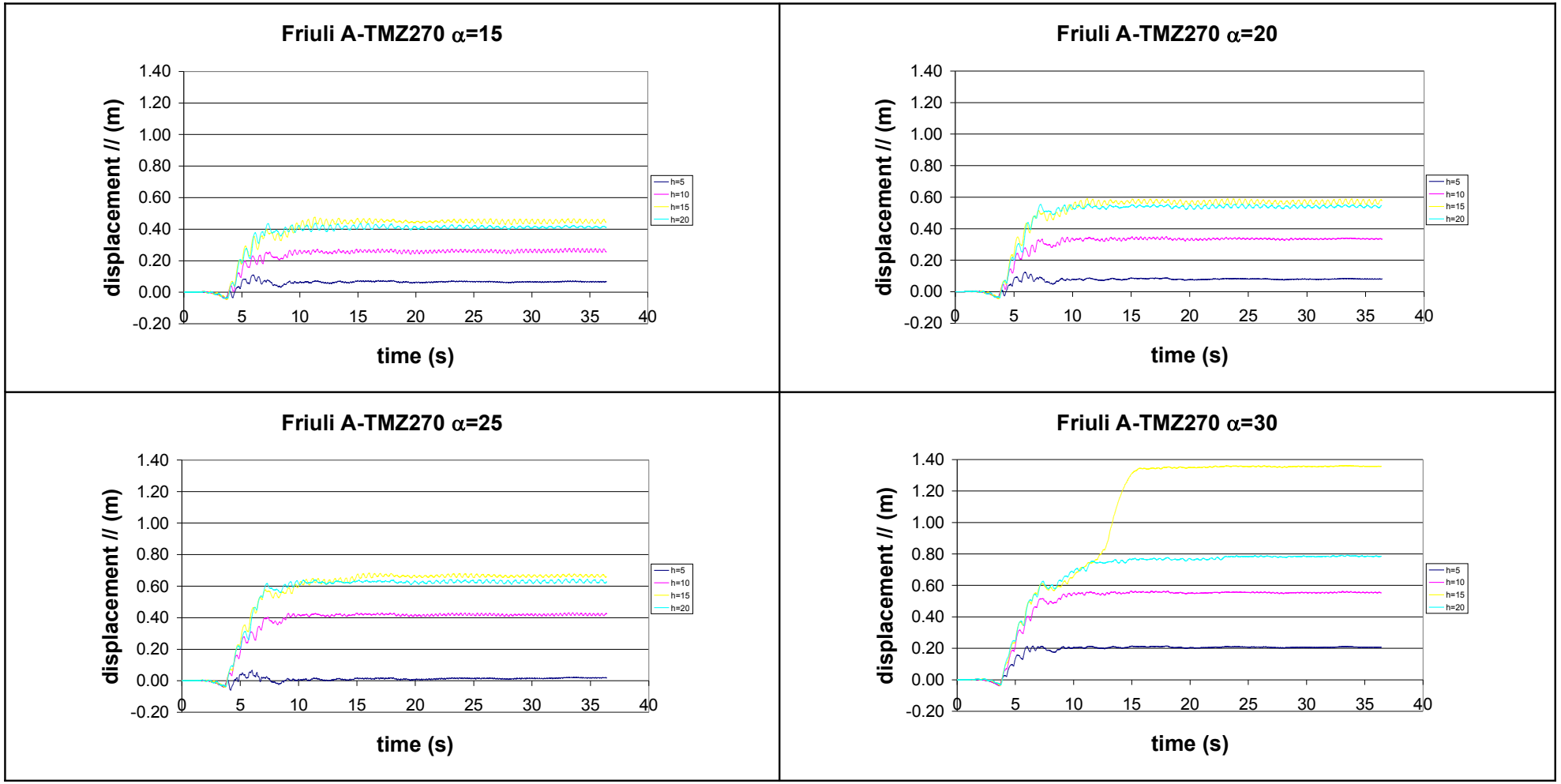

Figure 4.40. Permanent horizontal displacement, accelerogram A-TMZ270, soil type A.

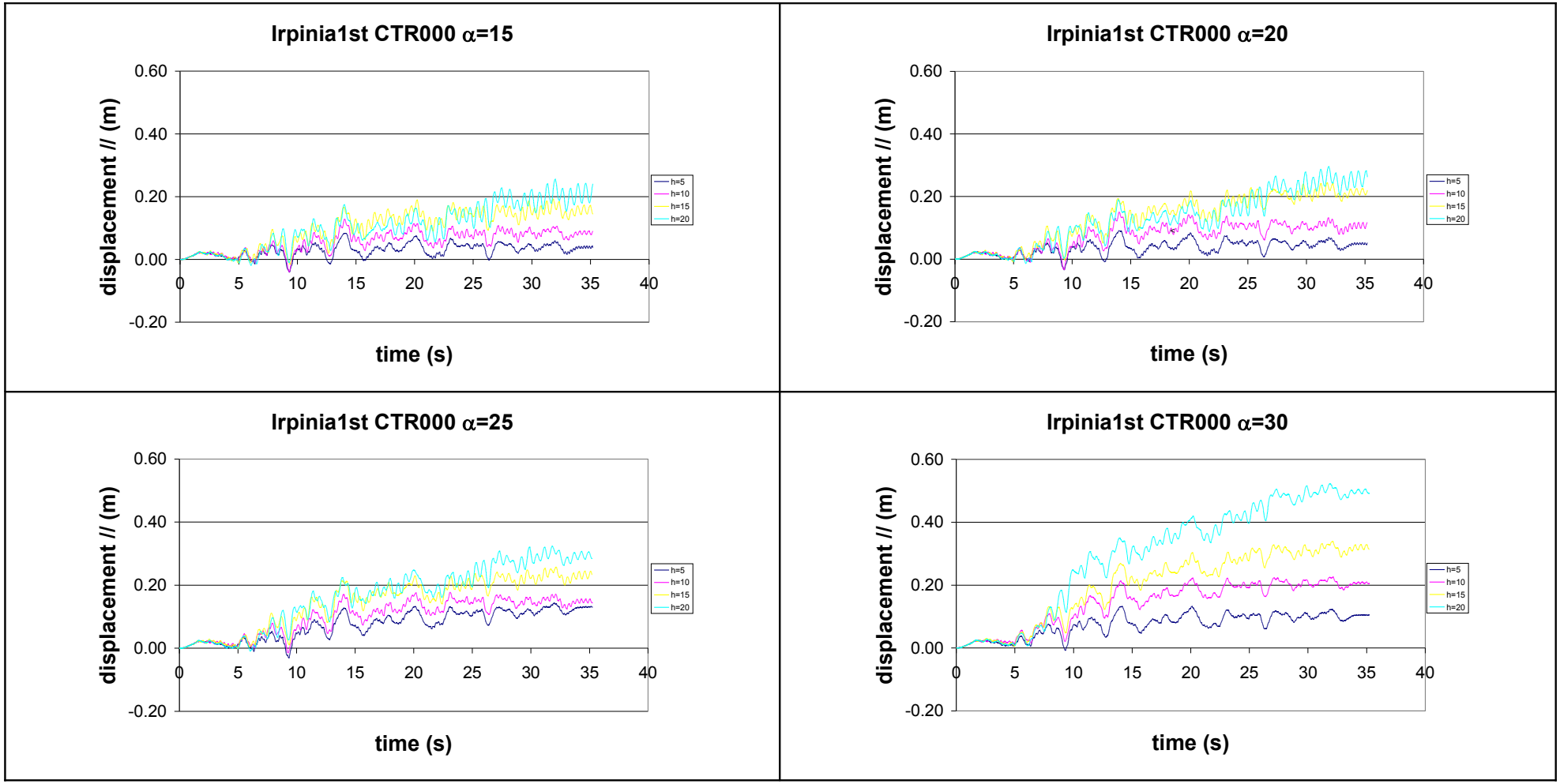

Figure 4.41. Permanent horizontal displacement, accelerogram CTR000, soil type A.

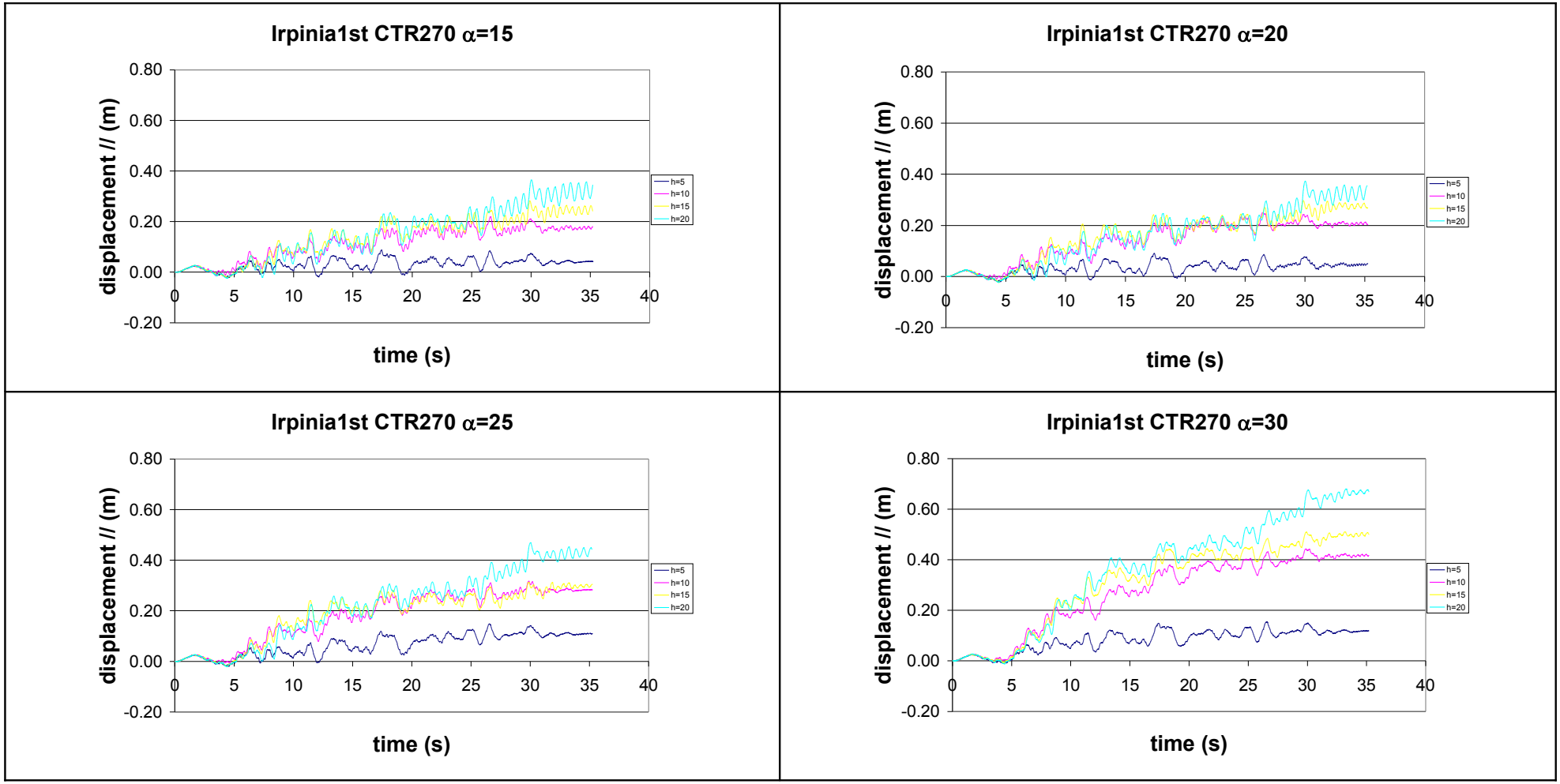

Figure 4.42. Permanent horizontal displacement, accelerogram CTR270, soil type A.

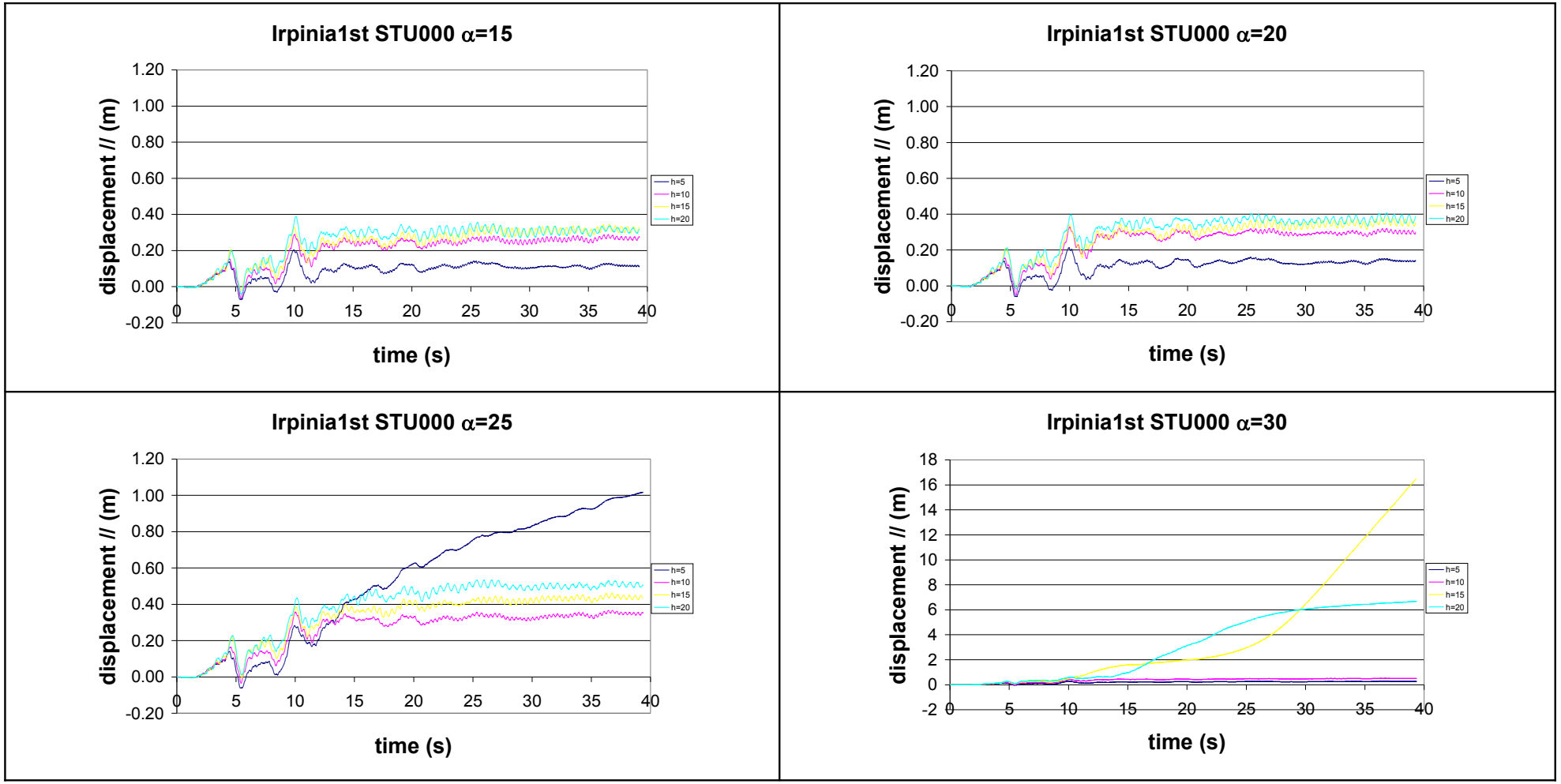

Figure 4.43. Permanent horizontal displacement, accelerogram STU000, soil type A.

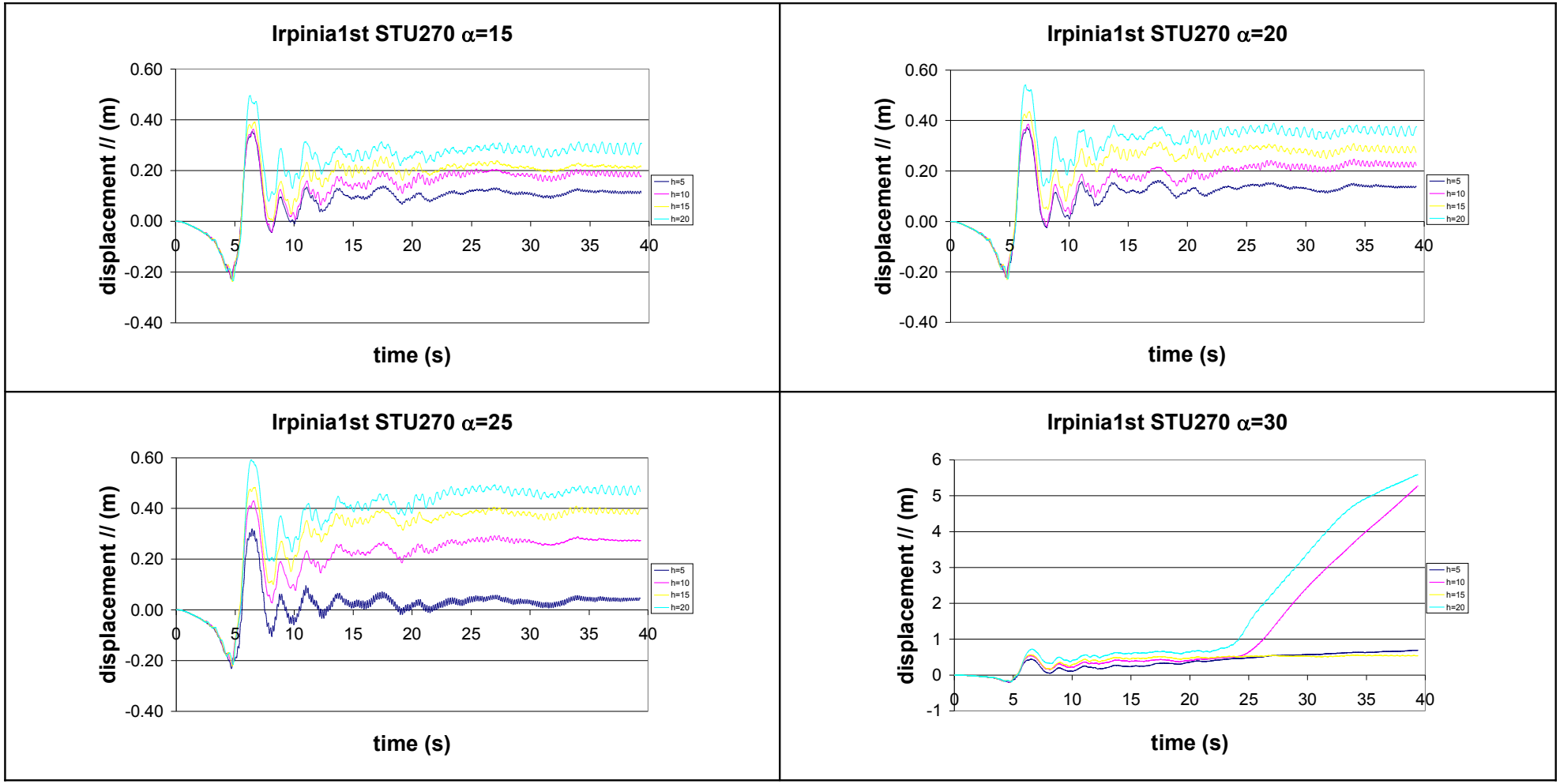

Figure 4.44. Permanent horizontal displacement, accelerogram STU270, soil type A.

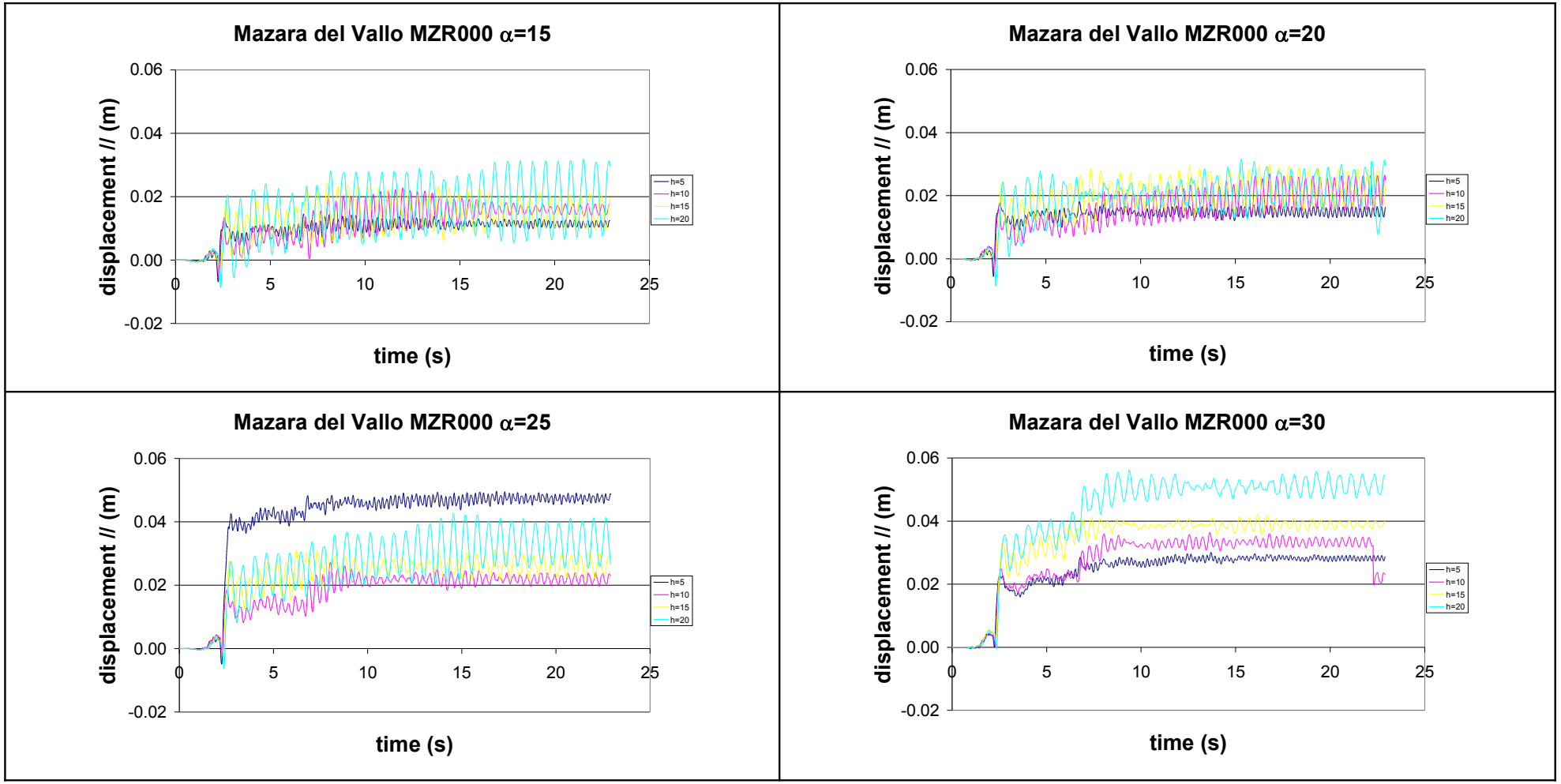

Figure 4.45. Permanent horizontal displacement, accelerogram MZR000, soil type A.

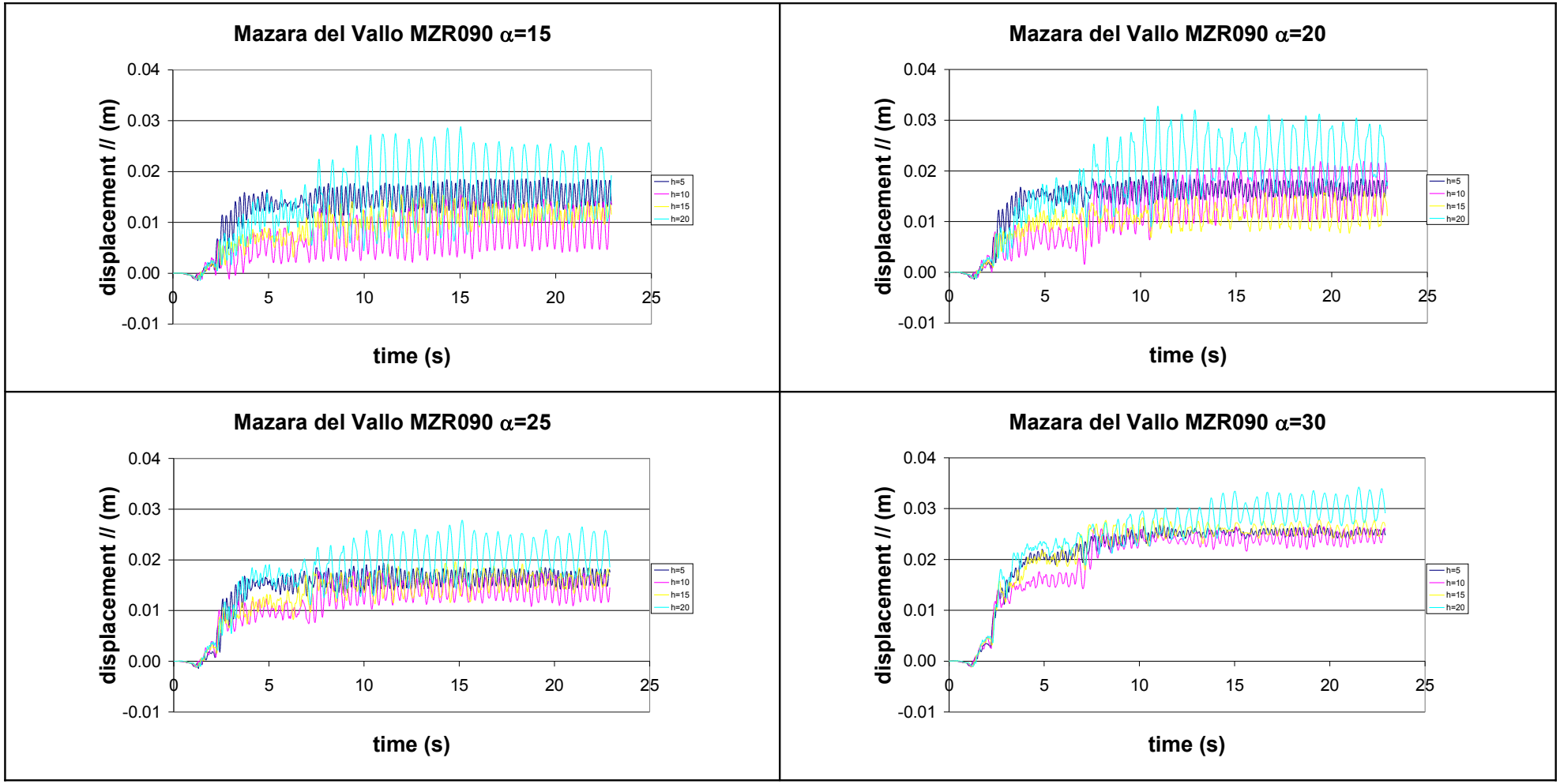

Figure 4.46. Permanent horizontal displacement, accelerogram MZR090, soil type A.

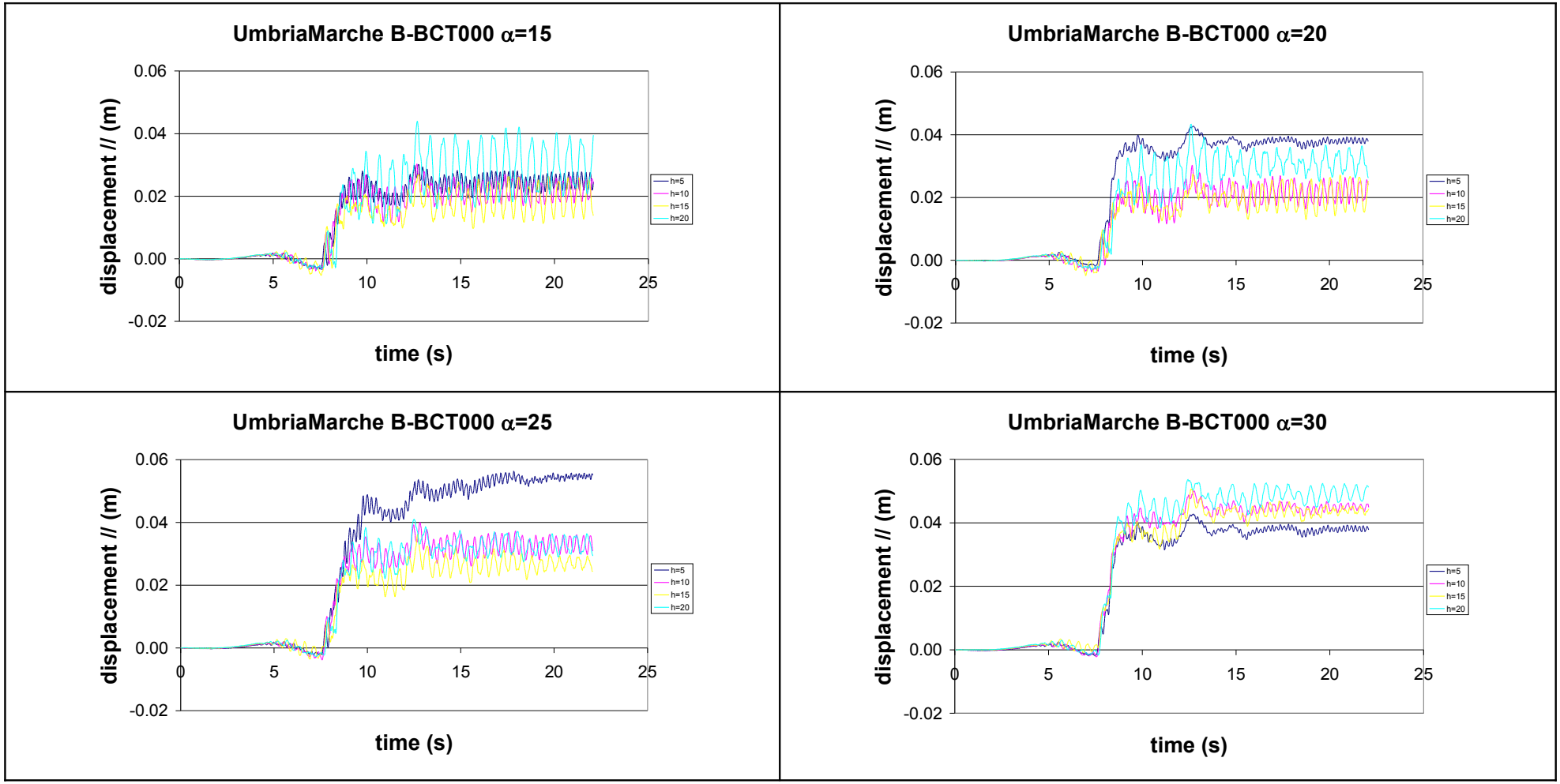

Figure 4.47. Permanent horizontal displacement, accelerogram B-BCT000, soil type A.

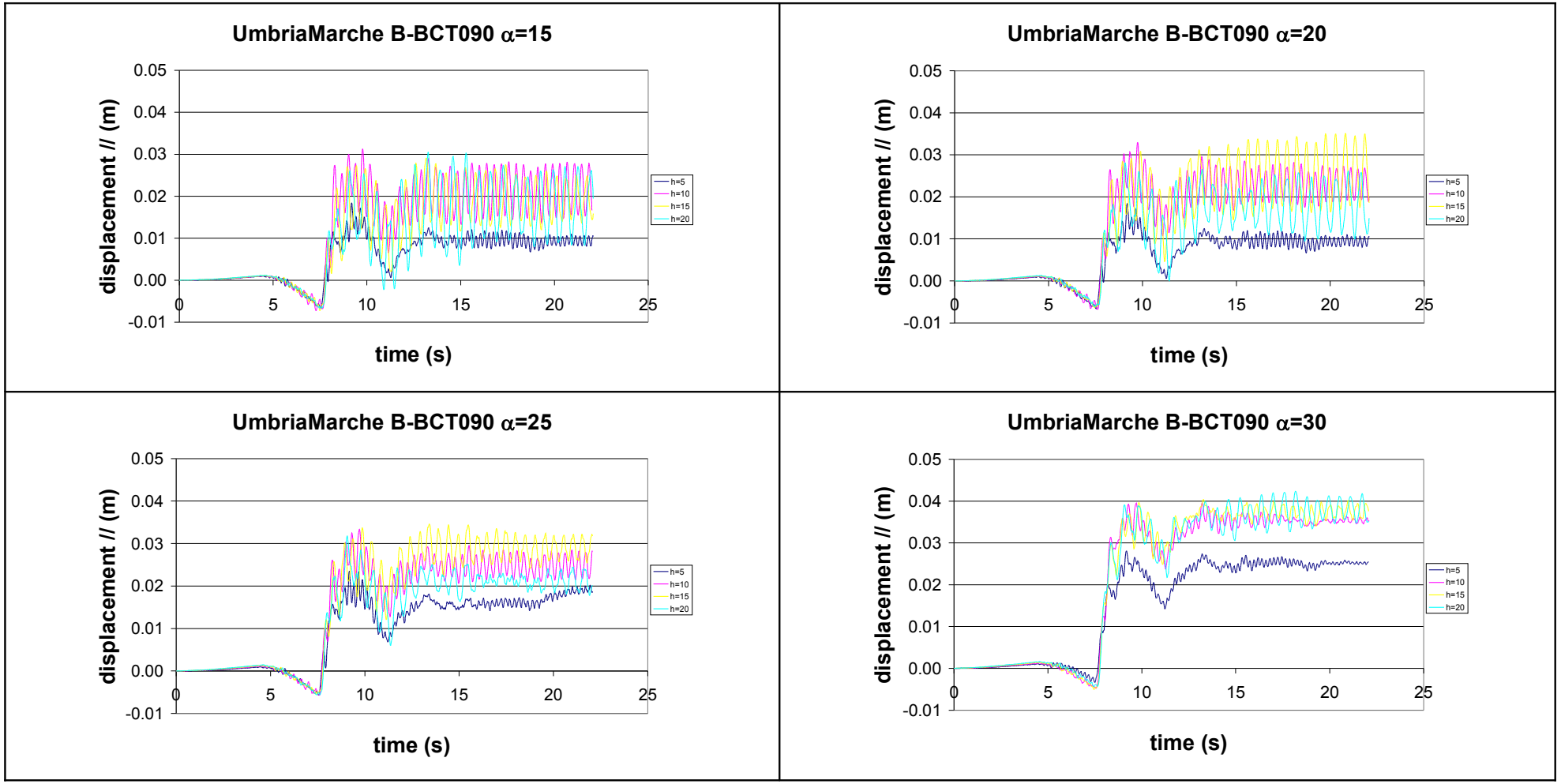

Figure 4.48. Permanent horizontal displacement, accelerogram B-BCT090, soil type A.

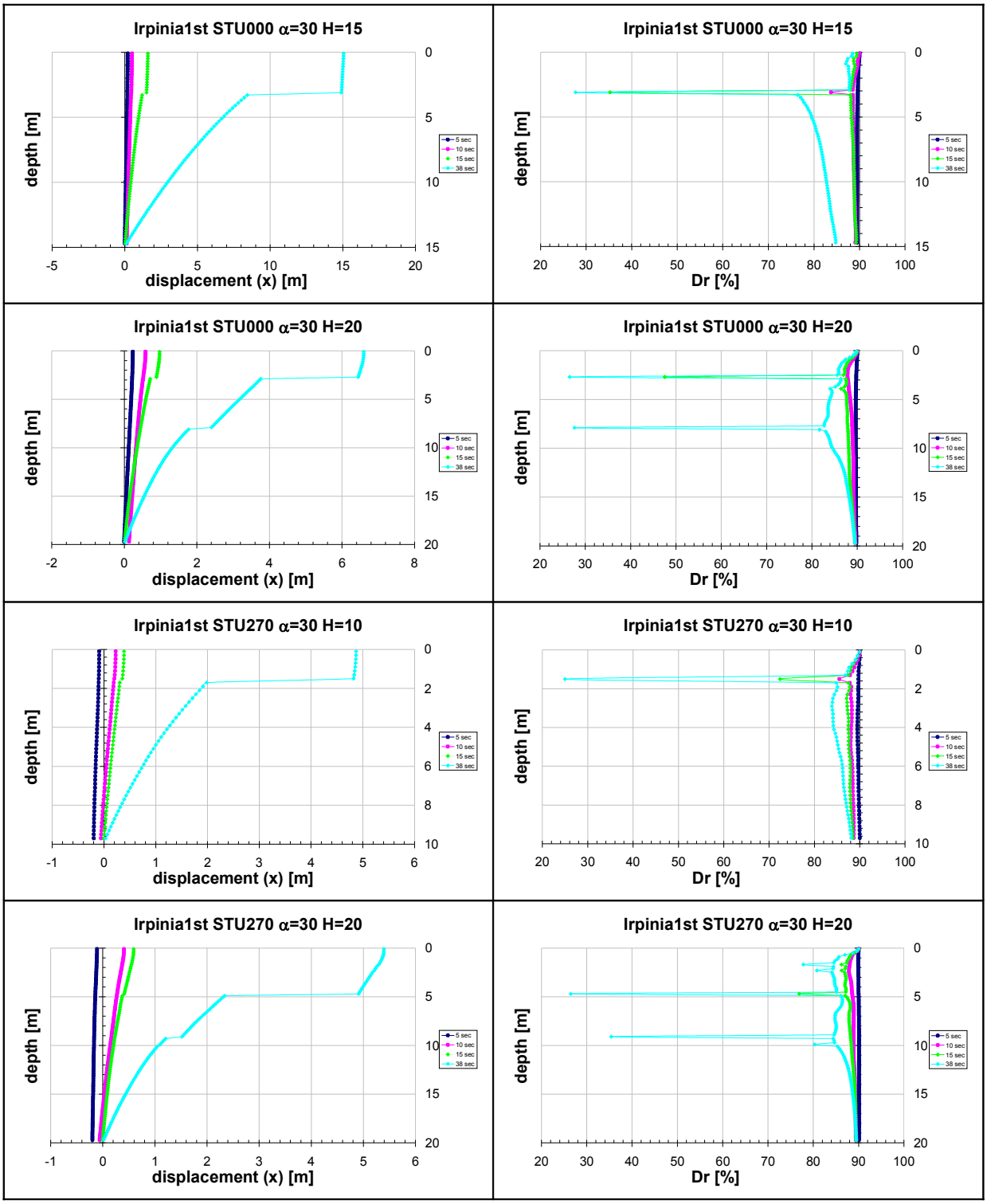

Figure 4.49. Isochrones: maximum horizontal displacements and relative density.

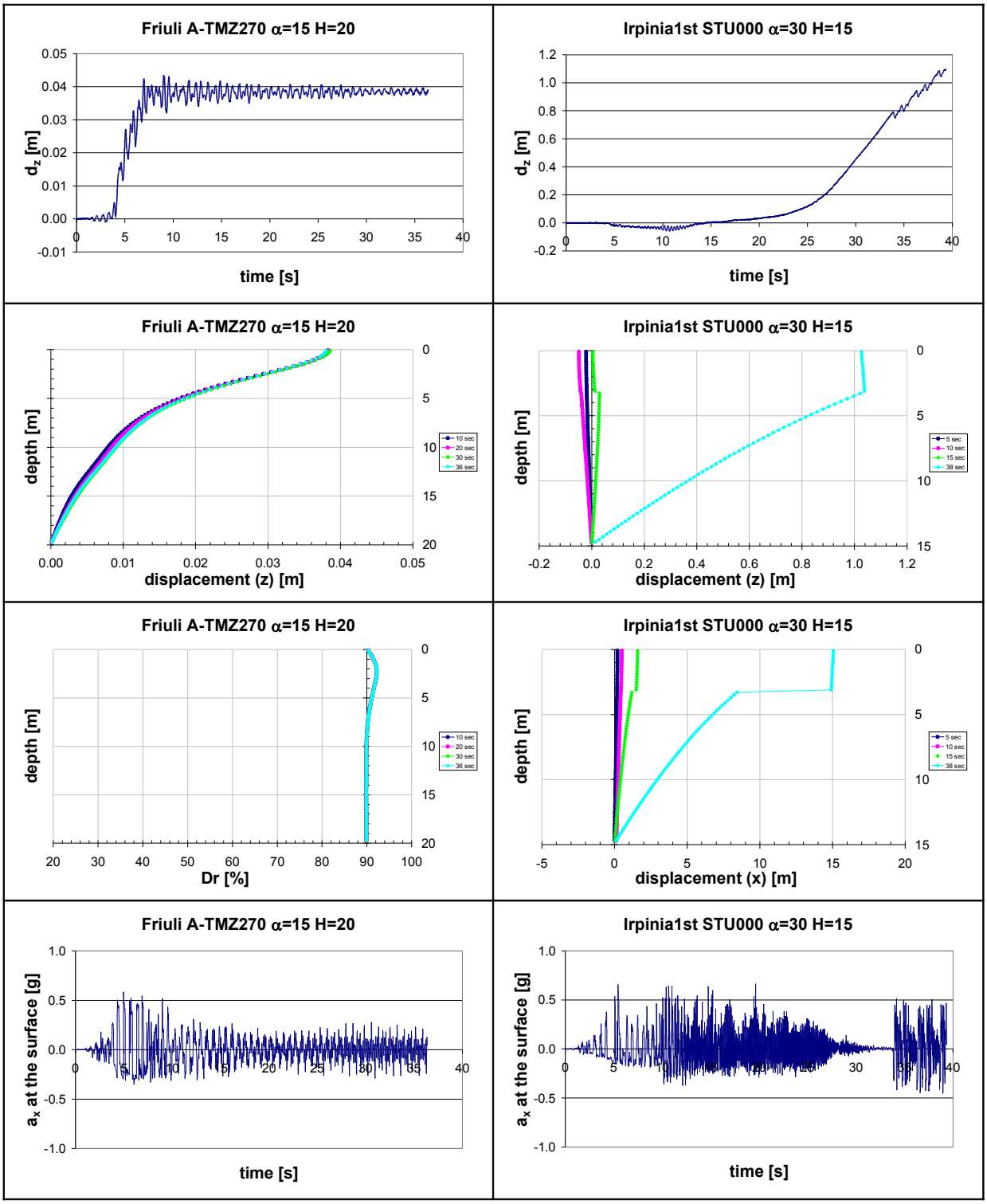

Figure 4.50. Vertical displacements and relative isochrones; horizontal acceleration.

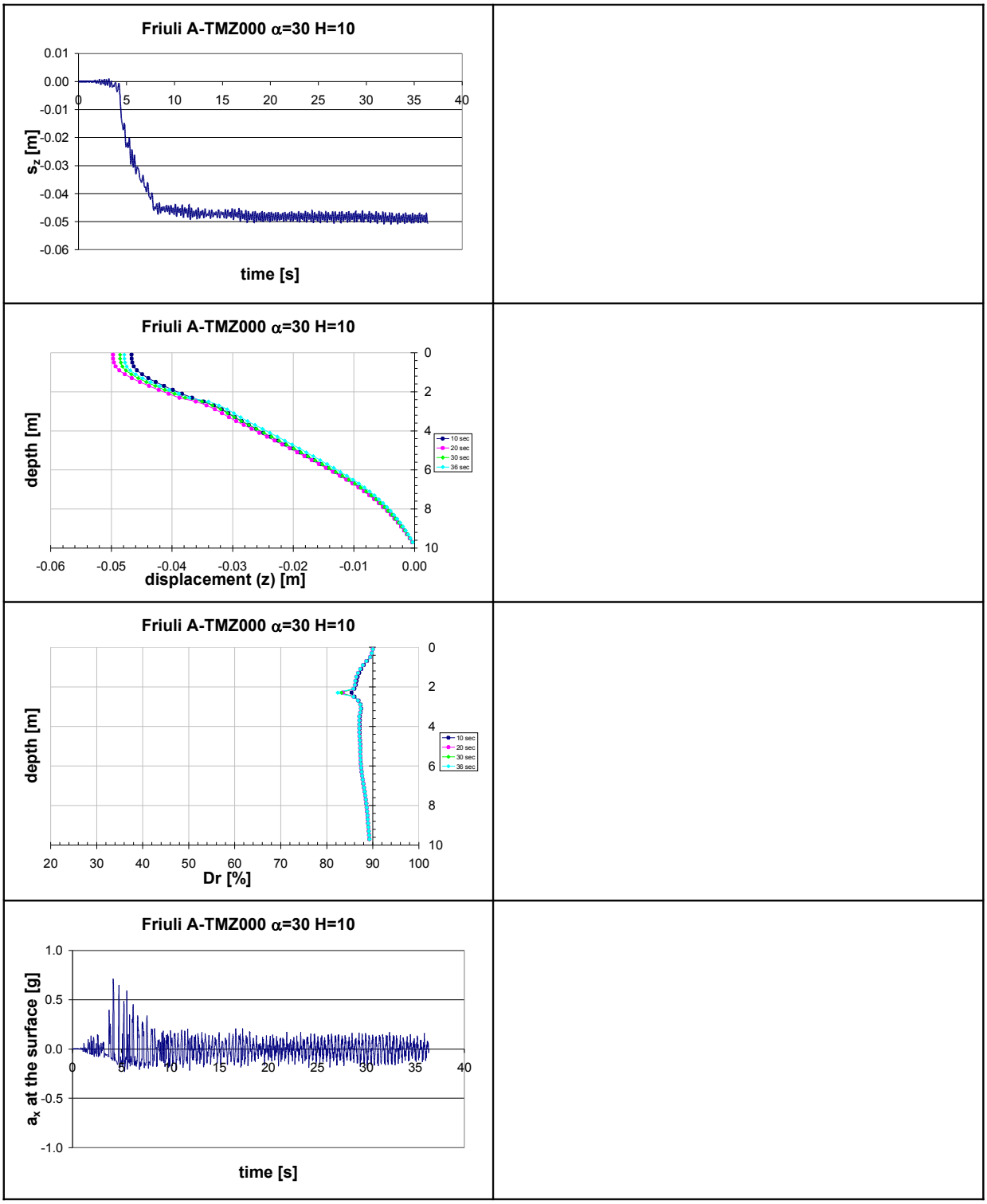

Figure 4.51. Vertical displacements and relative isochrones; horizontal acceleration.

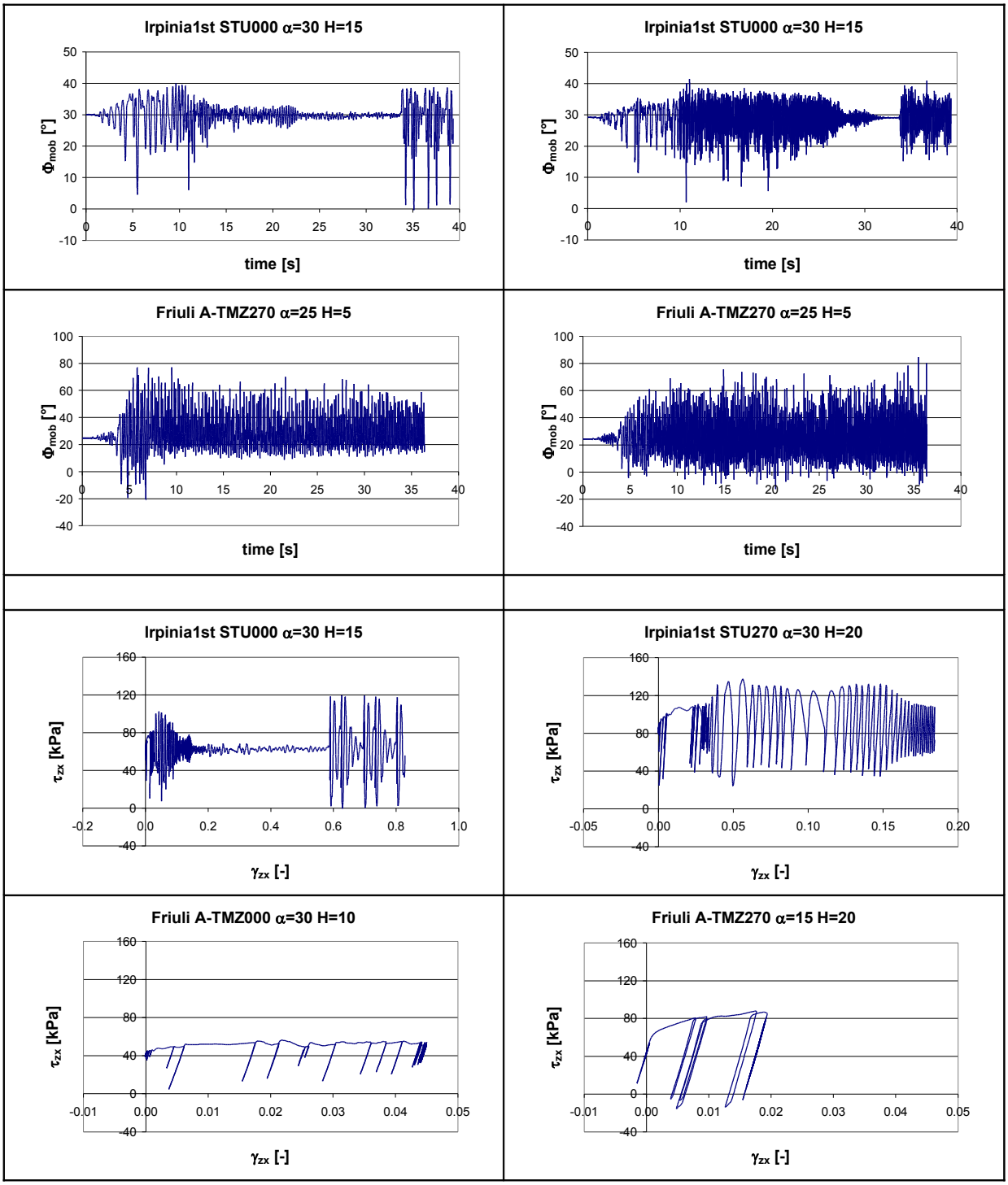

Figure 4.52. Friction angle mobilized (at the middle and on the surface of the slope) and load cycles (at the middle).

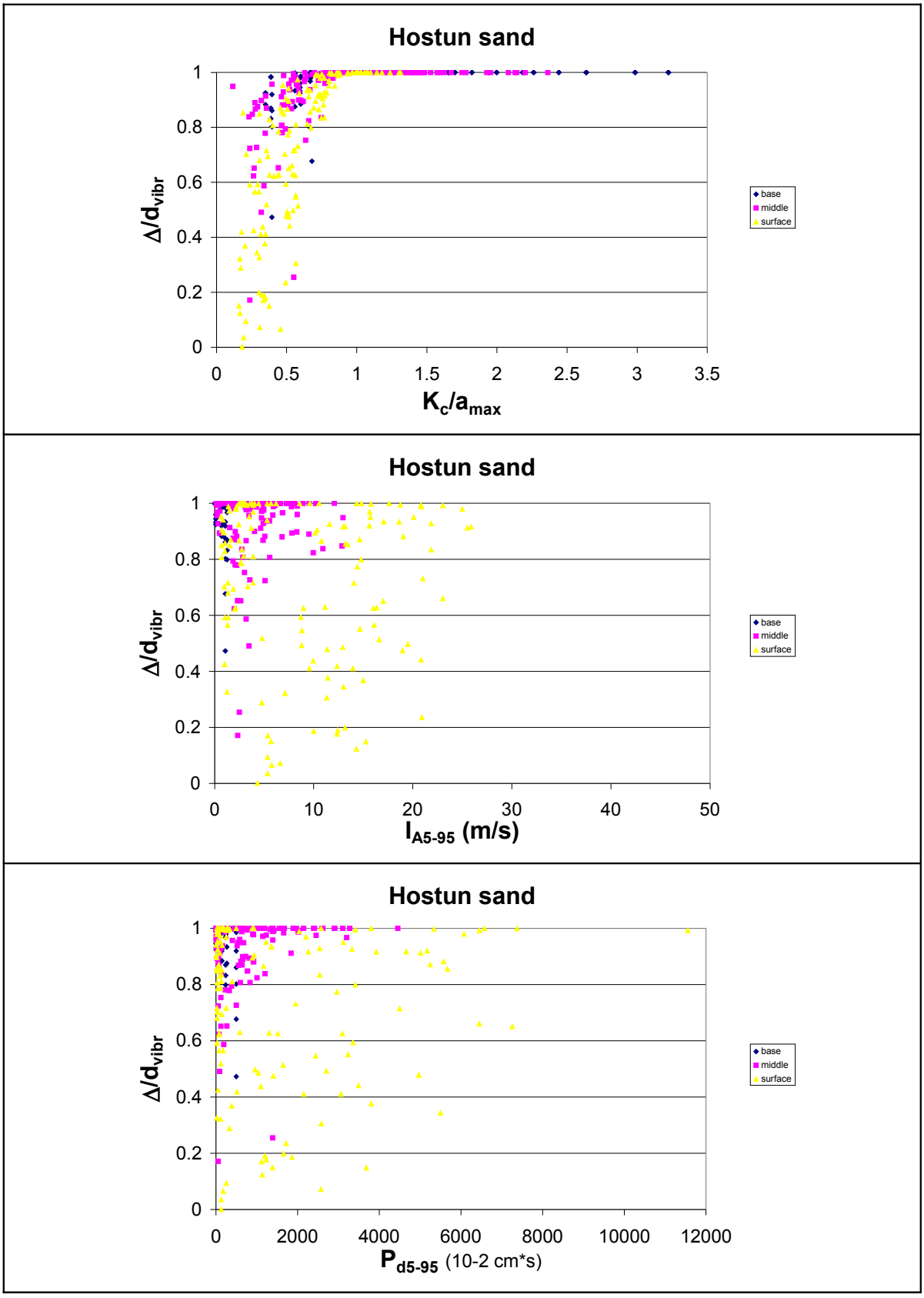

Figure 4.53. Ratio Δ/d_{vibr} in function of K_c/a_{max}, I_{A5-95} and P_{D5-95} respectively.

D_R = 20%

B_R (kPa)	R_F	λ	γ	$\hat{\theta}_c$	$\hat{\theta}_e$	ξ_c	ξ_e	B_P
1028	0.25	0.28	3.4	0.3649	0.2159	-0.4	-0.227	0.0049
c_P	β_{f0}	β_{flim}	r_{c0}	t_P	$\bar{\gamma}$	α	f_0	e_{max}
26	1.95	0.5	1	10	$2e^{-7}$	61	0.2	0.961

D_R = 90%

B_R (kPa)	R_F	λ	γ	$\hat{\theta}_c$	$\hat{\theta}_e$	ξ_c	ξ_e	B_P
1030	0.28	0.25	3.4	0.42	0.218	-0.24	-0.09	0.002
c_P	β_{f0}	β_{flim}	r_{c0}	t_P	$\bar{\gamma}$	α	f_0	e_{max}
100	2.7	0.9	1	10	$1e^{-6}$	61	0.2	0.624

Table 4.1. Constitutive model parameters for Hostun sand.

Loose sand			**Dense sand**		
p_c = 100 kPa	p_c = 200 kPa	p_c = 300 kPa	p_c = 100 kPa	p_c = 200 kPa	p_c = 300 kPa
32.36%	32.37%	32.38%	62.03%	62.2%	62.33%

Table 4.2. Relative density D_R at different confining pressures.

Soil type	Accelerograms	PGA (g)	I_A (m/s)	I_{A5-95} (m/s)	P_D (10^{-2} cm/s)	P_{D5-95} (10^{-2} cm/s)
A	TMZ000	0.357	0.786	0.708	83.14	142.59
	TMZ270	0.351	1.202	1.082	254.42	499.23
	CTR000	0.126	0.576	0.518	194.90	220.64
	CTR270	0.136	0.809	0.728	340.98	405.76
	STU000	0.223	1.184	1.065	240.23	268.00
	STU270	0.321	1.394	1.254	202.93	240.91
	MZR000	0.209	0.123	0.114	3.82	2.23
	MZR090	0.154	0.068	0.061	1.53	1.33
	B-BCT000	0.185	0.151	0.136	2.86	3.09
	B-BCT090	0.186	0.095	0.086	0.79	0.72
	CTR000 x4	0.507	9.271	8.344	3118.34	3530.17
	CTR270 x3	0.410	7.322	6.590	3068.79	3651.86
	STU000 x2	0.455	4.764	4.288	960.93	1071.99
	STU270 x1.5	0.643	5.608	5.047	811.71	963.63
	MZR000 x2	0.420	0.493	0.444	15.27	8.94
	MZR090 x3	0.465	0.618	0.556	13.73	11.95
	B-BCT000 x2.5	0.464	0.949	0.854	17.84	19.31
	B-BCT090 x2.5	0.466	0.596	0.536	13.09	4.41
B	P-ANR000	0.520	0.582	0.524	39.09	17.10
	P-ANR090	0.398	0.349	0.314	41.32	7.34
	Q-ANR000	0.466	0.286	0.257	10.31	15.18
	Q-ANR090 x2	0.428	0.440	0.396	15.88	12.67
	A-NCR000	0.474	2.492	2.243	141.95	169.91
	A-NCR270	0.384	2.385	2.147	210.30	251.35
	B-NCR000	0.475	1.168	1.051	50.79	52.58
	B-NCR270x2	0.526	3.541	3.187	209.51	202.32
	P-GEN000	0.407	0.655	0.590	26.19	23.69
	P-GEN090	0.465	0.973	0.875	35.34	42.54
C	A-CLF000 x2.5	0..498	2.967	2.670	565.97	551.14
	A-CLF270 x2	0.404	1.618	1.456	250.33	171.37
	B-CLF000 x1.5	0.511	1.578	1.420	242.44	368.80
	B-CLF270 x1.5	0.446	1.249	1.124	114.00	136.57
	Q-ANP000 (0.41g)	0.411	0.506	0.455	65.73	34.53
	Q-ANP090 x2	0.427	0.451	0.406	76.85	31.32
	R-ANP000	0.413	0.303	0.273	19.40	14.51
	R-ANP090 x2	0.414	0.573	0.516	150.04	44.07
	CPI000 x2	0.506	0.943	0.848	165.01	82.81
	CPI270	0.463	1.094	0.985	190.41	101.89

Table 4.3. Ground motion parameter values.

α (°)	φ' (°)	K_c
15	37.1	0.406
20	37.1	0.308
25	37.1	0.214
30	37.1	0.125

Table 4.4.

CHAPTER 5: ELASTOVISCOPLASTIC NUMERICAL ANALYSES OF INCLINED SHALLOW SLOPES OF TOYOURA SAND UNDER SEISMIC ACTION

5.1 *Introduction*

In this chapter the numerical results obtained by using the VIBRAZIONE code with constitutive parameters calibrated for Toyoura sand are illustrated.

Toyoura sand is a uniform clean fine sand and is widely used in Japan as a standard research sand.

Such as in the previous chapter, an inclined shallow infinitely long slope was studied considering four different angles of inclination (15°, 20°, 25° and 30°) and four different thicknesses H of the slope (5, 10, 15 and 20m).

Also in this case the spatial discretization Δz was set equal to 0.2m (only for H = 5m the value of Δz is equal to 0.1m).

In this chapter the author has taken, as seismic input, the accelerograms recording for recent Italian earthquakes for the soil types A (Database SISMA) reported in Chapter 3.

As was already explained in the previous chapters, before performing dynamic analyses the deposition process is necessary to be simulated, so that an initial estimate of the stress and internal variables is obtained. This phase was conducted, by adopting a purely elastoplastic model and imposing for Toyoura sand γ = 15.7 kN/m^3.

5.2 Mechanical characterization of Hostun sand

In this section the parameters used for the constitutive model are detailed. These have been obtained by simulating the experimental results of laboratory tests on Toyoura sand.

In this chapter only one sets of parameters (Table 5.1), representative of dense sand (D_R = 80%), is defined: in this case relative density is imposed to be constant; so it must give up one of the best qualities of the elastoviscoplastic model.

The stress-strain characteristics of Toyoura sand have been thoroughly explored by a large number of researchers (Tatsuoka et al., 1986, Tatsuoka and Shibuya, 1991) who have remarked that the difference of the mechanical properties of Toyoura sand in dry and saturated state is negligible.

The material consists mostly of quartz (around 90%) and chert (around 4%), the particles have an angular to sub-angular shape (Figure 5.1). The grain size distribution curve is given in Figure 5.1c.

The physical properties are specific gravity ρ_s = 2.654 g/cm^3, mean diameter D_{50} = 0.18 mm, uniformity coefficient U_c = 1.56, maximum void ratio e_{max} = 0.930, minimum void ratio e_{min} = 0.589 and no fine contents less than 74 μm are included. The two values of maximum and minimum density in dry conditions, for the two possible extreme state of thickening, are ρ_{max} = 1.671 g/cm^3 and ρ_{min} = 1.376 g/cm^3.

The values of specific gravity and density of the soil for a relative density D_R = 80% can be therefore determined:

$$\begin{aligned} e_{80} &= e_{\max} - D_R(e_{\max} - e_{\min}) = 0.657 \\ \rho_{80\%} &= 1.602 g/cm^3 \\ \gamma_{80\%} &= 15.7 kN/m^3 \end{aligned} \qquad (5.1)$$

For a relative density of 80% the value of the friction angle is equal to 42.1. Finally, as regards the dynamic properties of the material the average velocity of S waves V_S is equal to 229m/s while the shear modulus G = 84MPa.

5.3 ***Analysis of the dynamic response under real accelerograms***

In Figure 5.2 (a, b, c, d, e and f) the time histories of the main variables of the system monitored at the base, middle and surface of the slope are illustrated, which are:

- tangential stress and strain; displacement, velocity and acceleration in *x* direction;
- normal stress and strain; displacement, velocity and acceleration in *z* direction;
- relative density;
- loading cycles in $\gamma_{xz} - \tau_{xz}$ plane;
- friction angle along a horizontal plane, defined as the angle whose tangent is equal to the ratio between τ_{xz} and σ_z.

All these variables have been considered for the Friuli earthquake, Tolmezzo - Diga Ambiesta station (TMZ000) and geometry α = 15° and H = 5 m, while in the following only the most interesting variables will be analyzed, such as in the previous chapter for Hostun sand has been done.

In Figure 5.3 the isochrones given for 4 different time instants (variable depending on the accelerograms considered) are shown for TMZ000 (α = 15°, H = 5 m).

Analyzing the results obtained by employing the VIBRAZIONE code, the higher horizontal displacements, equal to 0.14m are obtained for Friuli earthquake, registration TMZ000, and Irpinia earthquake, registration STU270, in both case for an inclination angle of the slope α = 30° and a height H = 20m. Conversely to the previous cases, the horizontal displacement, obtained by using as seismic input the records of Campobello di Mazara and Borgo - Cerreto Torre, are quite similar to those obtained for Irpinia and Friuli earthquakes, in particular for Calitri station (Figures from 5.4 to 5.13).

The displacements are significantly lower than those obtained for Hostun sand, also because of "localization" is not allowed being unique the set of parameters used.

In any case, imposing an angle of inclination of the slope, the displacements are growing with increasing of the slope height.

The isochrones of horizontal displacements for any accelerograms employed and for the geometry α = 30° H = 20m are shown in Figure 5.14.

The higher surface settlements take place , instead, for the geometry α = 15° and H = 20 m, except for CTR000 being α = 20°, and the maximum value is 0.027m for STU270 accelerogram. (Figure 5.15).

No cases of heave of the ground level have been occurred.

With regard to the horizontal acceleration there is a large damping of the negative acceleration values for a slope inclination of 30° and, in particular, for height H = 20 m, such as for Hostun sand; some examples are reported in Figures 5.15 and 5.16.

Concerning the friction angle mobilized in many cases the limit breaking value of material, equal to 42.1°, is exceeded; in particular for Friuli earthquake and Irpinia earthquake (Sturno station). The inclination angles α = 25° and 30° are the most disadvantageous.

As was mentioned, the output of VIBRAZIONE provides the values of the variables calculated in the middle and at the surface of the slope, in particular, for this variable can be said that the breaking value is overcome only in the middle of the layer and not on the surface.

Finally looking at the load cycles (at the middle of the layer) can be noted that there are many yielding, but the deformations are lower with respect to Hostun sand, being less than 1% (Figures 5.15 and 5.16).

For Toyoura sand the amplification factor of PGA varies from 1.5 to 3.5 whereas for the Hostun the range is 1.5 – 3.5. In both cases the Irpinia earthquake is that for which there are the greatest amplification.

5.4 ***Comparison with Newmark method (real accelerograms).***

In this section the displacements already obtained by employing the code VIBRAZIONE are compared with those obtained by employing the Newmark method, for which the potential landslide body, subject to the weight force and the seismic action, moves along the sliding surface whenever the acceleration at the base, a(t), exceeds a threshold value, called critical acceleration K_c, characteristic of the incipient collapse conditions; in case of dry slope:

$$K_c = \frac{\cos\alpha * tg\varphi' - \sin\alpha}{\sin\alpha * tg\varphi' + \cos\alpha} \qquad (5.2)$$

where φ' is the friction angle and α the inclination angle of the slope. The values of K_c for different inclinations are shown in Table 5.2.

As for Hostun sand, the considered accelerograms for soil type A in addition to those obtained by VIBRAZIONE, in the middle and at the surface of the slope (for any geometry), are used as seismic input; in this case there are not variation of relative density and so of the friction angle to take into account in the displacement method.

The ratio Δ/d_{vibr} in function of the ratio K_c/a_{max}, the Arias Intensity 5-95% and the Destructive Power 5-95% respectively are reported in Figure 5.17.

By the comparison of results, in terms of displacements, obtained with the two methods appears that:

- using as seismic input the accelerogram at the base, in 97% of the cases the ratio Δ/d_{vibr} is between 0.8 and 1 and in 99.4% it is more than 0.5. In 85% of cases the threshold value K_c is not exceed, so no displacement occur using the Newmark approach;
- using as seismic input the accelerogram in the middle of the layer, in 87% of the cases the ratio Δ/d_{vibr} is between 0.8 and 1 and in 91% it is more than 50%. Only in 1 case Δ is negative but very few. In 50% a_{max} are less than K_c;
- using the accelerogram on the surface, only in the 70% of the cases the ratio Δ/d_{vibr} is between 0.8 and 1 and in 72% it is more than the 50%. In 18% of cases Δ is negative due to the amplification of the signal on surface, it happens only for Friuli earthquake, Tolmezzo station, and Irpinia earthquake, Sturno station. In 32% the threshold value is not reached.

This shows how the two methods are closer when it is taken into account the amplification of the accelerogram in the soil, such for Hostun sand.

In particular it should be noted that, for the recordings of Italian earthquakes on soil type A, in 85% of cases, using the Newmark approach, displacements do not occur because the critical acceleration K_c is not exceeded while with VIBRAZIONE not negligible displacements are obtained and in the majority of the cases the ratio Δ/d_{vibr} is more than 0.8, so the Newmark method gives no reliable results and, above all, not on the safety side.

Unfortunately it was not possible, for Toyoura sand, to identify a unique relationship between the values of seismic parameters, such as Arias Intensity and Destructive Potential, and the displacements calculated by the two methods.

5.5 ***Comparison with Newmark method (all accelerograms and sands)***

Considering, for Hostun and Toyoura sands, as seismic input, the accelerograms for soil types A, B and C (suitably amplified), those for soil A (Database SISMA) and, finally, those obtained by VIBRAZIONE in the middle and surface of the layer, and comparing the results obtained, in terms of displacement, with the two methods considered in this paper, Figure 5.18 shows the following results:

- when the ratio K_c/a_{max} is less than 0.5, a correlation between the calculated displacement with Newmark method and that one with VIBRAZIONE can not be found;
- when this ratio is between 0.5 and 0.7 the correlation is highly variable;
- when this ratio is more than 0.7 ratio Δ/d_{vibr} is more than 0.7.

Analysing this trend, the following relationship has been proposed:

$$\frac{K_c}{a_{\max}} = 0.5 + 0.45 * \left(\frac{\Delta}{s_{vibr}} \right)^2 \qquad (5.3)$$

This simple relationship allows to calculate the displacements that could be obtained by using the more refined elastoviscoplastic model starting from those obtained by the Newmark method. Unfortunately this relationship is applicable only when the ratio K_c/a_{max} is more than 0.5.

a)

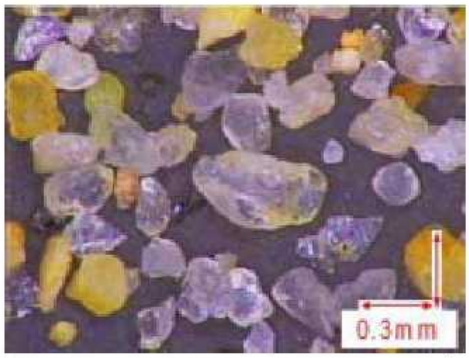

b)

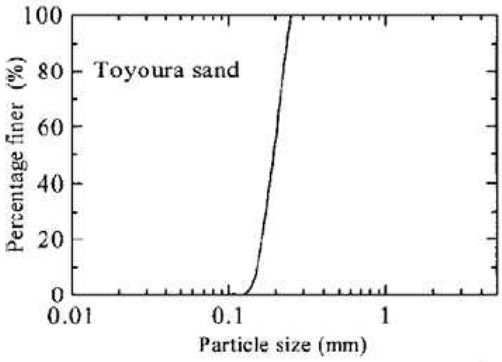

c)

$\rho_{min} = 1.339$ g/cm^3,
$\rho_{max} = 1.618$ g/cm^3

Figure 5.1. Toyoura sand (a), photomicrograph of its grains (b) and grain size distribution (c). (Zambelli, 2006)

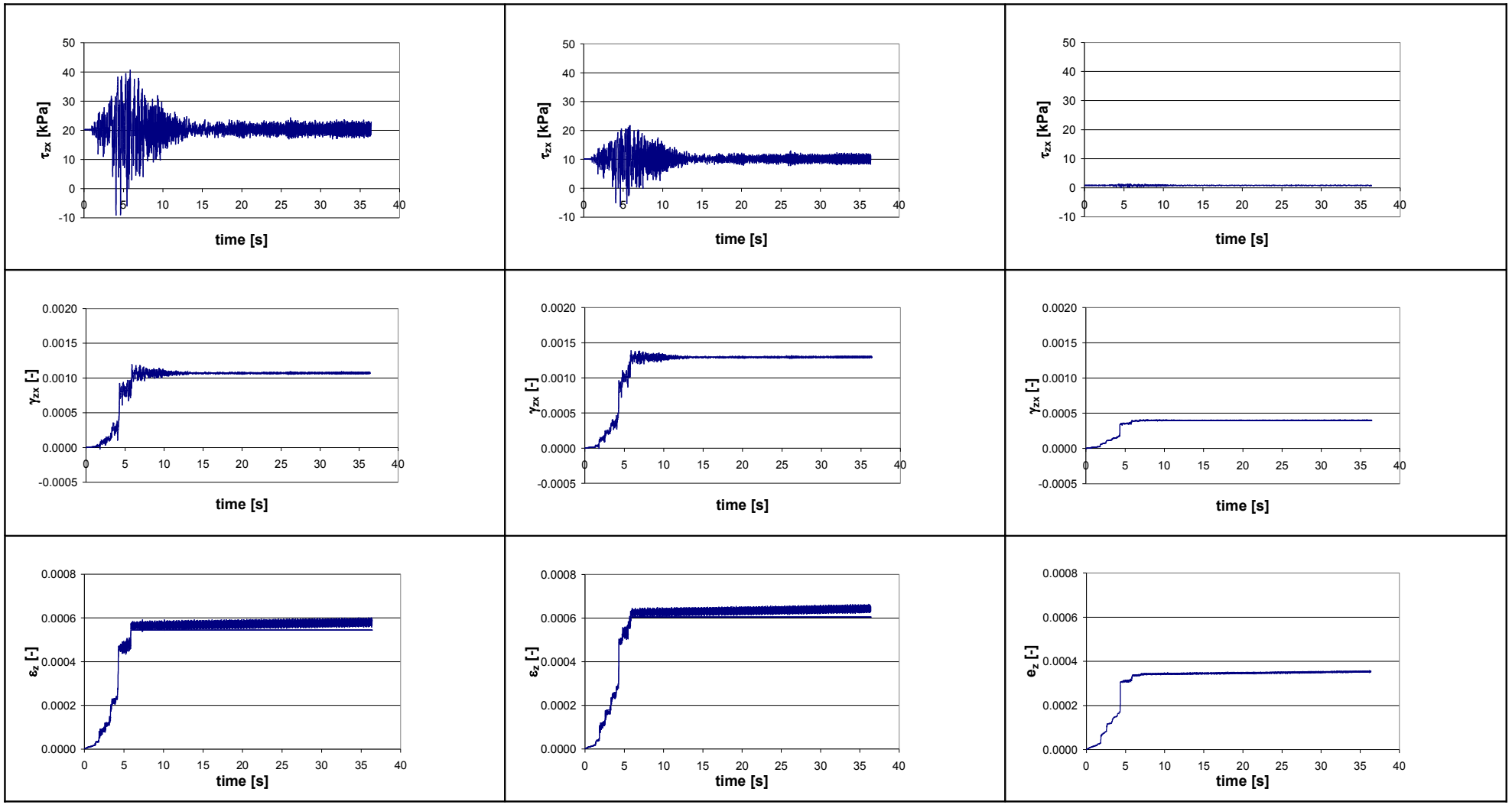

Figure 5.2 (a). Tangential stress and strain, vertical strain (base, middle and top of the layer), Toyoura sand.

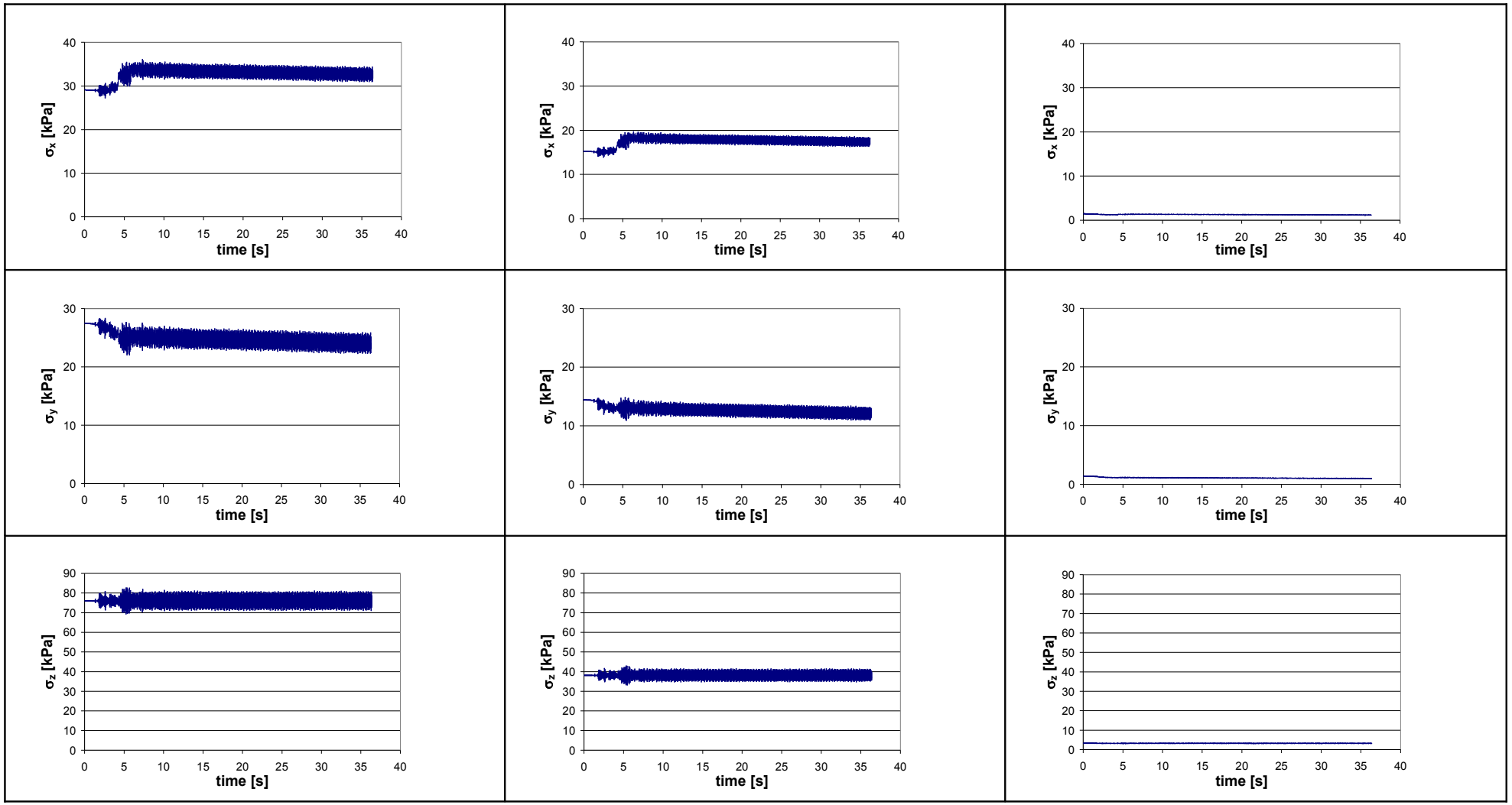

Figure 5.2 (b). Stress in x, y and z direction (base, middle and top of the layer), Toyoura sand.

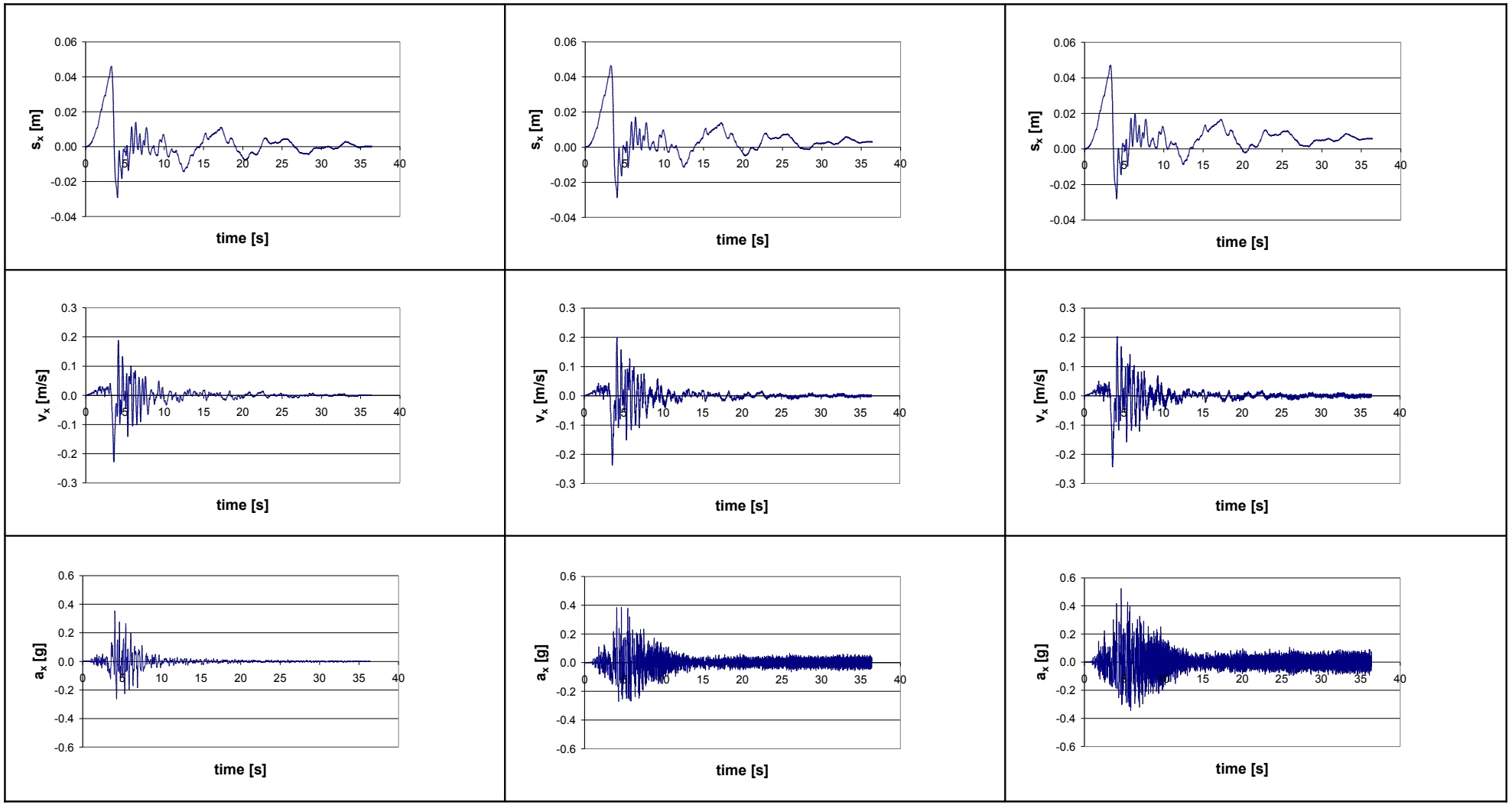

Figure 5.2 (c). Displacement, velocity and acceleration in x direction (base, middle and top of the layer), Toyoura sand.

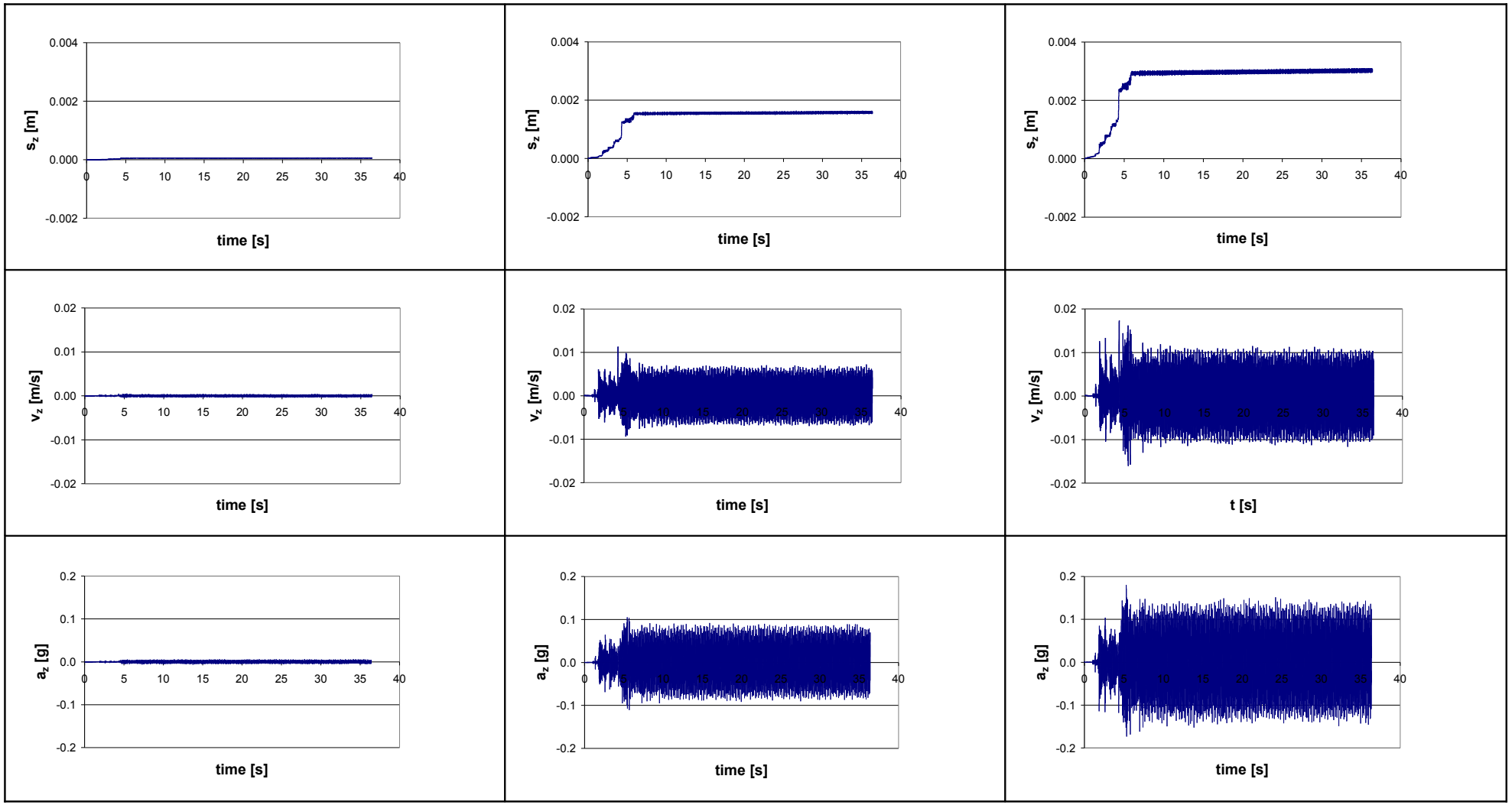

Figure 5.2 (d). Displacement, velocity and acceleration in z direction (base, middle and top of the layer), Toyoura sand.

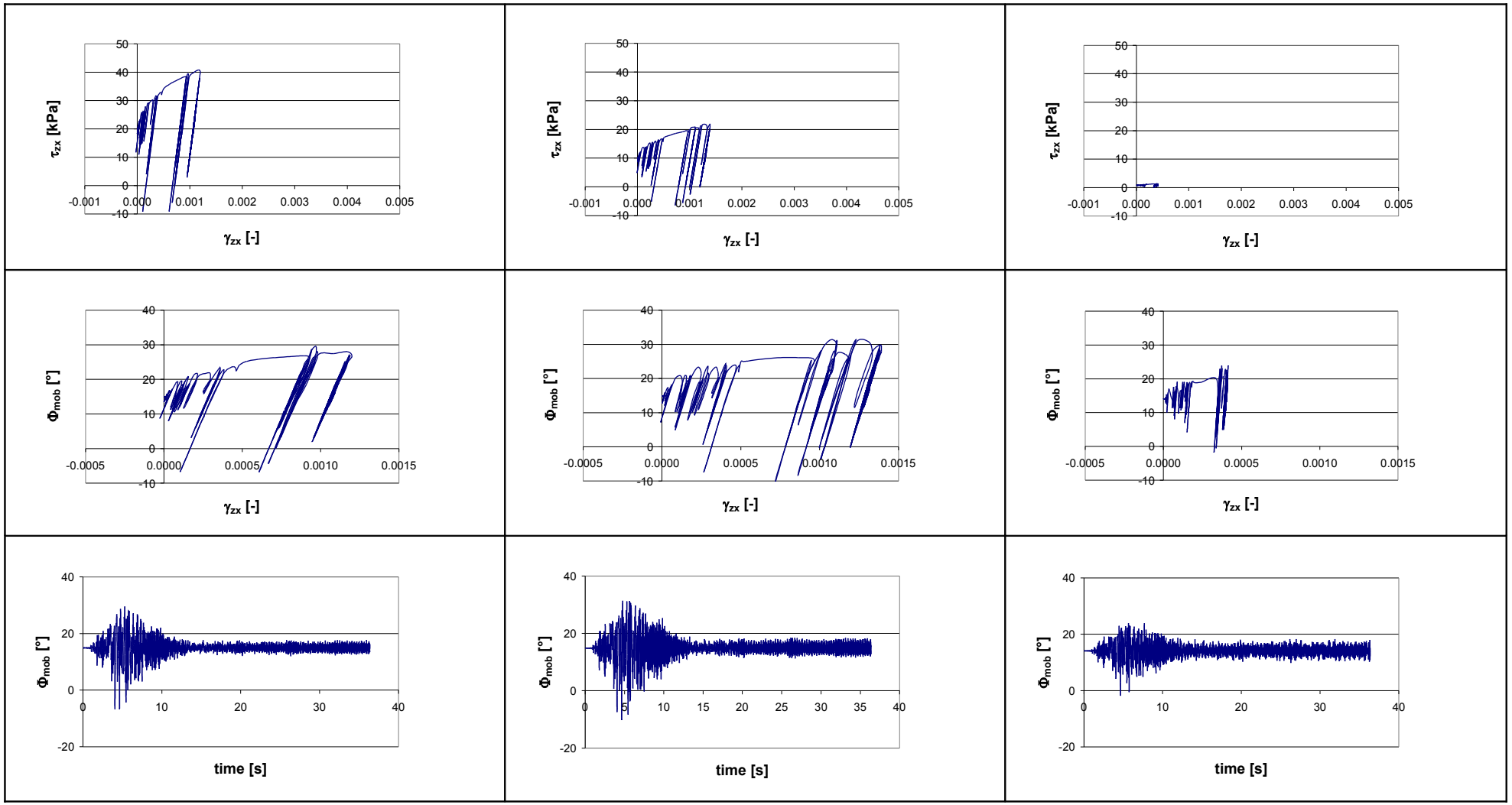

Figure 5.2 (e). Loading cycles and friction angle (base, middle and top of the layer), Hostun sand.

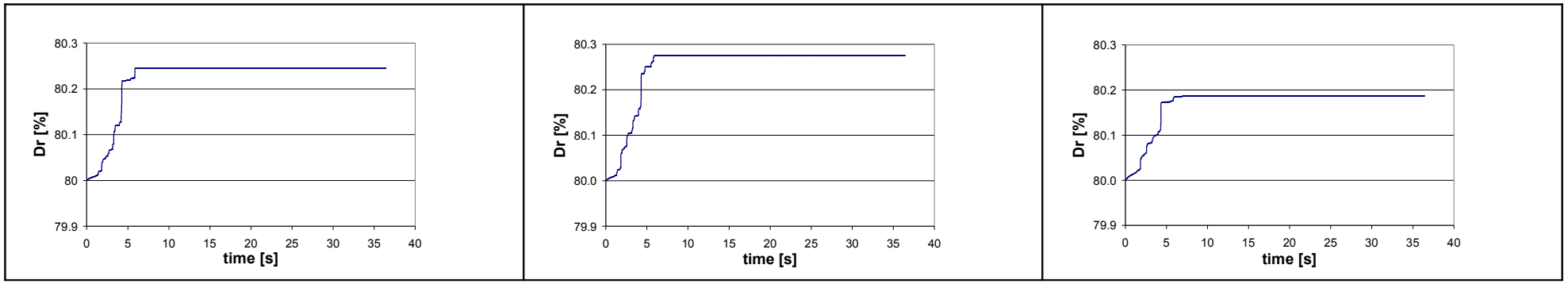

Figure 5.2 (f). Relative density (base, middle and top of the layer), Toyoura sand.

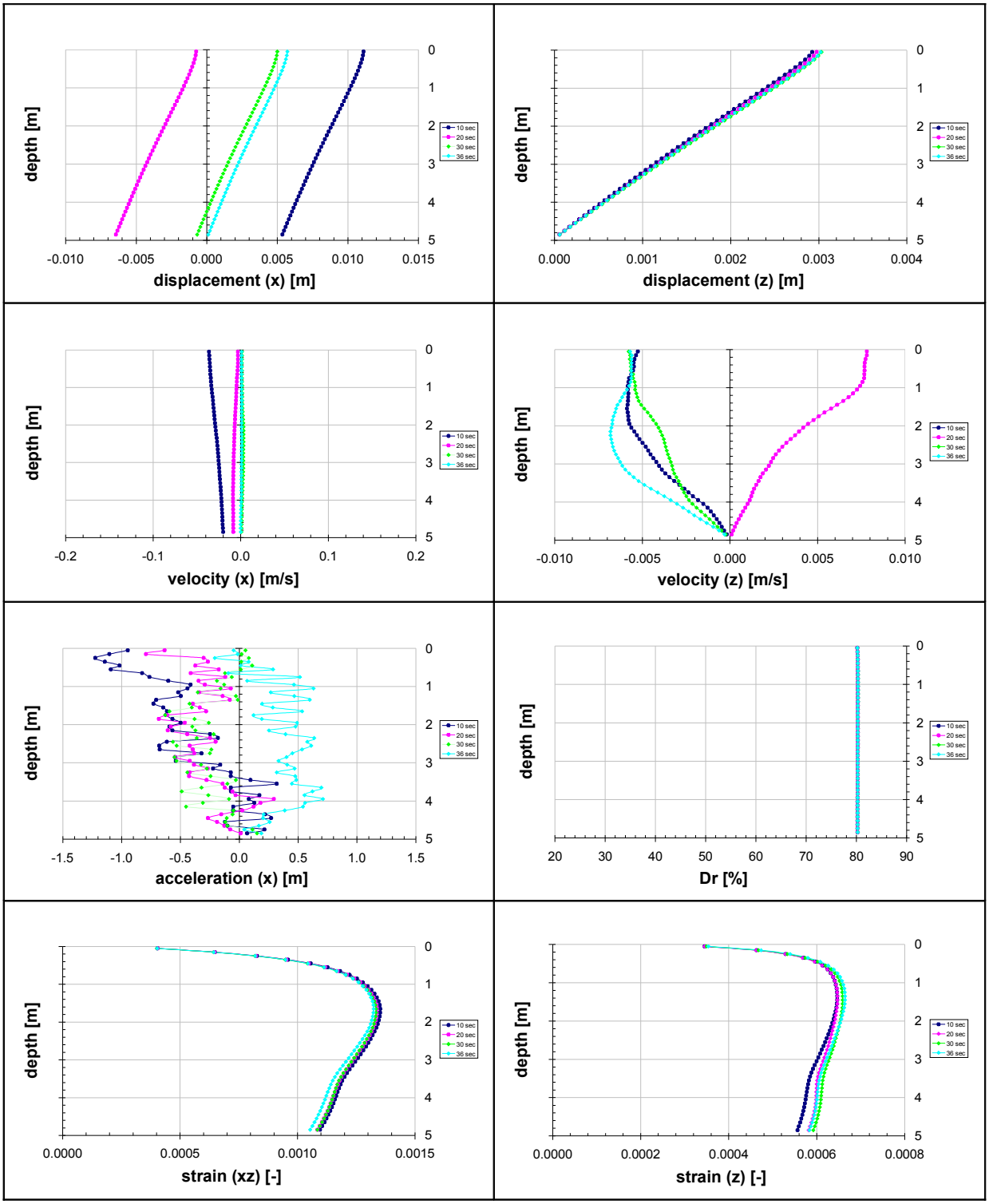

Figure 5.3. Isochrones of displacement and velocity (x and z), acceleration (x), relative density and strain, Toyoura sand.

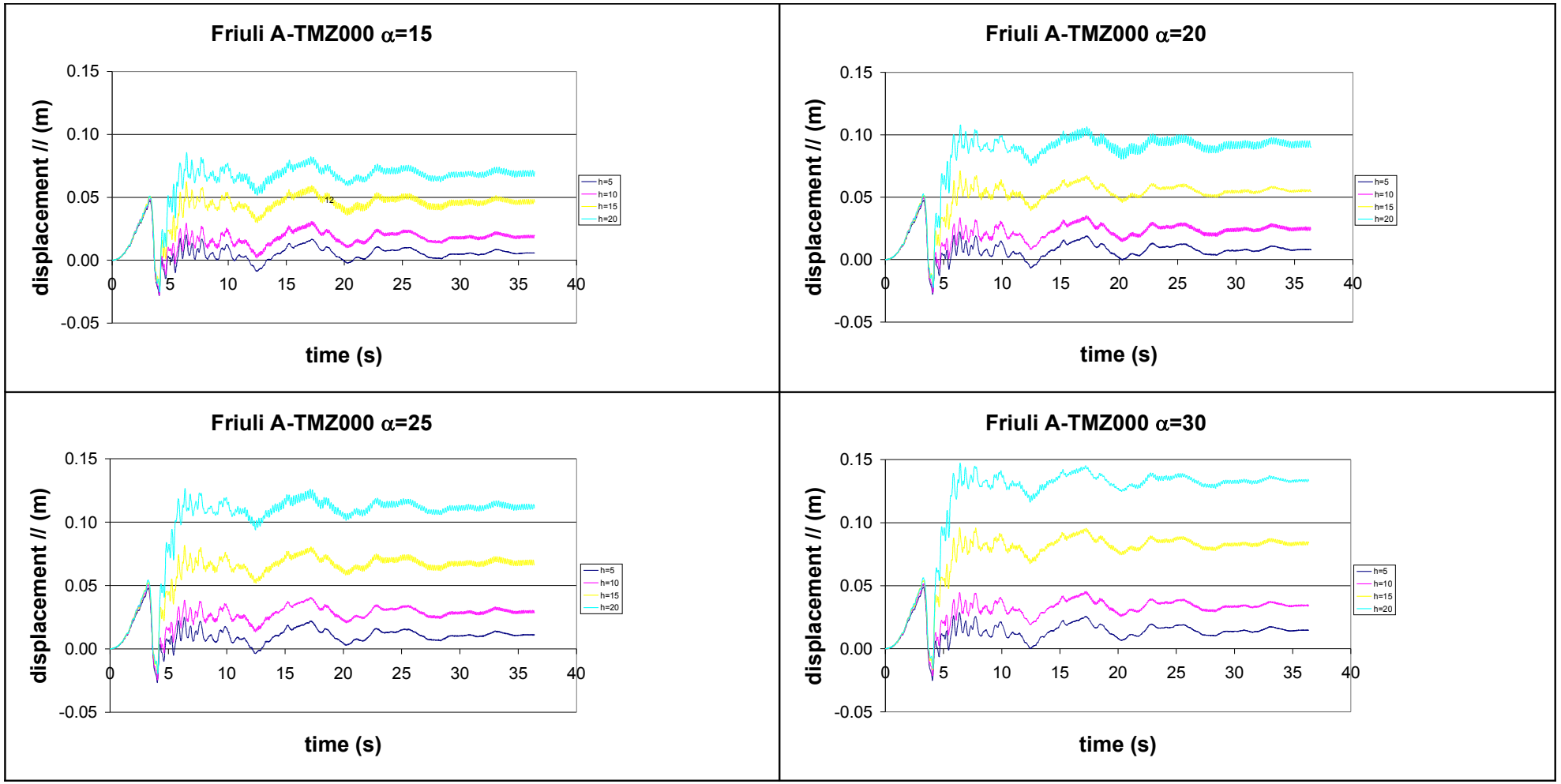

Figure 5.4. Permanent horizontal displacement, accelerogram A-TMZ000, soil type A, Toyoura sand.

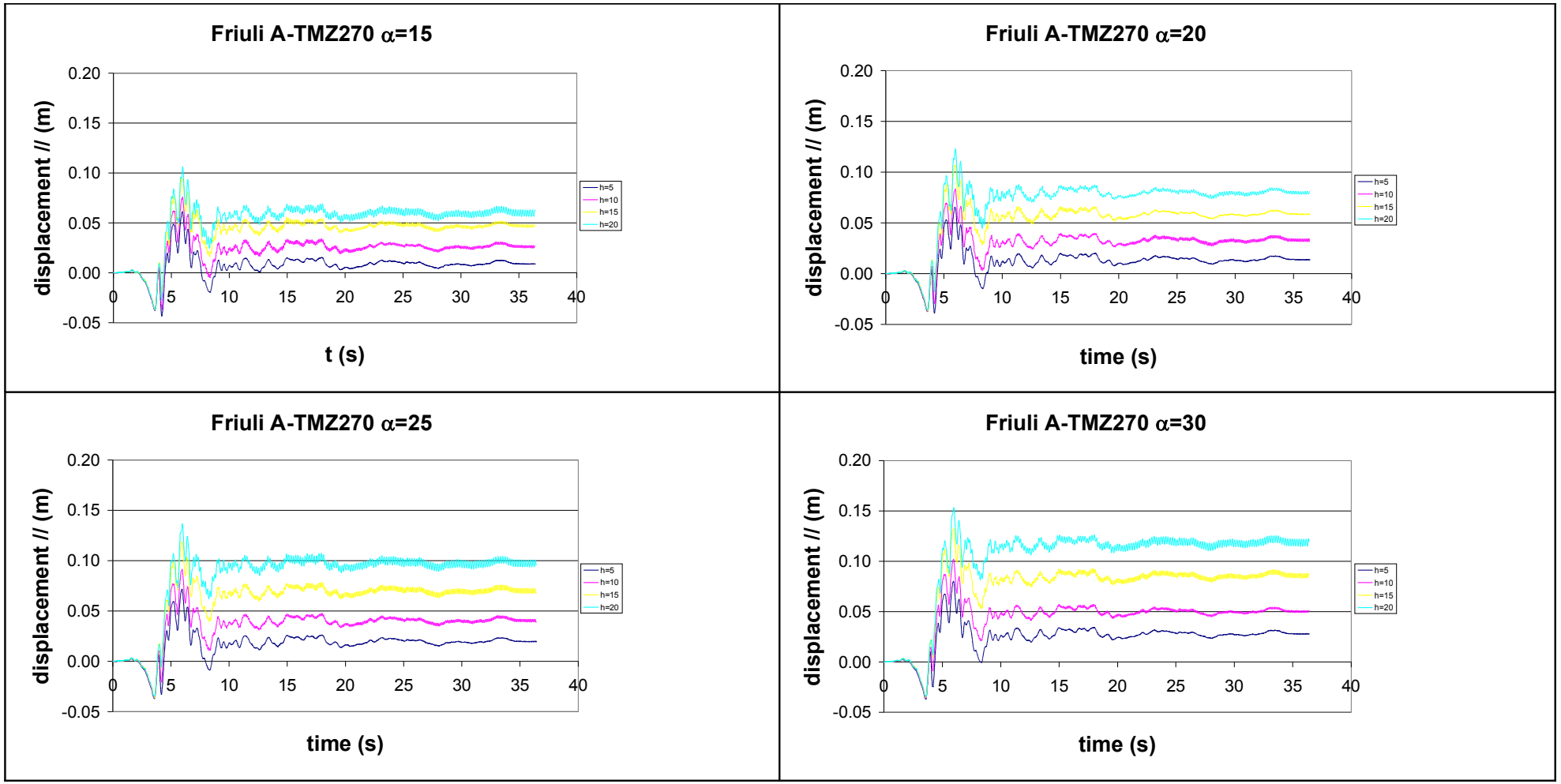

Figure 5.5. Permanent horizontal displacement, accelerogram A-TMZ270, soil type A, Toyoura sand.

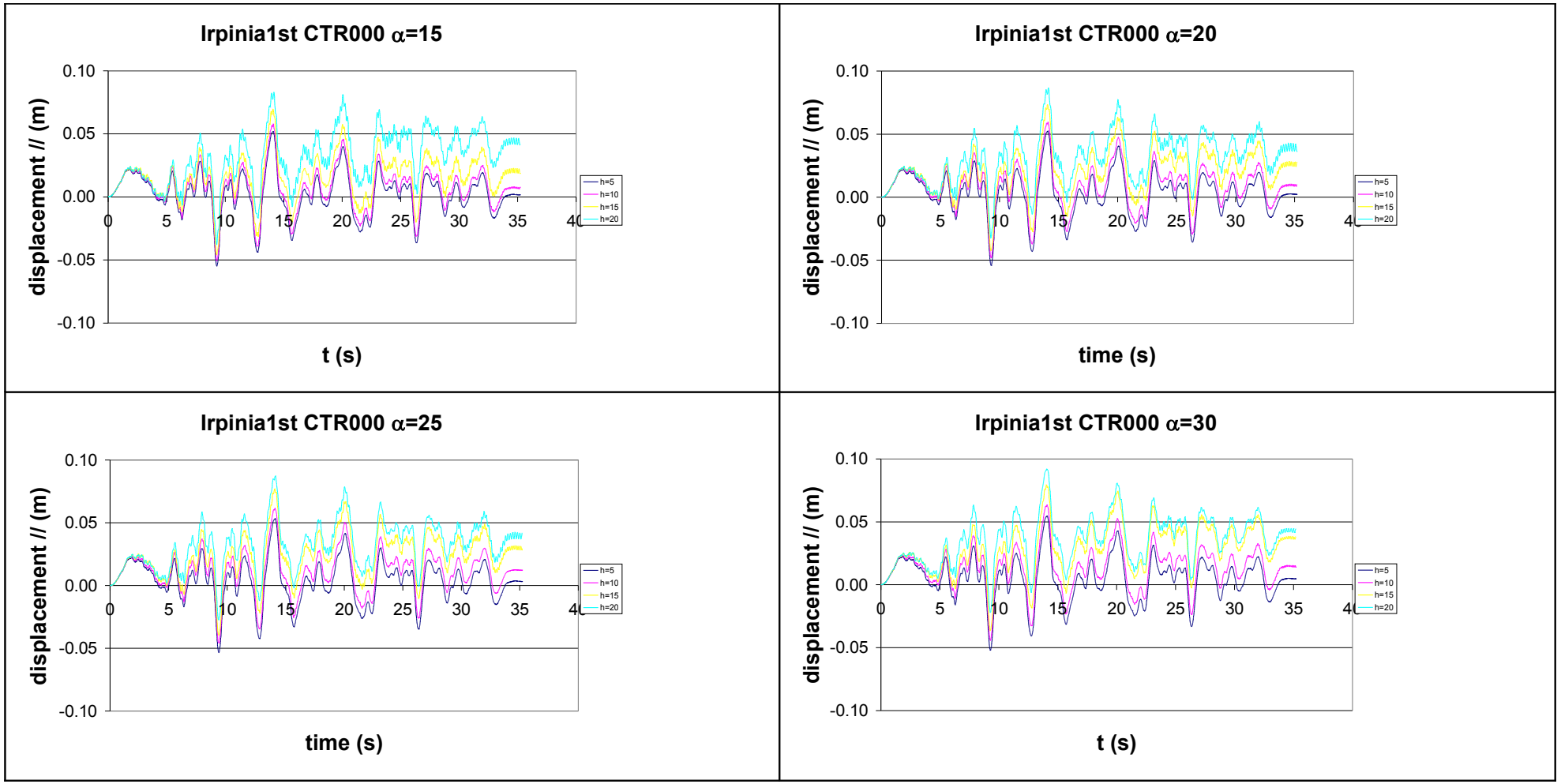

Figure 5.6. Permanent horizontal displacement, accelerogram CTR000, soil type A, Toyoura sand.

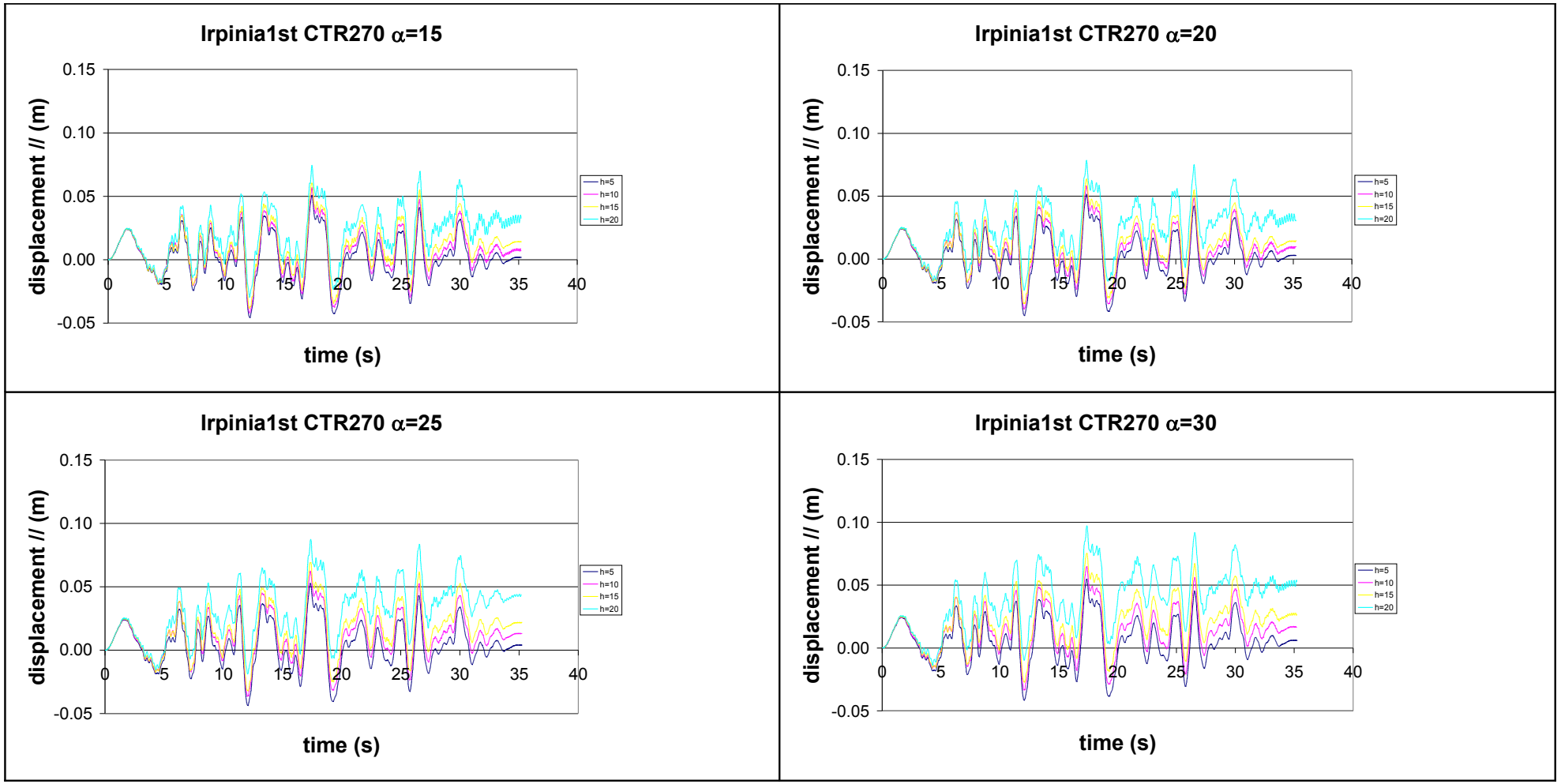

Figure 5.7. Permanent horizontal displacement, accelerogram CTR270, soil type A, Toyoura sand.

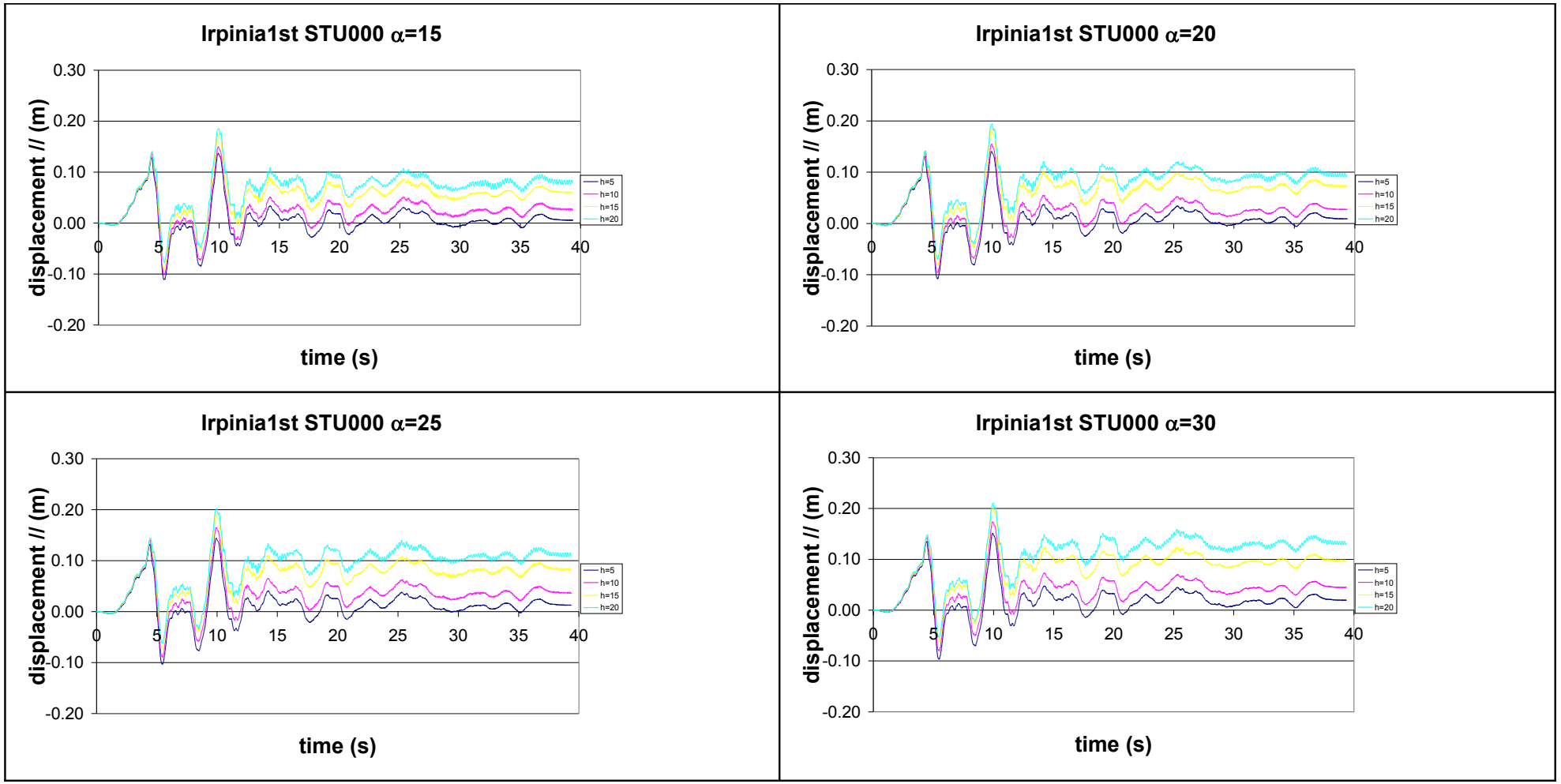

Figure 5.8. Permanent horizontal displacement, accelerogram STU000, soil type A, Toyoura sand.

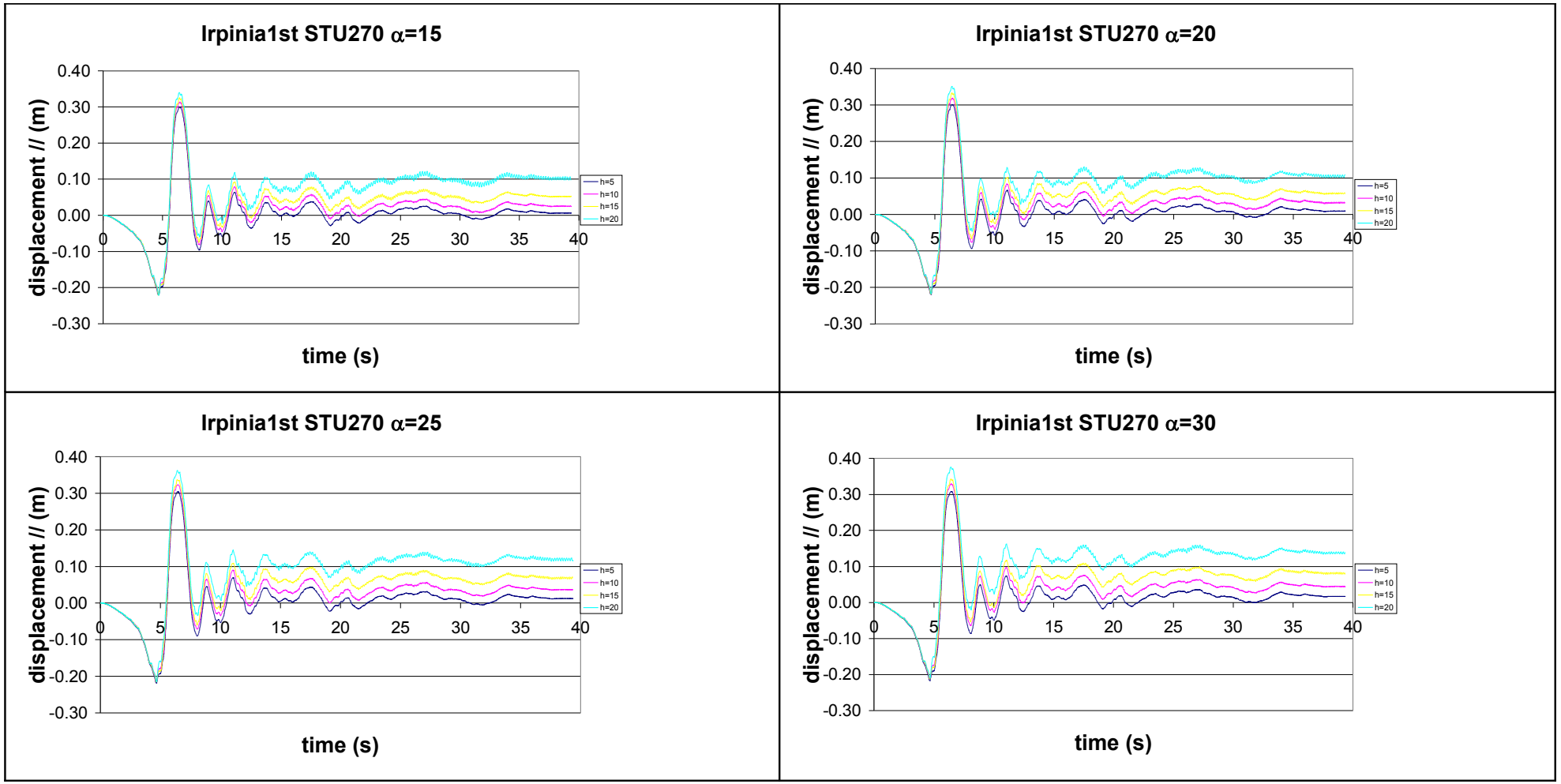

Figure 5.9. Permanent horizontal displacement, accelerogram STU270, soil type A, Toyoura sand.

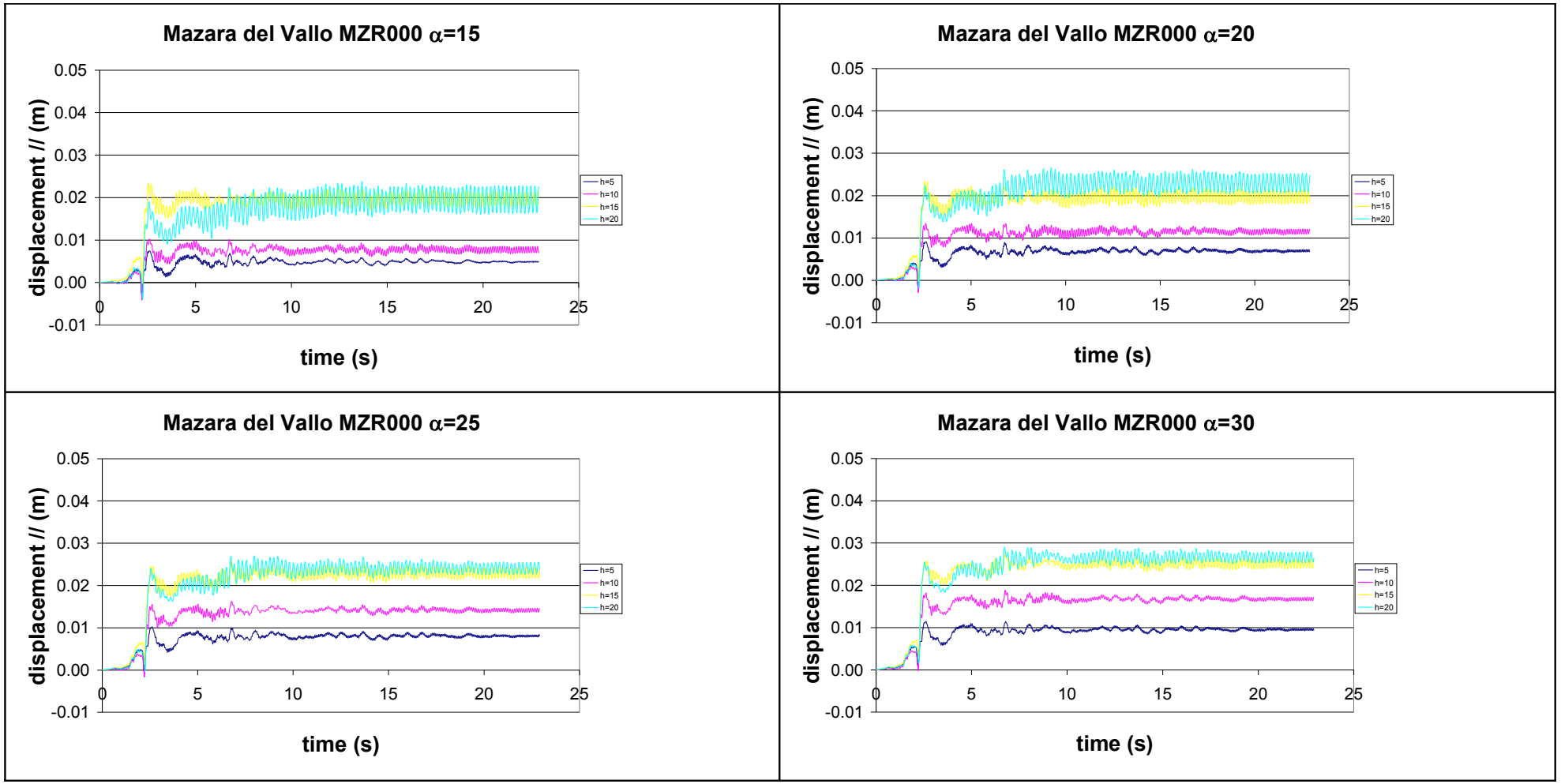

Figure 5.10. Permanent horizontal displacement, accelerogram MZR000, soil type A, Toyoura sand.

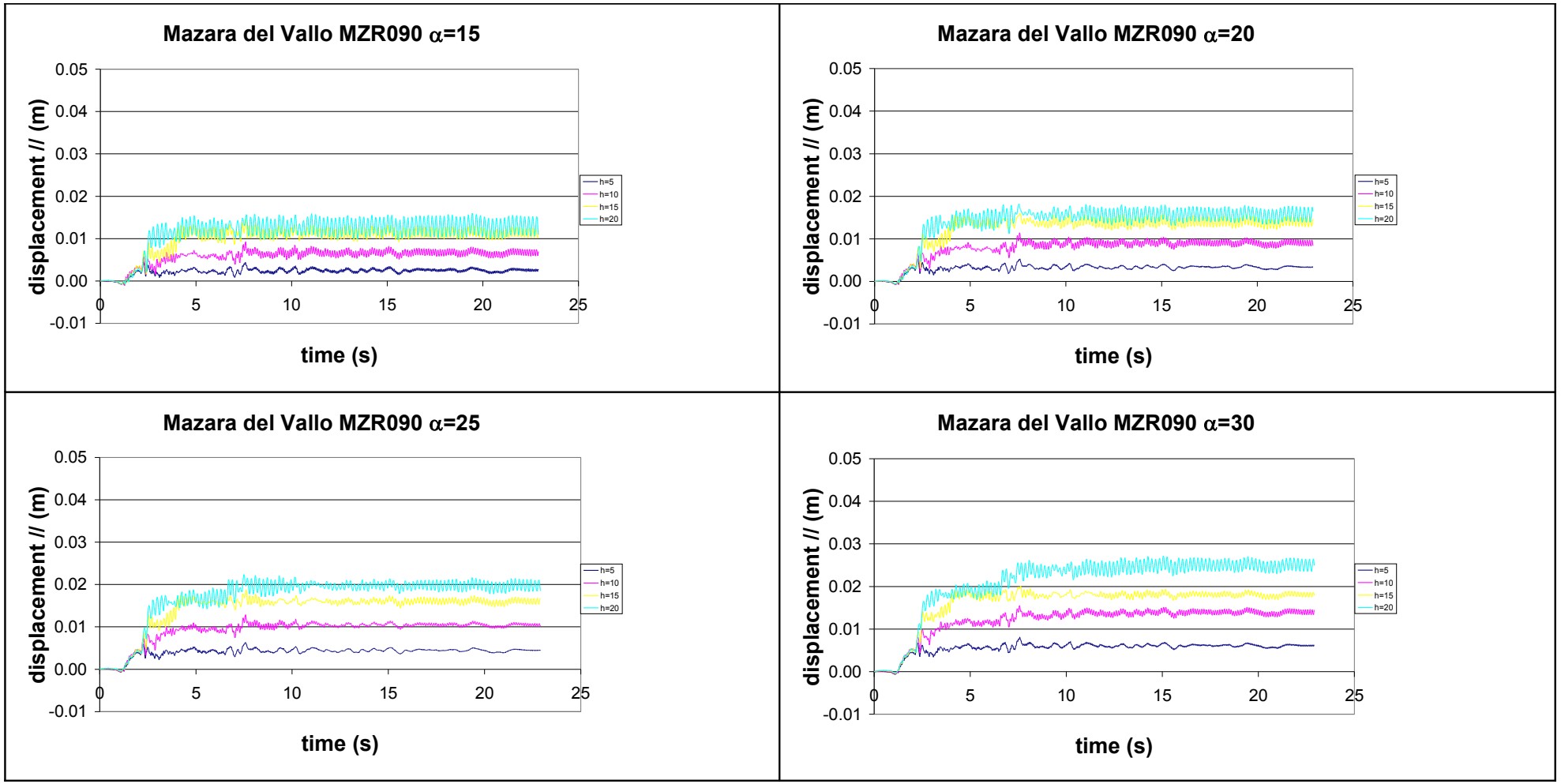

Figure 5.11. Permanent horizontal displacement, accelerogram MZR090, soil type A, Toyoura sand.

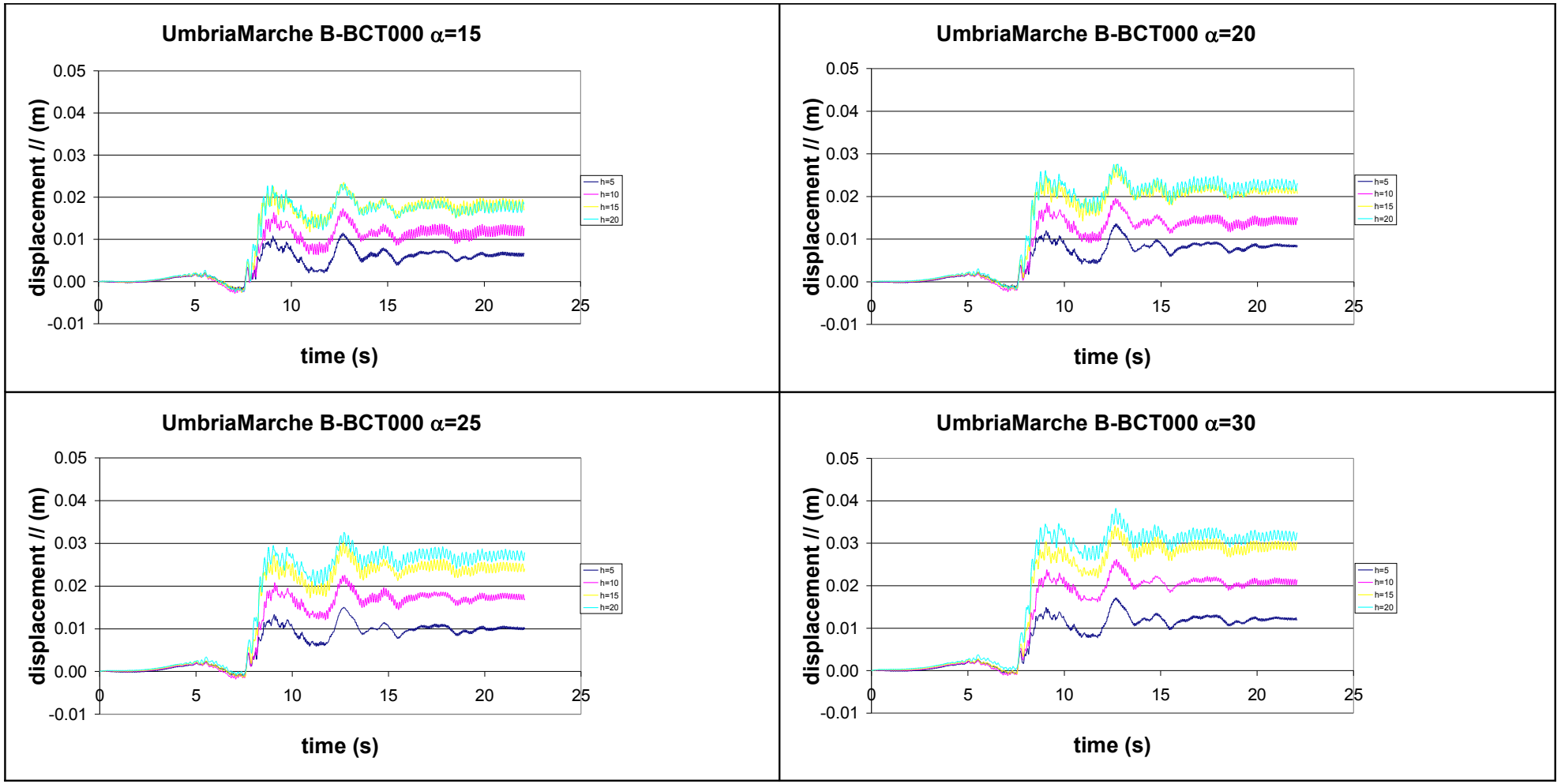

Figure 5.12. Permanent horizontal displacement, accelerogram B-BCT000, soil type A, Toyoura sand.

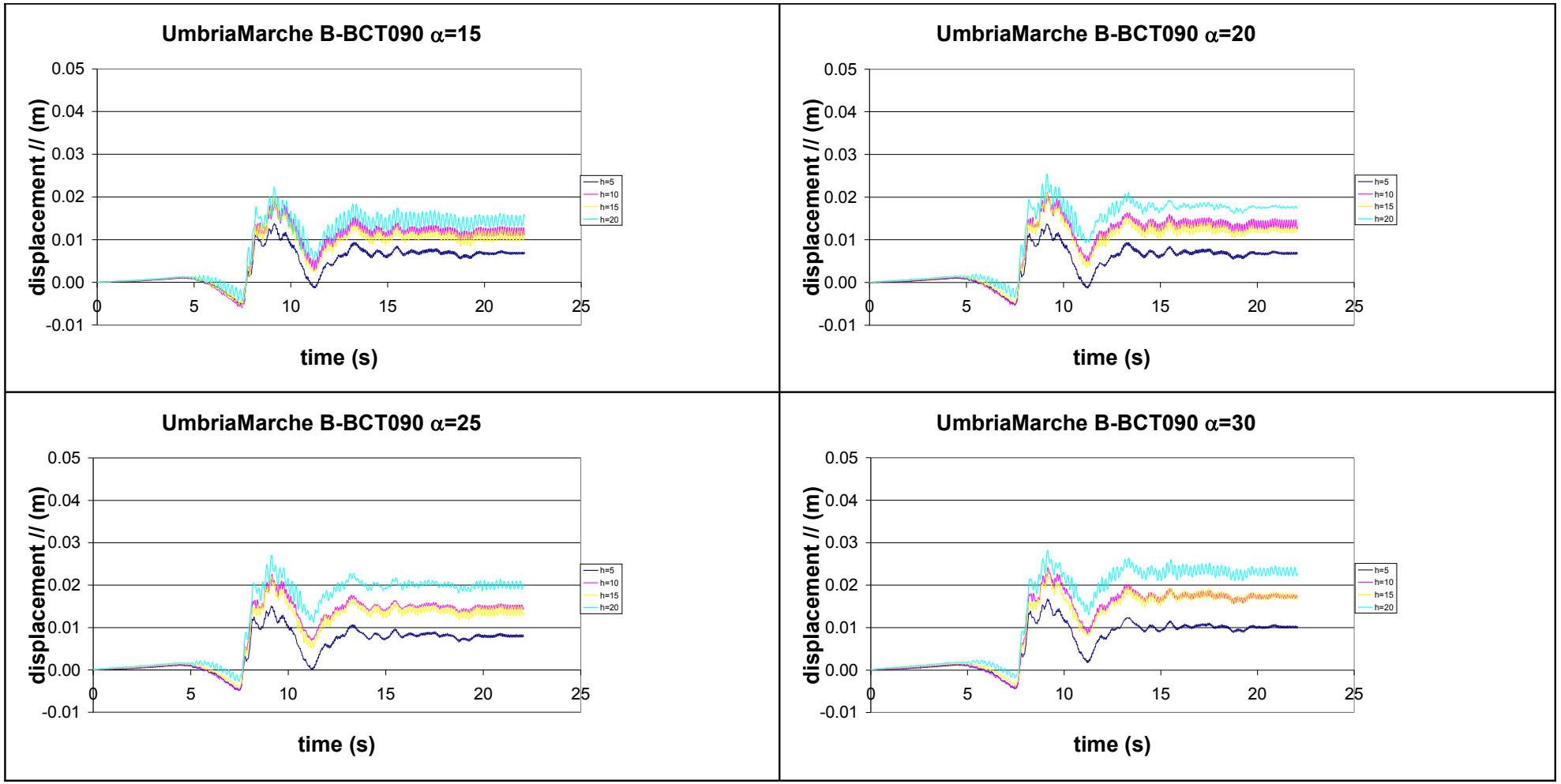

Figure 5.13. Permanent horizontal displacement, accelerogram B-BCT090, soil type A, Toyoura sand.

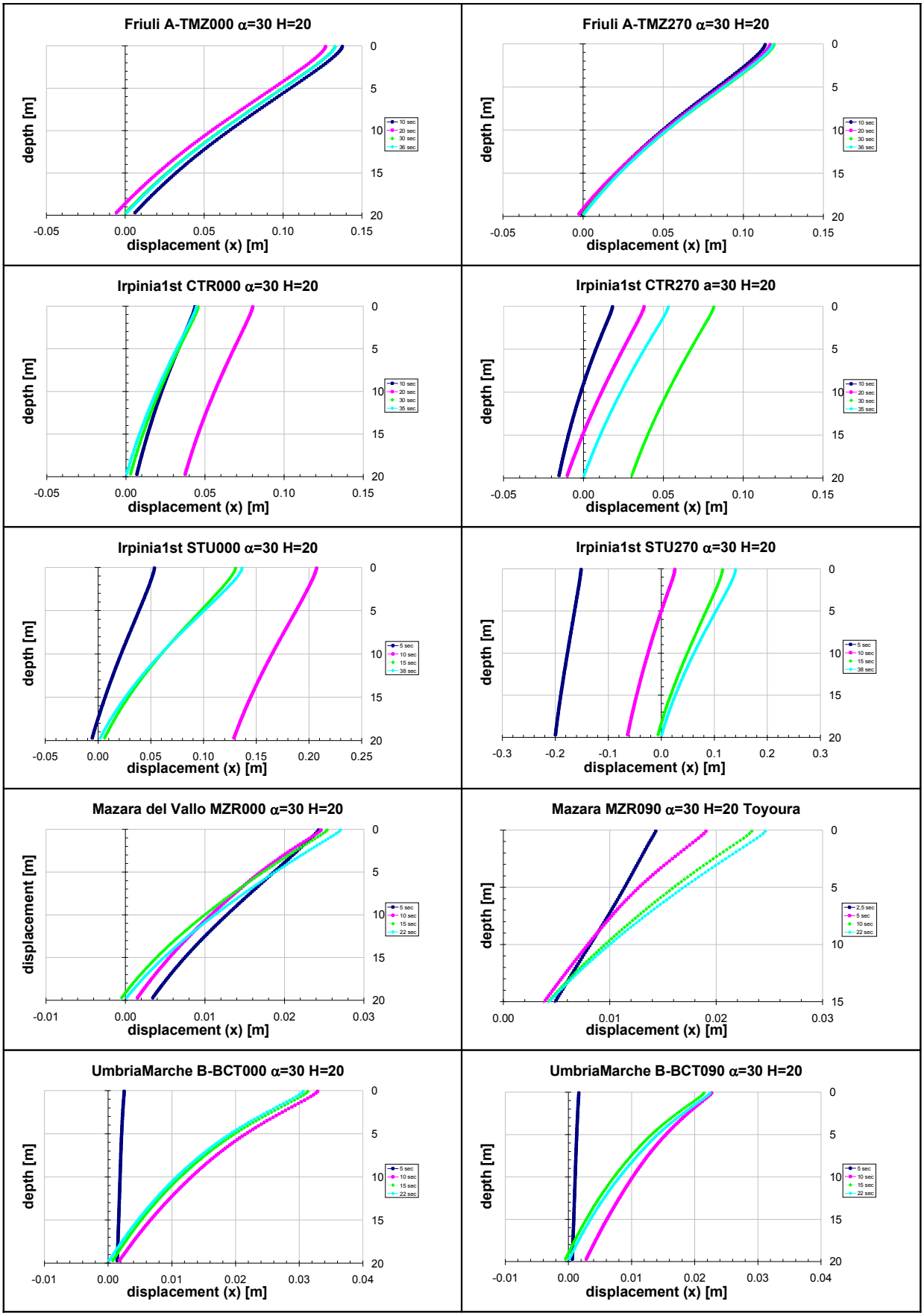

Figure 5.14. Isochrones for horizontal displacements.

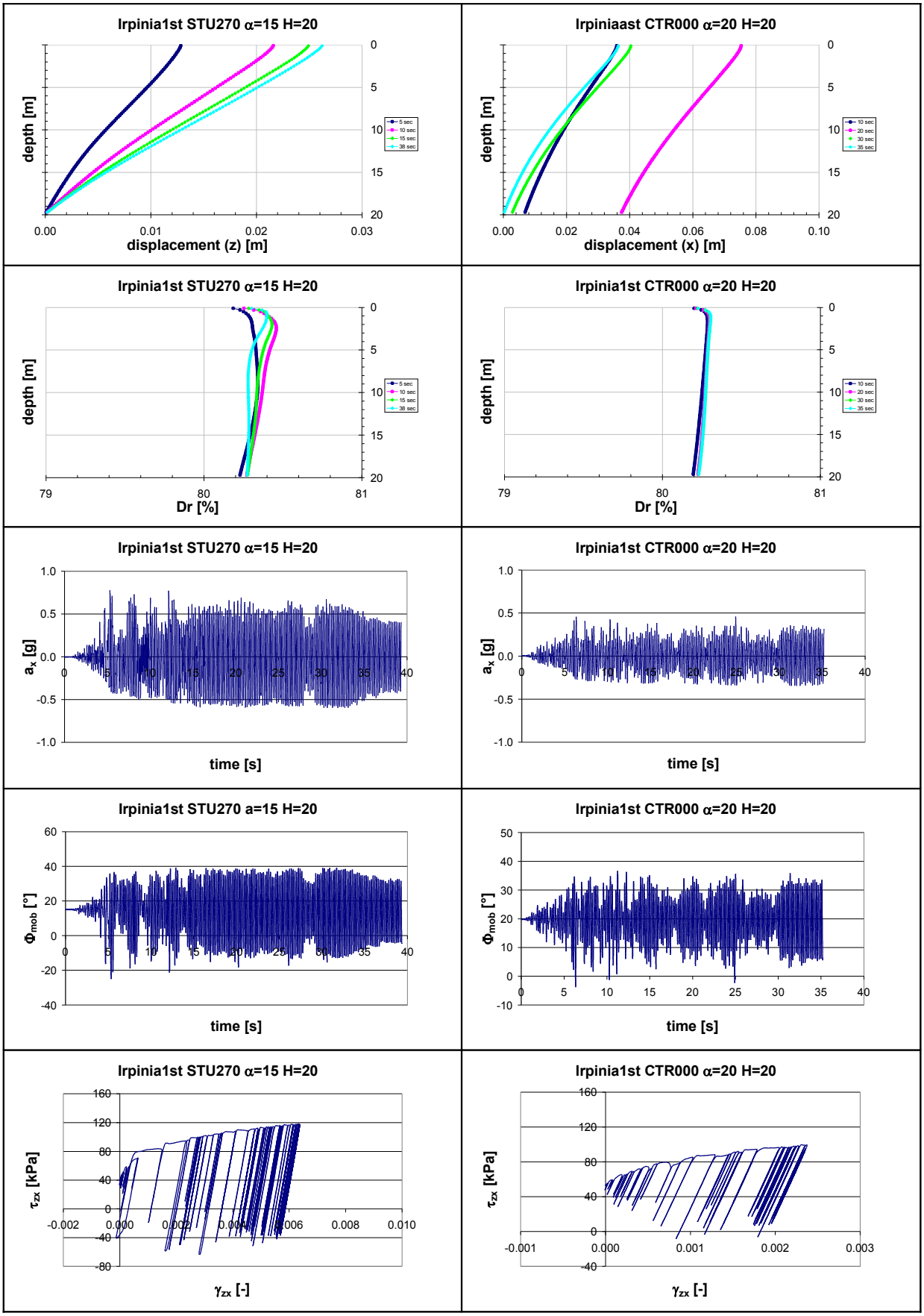

Figure 5.15. Isochrones relative to vertical displacement and relative density; horizontal acceleration on the surface; friction angle mobilized and load cycles (in the middle); Toyoura sand.

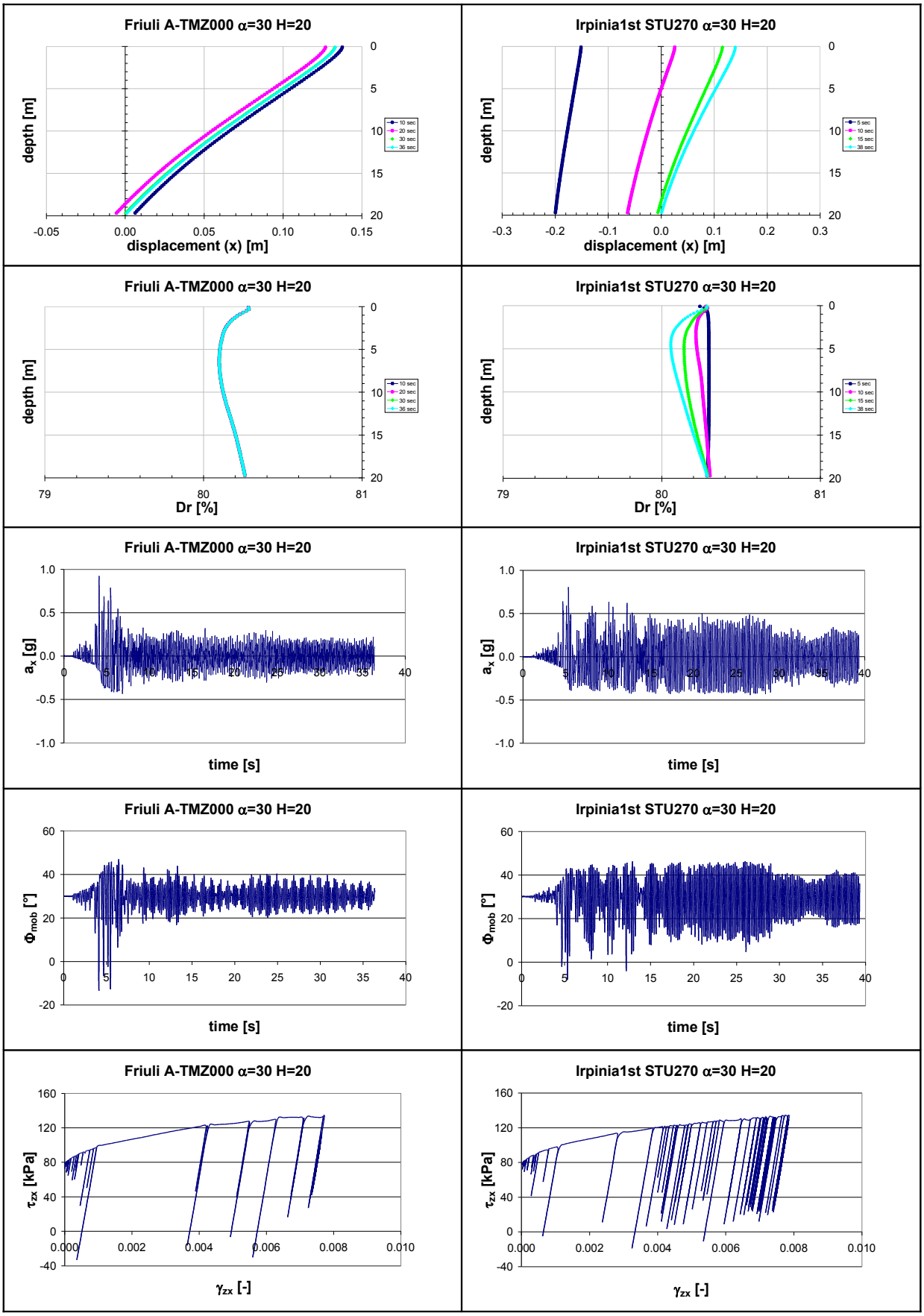

Figure 5.16. Isochrones relative to horizontal displacement and relative density; horizontal acc. on the surface; friction angle mobilized and load cycles (middle); Toyoura sand.

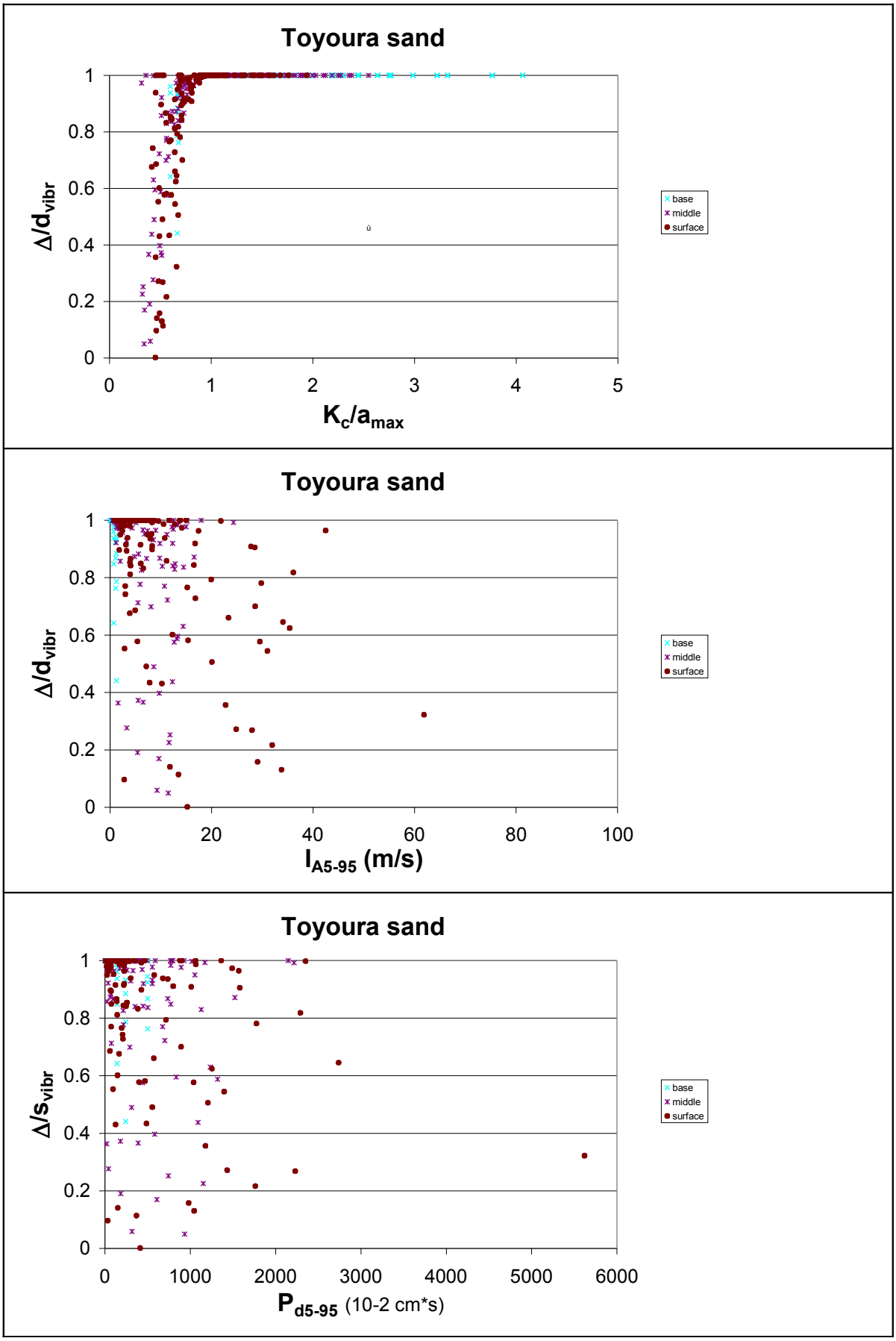

Figure 5.16. Ratio Δ/d_{vibr} in function of K_c/a_{max}, I_{A5-95} and P_{D5-95} respectively.

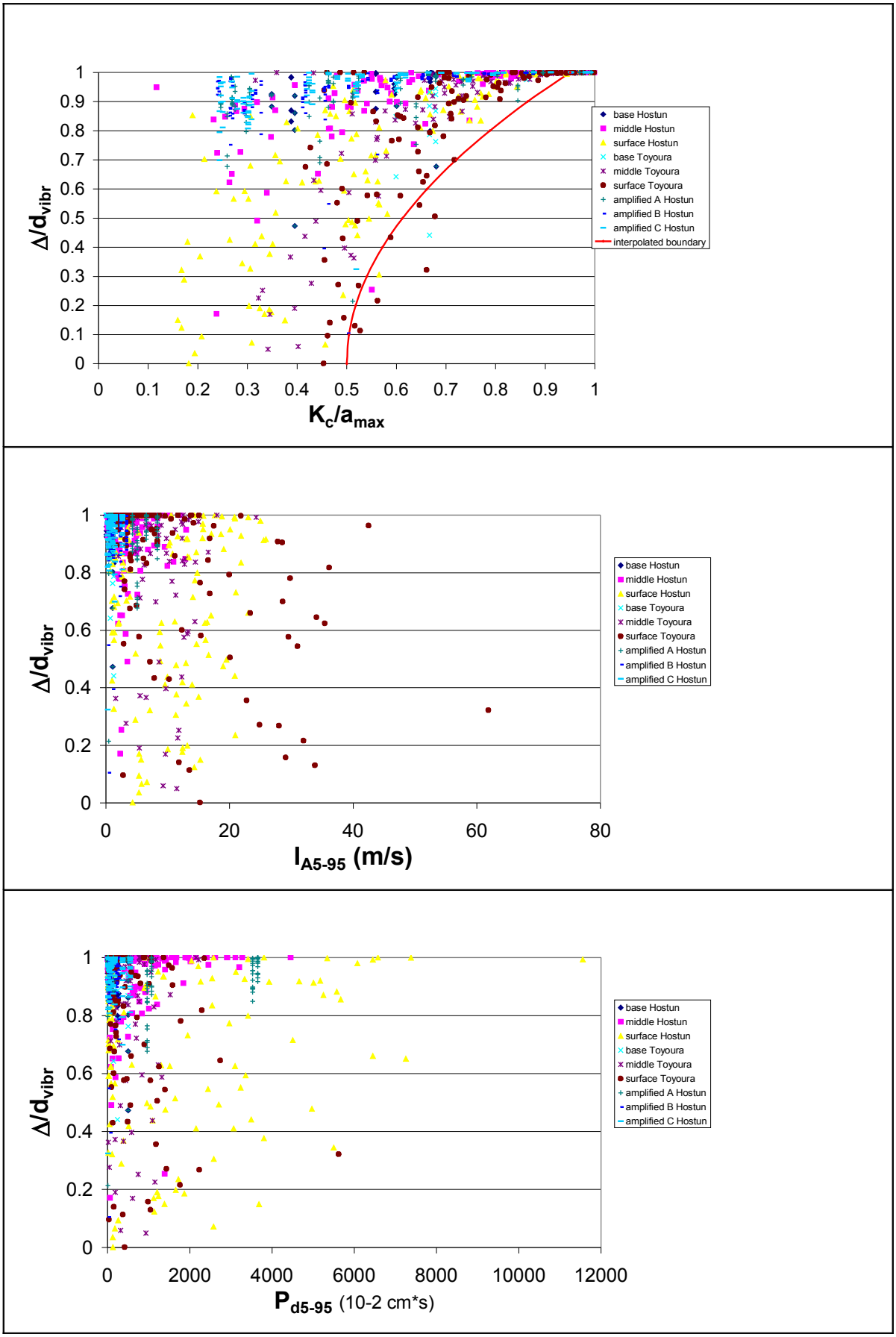

Figure 5.17. Ratio Δ/d_{vibr} in function of K_c/a_{max}, I_{A5-95} and P_{D5-95} respectively for all the considered cases.

D_R = 80%

B_R (kPa)	R_F	λ	γ	$\hat{\theta}_c$	$\hat{\theta}_e$	ξ_c	ξ_e	B_P
1100	0.0263	0.25	8.5	0.362	0.136	-0.17	-0.04	0.0004
c_P	β_{f0}	β_{flim}	r_{c0}	t_P	$\bar{\gamma}$	α	f_0	e_{max}
85	0.6	0.2	1	18	$1e^{-6}$	61	0.2	0.944

Table 5.1. Constitutive model parameters for Toyoura sand (Zambelli, 2006).

α (°)	φ' (°)	$\mathbf{K_c}$
15	42.1	0.512
20	42.1	0.406
25	42.1	0.308
30	42.1	0.214

Table 5.2. Critical acceleration values for different inclination angles of the slope.

CHAPTER 6: NUMERICAL ANALYSES WITH ARTIFICIALLY AMPLIFIED SEISMIC INPUT BY EERA CODE

3.7. *Introduction*

In this chapter the displacements evaluated, in the previous chapters, by means of VIBRAZIONE code, considering Hostun and Toyoura sands, are compared with those obtained by employing Newmark method considering as seismic input the accelerograms artificially provided by EERA.

Such as in the previous chapter, an inclined shallow infinitely long slope was studied considering four different angles of inclination (15°, 20°, 25° and 30°) and four different heights H of the slope (5, 10, 15 and 20m).

In this chapter the author has taken, as seismic input, the accelerograms of recent Italian earthqaukes for the soil types A (Database SISMA) for analysis performed with VIBRAZIONE, these one are also used as input in EERA and the accelerograms obtained in the middle and on the surface of the layer by means of this software are used as seismic input to evaluate displacements with the Newmark method.

3.8. *About EERA*

During past earthquakes, the ground motion on soft soil sites were found to be generally larger than those of nearby rock outcrops, depending on local soil conditions. These amplifications of soil site responses were simulated using several computer programs that assume simplified soil deposit conditions such as horizontal soil layers of infinite extent. One of the first computer programs developed for this purpose was SHAKE (Schnabel et al., 1972). SHAKE computes the response in a horizontally layered soil-rock system subjected to transient and vertical travelling shear waves and assumes that the cyclic soil behaviour can be simulated using an equivalent linear model, which is extensively described in the geotechnical earthquake engineering literature (e.g., Idriss and Seed, 1968; Seed and Idriss, 1970; and Kramer, 1996). SHAKE was modified many times and SHAKE91 is one of the most recent versions of SHAKE (Idriss and Sun, 1992).

The computer program EERA (Bardet et al., 2000) was developed in FORTAN 90 starting from the same basic concepts as SHAKE. EERA stands for Equivalent-linear Earthquake Response Analysis.

It is a modern implementation of the well-known concepts of equivalent linear earthquake site response analysis. EERA's input and output are fully integrated with the spreadsheet program Excel.

In figure 6.1 some terms used in site response analysis are defined. The *free surface motion* is the motion at the surface of a soil deposit. The *bedrock motion* is the motion at the base of the soil deposit. The *rock outcropping motion* is the motion at a location where bedrock is exposed at the ground surface.

3.9. ***EERA analysis***

In EERA the worksheet *Profile* is used to define the geometry and properties of the soil profile. As above mentioned four heights of the slope are considered H = 5, 10, 15 and 20 m, with a discretization in 50, 75 and 100 sub-layer of height Δz = 0.2 m, while Δz = 0.1 m for H = 5m.

The input data for Hostun sand are: total unit weight γ = 17.0 kN/m^3, the shear wave velocity V_S = 108 m/s and the maximum shear modulus G_{max} = 20.21 MPa.

The input data for Toyoura sand are: total unit weight γ = 15.7 kN/m^3, the shear wave velocity V_S = 343 m/s and the maximum shear modulus G_{max} = 188.3 MPa.

The input data for bedrock are: total unit weight γ = 20.0 kN/m^3, the shear wave velocity V_S = 1000 m/s and the maximum shear modulus G_{max} = 2038.7 MPa.

The cyclic stress-strain characteristics of the soil in shear are often defined by: the value of the shear modulus at small strains G_{max}, which can be also expressed in terms of the shear wave velocity $V_s = \sqrt{G_{\max} / \rho}$, where ρ is the mass density of the soil; the relation between the secant shear modulus G, and the cyclic shear strain amplitude γ_c, typically expressed as a curve of G / G_{max} versus γ_c; the curve relating the material damping ratio to γ_c.

The values of ratio G/G_{max} and of critical damping ratio corresponding to shear strain data for Hostun sand are obtained by Hameury (1995), see Figure 6.2, and by using ready-to-use charts (Vucetic et al., 1991), see Figure 6.3.

The values of ratio G/G_{max} and of critical damping ratio corresponding to shear strain data, instead, for Toyoura sand are obtained by Iwasaki et al. (1978) see Figure 6.4.

Considering Hostun sand, the higher values of peak acceleration (a_{max}) of the accelerogram, obtained by EERA in the middle and on the surface of the layer, are recorded for Friuli (TMZ000) and Irpinia (STU270) earthquakes respectively, in both cases for a slope height H = 5m.

The maximum values of Destructive Power 5-95% (P_{d5-95}), both in the middle of the layer that on the surface, are obtained for CTR270 accelerogram and a height H = 20m and are severally equal to 7867.85 *10^{-2} cm*s and 15969.87 *10^{-2} cm*s.

Finally, the maximum values of Arias Intensity are obtained for the accelerogram STU270 and a height H = 20m and it is equal to 4.694 m/s for that in the middle of the layer and equal to 5.706 m/s for that on the surface.

The above cited accelerograms for Hostun sand are shown in Figure 6.5.

Considering Toyoura sand, the higher values of peak acceleration (a_{max}), in the middle and on the surface of the layer, are recorded for the Irpinia (STU270) earthquakes, in both cases for a slope height H = 15m.

The maximum values of Destructive Power 5-95% (P_{d5-95}), in the middle and on the surface, are obtained for STU270 accelerogram and a height H = 20m, and are equal to 589.24 $*10^{-2}$ cm*s and 635.80 $*10^{-2}$ cm*s respectively.

The maximum values of Arias Intensity are obtained for accelerogram STU000 and a height H = 20m and are equal to 2.546 m/s for the accelerogram in the middle of the layer and equal to 3.363 m/s for that on the surface.

The above cited accelerograms for Hostun sand are shown in Figure 6.6.

65.. *Comparison of Newmark method with VIBRAZIONE*

In this section the results already obtained by using the code VIBRAZIONE, in terms of displacement, are compared with those obtained employing the Newmark method.

The seismic input in VIBRAZIONE are the ten accelerograms for soil type A, described in Chapter III, while in the Newmark method are the accelerograms obtained in the middle and on the surface of the layer given as output from EERA, using in this code the same ten accelerograms employed in VIBRAZIONE.

The ratio Δ/d_{vibr} in function of the ratio K_c/a_{max}, the Arias Intensity 5-95% and the Destructive Potential 5-95%, respectively, for Hostun sand are reported in Figure 6.7.

It is worth noting that:

- using as seismic input the accelerogram in the middle of the layer, in 86% of the cases the ratio Δ/d_{vibr} is higher than 0.8 and in 95% it is higher than 0.5. Only in 4 case Δ is negative and it happens for the geometry α = 25° and H = 5m, for Friuli earthquake, Tolmezzo station, and Irpinia earthquake, Sturno station. In 45% a_{max} is less than K_c and so there are not displacements with the Newmark method;
- using the accelerogram on the surface, in 81% of the cases the ratio Δ/d_{vibr} is higher than 0.8 and in 94% it is more than 0.5%. In 1% of cases Δ is negative, it occurs only for Irpinia earthquake (STU270) and for the geometry α = 30° and H = 10m and 15m. In 42% the threshold value is not reached.

The ratio Δ/d_{vibr} in function of the ratio K_c/a_{max}, the Arias Intensity 5-95% and the Destructive Potential 5-95%, respectively, for Toyoura sand are reported in Figure 6.8.

In this case:

- using as seismic input the accelerogram in the middle of the layer, in 86% of the cases the ratio Δ/d_{vibr} is higher than 0.8 and in 96% it is higher than 0.5% and this ratio is positive in all the cases considered. In 53% a_{max} is less than K_c and so there are not displacements with the Newmark method;
- using the accelerogram on the surface, in 85% of the cases the ratio Δ/d_{vibr} is higher than 0.8 and in 89% it is more thanare less than 50%. In 3% of cases Δ is negative, it occurs also in this case for the geometry α = 25° or 30° and H = 5m, it happens only for Friuli earthquake, Tolmezzo station, and Irpinia earthquake, Sturno station. In 44% the threshold value is not reached.

It should be noted that, for the Italian earthquakes recorded on soil type A, also if EERA code is used to take into account the amplification of the seismic input into the slope, in about 40% of cases, considering the Newmark method, displacements do not occur because the critical acceleration K_c is not exceeded while with VIBRAZIONE not negligible displacements are obtained.

Unfortunately it was not possible, for Hostun and Toyoura sands, to identify a unique relationship between the amount of seismic parameters, such as Arias Intensity and Destructive Power, and the displacements calculated by the two methods as it was underline in the previous chapters.

If the results obtained in this paper in terms of the difference Δ, between the displacements obtained by employing the elastoviscoplastic method (d_{vibr}) and those obtained by employing the Newmark approach, in function of the ratio between critical acceleration (K_c) and the peak acceleration (a_{max}) are considered, it is worth noting that similar results, using as seismic input for the analyses with the displacement based method those artificial obtained by means of VIBRAZIONE and EERA, in the middle and on surface of the layer, are obtained considering both Hostun and Toyoura sands.

Figure 6.9 shows the following results:

- when the ratio K_c/a_{max} is less than 0.45, a correlation between the calculated displacement with Newmark method and that one with VIBRAZIONE can not be found;
- when this ratio is between 0.45 and 0.7 the correlation is highly variable;
- when this ratio is more than 0.7 the ratio Δ/d_{vibr} is higher than 0.8 and also in this case it is difficult to find a correlation between the displacements calculated by means of VIBRAZIONE code and those obtained by employing the Newmark approach.

Analysing this trend, the following relationship is conceived:

$$\frac{\Delta}{s_{vibr}} = 0.45 + 0.45 * \left(\frac{K_c}{a_{\max}} \right)^2 \qquad (6.1)$$

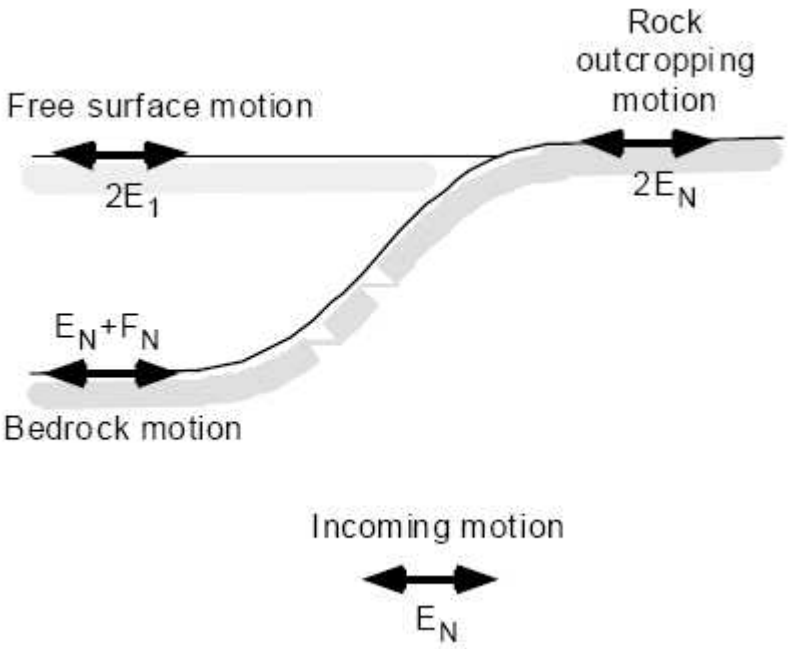

Figure 6.1. Terminology used in site response analysis (Bardet et al., 2000).

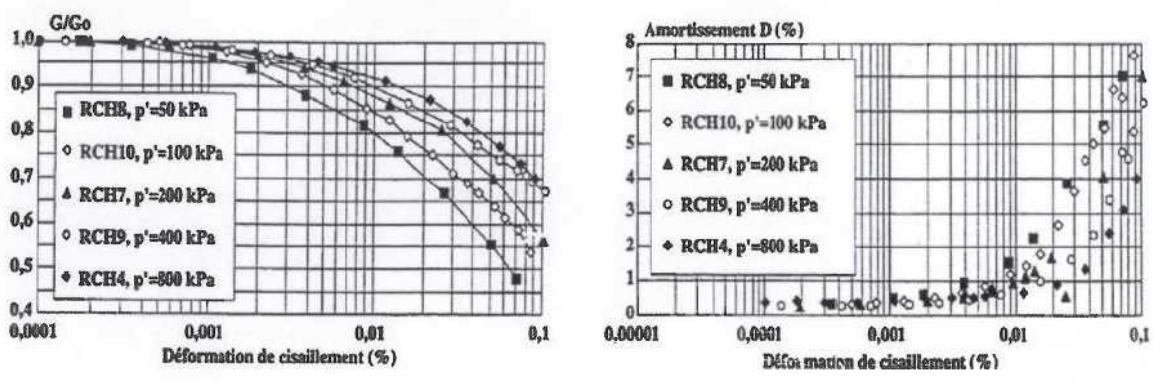

Figure 6.2. shear moduli and damping ratios for dense Hostun RF sand (Hameury, 1995)

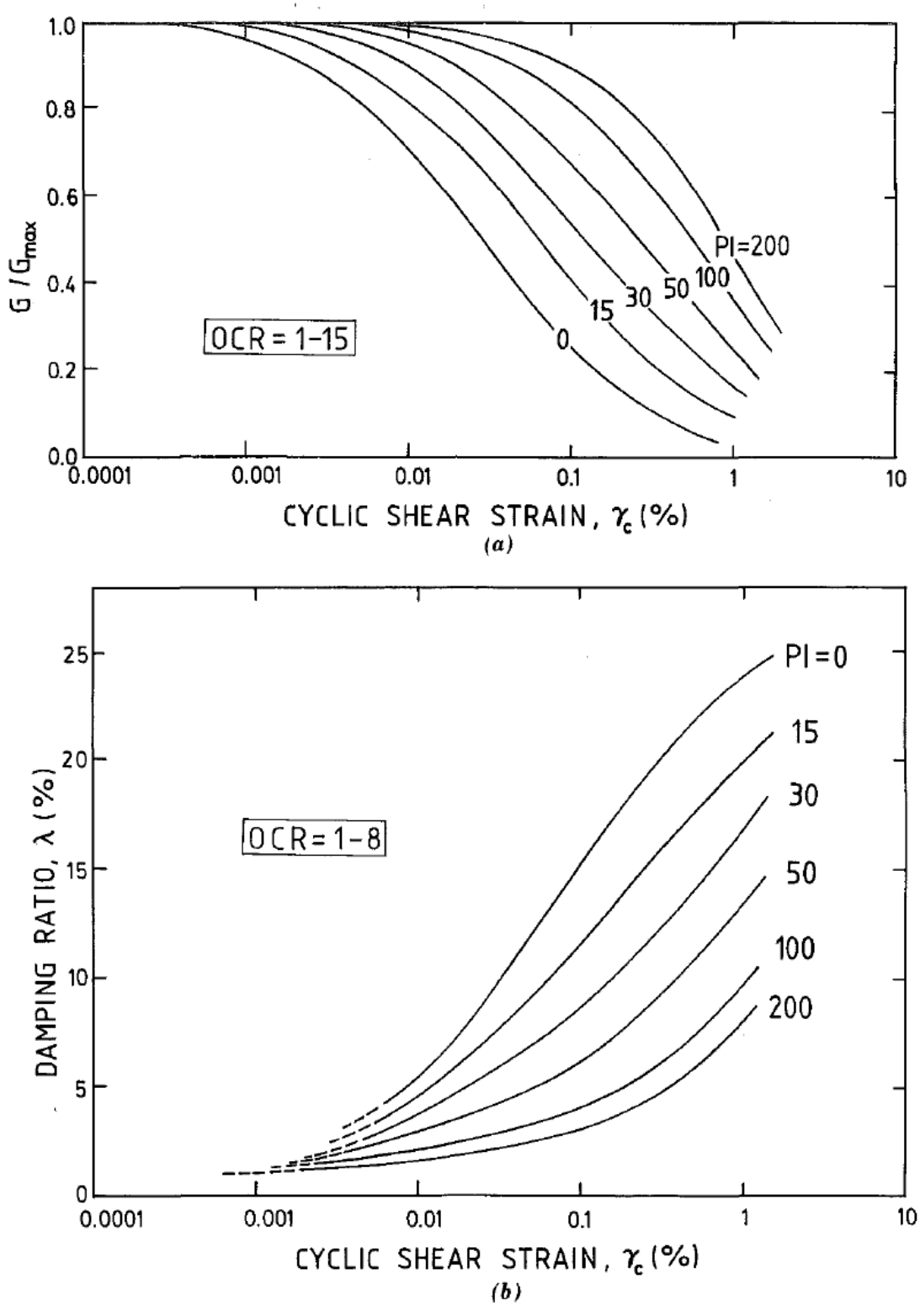

Figure 6.3. Relation between G/G_{max} versus γ_c *(a)* and λ versus γ_c *(b)*, Curves and Soil Plasticity for Normally and Overconsolidated Soils (Vucetic et al., 1991).

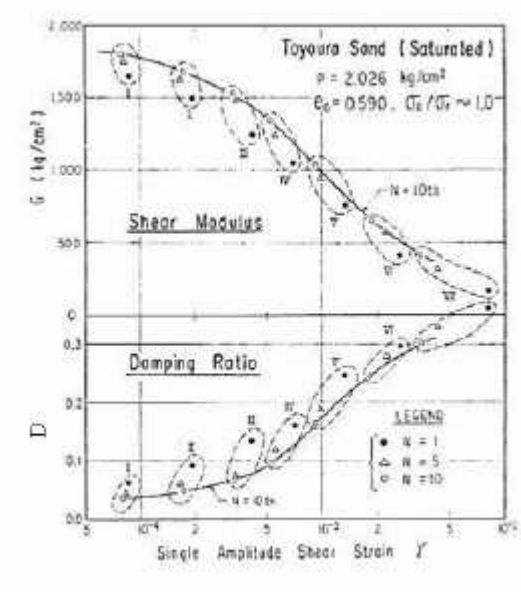

Figure 6.4. shear moduli and damping ratios (Iwasaki et al., 1978)

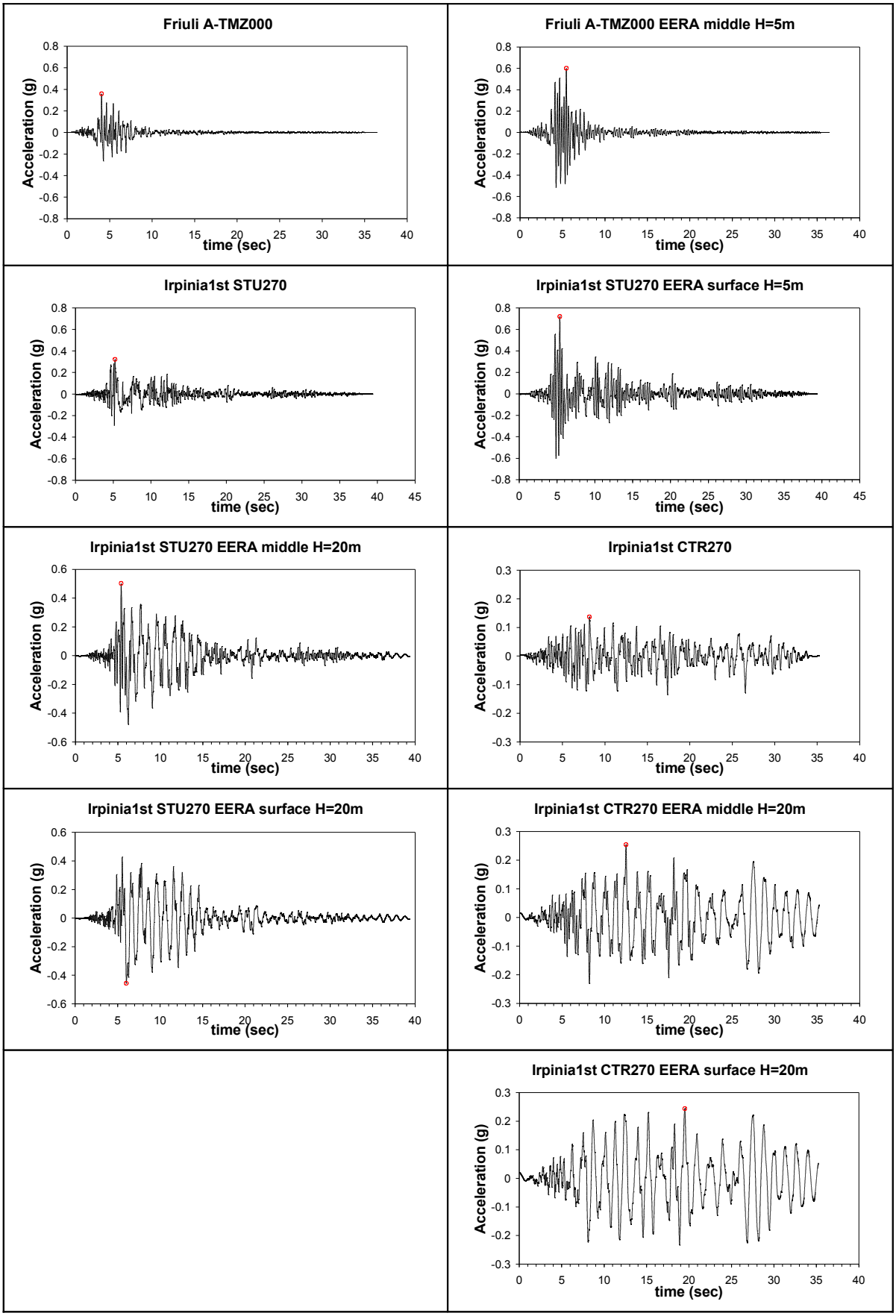

Figure 6.5. Considered accelerogram and the corresponding one at the middle and on surface of the layer employing EERA code for Hostun sand.

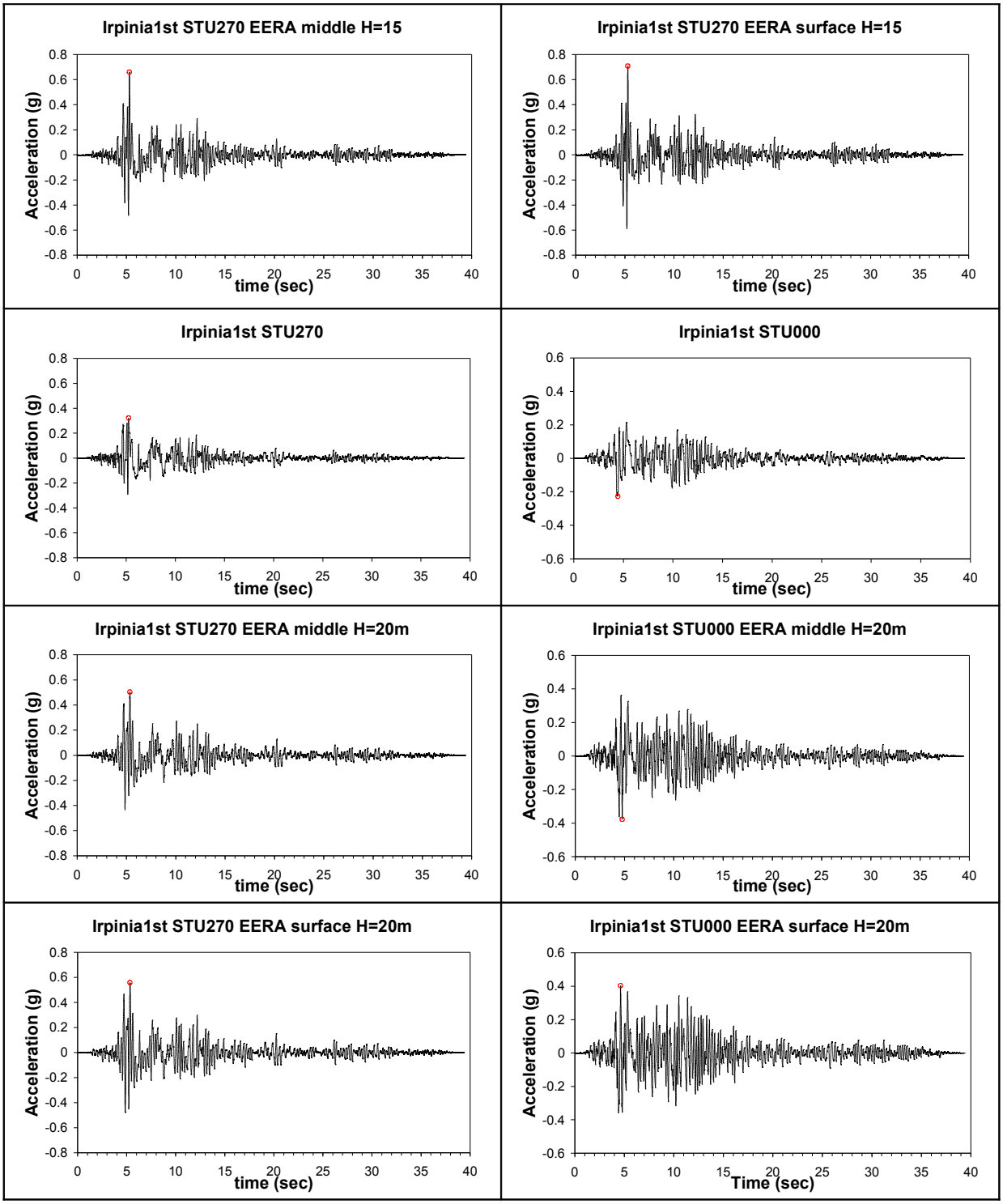

Figure 6.6. Considered accelerogram and the corresponding one at the middle and on surface of the layer employing EERA code for Toyoura sand.

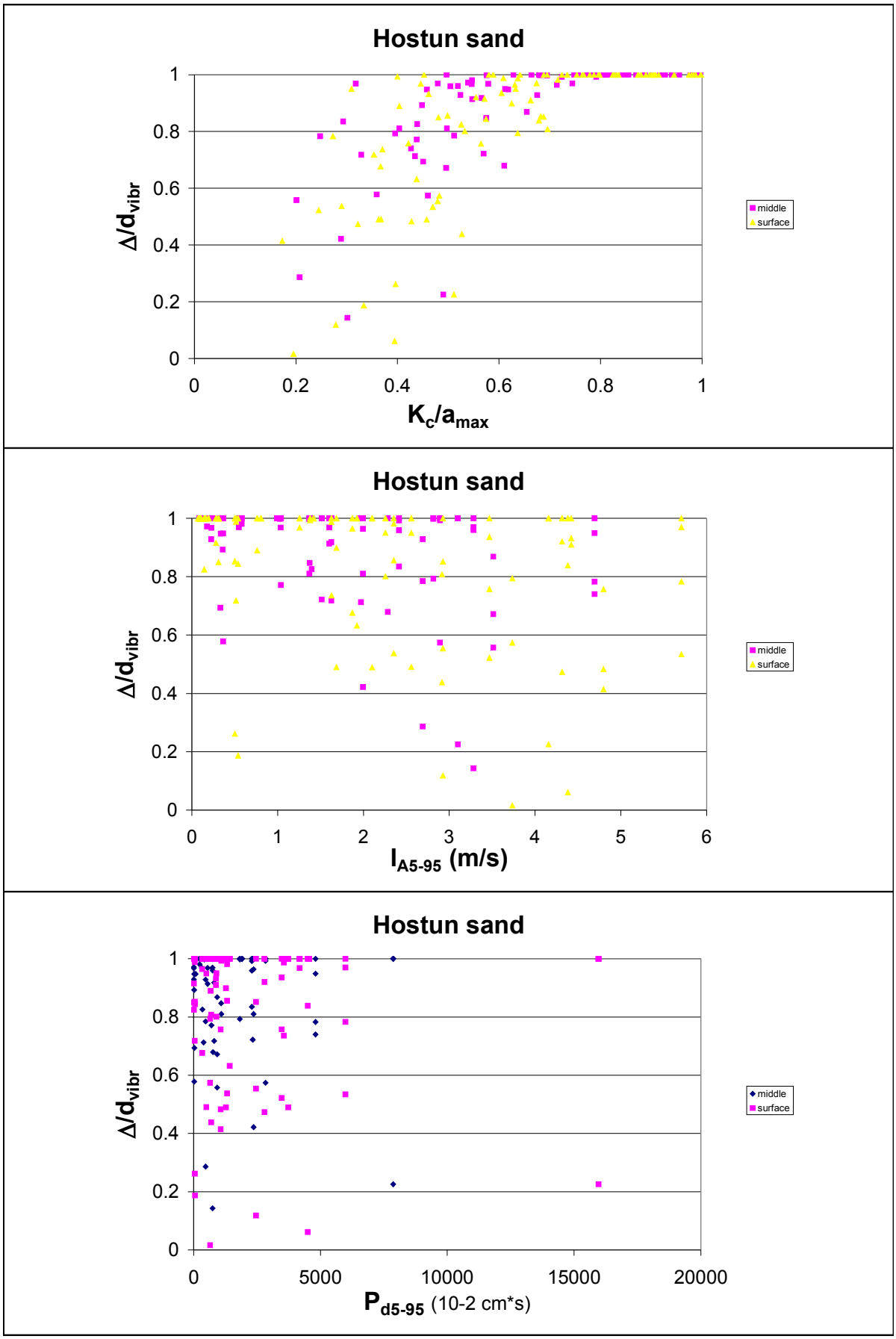

Figure 6.7. Ratio Δ/d_{vibr} in function of K_c/a_{max}, I_{A5-95} and P_{D5-95} respectively for Hostun sand.

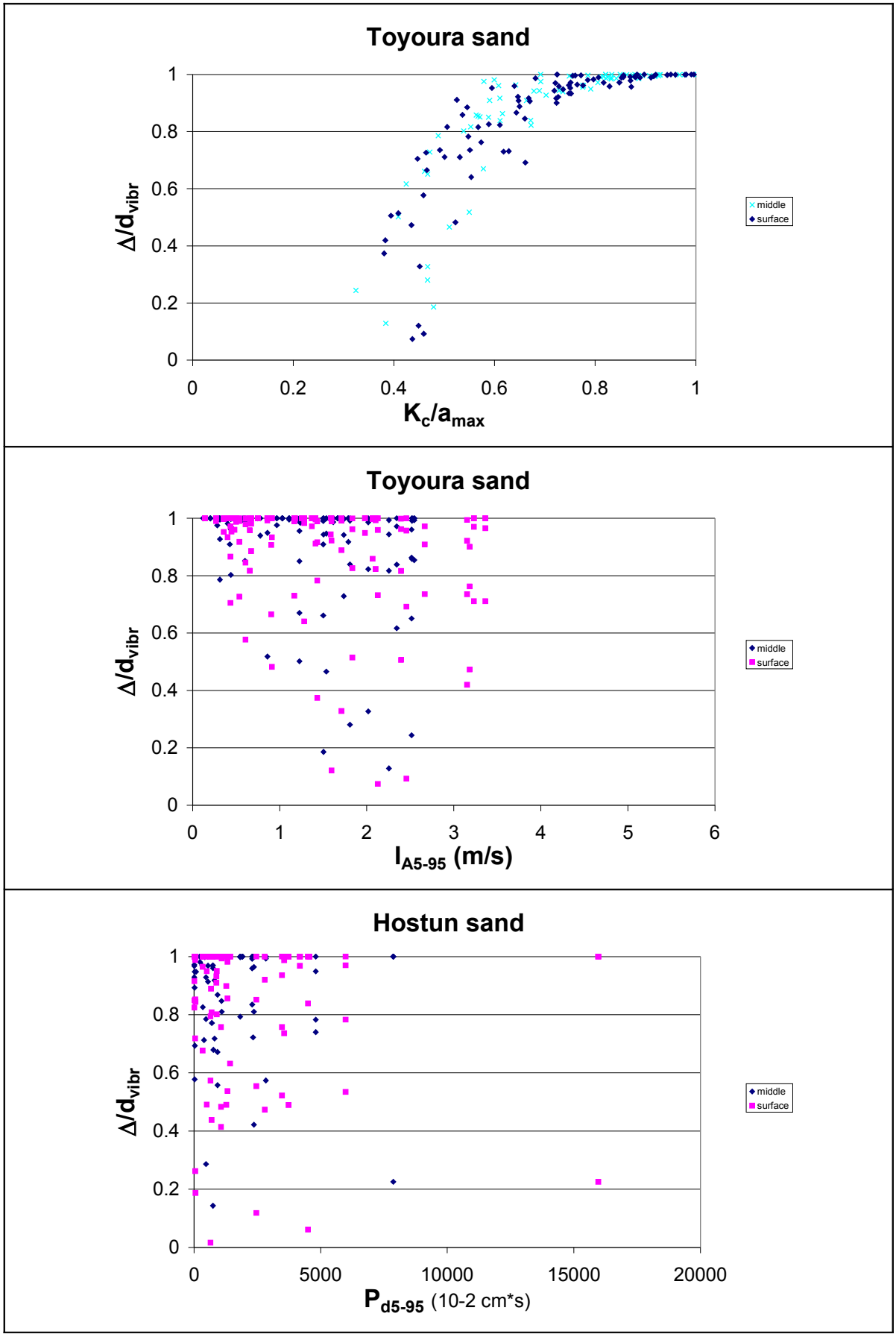

Figure 6.8. Ratio Δ/d_{vibr} in function of K_c/a_{max}, I_{A5-95} and P_{D5-95} respectively for Toyoura sand.

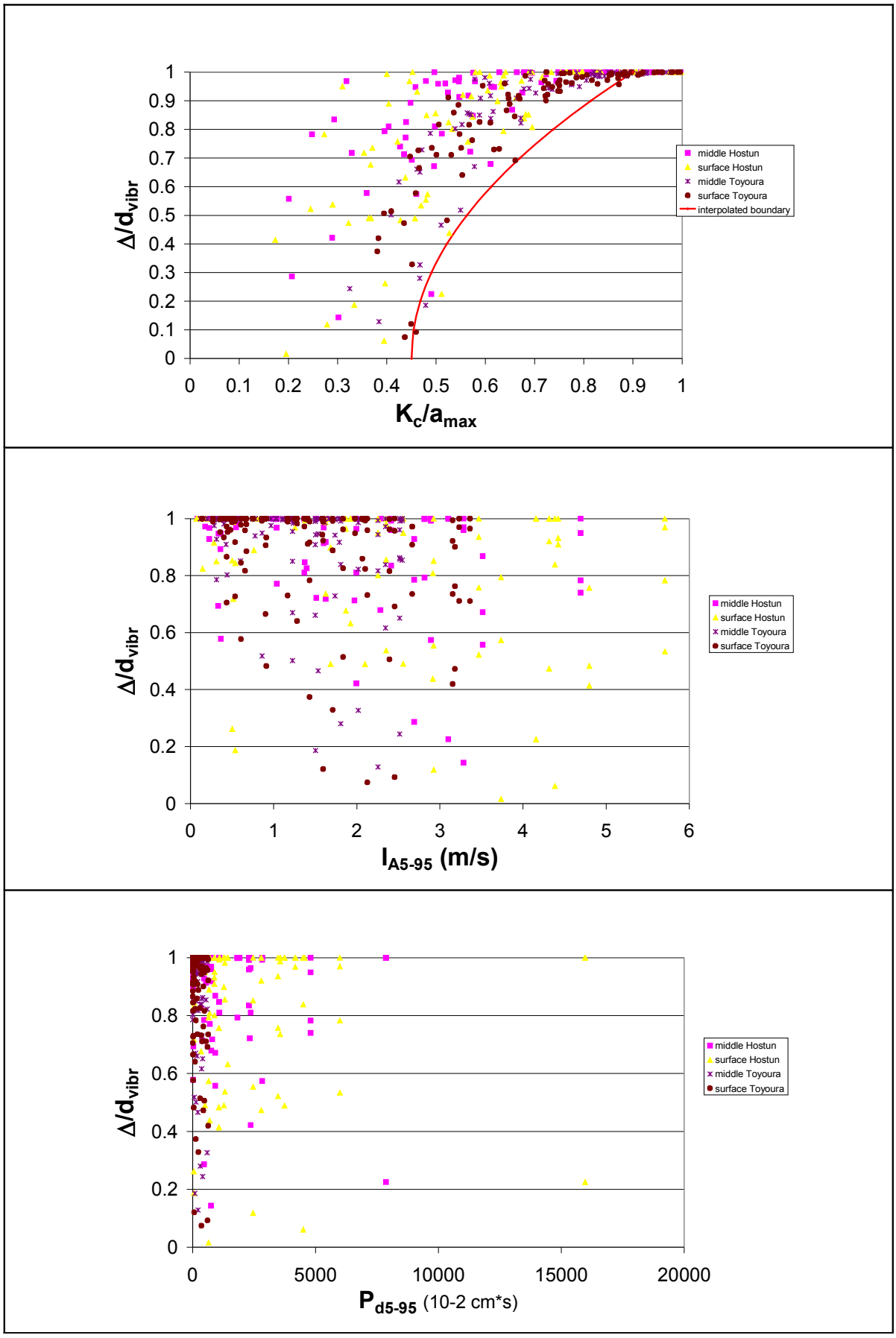

Figure 6.9. Ratio Δ/d_{vibr} in function of K_c/a_{max}, I_{A5-95} and P_{D5-95} respectively for all the considered cases.

CONCLUSIONS

The aim of this thesis consists to investigate the mechanical response of granular material in dynamic conditions. To this aim this work starts from the description of the elastoviscoplastic constitutive model whose first version, dates back to 1993, was developed at the Politecnico of Milan by prof. R. Nova and prof. C. di Prisco for loose sands.

In fact, the highlighting of the constitutive relationship is essential for the understanding of the response of any “geo-structure”. In this thesis the problem of the seismic response of a homogeneous infinitely long sandy slope is tackled.

In this perspective four different heights (H = 5, 10, 15 and 20m), four different inclination angles (α = 15°, 20°, 25° and 30°) of the slope and two different materials (Hostun and Toyoura sands) have been considered.

The post peak regime has been demonstrated to be fundamental for the dynamic response of the slope: in the case of Hostun sand a “critical condition” is assumed to be reached at large strains, while in the case of Toyoura sand the material is assumed to infinitely dilate.

A large number of numerical analyses were therefore performed to analyze what are the factors mainly affecting the response of the system.

As seismic input, ten acceleregrams (for the three types of soil A, B and C) recorded during recent Italian earthquake, have been chosen from the database SISMA; in particular the majority of the numerical analyses have been performed considering earthquake on soil type A.

Several comparisons were made starting from the analysis of the seismic response. Comparing to simpler constitutive models, eg. EERA analysis, the numerical code employed allows to describe and understand a wide variety of real phenomena, also typical of granular materials, such as the dependence of mechanical properties on relative density, localization phenomena, the dynamic amplification of earthquakes along the height of the slope: these are just some of the factors contributing to determine the dynamic response on site, however, essential to achieve reliable predictions.

For all the numerical analysis performed, the results obtained using the Newmark (1965) approach, widely used in current practice, also to test the elastoviscoplastic model with a simpler one, have been systematically compared. These results confirm what was expected; it is necessary to use extreme caution in simplify real physical problem to avoid unfounded assessments about its behavior.

Simplification can be an important key for engineers, but the importance of certain types of application, combined with the complexity of the system to be analyzed, requires the use of more sophisticated tools. In particular, the limitations of the Newmark approach have been demonstrate to be unacceptable , since this overlooks the phenomena of wave propagation and amplification effects: especially when the purpose is to predict the stresses of existing structures, it is easily to obtain disputable results and not on the safety side.

The numerical analyses carried out have repeatedly demonstrated how the software VIBRAZIONE reveals significant displacements of the slope against zero displacements conversely obtained by means of the Newmark approach, due to the fact that the peak acceleration of the seismic input does not exceed the critical acceleration.

It must be underline that, although the several years needed to arrive at constitutive formulations able to reproduce such a variety of phenomenological aspects, the research on this topic cannot be still considered to be completed.

The elastoviscoplastic model has several issues that still need a better setup as well as the structure of the software VIBRAZIONE, if it will be used for the simulation of complex seismic events, indeed in its current conception it takes to long time of computation.

In particular the model is not capable of simulating the ratcheting behavior of the granular materials: in fact, in small size cyclic loading, the anisotropic viscoplastic hardening is not activated, whereas the cyclic mechanism, after the first cycles, tends rapidly to stabilize and so is not able to produce a sufficient amount of axial strains.

Unfortunately it was not possible to identify a unique relationship between the amount of seismic parameters, such as Arias Intensity and Destructive Potential, and the difference of the displacements calculated by the two methods.

Considering the ratio K_c/a_{max}, when its value is more than 0.7, the difference Δ between the displacement obtained by means of VIBRAZIONE (d_{vibr}) and that calculated using the Newmark approach, that any engineer could easily employs, normalized by d_{vibr}, is at least equal to 0.7.

The aim of this thesis is not only to show how the Newmark method often leads to erroneous results but, also, to find relationships, as simple as possible, between a complex model and simpler methods, commonly used especially in professional practice, as the Newmark method and the software EERA.

REFERENCES

Adachi T. & Oka F. (1982). Constitutive equations for normally consolidated clays based on viscoplasticity. Solis and Foundations, **22**(4), 57-70.

Ambraseys, N. (1972). *Behaviour of foundation materials during strong earthquakes.* Proc. 4th European Symposium on Earthquake Engineering, London, Vol.7, pp.11-12.

Ambraseys, N. and Sarma, S.K. (1967). *The response of earth dams to strong earthquakes*. Geotecnique, London, englang, vol. 17, Sept. 1967, pp. 181-213.

Ambraseys, N. and Menu, J.M. (1988). *Earthquake-induced ground displacement.* Soil Dynamics and Earthquake Engineering, Vol. 16, pp.958-1006.

Ambraseys N., and Srbulov, M. (1994). *Attenuation of earthquake induced displacements*. Journal of Earthquake Engineering and Structural Dynamics, Vol. 23, pp.467-487.

Arulanandan, K. and Scott, R. F. (1993). *Project VELACS – control test results.* Journal of Geotechnical Engineering Division, ASCE, Vol. 119, No. 8, August, pp. 1276-1292.

Arias, A. (1970). *A measure of earthquake intensity*. Seismic design for nuclear power plants. R. J. Hansen, ed, MIT Press, Cambridge, Mass., 438-483.

Bardet, J.P., Mace, N., Tobita, T., Hu, J. (1999 a). *Large-scale modeling of liquefaction-induced ground deformation Part I: A four-parameter MLR model.* Technical Report MCEER-99-0019, Multidisciplinarity Center for Earthquake Engineering Research, State University of New York at Buffalo, Buffalo, NY, pp. 155-173.

Bardet, J.P., Mace, N., Tobita, T., Hu, J. (1999 b). *Large-scale modeling of liquefaction-induced ground deformation Part II: MLR model application and probabilistic model.* Technical Report MCEER-99-0019, Multidisciplinarity Center for Earthquake Engineering Research, State University of New York at Buffalo, Buffalo, NY, pp. 175-190.

Bardet J.P., Ichii K., Linn C.H (2000). EERA – A computer program for Equivalent Earthquake site Response Analyses of Layered Soil Deposits. University of Southern California, from the web-site: http://gees.usc.edu/GEES/Software/ EERA2000/Default.htm

Bartlett, S.F. and Youd, T.L. (1992). *Empirical analysis of horizontal ground displacement generated by liquefaction–induced lateral spread.* Technical Report NCEER – 92-0021, National Center for Earthquake Engineering Research , Buffalo, New York.

Bartlett S.F. & Youd T.L. (1995). Empirical Prediction of liquefaction-induced lateral spread. Journal of Geotechnical Engineering Division, ASCE, Vol. 121, No. 4, April, pp. 316-329.

Baziar M.H. (1991). Engineering evaluation of permanent ground deformation due to seismically-induced liquefaction. PhD. Thesis, Dept. of Civil and Evnironmental Engineering, Rensselaer Polytechnic Institute, Troy, Vew York, 297.

Baziar M.H., Dobry R., Elgamal A-W.M. (1992). Engineering evaluation of permanent ground deformations due to seismically-induced liquefaction. Tech. Rep. NCEER-92-0007, National Center for Earthquake Engineering Research, Buffalo, NY, March 24.

Bolt B.A. (1969). Duration of strong motion. Proc. 4th World Conference on Earthquake Engineering, Santiago, Chile, pp. 1304-1315.

Bouckovalas G., Gazetas G., Papadimitriou A.G. (1999). Geotechnical aspects of the 1995 Aegion, Greece, earthquake. Proc. 2nd International Conference on Earthquake Geotechnical Engineering, Lisboa, Portugal, 21-25 June, 1999, pp. 739-748

Bray J.D. & Rathjie E.R. (1998). Earthquake-induced displacement of solid waste landfills. Journal of Geotechnical and Geoenvironmental Engineering, Vol. 124, No. 3, pp. 242-253.

Byrne P. M. (1991). A model for for predicting liquefaction induced displacement. Proc. 46th Annual Canadian Geotechnical Conference, Saskatoon, Saskatchewan, pp. 271-281.

Byrne M., Jitno H., Ancerson D.L., Haile J. (1994). A procedure for predicting seismic dsplacement of earth dams. Proc. 13th International Conference on Soil Mechanics and Foundation Engineering, New Delhi, 5-10 January, 1994.

Cai Z. & Bathurst R.J. (1996). Deterministic sliding bloch mothods for estimatine seismic displacements of earth structures. Soil Dynamics and Earthquake Enginering, Vol. 16 (1996), pp. 255-268.

Cambou B., Lanier J. (1988). *Induced anisotropy in cohesionless soil: experiments and modelling*. Computers and Geotechnics, **6**, 291-311.

Cascone E., Maugeri M., Motta E. (1998). Seismic response of clay slopes. Proc. 11th European Conference on Earthquake Engineering, Paris.

Cascone E. & Rampello S. (2002). Decoupled seismic analysis of an earth dam. Accettato per la pubblicazione sulla rivista Soil Dynamic and Earthquake Engineering.

Castro G. (1987). On the behaviour of soil during earthquake liquefaction. In Developments in geotechnical engineering 42, Soil Dynamics and Liquefaction, A.S. Cakmak editors, Princeton University, Princeton, NJ 08544, 1987;169-204

Chang C.J., Kuo C.L., Selig E.T. (1983). Pore pressure development during ciclic loading. Journal of Geotechnical Engineering Division, ASCE, Vol. 109, No. 1.

Chen W.F. & Liu X.L. (1990). Limit analysis in soil mechanics. Development in geotechnical enginnering, 52, Elsevier, 1990.

Chopra A.K. & Zhang L. (1991). Base sliding response of concrete gravity dams to earthquakes. Earthquake Engineering Research Center, Report No. UCB/EERC-91/05, University of California, Berkeley, California, USA, May 1991, 165 pp.

Conte E. & Dente G. (1986). Deformazioni permanenti indotte da carichi sismici nei pendii sabbiosi in falda. A.G.I., XVI Convegno Nazionale di Geotecnica, Bologna 14-16 Maggio 1986.

Conte E. & Rizzo G. (1996). Un'analisi probabilistica degli spostamenti permanenti indotti nei pendii da carichi sismici. Rivista Italiana di Geotecnica, No.1/96.

Crespellani T., Ghinelli A., Madiai C., Vannucchi G. (1990). Analisi di stabilità dei pendii naturali in condizioni sismiche. Rivista Italiana di Geotecnica XXIV, No.2.

Crespellani T., Madiai C., Vannucchi G. (1992). Seismic stability analisys of slopes including amplification effects. Proc. of French-Italian Confrrence on Slope Stability in Seismic Areas, Bordighera, Italy, 14-15 May 1992.

Crespellani T., Madiai C., Vannucchi G. (1994). A Procedure for the seismic and post-seismic analysis of natural slopes. Proc. 13th Interantional Conference on Soil Mechanics and Foundation Engineering, New Delhi, 5-10 Gennaio, 1994

Crespellani T., Madiai C., Maugeri M. (1996). Analisi di stabilità di un pendio in condizioni sismiche e post- sismiche. Rivista Italiana di Geotecnica XXX, No.1.

Crespellani T., Madiai C., Vannucchi G. (1998). Earthquake destructiveness potential factor and slope stability. Geotèchnique 48, No. 3, pp. 411-419.

di Prisco C. (1993). *Anisotropia delle sabbie: indagine sperimentale e modellazione matematica.* Ph. D. Thesis, Milan, University of Technology.

di Prisco C., Imposimato S. (1996). *Time dependent mechanical behaviour of loose sand.* Mechanics of Cohesive-Frictional Materials; **17(1)**: 45-73.

di Prisco C., Imposimato S., Aifantis E. (2002). *A visco-plastic constitutive model for granular soils modified according to non-local and gradient approaches.* International Journal for numerical and analytical methods in geomechanics; **26**(2),121-138.

di Prisco C., Imposimato S. (2003). *Nonlocal numerical analyses of strain localisation in dense sand.* Mathematical and computer modelling, **37**, 497-506.

di Prisco C., Stupazzini M., Zambelli C (2007). *Nonlinear SEM numerical analyses of dry dense sand specimens under rapid and dynamic loading.* International Journal for numerical and analytical methods in geomechanics; **31**, 757-788.

Dobry R. & Baziar M.H. (1991). Evaluation of ground deformation caused by lateral spreading. Proc. 3rd Japan-U.S. Workshop on Earthquake Resistant Design of Lifeline Facilities and Countermeasure for Soil Liquefaction, Tech. Rep. NCEER-91-0001, T. D. O'Rourke and M. Hamada (eds.), February 1, pp. 209-223.

Dobry R & Baziar M.H. (1992). Modelling of lateral spreads in silty sands by sliding soil blocks. Stability and performance of slopes and embankments I., ASCE, Geotechnical Special Publication 1992, (31), pp.625-652.

Dobry R., O'Rourke T.D., Hamada M. (1992). Liquefaction and groun failure in the Imperial Valley, Southern California during the 1979, 1981 and 1987 Earthquakes. Chapter 4 in O'Rourke T.D. & Hamada M.

Faccioli, E. and Paolucci, R. (2005). *Elementi di sismologia applicata all'ingegneria*. Pitagora Editrice Bologna.

Finn W.D.L. (1999). Code, standards and seismic safety evaluation of earth structures. Proc. 2nd International Conference on Earthquake Geotechnical Engineering, Lisboa, Portugal, 21-25 June, 1999, pp. 1091-1106.

Franklin A.G. & Chang F.K. (1977). Permanent displacements of earth embankments by Newmark sliding block analysis. Report 5, Miscellaneous Paper S-71-17, U.S Army Corps of Engineers Waterways Experiment Station, Vicksburg, Mississippi.

Fukuy, J., Nakatani, S., Shirato, M., Kouno, T., Nonomura, Y., Asai, R. (2007 a). *Experimental study on the residual displacement of shallow foundations during large earthquakes*. Technical Memorandum of PWRI. Public Works Research Institute (4027).

Fukuy, J., Nakatani, S., Shirato, M., Kouno, T., Nonomura, Y., Asai, R, Saito, T. (2007 b). *Large-scale shake table test on the nonlinear seismic response of shallow foundations during large earthquakes*. Technical Memorandum of PWRI. Public Works Research Institute (4027).

Gazetas G., Debchaudry A., Gasparini D.A., (1981). Random vibration analysis for the seismic response oh earth dams. Geotecnique, Vol. 31, pp. 261-277.

Gazetas G. & Uddin N.(1994). Permanent deformazion on pre-exiting slidign surface in dams. Journal of Geotechnical Engineering Division, ASCE, Vol. 120 (11), pp. 2041-2061.

Goodman R.E. & Seed H.B. (1966). Earthquake-induced displacement in sand embankments. Journal of the Soil Mechanics and Foundations Division, ASCE, Vol. 92, No. SM2, pp.125-146.

Hadj-Hamou T. & Kavazanjian E. Jr. (1985). Seismic stability of gentle infinite slopes. Journal of Geotechnical Engineering Division, ASCE, Vol. 111 (6). pp. 681-697.

Hamada M., Yasuda S. Isoyama R., Emoto K. (1986). Study on liquefaction induced permanent ground displacements. Published by the Association for the Development of Earthquake Prediction in Japan, November 1, 87 pages.

Hameury O. (1995). "Quelques aspects du comportement des sables avec et sans rotation des axes principaux des petites aux grandes déformations", Thèse de doctorat. Paris: Ecole Centrale Paris.

Hardin B.O., Drnevich V.P. (1972). Shear modulus and damping in soils: Design equations and curves. Journal of Soil Mechanics and Foundation Division (ASCE). **98**(7):667-692.

Hynes-Griffin M.E. & Franklin A.G. (1984). Rationalizing the seismic coefficient methods. Miscellaneous paper GL-84-13, U.S. Army Corps pf Engineers, Waterways Experiment Station, Vicksbourg, 21 pp.

Iai S., Ichii K., Sato Y., Kuwazima R. (1999). Earthquake response analysis of a high embankment on a existing hill slope. Proc. 2nd International Conference on Earthquake Geotechnical Engineering, Lisboa, Portugal, 21-25 June, 1999, pp. 697-702.

Idriss, I. M. and Seed, H.B. (1968) "Seismic Response of Horizontal Soil Layers", Journal of the Soil Mechanics and Foundations Division, ASCE, Vol. 94, No. 4, pp. 1003-1031.

Idriss I.M. (1985). Evaluating seismic risk in engineering practice. Proc. 11th Int. conf, on Soil Mechanics and Foundation Engineering, San Francisco, Vol. 1, pp. 255-320.

Idriss, I. M. and Sun, J. I. (1992) "User's Manual for SHAKE91", Center of Geotechnical Modelling, Department of Civil Engineering, University of California, Davis.

Imposimato S. (1998). *Il ruolo della variabile temporale nel comportamento meccanico delle sabbie sciolte.* Ph. D. Thesis, Milan University of Technology.

Ishihara K. (1993). Liquefaction and flow failure during earthquakes. Geotèchnique Vol. 43, No. 3.

Ishihara K. (1994). Evaluation of residual strength of sandy soils. Proc. 13th Int. Conf. Soil Mech. Found. Engrg., Vol. 5, New Delhi, January, pp. 175-181.

Ishihara K., Verdugo R., Acacio A.A., (1991). Characterization of cyclic behaviour of sand and post-seismic stability analyses. Proc. 9th Asian Regional Conf. Soil Mech. Found. Engrg., Vol. 2, Bangkok, Thailand, December, pp. 45-67.

Iwasaki T., Tatsouka T., Takagi Y. (1978). "Shear modulus of sand under cyclic torsional shear loading", Soils and Foundations, 18 (1), 39-56.

Jibson R.W. (1993). *Predicting earthquake-induced landslide displacement using Newmark's sliding block analysis.* Transportation Research Record No. 1411, TRB, Washington, D.C., pp.9-17.

Jibson R.W. & Keefer D.K. (1993). *Analysis of the seismic origin of Landslides: examples from the New Madrid seismic zone.* Geological Society of America Bulletin, Vol. 105, No. 4,pp.521-536.

Jibson R.W., Harp E.L., Michael J.A. (1998). *A method for producting digital probabilistic seismic landslide hazard maps: an example from the Los Angeles, California.* Open-File report 98-113, http://geohazards.cr.usgs.gov/pubs/ofr/98-113/ofr98-113..html.

Keefer D.K. (1984). Landslides caused by earthquakes. Geological Society of America Bulletin, Vol. 95, No. 6, pp.406-421.

Keefer D.K. & Wilson R.C. (1989). Predicting earthquake-induced landslides, with emphasis on arid and semi-arid environments. In "Landslides in a semi arid environment", Inland Geological Society, Riverside, California, Vol. 2, pp.118-149

Kobayashi Y. (1981). Causes of fatalities in recent erthquake in Japan. Journal of Disaster Science, Vol. 3, pp. 15-22.

Kramer S.L. (1996). Geotechnical earthquake engineering. Prentice-Hall, Upper Saddle River, New Jersey; pp. 254-280.

Kramer S.L. & Smith M.W. (1997). Modified Newmark Model for Seismic Dislpacement of compliant slope. Journal of Geotechnical and Geoenvironmental Engineering Division, ASCE, Vol. 123, No. 7, pp.635-644.

Lade P. V. and Nelson R.B. (1987). *Modelling the elastic behaviour of granular materials*. Int. J. Num. and Anal. Methods in Geom., **11** (5), pp. 521-542.

Legg G. et al. (1982). Seismic Hazard mapping for lifeline vulnerability analysis. III Int. Conf. On Microzonation, Seattle, Vol. III.

Lemos L.J.L. & Coelho P.A.L.F. (1991). Displacements of slopes under earthquake loading. Proceedings of the 2nd International Conference on Recent Advances in Geotechnical Earthquake Engineering and Soil Dynamic, St. Louis, Missouri, Vol.2, pp. 1051-1056.

Lemos L.J.L., Gama A.M.P., Coelho P.A.L.F. (1994). Displacement of cohesive slopes induced by earthquakes loading. Proc. 13th Int. Conf. On Soil Mechanics and Foundation Engineering, New Delhi, 5-10 Gennaio, 1994.

Lin J.S. & Whitman R.V. (1983). Decoupling approximantion to the evaluation of ef earthqyake-induced plastic slip in earth dams. Earthquake Engineering and Structural Dynamics, Vol. 11, No. 5, pp. 667-678.

Lin J.S. & Whitman R.V. (1986). Earthquake induced displacement of sliding blocks. Journal of Geotechnical Engineering, ASCE, Vol. 112, No. 3, pp. 373-377.

Lindenberg, J. and Koning, H.L. (1981). *Critical density of sand*. Géotechnique, **131** (2), 231-245.

Lucia P.C., Duncan J.M., Seed H.B. (1981). Summary of research on case histories of flow failures of mine tailing impoundments. Information Circular 8857, Technology Transfer Workshop on Mine Waste Disposal Techniques, U. S. Bureau of Mines, Denver, Colorado, pp. 46-53.

Luzi L. & Pergalani F. (2000). A correlation between slope failures and accelerometric parameters: the 26 September 1997 earthquake (Umbria-Marche, Italy). Soil Dynamics and Earthquake Enginering, Vol. 20 (2000). pp. 301-313.

Madiai C. & Vannucchi G. (1997). Potenziale sismico distruttivo e stabilità dei pendii: abachi e tabelle per la stima degli spostamenti, Rivista Italiana di Geotecnica 3-4/1997.

Makdisi F.I. & Seed H.B. (1978). Simplified procedure for estimating dam and embankment earthquake - induced deformations. Journal of the Geotechnical Engineering Division, ASCE, Vol.104, No. GT7, pp. 849-867.

Manzari M.T., Arulanandan K., Scott R.F. (1994). VELACS Project: A summary of achievements. Proc. 5th U.S.-Japan Workshop on Earthquake resistant Design of Lifeline Facilities and Countermeasures Against soil liquefaction. Tech. Rep. NCEER-94-0026, T. D. O'Rourke & M. Hamada (eds.), November 7, pp. 389-404.

Marcuson W.F.III, Hynes M. E., Franklin A.G. (1990). Evaluation and use of residual strength in seismic safety analysis of embankments. Earthquake Spectra, Vol. 6, No. 3, pp. 529-572.

Matasovic N., Kavazanjian E.Jr., Giroud J.P. (1998). Newmark seismic deformation analysis for geosynthetic covers. Proc. of Geosynthetics International, Vol. 5, No. 1-2, pp. 237-264.

Mononobe N. (1929). Earthquake-proof construction of masonry dams, Proc. World Engineering Conference, 9, 275.

National Research Council (1985). Liquefaction of soils during earthquakes. National Academy Press, Washington, D. C., 240 pp.

Newmark N.M. (1965). Effect of earthquakes on dam and embankment, The Rankine lecture, Geotèchnique , Vol. 15, No.2.

Nova R., Hueckel T. (1980) *A geotechnical stress variables approach to cyclic behaviour of soils*. Proceedings of behaviour of soils under cyclic and transient loading, vol. 1, Swansea; 301-314.

Nova R. (1998). *Sinfonietta Classica: an exercise on classical soil modelling.* Proc. Int. Workshop on constitutive equations for granular non cohesive soils. Saada A. and Bianchini G. Eds. , Cleveland, 22-24 July 1987, Balkema, 501-520.

O'Rourke T.D. & Hamada M. (1992). The Case Studies on Liqiefaction and Lifgeline Performance during Past Large Earthquakes, vol. 2: U.S. Case Histories. National Center for Engineering Earthquake Research, SUNY-Buffalo, buffalo, NY, NCEER Report.

Oda M. (1972). *Initial fabrics and their relations to mechanical properties of granular materials*. Soils and Foundations, **12**(1), 17-36.

Oda M., Koishikawa I., Higuchi T. (1978). *Experimental study of anisotropic shear strength of sand by plane strain test*. Soils and Foundations, **18**(1), 25-38.

Okabe S. (1926). General theory of Earth Pressure. Journal of Japanese Society of Civil Engineering, Tokyo, Vol.12, No.1.

Perzyna P., *The constitutive equations for rate sensitive plastic materials*. Quarterly of Applied Mathematics 1963; **20:**321-332.

Perzyna P., *Fundamental problems in viscoplasticity*. Advances in Applied Mechanics, vol. 9. Academic Press: New York, 1966; 243-377.

Pisanò F. (2007). Depositi granulari infinitamente estesi sollecitati dinamicamente: Analisi numeriche e considerazioni teoriche, Degree Thesis, Milan University of Technology.

Rauch A.F. (1997). EPOLLS: an empirical method for predicting surface displacement due to liquefaction-induced lateral spreading in earthquakes. PdD Dissertation, virginia Polytechnic Institute and State University, Blacksburg, Va.

Rathje, E.M., Abrahamson, N. and Bray, J.D., 1998. Simplified frequency content estimates of earthquake ground motions. Journal of Geotechnical Engineering, Vol. 124, No. 2, pp. 150-159.

Robertson P.K. & Fear C.E. (1995). Liquefaction of sands and its evaluation. Proc. 1st International Conference on Earthquake Geotechnical Engineering.

Robertson P. K. & Fear C. E. (1996). Soil liquefaction and its evaluation based on SPT and CPT. Draft of paper presented at NCEER Workshop on Evaluation of Liquefaction Resistance, Salt Lake City, Utah, January, 4-5.

Romeo R. (1998). Seismically-induced landslides displacement: a predictive model. XXIII General Assembly of European Geophysical Society, Nice, 1998.

Romeo R. (2000). Seismically induced landslide displacement: a predictive model. Engineering Geology, 58, pp. 337-351.

Saragoni, R. (1981). *Influencia de la acceleración maxima, duratión y contenido de frecuencias en los daños producidos por terremotos*. Bol. Inf. Lab. Car. Geo. España Vol. 144, 15-32.

Sarma S.K. (1974). Critical acceleration versus static factor of safety in stability analisys of earth dam and embankement, Geotèchnique , Vol. 24, No.4.

Sarma S.K. (1975). Seismic stability of earth dam and embankments. Geotèchnique Vol. 25, No.4.

Sarma S.K. (1979). Response and stability of earth dams during strong earthquakes. Miscellaneous paper GL-79-13. U.S. Army engineer Waterways Experiment Station, Vicksburg.

Sarma S.K. (1981). Seismic displacement analisys of earth dams, Journal of Geotechnical Engineering Division, ASCE, Vol. 107 No. GT12.

Schnabel, P.B., Lysmer, J., and Seed, H.B. (1972) “SHAKE: A computer Program for Earthquake Response Analysis of Horizontally Layered Sites”, Report No. UCB/EERC-72/12, Earthquake Engineering Research Center, University of California, Berkeley, December, 120p.

Seed H.B. & Wilson D. (1967). The Turnagain Heights Landslides, Anchorage, Alaska. Journal of Soil Mechanics and Foundation Division, ASCE, Vol. 93, No. SM4, July, pp. 325-353.

Seed H.B., Idriss I.M. (1969). The influence of soil conditions on ground motions during earthquakes. Journal of the Soil and Mechanics Foundation Division (ASCE); **94**:93-137.

Seed, H.B. and Idriss, I. M. (1970) “Soil Moduli and Damping Factors for Dynamic Response Analysis”, Report No. UCB/EERC-70/10, Earthquake Engineering Research Center, University of California, Berkeley, December, 48p.

Seed H. B. (1976). Some aspects of sand liquefaction under cyclic loading. Proceedings, Conference on Behavior of Offshore Structures, Norwegian Institute of Technology, Oslo.

Seed H.B., Martin P.P., Lysmer J. (1976). Pore-water pressure change during soil liquefaction. Journal of Geotechnical Engineering Division, ASCE, Vol. 102 No. GT4.

Seed H.B., Makdisi F.I., Faiz I., De Alba P. (1978). Performance of earth dams durign earthquakes. Journal of Geotechnical Engineering Division, ASCE, Vol. 104 (2), pp.967-995.

Seed H.B. (1979 a). Soil liquefaction and cyclic mobility for level ground during earthquakes. Journal of Geotechnical Engineering Division, ASCE, Vol. 105 No. GT2.

Simonelli A.L. & Viggiani C. (1995). Effects of seismic motion characteristics on earth slope behaviour. Proc. First International Conference on Earthquake Geotechnical Engineering, Tokyo, 14-16 Novembre 1995.

Simonelli A.L. & Di Stefano P. (2001). Effect of vertical seismic accelertions on slope displacements. Proc. 4th Int. Confenrence on Recent Advances in Geotechnical Earthquake Engineering and Soil dynamics, San Diego, California, 26-31 Marzo, 2001, paper No. 5.34.

Skempton A.W. (1954). The pore pressure coefficients A and B. Geotèchnique , Vol 4, No.4.

Tanaka K. (1982). Seismic slope stability map (Present situation and several mooted points). Journal of Japan Landslide Society, 19-2, pp. 12-19.

Tatsuoka F., Ochi k., Fujiii S., Okamoto M. (1986). Cyclic undrained triaxial and torsional shear strength of sands for different sample preparation methods, Soils and Foundations, **26**(3), pp. 23-41.

Tatsuoka F., Shibuya S. (1991). Deformation characteristics of soils and rocks from field and laboratory tests. Keynote Lecture for Session No.1, Proc. of the 9th Asian Regional Conf. on SMFE, Bangkok, Vol. II, pp. 101-170.

TC4, ISSMGE (1999). Manual for zonation on seismic geotechnical hazard (revised version), 1999. Technical Committee for Earthquake Geotechnical Enginnering, TC4, ISSMGE

Terzaghi K. (1950). Mechanism of landslides. The geological survey of America Engineering Geology, Berkeley.

Tika-Vassilikos T.E., Sarma S.K., Ambraseys N. (1993). Seismic displacement of shear surfaces in cohesive soils. Earthquake Engineering and Structural Dynamics, Vol. 22, pp. 709-721.

Tika Th. & Pitilakis K. (1999). Liquefaction-induced failure of a bridge embankment. Proc. 2nd International Conference on Earthquake Geotechnical Engineering, Lisboa, Portugal, 21-25 June, 1999, pp. 631-636.

Tokida K., Matsumoto H., Azuma T., Towhata I. (1993). Simplified procedure to estimate lateral ground flow by soil liquefaction. Soil Dynamics and Earthquake Engineering. VI, A.S. Cakmak and C.A. Brebbia (eds.), Elsevier Applied Science, New York, pp.381-396.

Towata I., Sasaki Y., Tokida K.I., Matsumoto H., Tamari Y., Yamada K. (1992). Prediction of permanent displacement of liquiefied round by means of minimum energy principle. Soils and Foundations, JSSMFE, Vol. 32, No. 3, Settembre, pp. 97-116.

Towata I. & Mizutani T. (1999). Effect of subsurface liquefaction on stability of embankment resting upon surface. Proc. 2nd International Conference on Earthquake Geotechnical Engineering, Lisboa, Portugal, 21-25 June, 1999, pp. 1045-1057.

Trifunac, M.D. and Brady, A. G. (1975). On the correlation of seismic intensity scales with the peaks of recorded ground motion. Bull. Seism. Soc. Am., **65**, 139-162.

Vucetic, M., Dobry, R. (1991). “Effect of soil plasticity on cyclic response”, Journal of Geotechnical Engineering, 117, 89-107.

Xu J., Bielak J., Ghattas O., Wang J. (2003). Three-dimensional nonlinear seismic ground motion modelling in elastic basins. Physics of the Earth of the Earth and Planetary Interiors, **137**: 81-95.

Weekes L. & Wang R.X. (2001). Simplified assesment of seismic interactions due to sliding using the Newmark sliding block method. Proc. 12th European Conference on Earthquake Engineering, London, 2991.

Wieczorek G.F., Wilson R.C., Harp E.L. (1985). Map slowing slope stability during earthquakes in San Mateo County, California. Miscellaneous Investigations Map I-1257-E, scale 1:62,500. U.S. Geological Survey, 1985.

Wilson R.C. & Keefer D.K. (1983). Dynamic analysis of a slope failure from the 6 August 1979 Coyote Lake, California, Eartquake. Bulletin of the Seismological Society of America, Vol. 73, No. 3, 1983, pp.863-877.

Wilson R.C. & Keefer D.K. (1984). Analysis of the seismic orign of landslides: example from the New Madrid Seismic zone. Geological Society of American Bulletin, Vol. 105, No. 4, 1993, pp. 521-536.

Wilson R.C. & Keefer D.K. (1985). Predicting areal limits of earthqyake induced landsliding. In Evaluating earthquake hazard in the Los Angeles region – An Earth-Science Perspective. Ziony, J.I. ed., U.S. Geological survey, Reston, Virginia, Professional paper 1360, , 1985, pp. 316-345.

Yegian M.K., Marciano E.A., Ghahraman V.G. (1991). Earthquake-induced permanent deformations: Probabilistic approach. J. Geotech. Engrg., ASCE, Vol. 117, No. 1, January, pp.35-50.

Yegian M.K., Vitelli B.M. (1981). Analisys of liquefaction: Empirical approach. Int. Conf. on Recent Advances in Geotechnical Earthquake Engineerong and Soil Dynamics, St. Louis, Vol. 1, pp. 173-177.Youd T.L. (1978). Major causes of earthquake damage in ground failure. Civil Engineering, ASCE, Vol. 48, No. 4, pp. 47-51

Youd T.L. & Perkins D. M. (1987). Mapping of liquefaction severity index. Journal of the Geotechnical Engineering Division, ASCE, 1987; Vol. 113, No.11, pp.1347-1392.

Youd T.L., Perkins, D.M., Turner, W.G. (1989). Liquefaction severity index attenuation for the eastern United States. Proc. 2nd U.S.-Japan Workshop on Liquefaction, Large Ground Deformation and their Effects on Lifelines, Tech. Rep. NCEER-89-0032, T. D. O'Rourke and M. Hamada (eds.), December 1, pp. 438-452.

Zambelli C. (2002). Modellazione costitutiva del comportamento meccanico in campo dinamico. Degree Thesis, Milan University of Technology.

Zambelli C., di Prisco C., Imposimato S. (2004) *A cyclic elasto-viscoplastic constitutive model: theoretical discussion and validation.* In Cyclic Behaviour of Soils and Liquefaction Phenomena, Triantafyllidis Th (ed.). Balkema: Rotterdam, 99-106.

Zambelli C. (2006). Experimental and theoretical analysis of the mechanical behaviour of cohesionless soils under cyclic-dynamic loading. Ph. D. Thesis, Milan University of Technology.

Zienkiewicz O.C., Leung K.H., Pastor M. (1985). Simple model for transient soil loading in earthquakes analysis. I: basic model and its application. Int. J. Num. Anal. Meth. Geomech., **9**, 453-476.

APPENDIX A

The choice of the space-time discretization has a significant influence on the quality of the approximate solution in finite differences method. However, whether in non-linear analysis is usually impossible to find analytical constraints on the values of Δt and Δz, in linear elasticity such a possibility is typically given.

With reference to Moczo et al. (2004), considering the 1D dynamic elastic problem and being h and Δt the spacing of the space-time grid and c_0 the wave-propagation velocity, the dependence of the effective speed of the grid c^{grid} by the ratio h/λ can be studied at the varying of the stability ratio $p = c_0 * \Delta t/h$, as reported in Figure 1.

It is immediately noted as for less finely discretized domains and decreasing the stability ratio *p* the approximation of the material velocity by the "numerical velocity of the grid" makes worse, this is the phenomenon of grid dispersion.

However, it was observed that for values of the ratio h/λ less than 0.1 this approximation can be considered still satisfactory, hence the pseudo-empirical rule according to which the spatial discretization has to ensure at least ten sampling points for each wavelength of the signal:

$$h \leq \frac{\lambda}{10} \tag{1}$$

If instead the domain under consideration has already been discretized, the relationship (1) provides a limit on the frequency of the stress:

$$f_{\max} \leq \frac{c_0}{10h} \tag{2}$$

From a modelling point of view, because of the intrinsic challenging characteristics of the problem under examination, the approaches adopted can be essentially subdivided between empirical and theoretical.

This is true, however, in linear elasticity, so in this paper the construction of the numerical model should be therefore carried out with caution, preferring choices on the safety side.

Considering some numerical analyses performed by Pisanò (2007) and by the author of this paper, a spatial discretization Δz = 0.2 m could be considered satisfactory, in any case for a height H = 5 m of the slope considered in this work the spatial discretization Δz is imposed equal to 0.1 m.

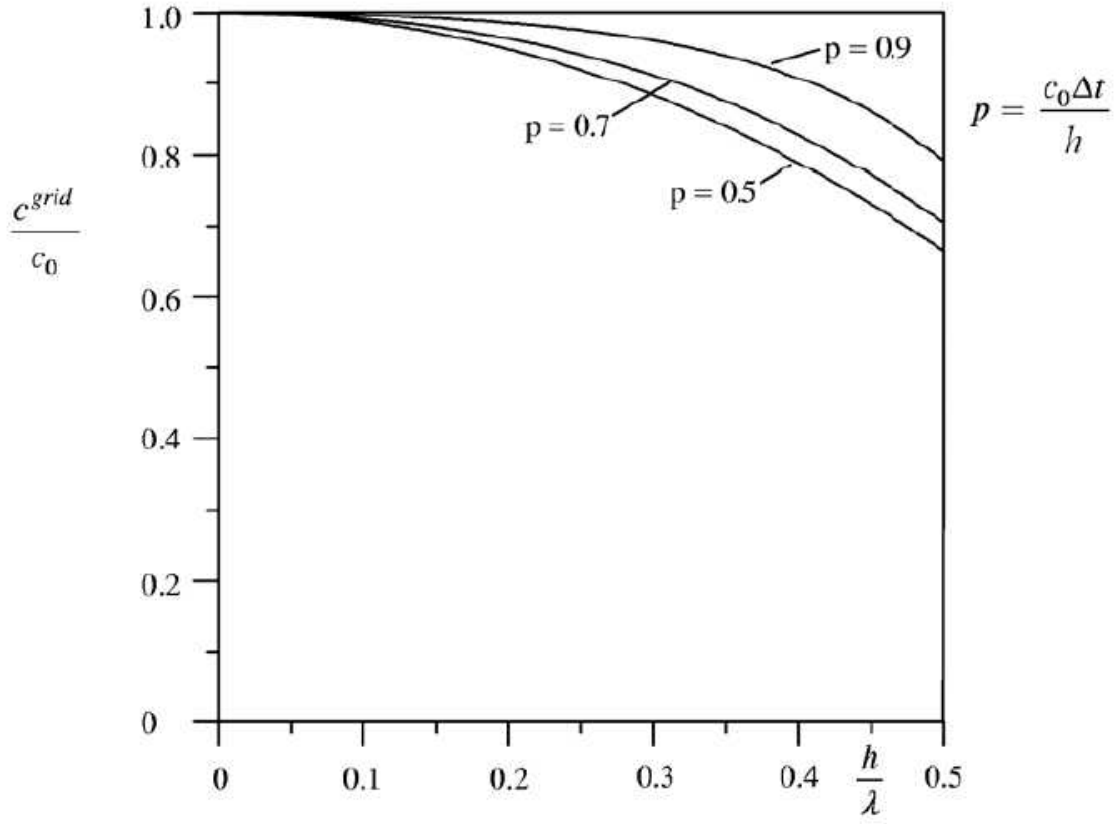

Figure 1. Grid dispersion curves (Moczo et al., 2004).